

INTERNATIONAL CONFERENCE
DAYS ON DIFFRACTION 2018

ABSTRACTS



June 4–8, 2018

St. Petersburg

ORGANIZING COMMITTEE

V. M. Babich /Chair/, A. S. Kirpichnikova /Secretary/,
T. V. Vinogradova /Visas/, N. V. Zaleskaya /Accommodation/,
I. V. Andronov, P. A. Belov, L. I. Goray, A. Ya. Kazakov,
N. Ya. Kirpichnikova, A. P. Kiselev, M. A. Lyalinov,
O. V. Motygin, M. V. Perel, V. P. Smyshlyaev,
R. Stone, N. Zhu

Conference e-mail: diffraction18@gmail.com

Web site: <http://www.pdmi.ras.ru/~dd/>

The conference is organized and sponsored by



St. Petersburg
Department
of V.A. Steklov
Institute of Mathematics



St. Petersburg State
University



The Euler International
Mathematical Institute



ITMO University



Russian Foundation
for Basic Research
(Project no. 18-01-20031)



IEEE Russia (Northwest)
Section AP/ED/MTT
Joint Chapter



FOREWORD

“Days on Diffraction” is an annual conference taking place in May–June in St. Petersburg since 1968. The present event is organized by St. Petersburg Department of the Steklov Mathematical Institute, St. Petersburg State University, the Euler International Mathematical Institute, and the ITMO University.

The abstracts of 261 talks to be presented at oral and poster sessions during 5 days of the conference form the contents of this booklet. The author index is located on the last pages.

Full-length texts of selected talks will be published in the Conference Proceedings. They must be prepared in \LaTeX format and sent not later than 25 June 2018 to diffraction18@gmail.com. Format file and instructions can be found at <http://www.pdmi.ras.ru/~dd/proceedings.php>. The final judgement on accepting the paper for the Proceedings will be made by the Editorial Board after peer reviewing.

As always, it is our pleasure to see in St. Petersburg active researchers in the field of Diffraction Theory from all over the world.

Organizing Committee



In memoriam of
Alexander Mikhailovich Samsonov
1948–2017

Alexander M. Samsonov, a theorist of high international reputation, passed away on Saturday, October 7, 2017, aged 69. He was a member of the Organizing Committee of the “Days on Diffraction” conference since 2003.

A. M. Samsonov, D.Sci., headed the Laboratory for Theory of Solids at the Ioffe Institute of the Russian Academy of Sciences, and was a Professor at the Peter the Great Polytechnic University in St. Petersburg. The main area of his interest and the lifelong topic of his studies concerned nonlinear strain solitary waves in solids, where he was a world renowned expert. His theoretical inventions served as a basis for his collaboration with experimentalists at the Ioffe Institute; it lasted for several decades and resulted in the prediction and observation of bulk longitudinal strain solitary waves in various solid waveguides. Another field of his research was application of methods of nonlinear mathematical physics to various models arising in biophysics and systems biology.

A. M. Samsonov was a meticulous and inspiring teacher, a supervisor to numerous students and young researchers, a colleague and dear friend to many of us. His passing away puts a dent in the community of nonlinear wave physicists, and it is an irreplaceable loss for his friends and colleagues. He is greatly missed.



70 years to A. P. Kiselev

The Organizing Committee of Days on Diffraction 2018 congratulates Aleksei Prokhorovich Kiselev on the occasion of his 70th birthday. Being a permanent member of the team of Days on Diffraction since 1997, currently he heads the Programme Committee and participates in editing of the Conference Proceedings. A. P. Kiselev is a Chief Research Scientist at the St. Petersburg Department of the V. A. Steklov Mathematical Institute, a Professor at the Faculty of Physics, Saint Petersburg State University; above all he is a Principal Research Scientist at the Institute for Problems in Mechanical Engineering of the Russian Academy of Sciences. He is a well known expert, profoundly competent in various aspects of the diffraction theory, and the mastery is successfully contributed to organization of Days on Diffraction. The main scientific results of A. P. Kiselev concern localized solutions of hyperbolic equations and high-frequency elastic waves (partly the results can be found in the recent book by V. M. Babich, A. P. Kiselev, *Elastic Waves: High Frequency Theory*, CRC Press, 2018). The Organizing Committee wishes Aleksei Prokhorovich new scientific achievements, in addition to good health and energy needed to organize many further Days on Diffraction.



65 years to S. A. Nazarov

The Organizing Committee of Days on Diffraction 2018 congratulates Sergei Aleksandrovich Nazarov on the occasion of his 65th birthday. S. A. Nazarov is a Principal Research Scientist at the Institute for Problems in Mechanical Engineering and at the Faculty of Mathematics and Mechanics, Saint Petersburg University. He is widely known as an extraordinary prolific scientist and for his outstanding results in Mathematical Physics; they are based on masterly application of various asymptotic techniques to numerous problems that involve differential equations and their applications to Mechanics, Biology, Acoustics, etc. Days on Diffraction highly appreciate that S. A. Nazarov is a permanent participant of this annual conference; his talks always attract much interest in view of high-level scientific results presented in a clear and vivid style. The Organizing Committee wishes Sergei Aleksandrovich new achievements and hopes to hear about them at many spring Days on Diffraction ahead.

List of talks

Eugeny G. Abramochkin, Evgeniya V. Razueva Light beams based on diffraction catastrophes	23
Alekseeva E.L., Alkhimenko A.A., Grishchenko A.I., Semenov A.S., Tretyakov D.A., Belyaev A.K., Polyanskiy V.A., Yakovlev Yu.A. Propagation of acoustic waves during the control of hydrogen-induced destruction of metals by the acoustoelastic effect	24
Altaisky M.V., Kaputkina N.E., Krylov V.A. Simulation of 3 quantum dot network dynamics	25
Khimya Amlani Approximate solution of MHD boundary layer flow of a non-Newtonian power-law fluids over a continuous moving surface using B-spline collocation	25
R. Anastasia, I. Magdalena, H.Q. Rif'atin Seiches and harbour oscillation in a semi-closed basin of various geometric shape with porous media	25
Anikin A.Yu., Dobrokhotov S.Yu., Nazaikinskii V.E. Efficient asymptotic formulas for waves generated by a localized source with finite duration	26
A.Yu. Anikin, S.Yu. Dobrokhotov, V.E. Nazaikinskii Simple asymptotics for a generalized wave equation with degenerating velocity and their applications to the linearized long wave run-up problem	27
Anatoly Anikin, Sergey Dobrokhotov, Vladimir Nazaikinskii, Michel Rouleux Semi-classical Green functions	27
Asadchikov, V.E., Goray, L.I., Rosshin, B.S., Tikhonov, A.M., Volkov, Yu.O. Fluorescence analysis of X-ray whispering gallery waves propagating along liquid meniscuses	28
Mikhail Babich, Sergey Slavyanov Fuchsian Heun equation, equivalent Fuchsian linear systems and Painlevé P^{VI} equation	29
Andrey Badanin Third order operator for the good Boussinesq equation on the circle	30
I.V. Baibulov, A.M. Budylin, S.B. Levin The asymptotics of the solution of three one-dimensional quantum particles scattering problem. The case of finite repulsive pair potentials	30
Bakharev F.L., Matveenko S.G. Localization effect for eigenfunctions in narrow Kirchhoff plates with clamped edges	30
Bakharev F.L., Nazarov S.A. Some spectral problems for thin Kirchhoff plates	31
M.I. Belishev, S.A. Simonov Isometric model of metric spaces and the wave model of symmetric operators	31
Belolipetskaia A.G., Popov I.Y. On the spectrum discreteness for quantum graph in a magnetic field	32
Beltukov Y.M., Belashov A.V., Garbuzov F.E., Semenov A.A., Semenova I.V. Solitary strain waves in two-layered nanocomposites	32
Alexander K. Belyaev Some approaches to harmonic wave propagation in elastic solids with random microstructure	33

Alexander S. Blagoveshchensky, Azat M. Tagirdzhanov, Aleksei P. Kiselev Two classes of localized solutions of the wave equation	34
Borzov V.V., Damaskinsky E.V. Generalized Chebychev polynomials connected with a point interaction for the discrete Schrödinger equation	34
Brezhnev Yu.V., Dobrokhotov S.Yu., Tsvetkova A.V. Integrable in elliptic functions equations for the fronts of linear water waves generated by a localized source	35
Budiasih L.K., Wiryanto L.H. Boussinesq-type model to simulate the development of an undular bore on a small slope ...	36
Bulatov V.V., Vladimirov Yu.V. Unstable regimes of surface gravity waves generation	36
Bulygin A.N., Pavlov Yu.V. Complex representation of general solution of equations for nonlinear model of plane deformation of crystal media with a complex lattice	37
Buslov V.A. Different asymptotic limits of average evolution of quantum particle under small random perturbations	38
Jen-Hsu Chang The Le-diagram for the resonance of modified KP equation	39
Chehade S., Darmon M., Lebeau G. The spectral functions method for elastic plane wave diffraction by a wedge	40
Danilov V.G., Gaydukov R.K. Equations for velocity oscillations in problems of a fluid flow along a plate with small periodic irregularities on the surface for large Reynolds numbers	40
M.N. Demchenko Reconstruction of solution to the wave equation from Cauchy data on the boundary	41
E. Dinvai, H. Kalisch, D. Dutykh, John D. Carter Bidirectional fully dispersive models for water waves over a rough bottom	42
Dmitrieva L.A., Kuperin Yu.A., Smetanin N.M. Differentiation of brain waves patterns in different states by multifractal analysis	42
Dobrokhotov S.Yu. The problem of the wave overturning for the Burgers equation with an imaginary dispersive second derivative	43
Dobrokhotov S.Yu., Sekerzh-Zenkovich S.Ya., Tolstova O.L., Vargas C.A. The linear water waves in the basin with elastic base created by the localized underground source	44
Dorodnyi M.A., Suslina T.A. Homogenization of a nonstationary model equation of electrodynamics	44
Doroshenko O.V. Modelling of damaged interface dynamic behaviour via random and periodic distributions cracks	45
Dugin N.A., Belyaev G.R., Lobastov V.G., Zaboronkova T.M. Polarization characteristics of graphene-containing composite L-band antenna	46

Farafonov V.G., Ustimov V.I., Tulegenov A.P., Sokolovskaya M.V., Il'in V.B.	
A spheroidal model for axisymmetric scatterers based on the quasistatic approach	47
Fedotov A., Klopp F.	
Difference equations, uniform quasiclassical asymptotics and Airy functions	47
Fedotov A., Shchetka E.	
Monodromy matrices for Harper equation	48
Fialkovsky I.V., Perel M.V.	
Interaction of modes near an eigenvalue crossing for the diagonalizable perturbed Hamiltonian	49
Filippenko G.V., Wilde M.V.	
Low-frequency backward waves in an elastic cylindrical shell filled with fluid: comparison of shell theories and 3D theory of elasticity	50
Garbuzov F.E., Khusnutdinova K.R.	
Modelling longitudinal bulk strain waves in elastic waveguides with Boussinesq and Korteweg–de Vries type equations	50
Gavrikov A.A.	
Natural vibrations of some inhomogeneous rod-like systems	51
Gavrilov S.N., Mochalova Yu.A., Shishkina E.V.	
Evolution of a trapped mode of oscillation in a Bernoulli–Euler beam on the Winkler foundation with point inhomogeneity	52
Golub M.V., Eremin A.A., Glushkov E.V., Glushkova N.V.	
Theoretical and experimental study of resonance Lamb wave scattering by an impact-induced damage	53
Golub M.V., Shpak A.N., Fomenko S.I., Zhang Ch.	
Semi-analytical hybrid approach for modelling wave motion excited by a piezoelectric transducer in periodic layered composite with a crack	54
Gómez D.	
High frequencies for some spectral problems in thin structures	55
Grekova E.F.	
Harmonic waves in simplest reduced Kelvin's and gyrostatic media under external body follower torque	55
Grigoreva A.A., Tyukhtin A.V., Vorobev V.V., Galyamin S.N.	
Electromagnetic field structure of a charge flying out from a vacuum area to bilayer one in a circular waveguide	56
Gusev V.A.	
Surface acoustical waves at the boundary of bimodule medium	57
A.M. Ishkhanyan	
Appell hypergeometric expansions of the solutions of the general Heun equation	58
T.A. Ishkhanyan, C. Leroy, A.M. Ishkhanyan	
Generalized confluent hypergeometric solutions of the confluent Heun equation	58
Ivanov A.V.	
Transversal connecting orbits of Lagrangian systems with turning points: Newton–Kantorovich method	59
Boris Katsnelson	
Variability of the phase and pulse fronts of the sound signal due to horizontal refraction in shallow water waveguide	60

A.Ya. Kazakov

“Separation of variables” in the model problems of the diffraction theory 60

Anna Kirpichnikova, Nataliya Kirpichnikova

Asymptotical and numerical investigation of the currents in a short-wave diffraction problem of a plane incident wave by smooth prolate bodies of revolution with Dirichlet and Neumann boundary conditions 61

Aleksei P. Kiselev, Alexandr B. Plachenov

Astigmatic Gaussian beam: exact solution of the Helmholtz equation 61

Kislin D.A., Knyazev M.A., Shpolyanskiy Y.A., Kozlov S.A.

Self-focusing of non-paraxial single cycle optical pulses in nonlinear media 62

Knyazkov D.

Inverse problem of tomography of thick layer 63

Korikov D.V., Plamenevskii B.A.

Asymptotics of solutions to non-stationary Maxwell systems in a domain with small cavities 64

Kovaleva M., Manevitch L.I., Pilipchuk V.

Non-conventional phase attractors and repellers in weakly coupled autogenerators with hard excitation 64

A.E. Kovtanyuk, A.Yu. Chebotarev, A.A. Dekalchuk, N.D. Botkin, R. Lampe

Analysis of a mathematical model of oxygen transport in brain 65

Kozitskiy S.B.

Dynamic patterns in double-diffusive convection 66

V. Kozlov

A comparison theorem for super- and subsolutions of $\nabla^2 u + f(u) = 0$ and its application to water waves with vorticity 67

Vladimir Kozlov, Sergei Nazarov, German Zavorokhin

On effective lengths of blood vessels 68

I.J. Kristianto, I. Magdalena

Wave reduction on a shoaling phenomenon by a porous structure 68

Kudrin A.V., Zaboronkova T.M., Zaitseva A.S., Krafft C.

Current distribution and input impedance of a circular loop antenna located on the surface of a gyromagnetic cylinder 69

Kurseeva V.Yu.

Electromagnetic non-polarized symmetric hybrid wave propagation in nonlinear media with saturation 69

Nikolay Kuznetsov

An indefinite integral equation without irregular frequencies for the floating-body problem . 70

M.A. Lyalinov

Surface waves in a polygonal domain with Robin boundary conditions 71

I. Magdalena, Kevin

Numerical studies for resonant phenomena during wave run-up 72

Matias, D.V.

Propagation process of the coupled hyperbolic waves in gas thermoelastic medium 72

Matveev V.B.

Linear and nonlinear aspects of scattering on oscillating potentials 73

Melikhova A.S., Popov I.Y.	
Spectral problem for Dirac operator for Y-type splitted chain of nanospheres	73
Miakisheva O.A., Fomenko S.I.	
Leaky wave asymptotics in the case of stationary point and complex pole approaching	74
A.S. Mikhaylov, V.S. Mikhaylov	
Dynamic inverse problem for canonical system with smooth positive Hamiltonian	75
Minenkov D.S.	
On analytical modeling of cold field electron emission from nanotube films in irregular and aperiodic cases	76
Oleg V. Motygin	
On evaluation of the confluent Heun functions	77
Sergei A. Nazarov	
“Blinking and wandering” eigenvalues: Blunted elastic cusps and rounded plasmonic singularities	77
Sergei A. Nazarov	
Spectral problems for long and infinite Kirchhoff plates	78
Pastukhova S.E.	
Operator estimates in homogenization of second-order divergence elliptic equation with coefficient matrix in BMO	79
Pavlova A.V., Rubtsov S.E., Telyatnikov I.S.	
Steady-state oscillations of the volume of liquid on an elastic layer	80
Pérez E.	
Asymptotics for the spectrum in boundary value problems with strongly alternating boundary conditions	81
Pestov L.N., Danilin A.N.	
Various options for migration in elastic environments based on the method of Reverse Time Migration	82
Pestov L.N., Filatova V.M., Nosikova V.V., Rudnitskii A.G.	
Sound speed determining in weak inclusions degraded by noise in the ultrasound tomography problem	82
Petrov P.N., Dobrokhotov S.Yu.	
Asymptotic solution of the Helmholtz equation in a three-dimensional layer of variable thickness with a localized right-hand side	83
Petrov P.S., Burenin A.V., Golov A.A., Morgunov Yu.N.	
Transformation of the modal structure of acoustical field in course of the sound propagation from continental shelf to the deep ocean	84
Petrov P.S., Tyshchenko A.G., Ehrhardt M.	
Numerical solution of iterative parabolic equations approximating the nonlinear Helmholtz equation	85
Vladimir Petrov	
Diffraction of high-frequency hadronic waves	86
Polyanskiy V.A., Belyaev A.K., Tretyakov D.A., Yakovlev Yu.A., Polyanskiy A.M.	
Averaged equations bi-continuum material in the long-wavelength approximation	86
Popov A.V., Edemsky F.D., Prokopovich I.V.	
GPR image deconvolution from antenna current waveform	87

Popov M.M.	
On Morse index calculations for geodesic lines on smooth surfaces imbedded in \mathbb{R}^3	88
Porubov A.V.	
Two dimensional nonlinear waves in crystalline media	89
Prozorova E.V.	
Mathematical theory of continuum mechanics with angular momentum	89
Evgeniya V. Razueva, Eugeny G. Abramochkin	
Basic multiple-twisted spiral beams	90
Ryadovkin K.S.	
Laplacians on periodic graphs with boundary	91
Saburova N.Yu.	
Invariants and spectral estimates for Laplacians on periodic graphs	91
Pavle Saksida	
Nonlinear Fourier transform, nonlinear modes and nonlinear superposition	92
Sazonov S.V., Kalinovich A.A., Zakharova I.G., Komissarova M.V.	
Light bullets in a planar waveguide with quadratic nonlinearity and normal group velocity dispersion	92
Schadko A.O., Zaytsev K.I., Chernomyrdin N.V., Nosov P.A.	
Simulation of the optical components surface quality influence on the propagation of high-power laser radiation	93
Nikita N. Senik	
On homogenization for strongly elliptic operators with “Hölder continuous” locally periodic coefficients	94
Sergeev S.A., Tolchennikov A.A., Petrov P.S.	
Maslov’s canonical operator in the problem of acoustic pulse signal propagation in a shallow sea with penetrable bottom	95
Setukha A.V., Fetisov S.N.	
Numerical method for solving the problem of electromagnetic wave scattering by a perfectly conducting object of small thickness	96
Shanin A.V., Korolkov A.I.	
Method of parabolic equation in diffraction theory. When it is applicable?	97
Shanin A.V., Korolkov A.I., Belous A.A.	
Experimental study of diffraction by a thin cone	97
Shirokov E.A.	
Scattering of quasi-electrostatic waves on the conducting bodies of revolution in media with dielectric anisotropy	98
Slunyaev A.V.	
Inverse scattering technique for deep water waves	99
Eugene Smolkin, Maxim Snegur	
Numerical study of the electromagnetic wave propagation problem in an anisotropic waveguide	100
Starkov I.A., Starkov A.S.	
The effect of curvature and torsion of inclusions on effective permittivity	100
Stavtsev S.L.	
Low-rank matrices with a hierarchical basis in an electromagnetic problem of diffraction ...	101

I.O. Sukharevsky, M. Lebental, B. Dietz, C. Lafargue, S. Bittner	
Supercar model for dielectric equilateral triangle microresonators validated by the integral equation method	102
Suleymanova A.	
Spectral geometry of surfaces with curved conic singularities	103
Sushchenko A.A., Kovalenko E.O., Kan V.A.	
Focusing of the seabottom images	103
Suslina T.A.	
On spectral approach to homogenization of elliptic operators in a perforated space	104
Telyatnikov I.S.	
On the method of the block element in the problem of vibration of an elastic medium with a composite coating	105
Tikhov S.V., Valovik D.V.	
Propagation of electromagnetic waves in a shielded dielectric layer with cubic nonlinearity ..	106
M.D. Todorov	
Nonlinear waves: theory, computer simulation, experiment	107
Vasilchuk V.	
Distribution of the spectrum of symmetrically deformed unitary invariant random matrix ensemble	108
Vedenyapin V.V.	
Hamilton–Jacobi method in non-Hamiltonian situation and Boltzmann extremals	108
Ngoc Nguyen Vu, Rolf Lammering	
Numerical simulation of nonlinear wave propagation in symmetric cross-ply laminates with hyperelastic material behavior	109
Wilde M.V., Sergeeva N.V.	
Analysis of longitudinal impact waves in a thin viscoelastic rod on the basis of 3D equations for a Rabotnov’s hereditary elastic body	110
Yakovlev Yu.A , Belyaev A.K., Polyanskiy V.A., Tretyakov D.A., Arseniev D.G.	
Gradient method for detecting sites of local hydrogen embrittlement of metals	111
Yashina N.F., Zaboronkova T.M., Krafft C.	
Interaction of nonsymmetric electromagnetic waves guided by cylindrical duct with enhanced density in magnetoactive plasma	112
D.D. Zakharov	
Low frequency spectra of layered plates and their parametrical study	113
V. Zalipaev, S. Kosulnikov, S. Glybovski	
Electromagnetic resonance structures made of thin metallic wires	113
Zhuchkova M.G.	
Ice-coupled surface water waves near a vertical barrier	114
Ekaterina A. Zlobina, Aleksei P. Kiselev	
High-frequency diffraction by a contour with a jump of curvature	115

Workshop on Nanophotonics and Metamaterials

Redha Abdeddaim, Stefan Enoch	
M-Cube project: objectives and some results	116
Muhammad U. Afzal, Karu P. Esselle, Ali Lalbakhsh, Mst Nishat Yasmin Koli	
A metasurface-based beam-steering solution for microstrip patch arrays	117
A.G. Balanov, A. Apostolakis, K.N. Alekseev, F.V. Kusmartsev, F. Wang, C.L. Poyser, A.V. Akimov, A.J. Kent, M.T. Greenaway, T.M. Fromhold	
Charge transport in a semiconductor multilayer heterostructures driven by a high-frequency acoustic wave	118
Miguel A. Bandres, Mordechai Segev	
Embedded photonic topological insulators	118
Baranov, D.G., Li, S., Generalov, A., Krasnok, A., Alù, A.	
Coherent control of light for virtual absorption and wireless power transfer	119
Baranov, D.G., Verre, R., Karpinski, P., Käll, M.	
Enhanced Raman emission by non-scattering anapole state of a silicon nanodisk	120
Hani Barhom, Andrey Machnev, Ivan I. Shishkin, Roman Noskov, Pavel Ginzburg	
Optomechanical manipulation and optical properties of vaterites	121
Barsukova M.G., Shorokhov A.S., Musorin A.I., Luk'yanchuk B.S., Fedyanin A.A.	
Enhanced Faraday effect in hybrid metasurfaces	122
Ray H. Baughman, Alan G. MacDiarmid	
Stronger, faster, and more powerful artificial muscle yarns and fibers	123
Benimetskiy F.A., Alekseev P.A., Sinev I.S., Mukhin I.S., Samusev A.K.	
Strain engineering in MoSe ₂ monolayers	123
Berestennikov A.S., Tiguntseva E.Y., Iorsh I.V., Makarov S.V.	
Optical properties of spatially dispersive Mie-resonant halide perovskite nanoparticles	124
M. Beruete	
The role of leaky waves in extraordinary transmission hole arrays and corrugated antennas	126
Bleu O., Malpuech G., Solnyshkov D.D.	
Topological polaritonics	127
Bliokh K.Y., Bekshaev A.Y., Nori F.	
Optical momentum and angular momentum in complex media	128
A.A. Bogdanov, M.V. Rybin, K.L. Koshelev, Z.F. Sadrieva, K.B. Samusev, M.F. Limonov, Yu.S. Kivshar	
High-Q modes in subwavelength dielectric resonators	128
Bruil E.A., Shchelokova A.V., Zubkov M.A., Melchakova I.V., Glybovski S.B., Andreychenko A.E., Slobozhanyuk A.P.	
Adjustable metasurface-based resonator for in vivo MRI	129
Hrvoje Buljan	
Engineering Weyl semimetals and anyons	130
Chestnov I.Yu., Sedov E.S., Kavokin A.V.	
One-dimensional optical Tamm plasmons	130
Chubchev E.D., Dorofeenko A.V., Vinogradov A.P.	
Transmission properties of a chain of plasmonic nanoparticles beyond the point dipole approximation	131

Christopher M. Collins, Giuseppe Carluccio, Gillian Haemer	
Potential to improve performance of state-of-the-art receive arrays with high-permittivity materials	132
M. Conforti, G. Xu, C. Mas Arabí, T. Marest, A. Bendahmane, A. Kudlinski, A. Mussot, S. Trillo	
Dispersive shock waves in optical fibers	133
Dadoenkova N.N., Dadoenkova Yu.S., Panyaev I.S., Sannikov D.G., Lyubchanskii I.L.	
Multi-periodic one-dimensional photonic crystals	134
V.I. Demidchik, R.V. Kornev	
Antenna approach for calculating dynamic polarizability of carbon nanotubes	135
Aldo Di Carlo	
2D materials for mesoscopic perovskite photovoltaics	136
Marco Di Liberto	
Two-body physics in topological models	136
Alexey A. Dmitriev, Mikhail V. Rybin	
Coupling regimes of high-index dimer	137
Dolganov P.V.	
Peculiarities of the photonic density of states in liquid-crystalline photonic crystals	138
Dolganov P.V., Shuravin N.S., Dolganov V.K.	
Structures and optical properties of smectic liquid crystals with multilayer periodicity	138
Jian-Wen Dong	
All-dielectric valley photonic crystals: Paving the way to topological nanophotonics	139
I.V. Doronin, E.S. Andrianov, A.A. Zyablovsky, A.P. Vinogradov, A.A. Lisyansky	
Second-order autocorrelation function for amplified spontaneous emission	140
Doskolovich L.L., Bezus E.A., Bykov D.A.	
High-Q resonances and bound states in the continuum in photonic elements integrated into a slab waveguide	141
R. Driben, V.V. Konotop, A.V. Yulin, T. Meier	
Bloch oscillations and related phenomena in multidimensional nonlinear settings	142
Drozdov A.A., Knyazev M.A., Kozlov S.A., Boyd R.W.	
Disappearance of self-focusing phenomena for few-cycle pulses	143
M. Dubois, R. Abdeddaim, S. Enoch, L. Leroi, Z. Raolison, A. Vignaud	
Shaping electromagnetic fields with meta atom for ultra-high field MRI	144
Dyakov, S.V., Gippius, N.A.	
Engineering of resonances in modulated structures	145
Egorov, O.A., Skryabin, D.V.	
Frequency comb generation in a exciton-polariton microring resonator	145
S.V. Fedorov, N.N. Rozanov, N.A. Veretenov	
3D-topological — vortex, knotted, and tangled — dissipative optical solitons	146
Fedyanin A.E., Mogunov Ia.A., Scherbakov A.V., Lysenko S., Akimov A.V., Kalashnikova A.M.	
Picosecond photo-elastic effect in a VO ₂ thin film in insulating and metallic phases	147
Dmitry Filonov, Pavel Ginzburg	
Metamaterial-based super-scatterers	148

Frizyuk K.S., Zograf G.P., Tarasov M.G., Makarov S.V., Grange R., Petrov M.I. Polarization effects in second-harmonic generation from inorganic BaTiO ₃ perovskite resonant nanoparticles	149
Furasova A.D., Zakhidov A.A., Di Carlo A., Makarov S.V. Silicon nanoantennas in perovskite photovoltaics	150
Aitzol García-Etxarri Optical vortices and polarization Möbius strips on all-dielectric optical antennas	151
Gets D.S., Ishteev A.R., Liashenko T.G., Saranin D.S., Makarov S.V., Zakhidov A.A. Switchable light emitting perovskite solar cells	151
Gorkunov M.V., Kondratov A.V., Rogov O.Y., Artemov V.V., Gainutdinov R.V., Ezhov A.A. Visible guided-mode resonances of FIB-nanopatterned mono-c-Si chiral metasurface	152
Gorlach A.A., Zhirihin D.V., Slobozhanyuk A.P., Gorlach M.A., Khanikaev A.B. Valley Zak topological states in all-dielectric structures	153
Gorlach M.A., Savelev R.S., Poddubny A.N. Topological transition due to spontaneous symmetry breaking	154
Mohammad Hafezi Quantum directions in topological photonics	155
P. del Hougne, M.F. Imani, M. Fink, D.R. Smith, G. Lerosey Precise localization of multiple non-cooperative objects in a disordered cavity by wavefront shaping	156
Husakou A., Alharbi, M., Chafer, M., Debord, B., Gerome, F., Benabid, F. Coupled wave propagation and nanotrap lattice in hollow fiber filled with Raman-active gas	157
Artur Ishteev, Ross Haroldson, Masoud Alahbakhshi, Alisha Whitehead, Sergey Makarov, Anvar Zakhidov Tunable color bright LED tandems with nanostructured perovskite-polymer composites	158
E.L. Ivchenko Photogalvanic effects in gyrotropic Weyl semimetals	158
Jalali M., Erni D., Nadgaran H. Semi-periodic nanostructures: an apt solution to broadband optical applications	159
Kafesaki M., Katsantonis I., Economou E.N., Droulias S., Soukoulis C.M. Combining chirality and Parity-Time symmetry in metamaterials	160
Kaliteevski M.A., Ivanov K.A., Gubaydullin A.R. Purcell factor in periodic metal-dielectric structures	161
Ido Kaminer Ultrastrong coupling of electrons and 2D polaritons	162
D. Kartashov, R. Sollapur, M. Zürich, M. Chemnitz, M. Schmidt, C. Spielmann Nonlinear wave dynamics in anti-resonant hollow-core fibers	163
A.B. Khanikaev All-dielectric topological photonics	164
Kiselev A.D., Pasechnik S.V., Shmeliova D.V., Dubtsov A.V. Waveguide modes of biaxially anisotropic fiber and electro-optics of porous films filled with nematic liquid crystals	164
Kivshar Yu.S. Meta-optics and Mie-resonant nanophotonics	165

Vasily V. Klimov	
Breaking of bulk-surface correspondence in topological photonics	165
Knyazev M.A., Kozlov S.A.	
Noncollinear interaction features of optical waves with wide spectrum in nonlinear dielectric medium	166
Kolodny S.A., Yudin D.I., Iorsh I.V.	
Resonant excitation of TMOKE-based spin waves in hybrid nanostructures via frequency comb	167
Kozin V.K.	
Quantum rings in the regime of strong light-matter coupling. Topological insulators	168
Kretov E.I., Shchelokova A.V., Slobozhanyuk A.P.	
Wire metasurface eigenmode impact on receive sensitivity enhancement of 1.5 T MRI machine	169
Dmitriy Krizhanovskii	
Polaritons in photonic structures with (In)GaAs and transition metal dichalcogenides as an active media	170
Sylvain Lannebère, Mário G. Silveirinha	
Photonic analogues of the Haldane and Kane–Mele models	170
Lapine M.	
Sorting resonances and non-resonant enhancements: a kaleidoscope of recent highlights	171
Larin A.O., Sun Y., Savelev R.S., Zuev D.A.	
Numerical design of Au/Si core-shell nanoparticles	172
Lavrinenko A.V., Shkondin E., Takayama O., Repän T., Panah M.E.A.	
Lamellas metamaterials: fabrication, characterization and applications	173
Lepeshov S., Krasnok A., Kotov O., Alù A.	
Strong coupling between silicon spherical nanoparticle and monolayer WS ₂	174
D. Leykam, S. Mittal, M. Hafezi, Y.D. Chong	
Topologically-protected transport in next-nearest-neighbour coupled ring resonator lattices.	175
Li, S.V., Krasnok, A.E.	
Dielectric Yagi–Uda nanoantennas for unidirectional excitation of plasmons	176
Lyubarov M.D., Poddubny A.N.	
Exceptional points in energy spectrum of nonlinear cavity arrays	177
T. Marest, C. Mas Arabí, M. Conforti, A. Mussot, A. Kudlinski, C. Milian, D.V. Skryabin	
Dispersive wave emission from dark solitons and their collision in optical fibers	178
Ekaterina E. Maslova, Mikhail V. Rybin	
All-dielectric metamaterials with Mie-driven resonant electric response	180
Medvedev Iu., Ferreira H., Maslovski S.	
Modeling of metamaterial superabsorbers in two dimensions	181
Mikheeva E., Lumeau J., Enoch S., Wenger J., Moreau A., Lemarchand F., Voznuk I., Abdeddaim R.	
Development of hyperbolic metamaterials for the control of biological molecules fluorescence	182
Andrey Miroshnichenko	
Nonradiating excitations with dielectric nanoparticles	183
Morozov K.M., Gubaydullin A.R., Ivanov K.A., Pozina G.P., Kaliteevski M.A.	
Purcell effect in a disordered photonic crystals	183

Arnaud Mussot, Pascal Szriftgiser, Corentin Naveau, Matteo Conforti, Alexandre Kudlinski, François Copie, Stefano Trillo	
Full characterisation in phase and amplitude of the Fermi–Pasta–Ulam recurrence process in optical fibers	184
Neerad Nandan, Mikhail V. Rybin	
Study of high-index dielectric nanoparticles by means of virtual surface currents method	186
N.E. Nefedkin, E.S. Andrianov, A.A. Pukhov, A.P. Vinogradov, A.A. Lisyansky	
Control of second order correlation function of plasmonic resonator by NV-center	187
Nestoklon M.O., Goupalov S.V., Dzhioev R.I., Ken O.S., Korenev V.L., Kusrayev Yu.G., Sapega V.F., de Weerd C., Gomez L., Gregorkiewicz T., Lin Junhao, Suenaga Kazutomo, Fujiwara Yasufumi, Matyushkin L.B., Yassievich I.N.	
Optical orientation of excitons in nanocrystals of inorganic perovskites	187
A. Nikulin, A. Ourir, J. de Rosny	
Metacage for controllable field distribution in MRI	188
A. Nikulin, A. Ourir, J. de Rosny, G. Lerosey, B. Larrat, F. Kober, R. Abdeddaim, S. Glybovski	
Double-tuned birdcage-like coil based on metasurfaces	189
Franco Nori	
Parity-Time-Symmetric Optics, extraordinary momentum and spin in evanescent waves, and the quantum spin Hall effect of light	190
Okhlopkov K.I., Ezhov A.A., Shafrin P.A., Orlikovsky N.A., Shcherbakov M.R., Fedyanin A.A.	
Optical coupling between dielectric Mie-resonant nanodisks and waveguides probed by third harmonic generation microscopy	192
Willie J. Padilla, Andrew Cardin, Kebin Fan	
All-dielectric metasurfaces for unconventional scattering	193
Dmitry Panna, Nadav Landau, Leonid Rybak, Shai Tsesses, Guy Adler, Sebastian Brodbeck, Christian Schneider, Sven Hofling, Alex Hayat	
Reversible light-by-light control through a giant ac Stark effect in a strongly coupled light-matter system	194
V. Petranovskii, Y. Kotolevich, S. Miridonov, P. Sánchez-Lopez, F. Chávez-Rivas, R. Machorro, S. Fuentes	
Self-assembling of ordered domains of silver nanoparticles into the mordenite channel system	194
Alexander Yu. Petrov, Dirk Jalas, K. Marvin Schulz, Manfred Eich	
Emission enhancement in dielectric nanocomposites	195
Pidgayko D., Sinev I., Permyakov D., Samusev A., Sychev S., Bogdanov A., Lavrinenko A., Rutckaia V., Schilling J.	
Visualization of elliptic and hyperbolic dispersion regimes of guided optical modes in all-dielectric metasurface	196
Poddubny A.N.	
Routing emission of plasmons by a magnetic field	197
L.Yu. Pogorelskaya, A.A. Bogdanov, K.B. Samusev, A.D. Sinelnik	
Bound state in the continuum supported by a low refractive index contrast waveguide in a woodpile structure	197
Poutrina E., Urbas A.M.	
Inherently nonreciprocal: nonlinear nanomaterials	198

Pushkarev A.P., Korolev V.I., Markina D.I., Komissarenko F.E., Sannikov D.A., Zasedatelev A.V., Lagoudakis P.G., Zakhidov A.A., Makarov S.V.	
Synthesis of high-quality CsPbBr ₃ nanolasers at ambient conditions	199
Andreas Rennings, Zhichao Chen, Benedikt Sievert, Jan Taro Svejda, Daniel Erni	
Metamaterial based enhancements of RF-coils for ultra high-field magnetic resonance imaging	200
Julien de Rosny, Redha Abdeddaim, Camille Jouvaud, Benoît Larrat, Anton Nikulin, Abdelwaheb Ourir	
Hybridized magnetic enhancer and metacage as new volume antenna for high field MRI . . .	201
Sáenz J.J.	
Light induced collective dynamics and “Mock Gravity” interactions between plasmonic nanoparticles	202
Sarychev A.K., Afanasev K.N., Bykov I.V., Boginskaya I.A., Ivanov A.V., Lagarkov A.N., Merzlikin A.M., Ryzhikov I.A., Sedova M.V., Evtushenko E.G., Kurochkin I.N., Mikheev V.V., Negrov D.V.	
Tunable metasurface composed of periodic metal-dielectric resonators	203
Moti Segev	
Topological photonics and topological insulator lasers	204
Shamkhi H.K., Baryshnikova K.V., Shalin A.S.	
Simultaneous forward-backward scattering suppression through nonresonant multipole excitation	204
Sharapova, P.R., Reichelt, M., Nikitin, A., Meier, T., Luo, K.H., Herrmann, H., Höpker, J.P., Krapick, S., Bartley, T.J., Silberhorn, C., Lita, A., Verma, V., Gerrits, T., Nam, S.W., Mirin, R.	
Quantum optics with LiNbO ₃ integrated waveguide circuits: Generation and manipulation of two-photon interference and progress towards the integration of superconducting detectors	205
Timur Shegai	
Modified excited states dynamics in the localized plasmon — molecular exciton hybrids . . .	206
K.V. Shulga, M.V. Fistul, I. Besedin, A.V. Ustinov	
Microwave transparency of a superconducting quantum metamaterial	206
Gennady Shvets	
Active nanophotonics: from graphene-integrated plasmonic metasurfaces and metagates to photon-accelerating semiconductor nanostructures	207
Simovski C.R., Voroshilov P.M., Papadimitratos A., Zakhidov A.A.	
Light-trapping in organic solar cells by silver nanoantennas	208
A.D. Sinelnik, M.V. Rybin, S.Y. Lukashenko, K.B. Samusev, M.F. Limonov	
Glassy metasurfaces: structural and optical studies	209
Slunyaev A.V., Pelinovsky E.N., Shurgalina E.G.	
Extreme states and statistics in the gas of solitons	210
Solomakha G.A., Glybovski S.B.	
Metamaterial inspired structures for enhancement performance of RF-coils for MRI	211
Stepanenko A.A., Gorlach M.A.	
Interaction-induced two-photon topological states	212
Sukhorukov A.A.	
Quantum photonics with dielectric metasurfaces	213

Tiguntseva E.Y., Pushkarev A.P., Makarov S.V., Zakhidov A.A., Kivshar Yu.S. Tunable resonant coupling of excitonic states with Mie modes in halide perovskite nanoparticles	214
Tiguntseva E.Y., Zakhidov A.A., Kivshar Yu.S., Makarov S.V. Halide perovskite nanoparticles with enhanced photoluminescence	214
Tikhodeev S.G. Chiral photonic crystal slabs and metasurfaces for emitters of circularly polarized light	215
Timofeev I.V., Pankin P.S., Vetrov S.Ya., Arkhipkin V.G., Lee W., Zyryanov V.Ya. Chiral optical Tamm states: method of images	216
Tsvetkov D.M., Bushuev V.A., Mantsyzov B.I., Konotop V.V. Short pulse propagation in PT-symmetric photonic crystals with material dispersion	217
R.M. Turtos, S. Gundacker, E. Auffray, P. Lecoq, B. Mahler, C. Dujardin CdSe nanoplatelets as a new generation of ultrafast ionizing radiation detectors	218
P. Velez, J. Mata-Contreras, F. Martin, K. Grenier, D. Dubuc Sensing strategies for dielectric characterization and solute concentration measurement in liquids based on metamaterials-inspired resonators in microstrip technology	219
Alexandre Vignaud, Zo Raolison, Marc Dubois, Lisa Leroi, Ana L. Neves, Franck Mauconduit, Stefan Enoch, Nicolas Malléjac, Pierre Sabouroux, Anne-Lise Adenot-Engelvin, Redha Abdeddaim Ultra-high field MRI radiofrequency excitation inhomogeneities mitigation in the head: optimization of dielectric pad mixture and locations	220
Vladimirov A.G., Pimenov A. Time-delay modeling of short pulse generation in lasers	221
Volkovskaya I.I., Smirnova D.A. Second-harmonic generation in Mie-resonant dielectric nanoparticles made of noncentrosymmetric materials	222
Voroshilov P.M., Saranin D.S., Simovski C.R., Zakhidov A.A. Multi-walled carbon nanotube sheet transparent electrode mediated ionic doping in organic photovoltaics	223
Ming Wang, Junbao Chen, Hui Hao, Dongmei Guo, Wei Xia A synthetic dual-frequency self-mixing interferometer	224
Xu-Chen Wang, Ana Díaz-Rubio, Viktor S. Asadchy, Sergei A. Tretyakov Flat asymmetric absorbers	224
Yermakov O., Hurshkainen A., Dobrykh D., Kapitanova P., Iorsh I., Glybovski S., Bogdanov A. Surface waves of mixed TE-TM polarization at Jerusalem-cross-based anisotropic metasurface in microwaves	225
Yulin A.V., Iorsh. I., Shelykh, I. Dynamics of solitons and slow light in optical systems with strong light-matter interactions	226
Yves S., Lemoult F., Fink M., Lerosey G., Fleury R., Berthelot T. Crystalline metamaterials for topological properties at the subwavelength scale	227
Zalogina A.S., Zuev D.A. Metal-dielectric nanoantenna for NV-center emission control	227
Li Zhang Manipulation of robust valley edge transport in ultrathin substrate-integrated photonic crystals	228

Alexander A. Zharov, Nina A. Zharova, Alexander A. Zharov, Jr. Light-assisted spontaneous birefringence and magnetic domains formation in suspension of gyrotropic nanoparticles	229
Alexander A. Zharov, Jr., Nina A. Zharova, Alexander A. Zharov Self-focusing of electromagnetic surface waves in gyrotropic liquid metacrystals	230
Zhirihin D.V., Gorlach M.A., Slobozhanyuk A.P., Belov P.A., Ni X., Smirnova D.A., Korobkin D., Alù A., Khanikaev A.B. Leaky topological states: from near- to far-field investigation	230
A.A. Zyablovsky, E.S. Andrianov, N.E. Nefedkin, I.A. Nechepurenko, A.V. Dorofeenko, A.A. Pukhov, A.P. Vinogradov Multimode theory of plasmonic distributed feedback laser	231

Propagation of acoustic waves during the control of hydrogen-induced destruction of metals by the acoustoelastic effect

Alekseeva E.L., Alkhimenko A.A., Grishchenko A.I., Semenov A.S., Tretyakov D.A.

Peter the Great Saint-Petersburg Polytechnic University, 29, Polytechnicheskaya, St. Petersburg, 195251, Russia

e-mail: dmitry.tretyakov93@yandex.ru

Belyaev A.K., Polyanskiy V.A., Yakovlev Yu.A.

Institute for Problems in Mechanical Engineering RAS, 61, Bolshoj pr. V.O., St. Petersburg, 199178, Russia

e-mail: vice.ipme@gmail.com, vapol@mail.ru, yura.yakovlev@gmail.com

The propagation of acoustic waves in metals with an inhomogeneous microstructure does not lead to an additional reflection of the sound wave. As a rule, its length exceeds the dimensions of individual microstructural elements by orders of magnitude. The additional absorption of the acoustic wave, associated with the excitation of additional degrees of freedom, is possible. The change in the velocity of wave propagation also occurs [1].

The implementation of advanced high-strength materials in the nuclear power industry, oil and gas industry, aviation and construction is accompanied by an increase in accidents. The development of main cracks occurs in high-strength materials very quickly. They are well detected by the acoustic method.

The prehistory of destruction accompanied by the formation of microdefects and a network of microcracks does not subject to non-destructive testing. Such an important phenomenon as hydrogen induced degradation of the mechanical properties of metals, developed as a result of corrosion and stress-corrosion processes, is also does not diagnosed. The velocity of propagation of sound wave depends on many factors besides microdefects, for example, on the temperature of the metal. The absence of reflections of sound wave from defects does not allow to detect them during the ultrasonic inspection. The methods of acoustic non-destructive testing, based on measuring the relative difference between the velocities of transverse waves with mutually perpendicular polarization [2], differ from other methods of non-destructive testing by the possibility of investigating of the small relative changes in the velocities propagation of ultrasonic waves comparable in magnitude with the influence of the degraded internal structure .

The investigation of the changes in the field of this relative difference during the development of hydrogen embrittlement was carried out. The results of theoretical estimates and experimental investigation of the influence of hydrogen embrittlement on the relative difference between the velocities of the corrosion-resistant steels during standard tests on hydrogen-induced cracking (HIC) are given. The relationship between the standard cracking parameters and the principal values of the damage tensor using the model of the material with anisotropic continuum damage [3] was obtained. This result allows us to expand the field of application of the model [3] to non-destructive acoustic control of the state of technical structures.

The support by the Russian Foundation for Basic Research, projects 17-08-00783 and 18-08-00201, is acknowledged.

References

- [1] L. B. Zuev, B. S. Semukhin, K. I. Bushmeleva, Variation of the ultrasonic velocity in Al under plastic deformation, *Technical Physics*, **45**, 50–54 (2000).
- [2] D. S. Hughes, J. L. Kelly, Second-order elastic deformation of solids, *Phys. Review*, **92**, 1145 (1953).
- [3] A. S. Semenov, Symmetrization of the effective stress tensor for anisotropic damaged continua, *St. Petersburg Polytechnical University Journal: Physics and Mathematics*, **3**, 271–283 (2017).

Simulation of 3 quantum dot network dynamics

Altaisky M.V.¹, Kaputkina N.E.², Krylov V.A.³

¹Space Research Institute RAS, Profsoyuznaya 84/32, Moscow 117997, Russia

²National University of Science and Technology “MISIS”, Leninsky prospect 4, Moscow 119049, Russia

³Joint Institute for Nuclear Research, Joliot Curie 6, Dubna 141980, Russia

e-mail: altaisky@mx.iki.rssi.ru, nataly@misis.ru, kryman@jinr.ru

We present results of numerical simulation of the dynamics of 3 quantum dot array with dipole-dipole interaction between quantum dots, which are linearly coupled to a common phonon bath. The simulation is performed by solving the von Neumann equation $i\dot{\rho} = [H, \rho]$ using the adiabatic path integral method by Makarov and Makri. Based on the symmetry properties of three quantum dot array, an attempt was made to implement NOT XOR operation using 3 QD array network with common heat bath.

Approximate solution of MHD boundary layer flow of a non-Newtonian power-law fluids over a continuous moving surface using B-spline collocation

Khimya Amlani

Applied Science and Humanities Department, Sardar Vallabhbhai Patel Institute of Technology, Vasad, Gujarat, India

e-mail: khimya_amlani@rediffmail.com

The problem of laminar boundary layer flow for non-Newtonian power-law fluid over a continuous moving surface in the presence of transverse magnetic field is studied. The governing partial differential equation is transformed into a non-linear ordinary differential equation using appropriate transformation. This non-linear ordinary differential equation is solved numerically by using B-spline collocation technique. It is found that solution depends on various parameters including magnetic field, power law index and velocity ratio parameter. It has been proved that B-spline is powerful tool to solve these types of problem due to ease of use and quality of results.

References

- [1] B. S. Reddy, N. Kishan, M. N. Rajasekhar, MHD boundary layer flow of a non-Newtonian power-law fluid on a moving flat plate, *Advances in Applied Science Research*, **3**, 1472–1481 (2012).
- [2] Govind R. Rajput, J.S.V.R. Krishna Prasad, M.G. Timol, Similarity flow solution of MHD boundary layer model for non-Newtonian power-law fluids over a continuous moving surface, *Gen. Math. Notes*, **24**, 97–102 (2014).
- [3] M. Kumari, G. Nath, MHD boundary layer flow of a non-Newtonian fluid over a continuously moving surface with a parallel free stream, *Acta Mechanica*, **146**, 139–150 (2001).
- [4] M. Guedda, Z. Hammouch, Similarity flow solutions of a non-Newtonian power-law fluid, *Int. J. Nonlinear Science*, **6**, 255–264 (2008).

Seiches and harbour oscillation in a semi-closed basin of various geometric shape with porous media

R. Anastasia, I. Magdalena, H.Q. Rif'atin

Industrial & Financial Mathematics Research Group, Faculty of Mathematics and Natural Sciences, Institut Teknologi Bandung, Indonesia, Jalan Ganesha 10, Bandung, West Java, Indonesia

e-mail: ikha.magdalena@gmail.com, hany.qoshirotur@gmail.com

Seiches are the long-period standing oscillation in an enclosed basin or in a locally isolated part of a basin. Harbour oscillations are a specific type of seiche motion that occur in partially enclosed

basins that are connected through one or more openings to the sea. When the period of these motions coincides with the natural period of sway, further resonance occurs, which can result in possible damage of a moored ship or port facilities. Porous wave absorber offers an excellent solution for protecting harbours against the action of resonance phenomenon. In this research, we propose a modification of shallow water equation involving the existence of porous media to investigate the effect of it for resonance phenomenon.

In this paper, we will observe wave profile that comes to a harbour of various geometric shape, which are rectangular, triangular, and semi-parabolic, with porous media at the edge of it. The governing equation is shallow water equation with friction term defined in the linearized Dupuit-Forcheimer's formula. The analytical solution is calculated to get the value of a natural resonant period of the basin, which causes resonance phenomenon. The equation will be solved numerically using finite volume method on a staggered grid to confirm the analytical solution. Effect of the porous media for wave's amplitude will be analyzed numerically.

References

- [1] A. Rabinovich, *Seiches and Harbor Oscillations*, World Scientific, 193–236, 2009.
- [2] I. Magdalena, Analytical and numerical solution for wave reflection from a porous wave absorber, (submitted).

Efficient asymptotic formulas for waves generated by a localized source with finite duration

Anikin A. Yu., Dobrokhotov S. Yu., Nazaikinskii V. E.

Ishlinsky Institute for Problems in Mechanics of the Russian Academy of Sciences, 101 Prospekt Vernadskogo, bld. 1, 119526, Moscow, Russia

e-mail: anikin83@inbox.ru, dobr@ipmnet.ru, nazaikinskii@yandex.ru

We consider the Cauchy problem for the two-dimensional non-homogeneous wave equation with variable coefficients

$$\frac{\partial^2 \eta}{\partial t^2} - \nabla c^2(x) \nabla \eta = \frac{\partial g(t)}{\partial t} V \left(\frac{x}{\mu} \right), \quad \eta|_{t=0} = 0, \quad \eta_t|_{t=0} = 0, \quad t \geq 0, \quad x \in \mathbf{R}_x^2, \quad (1)$$

where the function $g(t)$ is some smooth 'delta-like' function. Here $V(y)$ is smooth in \mathbf{R}_y^2 , decaying faster than $1/|y|_1^{\kappa_1}$ (where $\kappa_1 > 2$) as $|y| \rightarrow \infty$. Function $g(t)$ in case (b) is smooth on $[0, \infty)$, decaying faster than $1/t^{\kappa_2}$ (where $\kappa_2 > 1$) as $t \rightarrow \infty$, moreover, $g(t) = 0$ for $t \leq 0$.

This problem describes, in the linear approximation, tsunami waves appearing due to local bottom displacements (see e.g. [1, 2]). Usually, the size of the source, i.e. the domain, where these local displacements take place is much less than the size of the ocean. Their ratio μ , may be considered as a small parameter and used in the asymptotic analysis of the solution.

This model describes a time-spread source, i.e. its action has small but finite duration. In [3] the asymptotics for the solution was given in a form of Maslov's canonical operator. In [4], an approximation for the asymptotic solution was presented. More precisely, the approximation to this solution can be obtained by applying some differential operator to the solution of the Cauchy problem for the homogeneous equation. This formula is quite efficient from the point of view of practical calculations. It can be easily implemented using software like Wolfram Mathematica, Maple, etc.

We will recall the mentioned results and also discuss their application in a run-up problem.

References

- [1] C. C. Mei, *Applied Dynamics of Ocean Surface Waves*, World Sci., Singapore, 1989.
- [2] E. N. Pelinovskii, *Hydrodynamics of Tsunami Waves*, IPF RAN, Nizhnii Novgorod, 1996.

- [3] S. Dobrokhotov, D. Minenkov, V. Nazaikinskii, B. Tirozzi, Functions of noncommuting operators in an asymptotic problem for a 2D wave equation with variable velocity and localized right-hand side, *Operator Theory, Pseudo-Differential Equations, and Mathematical Physics*, 95–125, Oper. Theory Adv. Appl., 228, Birkhäuser/Springer Basel AG, Basel, 2013.
- [4] S. Yu. Dobrokhotov, A. Yu. Anikin, Approximation of solutions of the two-dimensional wave equation with variable velocity and localized right-hand side using some “simple” solutions, *Math. Notes*, **100**(5), 796–806 (2016).

Simple asymptotics for a generalized wave equation with degenerating velocity and their applications to the linearized long wave run-up problem

A.Yu. Anikin, S.Yu. Dobrokhotov, V.E. Nazaikinskii

Ishlinsky Institute for Problems in Mechanics of the Russian Academy of Sciences; Moscow Institute of Physics and Technology

e-mail: nazaikinskii@googlemail.com, nazaikinskii@yandex.ru

Asymptotic solutions of a wave equation degenerating on the boundary of the domain (where the wave propagation velocity vanishes on the boundary as the square root of the distance from the boundary) can be represented with the use of a modified canonical operator on an invariant Lagrangian submanifold of the nonstandard phase space constructed by the authors earlier. In the talk, we present simple expressions in a neighborhood of the boundary for the functions represented by the modified canonical operator and in particular for the solution of the Cauchy problem for the degenerating wave equation with initial data localized near an interior point of the domain.

The research described in the talk was supported by the Russian Science Foundation within the framework of project no. 16-11-10282.

Semi-classical Green functions

Anatoly Anikin, Sergey Dobrokhotov, Vladimir Nazaikinskii

Ishlinsky Institute for Problems in Mechanics and Moscow Institute of Physics and Technology, Moscow, Russia

email: anikin83@inbox.ru, dobr@ipmnet.ru, nazay@ipmnet.ru

Michel Rouleux

Aix Marseille Univ, Univ Toulon, CNRS, CPT, Marseille, France

e-mail: rouleux@univ-tln.fr

Let $H(x, p) \sim H_0(x, p) + hH_1(x, p) + \dots$ be a semi-classical Hamiltonian on $T^*\mathbf{R}^n$, and let f be a semi-classical distribution (the “source”) microlocalized on a Lagrangian manifold Λ which intersects transversally along L the flow-out Λ_+ of the Hamilton vector field X_{H_0} in a non critical energy surface Σ . The paradigm of this situation is when Λ is the conormal bundle to $x = 0$, and $H_0(x, p) = p_n$. This was considered in [1] from the point of view of asymptotics with respect to smoothness.

As in [2] we are interested in integral representations for the solution u , modulo $\mathcal{O}(h^N)$, verifying Sommerfeld radiation condition at infinity, of the inhomogeneous PDE $H^w(x, hD_x; h)u = f$.

Using Maslov canonical operator, we present u as the sum of terms microlocalized respectively on: (i) $\Lambda \setminus L$; (ii) the flow out of L by X_{H_0} in Σ for short times (near-field); (iii) the flow out of L through X_{H_0} in Σ for large times (far-field).

We give various applications: (i) $H^w(x, hD_x; h)$ is a geodesic flow and Λ a cylinder, as in the case for Bessel beams [3]; (ii) $H^w(x, hD_x; h)$ is Laplace operator and Λ is the conormal to an hypersurface, as for the diffusion by an antenna; (iii) H is the Dirichlet-to-Neumann operator for the linear waves equations in a domain with a non-uniform bottom, where Λ is the conormal bundle to a point [4].

We shall also discuss non-transverse (glancing) intersection, extending to the semi-classical case some results of [5].

References

- [1] R. B. Melrose, G. A. Uhlmann, Lagrangian intersection and the Cauchy problem, *Comm. Pure Appl. Math.*, **32**(4), 483–519 (1979).
- [2] A. Anikin, S. Dobrokhotov, V. Nazaikinski, M. Rouleux, The Maslov canonical operator on a pair of Lagrangian manifolds and asymptotic solutions of stationary equations with localized right-hand sides, *Doklady Math.*, **96**(1), 406–410 (2017).
- [3] S. Dobrokhotov, V. Nazaikinskii, A. Shafarevich, New integral representations of Maslov canonical operator in singular charts, *Izv. Math.*, **81**(2), 286–328 (2017).
- [4] A. Anikin, S. Dobrokhotov, V. Nazaikinski, M. Rouleux, Asymptotics of Green function for the linear waves equations in a domain with a non-uniform bottom, *Proceedings of “Days of Diffraction 2017”*, Saint-Petersburg, 18–23.
- [5] P. Laubin, B. Willems, Distributions associated to a 2-microlocal pair of Lagrangian manifolds, *Comm. Part. Diff. Eq.*, **19**(9, 10), 1581–1610 (1994).

Fluorescence analysis of X-ray whispering gallery waves propagating along liquid meniscuses

Asadchikov, V.E.¹, **Goray, L.I.**^{2,3}, Rosshin, B.S.¹, Tikhonov, A.M.⁴, Volkov, Yu.O.¹

¹A. V. Shubnikov Institute of Crystallography, Leninskii Pr. 59, Moscow, 119333, Russia

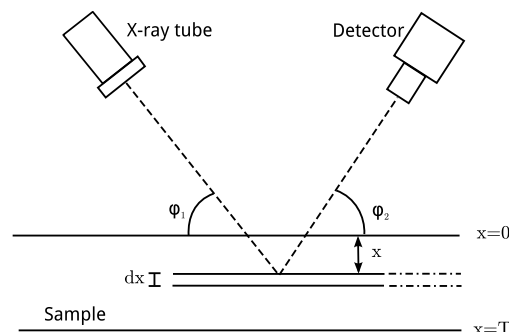
²Saint Petersburg Academic University, Khlopin 8/3, Let. A, St. Petersburg, 194021, Russia

³ITMO University, Kronverkskiy pr. 49, St. Petersburg, 197101, Russia

⁴P. L. Kapitza Institute for Physical Problems RAS, Kosygina Str. 2, Moscow, 119334, Russia

e-mail: lig@pcgrate.com

The extreme sensitivity of whispering gallery (WG) sensors not only lead to a breakthrough in biodetection, but also enables sensitive probing of physical and micromechanical oscillators via optomechanical coupling and laser resonators. In X-rays, WGs can be attractive for applications as beam splitters and beam rotators. We analyze X-ray WG waves, which propagate along the large-radius meniscus of silica hydrosols stabilized by CsOH. For analysis of intensities of the X-ray fluorescence, we have used a two-layer model of the liquid with the upper non-uniform corrugated layer in which the concentration of levitating Cs⁺ ions near the surface has a maximum derived from the experiment [1]. A quasi-grating model was chosen due to the presence of surface thermal capillary waves and near-zone clusters.



To determine the fluorescence intensity, we have used the numerical approach on the basis of the reciprocity theorem for gratings [2]. A similar theoretical approach was first applied in [3] to analyze the intensity of X-ray fluorescence on a multilayer stack with perfect plane boundaries. The intensity of the incident radiation at some boundary of the multilayer sample can be accurately determined by solving Maxwell's equations. For a conventional multilayer with perfect flat interfaces, this solution is Parratt's recurrence formulae. However, for structured interfaces the task is much more complicated and can be solved exactly, in general, only by using time-consuming numerical calculations ([2], Ch. 12). The intensity of the exciting electromagnetic field equal to $|E_{ex}(\phi_1, x)|^2$ is calculated for a given incidence angle ϕ_1 and the penetration depth into sample x (see Figure). Then

the fluorescence intensity obtained at the depth x is proportional to the intensity of the exciting field and the concentration of the unknown element $c(x)$:

$$|E_{fl}(\phi_1, x)|^2 = ac(x)|E_{ex}(\phi_1, x)|^2, \quad (1)$$

where a is a coefficient. The reciprocity theorem states that the electromagnetic field produced by the dipole source on a detector is identical to the field created at the source site by an analogous dipole located at the site of the detector. Taking into account that the distance from the source to the detector is much larger than the thickness of the layer, the quantity $|E_{fl}(\phi_2, x)|^2$ can be calculated using the same formalism as for $|E_{ex}(\phi_1, x)|^2$ under the assumption that the fictitious source is at infinity in the direction of detection:

$$|E_{fl}(\phi_1, \phi_2, x)|^2 = bc(x)|E_{ex}(\phi_1, x)|^2|E_{fl}(\phi_2, x)|^2, \quad (2)$$

where b is some coefficient. Thus, the concentration of an unknown element or substance (its mass volume) can be found using (2) when solving the inverse problem of X-ray fluorescence.

This work was partially supported by the Russian Foundation for Basic Research (17-02-00362).

References

- [1] V. E. Asadchikov, V. V. Volkov, Yu. O. Volkov, *et al.*, Condensation of silica nanoparticles on a phospholipid membrane, *JETP Letters* **94**(7), 585–587 (2011).
- [2] E. Popov (ed.), *Gratings: Theory and Numeric Applications*, 2nd rev. ed., Presses Universitaires de Provence, Marseille, 2014.
- [3] J.-P. Chauvineau, F. Bridou, Analyse angulaire de la fluorescence du fer dans une multicouche périodique Fe/C, *J. Physique IV*, **06**(C7), 53–64 (1996).

Fuchsian Heun equation, equivalent Fuchsian linear systems and Painlevé P^{VI} equation

Mikhail Babich^{1,2}, Sergey Slavyanov¹

¹Saint-Petersburg State University, St. Petersburg, Russia

²Petersburg Branch of Mathematical Institute RAS, St. Petersburg, Russia

e-mail: mbabich@pdmi.ras.ru, slav@ss2034.spb.edu

Famous Painlevé P^{VI} equation is connected with the linear Heun equation of Fuchsian type by different links. In these links there is a common point. It is the Hamiltonian nature of the Painlevé equation. We demonstrate these links introducing a proper first-order linear system which is also Fuchsian and obeys isomonodromic property. Two such systems are examined: one is with zero determinants of residues at singularities and the other is with zero traces at singularities. In both cases the accessory parameter of the Heun equation is obtained in terms of matrix elements of the system. Clearly, any chosen approach leads to the Painlevé P^{VI} either with technique of antquantization [1, 2] or as the isomonodromy condition [3, 4].

References

- [1] S. Slavyanov, Antiquantization and the corresponding symmetries, *Theoret. and Math. Phys.*, **185**, 1522–1526 (2015).
- [2] S. Slavyanov, Symmetries and apparent singularities for simplest fuchsian equations, *Theoret. and Math. Phys.*, **193**, 1754–1760 (2017).
- [3] A. Bolibruch, *Inverse Problems of Monodromie in Analytical Theory of Differential Equations*, Moscow – MNCMO, 2009 (in Russian).
- [4] A. Its, V. Novokshenov, *The Isomonodromic Deformation Method in the Theory of Painlevé Equations*, Lecture Notes in Math., **1191**, Springer, Berlin, New York, 1986.

Third order operator for the good Boussinesq equation on the circle

Andrey Badanin

Saint-Petersburg State University, Universitetskaya nab. 7/9, St. Petersburg, 199034, Russia
e-mail: a.badanin@spbu.ru

We consider the good Boussinesq equation on the circle. It is well known that this equation has a Lax pair, where the L-operator is a third order differential operator. In contrast with the KdV case, this operator is non-self-adjoint. The multipliers for this third order operator constitute a 3-sheeted Riemann surface with real and non-real ramifications. The ramifications are invariant with respect to the Boussinesq flow.

Moreover, we consider the auxiliary three-point Dirichlet problem for the third order operator. The spectrum of this problem consists of real and non-real eigenvalues. We determine asymptotics of the ramifications and of the auxiliary spectrum. We prove trace formulas in terms of the ramifications and of the auxiliary spectrum.

This is a joint work with E. L. Korotyaev.

The asymptotics of the solution of three one-dimensional quantum particles scattering problem. The case of finite repulsive pair potentials

I.V. Baibulov, A.M. Budylin, S.B. Levin

Saint Petersburg State University, 7/9 Universitetskaya Emb., St. Petersburg 199034, Russia
e-mail: molezz@bk.ru a.budylin@spbu.ru s.levin@spbu.ru

Basing on the results of the work [1] we derived the resolvent kernel asymptotics of the correspondent scattering problem with consequent separation of the absolutely continuous spectrum eigenfunction asymptotics. The obtained results were compared with the earlier results derived by the diffraction methods.

References

- [1] I. V. Baibulov, A. M. Budylin, S. B. Levin, The scattering problem of several one-dimensional quantum particles. Structure and asymptotics of the resolvent kernel limit values, *Zapiski Nauchnykh Seminarov POMI*, **461**, 52–64 (2017).

Localization effect for eigenfunctions in narrow Kirchhoff plates with clamped edges

Bakharev F.L.¹, Matveenko S.G.²

¹St. Petersburg State University, Universitetsky pr., 28, Peterhof, St. Petersburg, 198504, Russia

²Chebyshev Laboratory, St. Petersburg State University, 14th Line, 29b, St. Petersburg, 199178, Russia

e-mail: fbakharev@yandex.ru, matveiS239@gmail.com

It is well-known (see, for instance, [1–3]) that the eigenfunctions of the Laplacian in a thin domain with Dirichlet boundary conditions are localized near the thickest region. It appears that the same effect holds true for the bilaplace operator with Dirichlet boundary conditions. It should be mentioned that the problem for the bilaplace operator is much more complicated. In the report we discuss the asymptotics of the eigenvalues both of the Laplacian and the bilaplace operator with Dirichlet boundary conditions in a 2D narrow domain (a narrow Kirchhoff plate with clamped edges) as its width tends to zero. We explain that in both cases the main correction terms of the asymptotics can be derived from the ordinary differential equation of the harmonic oscillator, despite the different orders of the operators.

Acknowledgments. The authors were inspired by Sergei Nazarov from Institute for Problems in Mechanical Engineering (Saint Petersburg). This work is supported by the Russian Science Foundation grant № 17-11-01003.

References

- [1] D. Borisov, P. Freitas, Singular asymptotic expansions for Dirichlet eigenvalues and eigenfunctions of the Laplacian on thin planar domains, *Annales de l'Institut Henri Poincaré. Analyse Non Linéaire*, **26**(2), 547–560 (2009).
- [2] S. A. Nazarov, Localization effects for eigenfunctions near to the edge of a thin domain, *Mathematica Bohemica*, **127**(2), 283–292 (2002).
- [3] S. A. Nazarov, E. Perez, J. Taskinen, Localization effect for Dirichlet eigenfunctions in thin non-smooth domains, *Transactions of the American Mathematical Society*, **368**(7), 4787–4829 (2016).

Some spectral problems for thin Kirchhoff plates

Bakharev F.L., Nazarov S.A.

St. Petersburg State University, 198504, Universitetsky pr., 28, Peterhof, St. Petersburg, Russia
e-mail: fbakharev@yandex.ru

We are going to discuss several spectral problems for biharmonic operator in thin domains focusing on their difference from the same ones for Laplace operator. Starting with the simple model problem in thin rectangular domain where the main asymptotic terms are defined from the Dirichlet problem for ordinary differential equation of the second order, we follow with a discussion of T-shaped Kirchhoff plates. The asymptotic behavior of the eigenvalues now can be defined in terms of another limit problem in infinite semi-cross which describes the boundary layer phenomenon. We also going to discuss several other problems, solved and unsolved.

Research is financially supported by grant 17-11-01003 of the Russian Science Foundation.

Isometric model of metric spaces and the wave model of symmetric operators

M.I. Belishev^{1,2}, **S.A. Simonov**^{1,2,3}

¹St. Petersburg Department of V. A. Steklov Institute of Mathematics of the Russian Academy of Sciences, 27 Fontanka, St. Petersburg, 191023 Russia

²St. Petersburg State University, 7–9 Universitetskaya nab., St. Petersburg, 199034 Russia

³St. Petersburg State Technological Institute (Technical University), 26 Moskovsky pr., St. Petersburg, 190013 Russia

e-mail: belishev@pdmi.ras.ru, sergey.a.simonov@gmail.com

Let a metric space Ω be given. Consider the lattice of open sets \mathfrak{D} in it and the lattice \mathfrak{F} of functions from \mathbb{R}_+ to \mathfrak{D} . For every open set the family of metric neighborhoods defines a function from \mathfrak{F} , and such functions form a subset of \mathfrak{F} which we denote by $I\mathfrak{D}$. Consider its closure in a relevant topology of \mathfrak{F} . We show that under certain assumptions the atoms of this closure form a metric space $\tilde{\Omega}$ which is isometric to the original metric space Ω . This construction is related to solving inverse problems with the boundary control method and is used in developing the wave functional model of symmetric operators.

References

- [1] M. I. Belishev, A unitary invariant of a semi-bounded operator, *J. Operator Theory*, **69**(2), 299–326 (2013), *arXiv*: 1208.3084.

On the spectrum discreteness for quantum graph in a magnetic field

Belolipetskaia A.G., Popov I.Y.

ITMO University, Kronverkskiy, 49, St. Petersburg, 197101, Russia

e-mail: annabel11502@mail.ru, popov1955@gmail.com

The spectrum discreteness for the operators of various physical systems is an actual topic of research. There is well-known Molchanov's condition for the spectrum discreteness of the Sturm–Liouville operator on a half-line [1]. A version of the condition for the spectrum of the Schrödinger operator on quantum graph of some type was suggested in [2]. In the present paper we consider the analogous problem for quantum graph in a magnetic field. Namely, we deal with the graph embedded in \mathbb{R}^3 with the following operator acting on the edges:

$$Hf(t) = -\left(\frac{\partial}{\partial t} - ia\right)^2 f(t) + V(r(t))f(t),$$

where $r(t) = (r_1(t), r_2(t), r_3(t))$ is a separate edge given in the natural parametrization; $\vec{A} : \mathbb{R}^3 \rightarrow \mathbb{R}^3$ is a vector potential of the electromagnetic field; $V : \mathbb{R}^3 \rightarrow \mathbb{R}$ is the scalar potential of an electromagnetic field; $a(t) = \frac{dr}{dt}(t) \cdot \vec{A}(r(t))$.

For this problem, investigation of the spectrum discreteness problem for the Schrödinger operator with a magnetic field on quantum graph is carried out.

References

- [1] B. M. Levitan, I. S. Sargsyan, *Sturm–Liouville and Dirac Operators*, Nauka, Moscow, 1988.
- [2] M. O. Kovaleva, I. Y. Popov, On Molchanov's condition for the spectrum discreteness of a quantum graph Hamiltonian with δ -coupling, *Reports on Mathematical Physics*, **76**, 171–178 (2015).

Solitary strain waves in two-layered nanocomposites

Beltukov Y.M., Belashov A.V., Garbuzov F.E., Semenov A.A., Semenova I.V.

Ioffe Institute, St. Petersburg, 26 Polytekhnicheskaya st., 194021 Russia

e-mail: ybeltukov@gmail.com

Composite materials (composites) are of a great interest nowadays due to their advantageous mechanical properties, which differ from those of homogeneous materials. As was experimentally found a small concentration of nano-inclusions (3–5%) quite strongly affects (up to 30%) the 2nd order elastic moduli (Young's modulus, Poisson's ratio) [1]. However, their effect on the third-order moduli (Murnaghan moduli or Landau moduli) is much stronger and can lead to variations by several times, see, for example, [2].

A comprehensive study of dynamical behavior of composites is the challenging problem and can be performed through the non-destructive testing (NDT), based on evolution of a strain wave [3] propagating in the bulk of a nanostructured waveguide. The applied holographic technique in transmission configuration strictly limits the class of suitable materials by optically transparent ones and does not allow investigation of wave processes in opaque materials that are of interest for a variety of applications.

Although the nanoparticle inclusions even in small concentration often lead to a substantial decrease of transparency of material, the optical methods still can be used for investigation of strain waves. In order to investigate properties of opaque solids, we propose to use two-layered waveguides with one transparent layer [4]. We demonstrate that monitoring of soliton evolution in a two-layered waveguide made of adhesively bonded layers of a transparent material with known elastic parameters and an opaque material with unknown ones, can provide data on soliton velocity in the opaque material.

For mathematical description of the wave processes under study, an initial-boundary value problem was considered. We have shown that the propagation of long longitudinal strain solitary waves in such composite waveguides still can be described by doubly dispersive equation (DDE). For the complete description of the wave propagation, we used a multidomain pseudospectral numerical method to solve three-dimensional nonlinear elasticity equations. We have shown that for a high elastic contrast between layers (e.g. PMMA and brass), there is a strong mixing between longitudinal and flexural waves which leads to disintegration of the incoming soliton and formation of the oscillating wave in this case.

References

- [1] O. A. Moskalyuk, A. M. Samsonov, I. V. Semenova, V. E. Smirnova, Y. E. Yudin, Mechanical properties of polymeric composites with carbon dioxide particles, *Technical Physics*, **62**, 294–298 (2017).
- [2] A. I. Korobov, V. M. Prokhorov, D. M. Mekhedov, Second-order and third-order elastic constants of B95 aluminum alloy and B95/nanodiamond composite, *Physics of the Solid State*, **55**, 8–11 (2013).
- [3] A. M. Samsonov, I. V. Semenova, A. V. Belashov, Direct determination of bulk strain soliton parameters in solid polymeric waveguides, *Wave Motion*, **71**, 120–126 (2017).
- [4] A. V. Belashov, Y. M. Beltukov, N. V. Petrov, A. M. Samsonov, I. V. Semenova, Indirect assessment of bulk strain soliton velocity in opaque solids, *Appl. Phys. Lett.*, **112**, 121903 (2018).

Some approaches to harmonic wave propagation in elastic solids with random microstructure

Alexander K. Belyaev

Institute for Problems in Mechanical Engineering, Russian Academy of Sciences, St. Petersburg, Russia

e-mail: vice.ipme@gmail.com

From a perspective of propagating wave any structural material (cast iron, steel, concrete, composites etc.) seems to be an inhomogeneous elastic media because its microstructure is nothing else than a randomly heterogeneous field. This is an argument for applying the mathematical apparatus of the stochastic wave propagation to handle the problem. Three approaches to the problem of one-dimensional wave propagation in media with random elastic and mass properties are addressed, namely (i) the method of integral spectral decomposition, (ii) the Fokker–Planck–Kolmogorov equation and (iii) the Dyson integral equation. A lot of methods have been developed for studying the stochastic wave propagation however these approaches deal with the wave propagation in medium with a single random function. In the problem of wave propagation in random elastic media two random fields, namely random elastic modulus and random mass density should be taken into account.

As a stationary harmonic wave is considered, the wave equation in frequency domain is transformed into the ordinary differential equation. Two boundary conditions will be discussed: (i) the Dirichlet boundary condition which implies a prescribed displacement at $x = 0$ and (ii) the Neumann boundary condition with a prescribed axial stress at $x = 0$. It is necessary to mention that each of these boundary conditions is deterministic in contrast to the propagating random wave.

The method of integral spectral decomposition implies the medium parameters to be represented in the form of the Fourier–Stieltjes integrals in terms of the random Fourier spectra. The particular case under consideration is that in which the Young modulus and the mass density to be statistically independent random functions of diffuse type. It results in the characteristic equation which is a polynomial of sixth order. Since its analysis is rather laborious an asymptotic analysis is carried out for weakly heterogeneous media. A complete analysis is performed for the case in which the randomness in the Young modulus and mass density is fully correlated.

The second approach to the stochastic wave propagation in a 1-D solid with random parameters is based on the theory of continuous Markov processes. The analysis will be reduced to derivation of equations for the first and second moments.

The third approach operates with the velocity of sound and the acoustic impedance rather than with random elastic modulus and random mass density. These new independent variables allow one to reduce the problem to the Dyson integral equation which is solved for some asymptotic cases. It is shown that the approach is applicable even for the general case of random medium with an arbitrary short-range heterogeneity.

Merits and shortcomings of each approach are discussed. It is demonstrated that these three approaches cover actually all possible problems of the harmonic wave propagation in heterogeneous or stochastic media, hence, by means of the preliminary analysis of a particular problem and considering the strong and weak sides of each approach, one can choose an appropriate solution strategy.

The support by the Russian Foundation for Basic Research, projects 17-08-00783 and 18-08-00201, is acknowledged.

Two classes of localized solutions of the wave equation

Alexander S. Blagoveshchensky¹, Azat M. Tagirdzhanov^{1,2}, Aleksei P. Kiselev^{1,3,4}

¹St. Petersburg State University, St. Petersburg, Russia

²St. Petersburg Electrotechnical University, St. Petersburg, Russia

³Steklov Mathematical Institute, St. Petersburg Branch, St. Petersburg, Russia

⁴Institute for Problems in Mechanical Engineering RAS, St. Petersburg, Russia

e-mail: a.blagoveshchensky@spbu.ru, aztagr@gmail.com, kiselev@pdmi.ras.ru

We present a short review of two classes of simple exact solutions of the wave equation $u_{xx} + u_{yy} + u_{zz} = c^{-2}u_{tt}$, $c = \text{const} > 0$. First, we describe analytic solutions dependent on a certain parameter and becoming highly localized as it tends to infinity. Here, we are mainly concerned with the particular cases of the complexified Bateman solution (see, e.g., [1]). Second, we discuss simple solutions of the homogeneous wave equation, having a singularity at a running point. Attention is paid to analytical analysis of the solution given by Hörmander [2]. Also, we consider a specialized singular complexified Bateman solution which was dealt with in [3].

References

- [1] A. P. Kiselev, Localized light waves: Paraxial and exact solutions of the wave equation (a review), *Opt. Spectr.*, **102**, 661–681 (2007).
- [2] L. Hörmander, *The Analysis of Linear Partial Differential Operators I, Distribution Theory and Fourier Analysis*, Springer, Berlin, 1983.
- [3] A. S. Blagovestchenskii, A. P. Kiselev, A. M. Tagirdzhanov, Simple solutions of the wave equation with a singularity at a running point, based on the complexified Bateman solution, *J. Math. Sci.*, **224**, 47–53 (2017).

Generalized Chebychev polynomials connected with a point interaction for the discrete Schrödinger equation

Borzov V.V.¹, Damaskinsky E.V.²

¹Mathematical Department, The Bonch-Bruевич SPbGUT, Russia

²Mathematical Department, VI(IT), Russia and PDMI Russia

e-mail: borzov.vadim@yandex.ru, evd@pdmi.ras.ru

We consider a semi-infinite Jacobi matrix $\mathcal{J}_k^{(a)} = \{j_{i,n}^{(a,k)}\}_{i,n=0}^{\infty}$ (where a is a positive and k is a positive integer) corresponding to a point interaction for the discrete Schrödinger operator. The

elements $j_{i,n}^{(a,k)} = 0$, if $|n - i| \neq 1$; and $j_{i,n}^{(a,k)} = 1$, if $|n - i| = 1$, $i \neq k$, $n \neq k$; and $j_{k-1,k}^{(a,k)} = j_{k,k+1}^{(a,k)} = a$. As follows from recent work (see [1]) the spectral analysis of this problem (for $k = 1$) leads to a new class of orthogonal polynomials generalizing the classical Chebyshev polynomials. Our goal is to extend the class of generalized Chebyshev polynomials, considered in this paper from the case $k = 1$ to the case of any integer $k \geq 1$. Spectral analysis of this problem is almost exactly the same the analysis carried out in the work [2]. Therefore, we focus on the study of basic properties of the generalized Chebyshev polynomials. Namely, we find for these polynomials expressions using the classical Chebyshev polynomials. In addition we obtain explicit form of the measure orthogonality and differential equations for generalized Chebyshev polynomials. This report is a continuation of author's work (see [2]).

References

- [1] D. R. Yafaev, A point interaction for the discrete Schrödinger operator and generalized Chebyshev polynomials, *J. Math. Phys.*, **58**, 063511 (2017); arXiv:1703.06624.
- [2] V. V. Borzov, E. V. Damaskinsky, On the spectrum of discrete Schrödinger equation with one-dimensional perturbation, *Proceedings of "DAYS ON DIFFRACTION 2016"*, 73–78; arXiv:1609.05527.

Integrable in elliptic functions equations for the fronts of linear water waves generated by a localized source

Brezhnev Yu.V.¹, Dobrokhotov S.Yu.^{2,3}, Tsvetkova A.V.^{2,3}

¹Tomsk State University, 36 Lenin Ave., Tomsk, Russia 634050

²Ishlinsky Institute for Problems in Mechanics of the Russian Academy of Sciences, 101-1 pr. Vernadskogo, Moscow, Russia 119526

³Moscow Institute of Physics and Technology (Technical University), Dolgoprudny, Moscow Region, Russia 141701

e-mail: brezhnev@mail.ru, dobr@ipmnet.ru, annatsvetkova25@gmail.com

The front of the water wave generated by a localized source at each instant of time t is defined by the solution of the Cauchy problem $p|_{t=0} = (\cos \psi, \sin \psi)^T$, $\psi \in [0, 2\pi]$, $x|_{t=0} = x^0 \in \mathbf{R}^2$ for the Hamiltonian system with Hamiltonian $H = |p|C(x)$, $C(x) = \sqrt{gD(x)}$. Here $D(x)$ is the basin depth function, g is the acceleration due to gravity and the 2-vector x^0 specifies the source position. We consider two types of the depth function $D(x)$: $D(x) = \frac{b+r^2}{a+r^2}$ (r is the polar radius) and $D(x) = \frac{b+x_1^2}{a+x_1^2}$, where $a > b > 0$ are constants. First depth function describes an underwater bank, the second describes an underwater ridge.

We obtain exact analytical solutions of the Cauchy problem in cases reviewed here. This result can be applied to the asymptotic theory. In particular, we can visualize the curves of the fronts. For non-trivial depth function in case $t = 0$ the front is the point x^0 , for small $t > 0$ it is a smooth curve and for larger t the front may have focal points and points of self-intersection. Also using obtained formulas we describe asymptotic solutions of some stationary equations with localized right-hand sides.

References

- [1] P. H. LeBlond, L. A. Mysak, *Waves in the Ocean*, Elsevier, Amsterdam, 1978.
- [2] S. Yu. Dobrokhotov, A. I. Shafarevich, B. Tirozzi, Localized wave and vortical solutions to linear hyperbolic systems and their application to linear shallow water equations, *Rus. J. Math. Phys.*, **15**(2), 192–221 (2008).
- [3] A. Yu. Anikin, S. Yu. Dobrokhotov, V. E. Nazaikinskii, M. Rouleux, The Maslov canonical operator on a pair of Lagrangian manifolds and asymptotic solutions of stationary equations with localized right-hand sides, *Doklady Mathematics*, **96**(1), 406–410 (2017).

Boussinesq-type model to simulate the development of an undular bore on a small slope

Budiasih L.K.^{1,2}, **Wiryanto L.H.**¹

¹Department of Mathematics, Institut Teknologi Bandung, Indonesia

²Department of Mathematics, Sanata Dharma University, Indonesia

e-mail: lusia_kris@usd.ac.id, leo@itb.ac.id

Undular bore is a wave phenomenon, which is induced by a sudden increase of water flow and accompanied by wave trains without any wave breaking. In this study, the development of undular bores progressing downstream over a flat bottom and on a small slope have been numerically investigated. The Boussinesq-type equations are chosen as the governing equation, which solved using a finite difference method with predictor-corrector procedure. Numerical results show the ability of the scheme to simulate the development of an undular bore generated by a sudden discharge over flat bottom with the various Froude numbers. The Froude number affects the formation of undular bore. The greater Froude number, the wave train will become a steep traveling bore and the amplitude of undulations increases with faster phase velocity. The effects of channel slope on the amplitude of undular bore and the wave height have been shown. For a small slope, the greater slope will lead to small undulations, with lower phase velocity.

Unstable regimes of surface gravity waves generation

Bulatov V.V., **Vladimirov Yu.V.**

Institute for Problems in Mechanics RAS, 119526, Moscow, pr. Vernadskogo 101-1

e-mail: internalwave@mail.ru

The surface wave motions in the marine environment can either originate due to natural causes (wind waves, flow past underwater obstacles, bottom relief variations, density and flow fields) or be generated by the flow past natural obstacles (platforms, underwater pipelines, complex hydraulic facilities). The general system of hydrodynamic equations describing the surface perturbations is a rather complicated mathematical problem from the standpoint of proving the existence and uniqueness theorems for solutions in the corresponding function classes and from the computational standpoint. The main results of solving the problems of generation of surface wave perturbations are represented in most general integral form, and to obtain the integral solutions, it is thus necessary to develop asymptotic methods for their investigation which admit a qualitative analysis and rapid estimations of the obtained solutions. The fact that the structure of the heavy sea surface is three-dimensional is also significant, and there are currently no possibilities for large-scale computational experimental modelling of three-dimensional ocean flows at large times with a sufficient accuracy. But in several cases, the initial qualitative concept of the considered class of wave phenomena can be obtained by using simpler asymptotic models and analytic methods for studying them. So several results of asymptotic analysis of linear problems describing different regions of generation and propagation of surface perturbations also underlie the currently actively developing non-linear theory of generation of ocean waves of extremely large amplitude, the so-called rogue waves (killer waves). The goal in this paper is to construct uniform far field asymptotics of surface perturbations generated in the flow of a heavy homogeneous liquid of infinite depth around a localized harmonic source of perturbations. We have shown that, in certain generation regimes, the far fields of surface perturbations from a non-stationary source localized in the flow of a heavy liquid of infinite depth form a hybrid system of waves of the following two types: annular (transverse) and wedge-shaped (longitudinal). The qualitative picture of wave fields at a far distance from a non-stationary source is significantly more complicated compared to the case of wave generation by a moving stationary source when the wave fronts come to a fixed observation point. The unsteadiness of the perturbation source amplitude results not only in the appearance of annular waves diverging on the liquid surface directly from the

source but also in generation of hybrid surface perturbations propagating upstream from the source. The obtained asymptotics of surface wave perturbations far field allow one efficiently to calculate the basic amplitude-phase characteristics of wave fields and, in addition, qualitatively to analyze the obtained solutions, which is important in developing of well-posed mathematical models of wave dynamics of surface perturbations of the real natural environments. This opens wide opportunities for investigating the wave fields in general, which is also important for formulating correct statements of mathematical models of wave dynamics and for obtaining express evaluations in the surface field measurements in ocean [1–4].

References

- [1] V. Bulatov, Yu. Vladimirov, *Wave Dynamics of Stratified Mediums*, Nauka Publishers, Moscow, 2012.
- [2] C. Mei, M. Stiassnie, D. Yue, *Theory and Applications of Ocean Surface Waves*, World Scientific Publishing, London, 2017.
- [3] V. Bulatov, Yu. Vladimirov, I. Vladimirov, Uniform asymptotics of the far fields of the surface disturbances produced by a source in a heavy infinite-depth fluid, *Fluid Dynamics*, **49**, 655–661 (2014).
- [4] V. Bulatov, Yu. Vladimirov, I. Vladimirov, Far fields of the surface disturbances produced by a pulsating source in an infinite-depth fluid, *Fluid Dynamics*, **52**, 617–622 (2017).

Complex representation of general solution of equations for nonlinear model of plane deformation of crystal media with a complex lattice

Bulygin A.N., Pavlov Yu.V.

Institute for Problems in Mechanical Engineering of Russian Academy of Sciences, Saint Petersburg, Russia

e-mail: bulygin_an@mail.ru

In nonlinear model [1, 2] deformation of crystal medium is described by vector of acoustic mode \mathbf{U} and vector of optical mode \mathbf{u} . In the case of plane deformation they can be found from system of four connected nonlinear equations

$$\lambda_{44}\Delta\mathbf{U} + (\lambda_{12} + \lambda_{44}) \text{grad div } \mathbf{U} + C_{44}\Delta\mathbf{u} + (C_{12} + C_{44}) \text{grad div } \mathbf{u} = s \text{grad } \Phi(u_s), \quad (1)$$

$$k_{44}\Delta\mathbf{U} + (k_{12} + k_{44}) \text{grad div } \mathbf{U} + C_{44}\Delta\mathbf{u} + (C_{12} + C_{44}) \text{grad div } \mathbf{u} = \mathbf{B}(p - s \text{div } \mathbf{U}) \sin u_s, \quad (2)$$

Here

$$\mathbf{U} = U_x\mathbf{i} + U_y\mathbf{j}, \quad \mathbf{u} = u_x\mathbf{i} + u_y\mathbf{j}, \quad \Phi(u_s) = 1 - \cos u_s, \quad u_s = \mathbf{B}\mathbf{u}, \quad \mathbf{B} = \frac{\mathbf{i} + \mathbf{j}}{b}, \quad \Delta = \frac{\partial^2}{\partial x^2} + \frac{\partial^2}{\partial y^2}, \quad (3)$$

$\lambda_{12}, \lambda_{44}$ are macroelasticity modules, k_{12}, k_{44} are microelasticity modules, C_{12}, C_{44} are modules of interaction of the acoustic and optical modes, p is half of height of a potential barrier, s is a coefficient of mechanical striction, b is size of a cubic cell of a crystal.

In the equations of acoustic modes the nonlinear terms have an form of gradient of nonlinear function $\Phi(u_s)$. It has allowed to obtain a complex representation for general solution of the acoustic mode. The common solution is given by the N. I. Muskhelishvili's modified formulas [3] in which volume sources of potential type are considered. In nonlinear model a role of volume sources is played by microshift along a vector of inverse lattice. The equation of the optical mode has a form of the sine-Gordon equations with variable coefficient (amplitude) before the sine. A complex representation of general solution for optical mode is obtained in assumption of a certain type of nonlinear terms. Complex representations for a tensor of macrotension and a tensor of microtension are obtained also. They have a form of Kolosov–Muskhelishvili's generalized formulas in which

volume sources are considered. The obtained results allow to apply effective methods of the theory of functions of a complex variable to the solution of specific boundary problems of plain deformation on the basis of nonlinear model.

References

- [1] E. L. Aero, Microscale deformations in a two-dimensional lattice: Structural transitions and bifurcations at critical shear, *Phys. Solid State*, **42**, 1147–1153 (2000).
- [2] E. L. Aero, A. N. Bulygin, Yu. V. Pavlov, Nonlinear model of deformation of crystal media with complex lattice: mathematical methods of model implementation, *Math. Mech. Solids*, **21**, 19–36 (2016).
- [3] N. I. Muskhelishvili, *Some Base Problems of the Mathematical Theory of Elasticity*, Nauka, Moscow, 1966 [In Russian].

Different asymptotic limits of average evolution of quantum particle under small random perturbations

Buslov V.A.

Physical Faculty, Saint-Petersburg State University, Ulianovskaja st. 3, Saint-Petersburg, 198504
e-mail: abvabv@bk.ru, v.buslov@spbu.ru

Let the quantum particle trajectories x_t satisfy stochastic differential equation

$$dx_t = B(x)dt + \sqrt{\varepsilon}dw_t \quad (1)$$

where B is drift field on a smooth manifold Ω without a boundary, ε is small parameter, w_t is a proper dimension Wiener process. Quantum operator H (responsible for transitions from ground state to excited for example [1]) one can consider as a multiplication operator on smooth matrix-function $h_{ik}(x)$ operator at quantum variables space \mathbb{C}^n of some dimension n . The result of averaging of the quantum evolution operator $\exp(i \int_0^t H(x_s)ds)$ over all trajectories of stochastic process (1) is equal to $\int_{\Omega} \Psi dx$, where Ψ satisfies

$$\frac{\partial \Psi}{\partial t} = (iH \otimes I_s - L_{\varepsilon}^* \otimes I_q)\Psi. \quad (2)$$

Here $-L_{\varepsilon}^* = \varepsilon \Delta \cdot - \operatorname{div}(B \cdot)$ is formally conjugated to $-L_{\varepsilon} = \varepsilon \Delta \cdot + (B, \cdot)$, which is diffusion generating operator and describes evolution of distribution function of (1). If the field is potential one $B = -\nabla \varphi$, diffusion operator is self-adjoint at weighted space with weight $e^{-\varphi/\varepsilon}$ and has a series of exponentially small eigenvalues $\lambda_i = \Lambda_i e^{-W_i/\varepsilon}$, $W_i > 0$, $i = 1, \dots, N$; N is the number of potential minima. Corresponding eigenfunctions v_i of L are practically constant at attraction regions Ω_i of minima x_i of dynamic system $\dot{x} = -\nabla \varphi$. The corresponding eigenfunctions of L_{ε}^* up to normalization ($\langle u_i, v_j \rangle = \delta_{ij}$) are equal to $u_i = v_i e^{-\varphi/\varepsilon}$ and tend to some combination of $\delta(x - x_i)$ as $\varepsilon \rightarrow 0$.

Contracted on its lowest spectrum operator L_{ε} is a singular Laplace matrix \mathbf{L}_{ε} and it is convenient to investigate its proper spaces by graph methods [2]. Limit constant values of eigenvectors \vec{v}_i and \vec{u}_i of \mathbf{L}_{ε} and $\mathbf{L}_{\varepsilon}^*$ correspondingly compose up to numeration upper-block matrices \mathbf{V}^T and \mathbf{U} having no dependence on ε . Coarsened vector $\vec{\Psi}^{\varepsilon}$ ($\Psi_i^{\varepsilon} = \int_{\Omega_i} \Psi(x, t)dx$) in a lead term behaves as $\vec{\Psi}^{\varepsilon}(t) = \exp(i\omega \operatorname{diag}(h_1, h_2, \dots, h_N)t - \mathbf{L}_{\varepsilon} t)\vec{\Psi}^{\varepsilon}(0)$, where $h_i = h(x_i)$ and H is operator of multiplication by smooth function $h(x)$, $H\Psi = \omega h(x)\Psi$, ω is introduced for convenience characteristic frequency of quantum process.

If the exponential order W of characteristic frequency ω is equal to exponential order of eigenvalues $\lambda_k, \dots, \lambda_m$, vector $\vec{\Psi}(\tau) = \lim_{\varepsilon \rightarrow 0} \vec{\Psi}^{\varepsilon}(\tau e^{W/\varepsilon})$ demonstrates the following behavior at “slow” time τ

$$\vec{\Psi}(\tau) = \mathbf{U} \exp[(i\mathbf{H} - \operatorname{diag}(0, \dots, 0, \Lambda_k, \dots, \Lambda_m, \infty, \dots, \infty))\tau] \mathbf{V}^T \vec{\Psi}(0), \quad (3)$$

where $\mathbf{H} = \mathbf{V}^T \text{diag}(h_1, h_2, \dots, h_N) \mathbf{U}$ is upper-block matrix. $\vec{\Psi}$ is continuous at zero as a function of slow time: $\lim_{\tau \rightarrow 0} \vec{\Psi}(\tau) = \vec{\Psi}(0)$, if the initial distribution of particles decomposes into first m eigenvectors $\vec{u}_i(\vec{v}_i)$. The number of different types of average evolution is equal to the number of different exponential orders W_i of lower eigenvalues of infinitesimal operators $-L_\epsilon$ and $-L_\epsilon^*$ of semigroup connected with transition function of Markov process (1).

References

- [1] V. A. Buslov, Modeling asymmetric Mössbauer spectra of a super-paramagnetic in the framework of DOM (Discrete Orientation Model), *Proceedings of the International Conference DAYS on DIFFRACTION 2015*, 60–62 (2015).
- [2] V. A. Buslov, On the relationship between multiplicities of the matrix spectrum and signs of components of its eigenvectors in a tree-like structure, *Zap. Nauchn. Sem. POMI*, **464**, 5–36 (2017) (in Russian).

The Le-diagram for the resonance of modified KP equation

Jen-Hsu Chang

Department of Computer Science and Information Engineering, National Defense University, Taiwan, 33551
 e-mail: jhchang@ndu.edu.tw

The Le-diagram is a Young diagram filling with “+” or “o” in each box, which has the Le-property: there is no “o” which has “+” above it and its left. In KP equation, we use the Le-diagram to describe the resonance between line solitons. But in the Modified KP equation (MKP), the Le-diagram is different from KP equation due to kink-solitons. One will utilize the Le-diagram to describe the resonance structure between kink-solitons and line-solitons in the MKP equation. In particular, we focus on the case of totally non-negative Grassmannian manifold $Gr_{\geq 0}(2, 4)$.

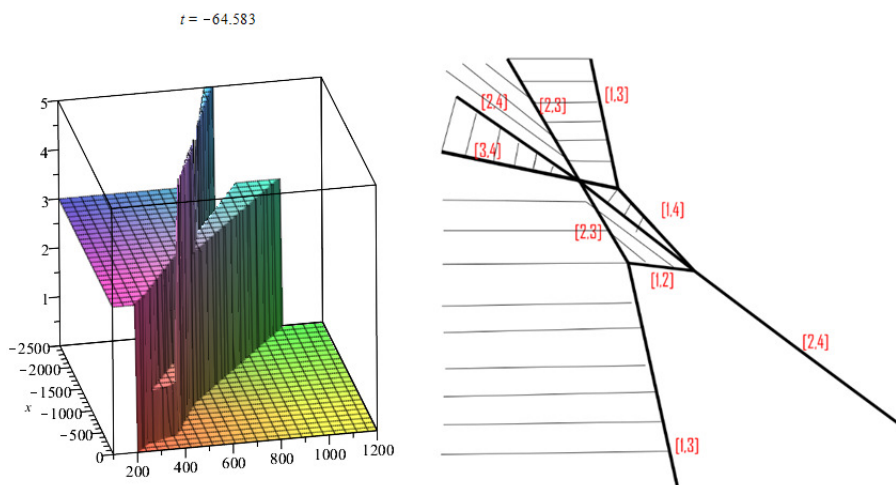


Fig. 1: T-type resonant solution of MKP equation.

References

- [1] A. Postnikov, Total positivity, Grassmannian, and networks, *arXiv: math/0609764* (2006).
- [2] Y. Kodama, L. Williams, KP solitons and total positivity for the Grassmannian, *Inventiones Mathematicae*, **198**, 637–699 (2014).
- [3] J.-H. Chang, Soliton interaction in the modified Kadomtsev–Petviashvili-(II) equation, *arXiv: 1705.04827* (2017).

The spectral functions method for elastic plane wave diffraction by a wedge

Cehade S., Darmon M.

CEA, LIST, Department of Imaging & Simulation for Nondestructive Testing, CEA-Saclay, DIGITEO LABs, bât 565, 91191 Gif-sur-Yvette, France

e-mail: samar.chehade@cea.fr, michel.darmon@cea.fr

Lebeau G.

Laboratoire J.A. Dieudonné, UMR CNRS 7351, Université de Nice Sophia-Antipolis, Parc Valrose, 06108 Nice, France

e-mail: lebeau@unice.fr

NDE examination of industrial structures requires the modeling of specimen geometry echoes generated by the surfaces (entry, back-wall, ...) of inspected blocks. For that purpose, the study of plane elastic wave diffraction by a wedge is of great interest since surfaces of complex industrial specimen often include dihedral corners.

These inspections often deal with high frequency ($f = 2 - 5$ MHz) ultrasonic waves. Simulation of realistic inspections by finite elements and finite differences can therefore be time consuming because such methods must keep the mesh step very small (on the order of 10 elements per wavelength $\lambda \sim 1$ mm) for a better description of the scattered wave. Semi-analytical methods are then preferred for high frequency problem.

There exist various approaches for semi-analytical modeling of plane elastic wave diffraction by a wedge but the theoretical and numerical aspects of these methods have so far only been developed for wedge angles lower than π .

Croisille and Lebeau [1] have introduced a resolution method called the Spectral Functions method in the different case of an immersed elastic wedge of angle less than π . Kamotski and Lebeau [2] have then proven existence and uniqueness of the solution derived from this method to the diffraction problem of stress-free wedges embedded in an elastic medium. The advantages of this method are its validity for wedge angles greater than π and its adaptability to more complex cases. The methodology of Croisille and Lebeau [1] has been first applied by the authors to the simpler case of an immersed soft wedge. It has then been developed here for the scattering problem of an elastic wave and a numerical validation of the method for all wedge angles is proposed.

References

- [1] J.-P. Croisille, G. Lebeau, *Diffraction by an Immersed Elastic Wedge*, Lecture Notes in Mathematics, Springer, Berlin, New York, 1999.
- [2] V. V. Kamotski, G. Lebeau, Diffraction by an elastic wedge with stress-free boundary: existence and uniqueness, *Proc. R. Soc. A*, **462**(2065), 289–317 (2006).

Equations for velocity oscillations in problems of a fluid flow along a plate with small periodic irregularities on the surface for large Reynolds numbers

Danilov V.G., Gaydukov R.K.

National Research University Higher School of Economics, Moscow, Russia

e-mail: vgdanilov@mail.ru, roma1990@gmail.com

Depending on the scales of irregularities in the problem under study, a solution arises which describes two (“double-deck”) or three (“triple-deck”) boundary layers on the plate. It is of interest to study the equations describing the velocity oscillations in the boundary layers.

In the double-deck case, this equation is a Rayleigh-type equation

$$\varepsilon^{1/3} \frac{\partial}{\partial t} \int_{\xi}^{\xi} \Delta_{\xi, \tau} \tilde{v} d\xi + f'(\tau/\sqrt{x}) \Delta_{\xi, \tau} \tilde{v} - \frac{f'''(\tau/\sqrt{x})}{x} \tilde{v} = 0, \quad (1)$$

which was obtained and investigated in our papers [2, 3].

In the triple-deck case, this equation is a Benjamin–Ono-type equation

$$\varepsilon^{1/2} \frac{\partial A}{\partial t} + A \frac{\partial A}{\partial \xi} = \int_0^{2\pi} \frac{\partial^2 A}{\partial \xi^2}(t, \xi') \cot\left(\frac{\xi - \xi'}{2}\right) d\xi'. \quad (2)$$

In the case of localized irregularities (a “hump”) on the plate surface, similar equation was obtained by O. S. Ryzhov and investigated by S. Yu. Dobrokhotov and I. M. Krichever [1].

In the fluid flow problems, there are some specialities.

- The above equations are considered on a semi-infinite cylinder.
- If the Navier–Stokes system is considered on finite times, then the solutions of these equations should be considered on large times.
- In hydrodynamic papers, the function A is a special parameter and is called a displacement. From the viewpoint of the boundary layer theory, this function describes the velocity oscillations on the boundary of the thin (near-wall) boundary layer. In the triple-deck case, this function A satisfies Benjamin–Ono-type equation (2) and is a lower boundary condition for Rayleigh-type equation (1) in the double-deck case.

It turns out that, in both cases, this function may be calculated from Prandtl-type equations describing the flow in the near-wall region.

Acknowledgment. This paper was prepared within the framework of the Basic Research Program at the National Research University Higher School of Economics (HSE) and supported within the framework of a subsidy by the Russian Academic Excellence Project ‘5-100’.

References

- [1] S. Yu. Dobrokhotov, I. M. Krichever, Multi-phase solutions of the Benjamin–Ono equation and their averaging, *Math. Notes*, **49**, 583–594 (1991).
- [2] V.G. Danilov, R.K. Gaydukov, Vortices in the Prandtl boundary layer induced by irregularities on a plate, *R. J. Math. Phys.*, **22**, 161–173 (2015).
- [3] R. K. Gaydukov, D. I. Borisov, Existence of the stationary solution of a Rayleigh-type equation, *Math. Notes*, **99**, 636–642 (2016).

Reconstruction of solution to the wave equation from Cauchy data on the boundary

M.N. Demchenko

St. Petersburg Department of V. A. Steklov Institute of Mathematics of the Russian Academy of Sciences, Fontanka 27, St. Petersburg
e-mail: demchenko@pdmi.ras.ru

We consider the problem of determining solution to the wave equation in $\Omega \times \mathbb{R}$ (Ω is an Euclidean domain) from Cauchy data given on $S \times I$, where $S \subset \partial\Omega$, $I \subset \mathbb{R}$. The set S and the time interval I are determined by the part of the cylinder $\Omega \times \mathbb{R}$ in which the solution is to be recovered. We provide a reconstruction algorithm based on analytic expressions. Possible reformulations of the problem in consideration are the source identification problem and the problem of recovering initial data in the IBVP for the wave equation. Such problems arise in geophysics (ground-penetrating radar), photoacoustic tomography with limited data, and tsunami source recovery.

The research was supported by the grant RFBR 17-01-00529-a.

Bidirectional fully dispersive models for water waves over a rough bottom

E. Dinvoy, H. Kalisch

Department of Mathematics, University of Bergen, Postbox 7800, 5020 Bergen, Norway
e-mail: evgueni.dinvay@math.uib.no, henrik.kalisch@math.uib.no

D. Dutykh

LAMA, UMR5127, CNRS - Université Savoie Mont Blanc, Campus Scientifique, 73376 Le Bourget-du-Lac Cedex, France
e-mail: denys.dutykh@univ-savoie.fr

John D. Carter

Seattle University, 901 12th Ave, Seattle, WA 98122, USA
e-mail: carterj1@seattleu.edu

The long-wave approximation is applied to the Hamiltonian formulation of the water wave problem

$$\eta_t = \frac{\delta \mathcal{H}}{\delta \Phi}, \quad \Phi_t = -\frac{\delta \mathcal{H}}{\delta \eta}.$$

We show that changing only the total energy, \mathcal{H} , while staying in the same framework of accuracy, one can arrive at different Whitham–Boussinesq systems. Some of these systems have been given attention in recent years and some are new. In fact, all of these systems are different in the sense of well-posedness and numerical stability. They all approximate the Euler system for an inviscid potential fluid. They are all fully dispersive in the linear part and have nonlinear parts that are asymptotically equivalent to the standard Boussinesq nonlinearity. These systems are suitable for describing problems with variable topography. They can combine gravitational and capillary or elastic effects. Their accuracy is checked by comparing with solutions of the Euler system given by the conformal mapping technique and with laboratory experiments.

Differentiation of brain waves patterns in different states by multifractal analysis

Dmitrieva L.A., Kuperin Yu.A.

Saint Petersburg State University, University Embankment, 7/9, Saint Petersburg, 199034
e-mail: l.dmitrieva@spbu.ru, y.kuperin@spbu.ru

Smetanin N.M.

National Research University Higher School of Economics, School of Data Analysis and Artificial Intelligence, Moscow, 3, Kochnovsky Proezd, 3, Moscow
e-mail: nsmetanin@hse.ru

Multifractal analysis is currently considered as the systematic technique for finding and describing the heterogeneity of fractal objects. Initially proposed for analysis of turbulence data, it is currently applied in many fields, including geophysics, financial modeling, biological systems, and time series analysis. The present paper makes a differentiation between brain waves patterns revealed in the multifractal spectra of multichannel electroencephalogram (EEG) records. Two characteristics of the multifractal spectrum of EEG time series have been chosen as differentiation indicators. These indicators are: the right tail width and the left tail width. These characteristics have been calculated for all EEG channels for a number of test subjects divided into two groups. The first group was subjected to a long practice of immersion in a state of consciousness characterized by the dominance of Mu waves (7–9 Hz), which are also known as slow Alpha waves. The second group had no such practice. The non-stationarity of the EEG records was overcome by splitting the entire EEG time series into stationary sections by moving windows. Statistical processing of the above indicators

computed on the stationary fragments was carried out by using the Repeated ANOVA (analysis of variance) approach. Statistical results obtained in the investigation of the right tail of the multifractal spectrum allowed us to make a conclusion that synchronization of large neural ensembles occurs mostly in test subjects from the first group in a state characterized by Mu waves dominance. The study of the left tail of the multifractal spectrum has shown that in a state of Mu waves dominance, the level of physiological noise in large neural ensembles significantly decreases for both groups of test subjects. However, the noise level in large neural ensembles is significantly higher for the second group of subjects, both in a background state with high Alpha waves (9–13 Hz) dominance (closed eyes) and in a state with Mu waves dominance, than it is for test subjects from the first group.

References

- [1] J. Feder, *Fractals*, Plenum, New York, 1988.
- [2] J. W. Kantelhardt, Fractal and multifractal time series, in: R. Meyers (Ed.), *Encyclopedia of Complexity and System Science*, Springer, 3754–3779 (2002).
- [3] H. Stanley, P. Meakin, Multifractal phenomena in physics and chemistry, *Nature*, **335**, 405–409 (1988).
- [4] C. B. Maity, R. Pratihari, etc., Multifractal detrended fluctuation analysis of alpha and theta EEG rhythms with musical stimuli, *Chaos Solitons Fractals*, **81**, 52–67 (2015).

The problem of the wave overturning for the Burgers equation with an imaginary dispersive second derivative

Dobrokhotov S.Yu.

Ishlinsky Institute for problem in Mechanics and Moscow Institute of Physics and Technology
e-mail: dobr@ipmnet.ru

The problem of the appearance and description of the oscillation zone of solutions of the Korteweg–de Vries equation with small dispersion h in the case when the Hopf limit equation (for a simple wave) describes the wave overturning was formulated and studied at the physical level of rigor in the well-known work of A. V. Gurevich and L. P. Pitaevsky more than 35 years ago. Later this problem was studied both for the Korteweg–de Vries equation and for other equations with weakly dispersive terms in the works of B. A. Dubrovin, S. P. Novikov, T. Grava, C. Klein, A. Moro, A. L. Krylov, G. El', A. Kamchatnov, Yu. Kodama, F. Tian, B. I. Suleimanov and many others. The basic assumption used in these papers is that in the oscillation zone solution are presented as a “one-phase” Kuzmak–Whitham ansatz $f(S(x, t)/h, x, t, h)$, where $S(x, t)$, $f(y, x, t)$ are smooth functions, $f(y, x, t, h)$ is 2π -periodic by the argument y . We consider a similar problem for the i-Burgers equation (the Burgers equation in which small viscosity is replaced by a small imaginary dispersion ih). Using the Coel–Hopf transformation and solutions of the Schrödinger equation for a free particle, we show that in the zone of oscillations solution has the two-phase form $F(S(x, t)/h, G(x, t)/h, x, t, h)$, and in the vicinity of the beginning and end of the zone of oscillations the solution is expressed in terms of Airy functions with a more complicated dependence on h . The main part of this work was done together with V. P. Maslov and V. B. Tsvetkov and published 1992 in [1], but it is almost unknown among specialists in nonlinear waves. In addition, we rewrite the solution in a more effective form based on recently obtained new asymptotic formulas.

The last part of this work was done in the frame of IPMech theme № AAAA-A17-117021310377-1.

References

- [1] S. Yu. Dobrokhotov, V. P. Maslov, V. B. Tsvetkov, Problem of the reversal of a wave for the model equation $r_t + rr_x - \frac{ih}{2}r_{xx} = 0$, *Mathematical Notes*, **51**(6), 624–627 (1992).

The linear water waves in the basin with elastic base created by the localized underground source

Dobrokhotov S.Yu., Sekerzh-Zenkovich S.Ya., Tolstova O.L., Vargas C.A.

Institute for Problem in Mechanics of Russian Academy of Sciences and Moscow Institute of Physics and Technology, 101-1, prosp. Vernadskogo, Moscow, Russia

e-mail: doobr@ipmnet.ru

We consider the propagation of the linear gravity waves in the basin with the elastic bottom. Usually the gravity water waves are considered in the layer with the hard lower boundary. If the length of the wave much larger than the depth of layer (or the basin) and the wave amplitude is small then one can use the shallow water approximation and reduce the original problem to the linear wave equation or its dispersive generalization like the linearized Boussinesq equation. Such type of models are used for instance for the description of the propagation of the tsunami waves. It is well-known so-called piston model of the creation tsunami wave: the underground source organizes the shift of the basin's bottom which in turn generates the perturbation of the free elevation and surface gravity water waves. Pod'japolskii in 1978 suggested to consider the process of generation and propagation tsunami waves in the frame of the combined water-elastic model that considers the effect of elastic foundations on propagation of water waves. The mathematical aspects of this model were discussed in particular by Sabatier (1983), Fragela (1989), Zvolinskii, Nikinin, Sekerzh-Zenkovich (1991), Chudinovich, Dobrokhotov, Tolstova (1993), Griniv, Dobrokhotov, Shkalikov (2000), numerical aspects was studied by V. Gusjakov (1987) and others (see bibliography in [1, 2]). The basic equations has a nonstandard form from of view of theory of partial differential equations because the boundary conditions contain the time-derivatives. Our previous results show that the basic equations with time derivatives in boundary conditions could be presented in a standard form for Cauchy problems for evolutionary equations but in the configuration space having the form of the tensor product of the 3-D Euclidean half-space and 2-D Euclidean planes. The Fourier analysis of this equations shows that solution of the Cauchy problem for this model breaks in the 3-D internal elastic modes and two 2-D surface modes: the mode describing the Rayleigh wave and the mode describing the waves on the water surface. In our talk we focus on the water waves mode and consider the situation when the water waves are created by the localized underground source. Using recent results from [2], we construct the effective asymptotic formulas for the leading edge front waves for a wide range of sizes of underground source. This allows one to estimate the influence of the elastic base on the velocity of the leading edge front propagation and also on the dispersive properties of such type of the waves. We also show that the waves near leading edge front could be described by the linearized Boussinesq equation with corrected velocity and dispersion coefficient before the 4th derivatives.

References

- [1] R. O. Griniv, S. Yu. Dobrokhotov, A. A. Shkalikov, An operator model of the problem of oscillations of a fluid on an elastic base, *Math. Notes*, **68**(1-2), 57–70 (2000).
- [2] S. Yu. Dobrokhotov, V. E. Nazaikinskii, Punctured Lagrangian manifolds and asymptotic solutions of the linear water wave equations with localized initial conditions, *Mathematical Notes*, **101**(6), 1053–1060 (2017).

Homogenization of a nonstationary model equation of electrodynamics

Dorodnyi M.A., Suslina T.A.

St. Petersburg State University, Universitetskaya emb. 7/9, St. Petersburg, 199034, Russia

e-mail: mdorodni@yandex.ru, t.suslina@spbu.ru

In $L_2(\mathbb{R}^3; \mathbb{C}^3)$, we consider a self-adjoint operator \mathcal{L}_ε , $\varepsilon > 0$, generated by the differential expression

$$\operatorname{curl} \eta(\mathbf{x}/\varepsilon)^{-1} \operatorname{curl} - \nabla \nu(\mathbf{x}/\varepsilon) \operatorname{div}.$$

Here the matrix function $\eta(\mathbf{x})$ with real entries and the real function $\nu(\mathbf{x})$ are periodic with respect to some lattice, are positive definite, and are bounded. We study the behavior of the operators $\cos(\tau\mathcal{L}_\varepsilon^{1/2})$ and $\mathcal{L}_\varepsilon^{-1/2}\sin(\tau\mathcal{L}_\varepsilon^{1/2})$ for $\tau \in \mathbb{R}$ and small ε . It is shown that these operators converge to $\cos(\tau(\mathcal{L}^0)^{1/2})$ and $(\mathcal{L}^0)^{-1/2}\sin(\tau(\mathcal{L}^0)^{1/2})$, respectively, in the norm of the operators acting from the Sobolev space H^s (with a suitable s) to L_2 . Here \mathcal{L}^0 is an effective operator with constant coefficients. In [1], the following sharp order error estimates were obtained:

$$\|\cos(\tau\mathcal{L}_\varepsilon^{1/2}) - \cos(\tau(\mathcal{L}^0)^{1/2})\|_{H^2(\mathbb{R}^3) \rightarrow L_2(\mathbb{R}^3)} \leq C_1(1 + |\tau|)\varepsilon, \tag{1}$$

$$\|\mathcal{L}_\varepsilon^{-1/2}\sin(\tau\mathcal{L}_\varepsilon^{1/2}) - (\mathcal{L}^0)^{-1/2}\sin(\tau(\mathcal{L}^0)^{1/2})\|_{H^1(\mathbb{R}^3) \rightarrow L_2(\mathbb{R}^3)} \leq C_2(1 + |\tau|)\varepsilon. \tag{2}$$

We confirm that (1), (2) are sharp (with respect to the operator norm) and distinguish conditions on the operator under which the result can be improved:

$$\|\cos(\tau\mathcal{L}_\varepsilon^{1/2}) - \cos(\tau(\mathcal{L}^0)^{1/2})\|_{H^{3/2}(\mathbb{R}^3) \rightarrow L_2(\mathbb{R}^3)} \leq C_3(1 + |\tau|)\varepsilon,$$

$$\|\mathcal{L}_\varepsilon^{-1/2}\sin(\tau\mathcal{L}_\varepsilon^{1/2}) - (\mathcal{L}^0)^{-1/2}\sin(\tau(\mathcal{L}^0)^{1/2})\|_{H^{1/2}(\mathbb{R}^3) \rightarrow L_2(\mathbb{R}^3)} \leq C_4(1 + |\tau|)\varepsilon.$$

The results are used for homogenizing the Cauchy problem for the model hyperbolic equation $\partial_\tau^2 \mathbf{v}_\varepsilon = -\mathcal{L}_\varepsilon \mathbf{v}_\varepsilon$, $\operatorname{div} \mathbf{v}_\varepsilon = 0$, appearing in electrodynamics. We study the application to a nonstationary Maxwell system for the case in which the magnetic permeability is equal to $\mathbf{1}$ and the dielectric permittivity is given by the matrix $\eta(\mathbf{x}/\varepsilon)$.

References

[1] M. A. Dorodnyi, T. A. Suslina, Homogenization of a nonstationary model equation of electrodynamics, *Mathematical Notes*, **102**(5), 645–663 (2017).

Modelling of damaged interface dynamic behaviour via random and periodic distributions cracks

Doroshenko O.V.

Institute for Mathematics, Mechanics and Informatics, Kuban State University, Krasnodar, 350040, Russia

e-mail: oldorosh@mail.ru

Micro-cracks of internal surfaces of solids may appear during operation or manufacturing process. The problem of detection and identification of interface damage can be solved ultrasonic non-destructive techniques. Mathematical models describing the elastic waves diffraction by cracks and delaminations are needed for internal defects sensing. A damaged interface can be simulated as a stochastic [1] or as a periodic distribution of defects [2]. One of the approaches for modelling of damaged interfaces between dissimilar media introduce special boundary conditions with a continuous distribution of springs characterized by stiffness constants [1].

Models of the imperfect interface assuming a random of planar circular or rectangular micro-cracks are presented. Numerical solution of a hypersingular integral equation (see, e.g. [3]) for a single crack is required for estimating the spring stiffness [2]. The crack opening displacement (COD) is an unknown function in the integral equation and it can be obtained by Bubnov–Galerkin method. Asymptotic representation for the kernel of the integral equation allows to derive analytical expressions for the components of displacement jump. Frequency-dependent representations for COD and spring stiffnesses in the case of circular interface cracks are constructed.

A damaged interface is also modelled as a doubly periodic array of planar circular or rectangular delaminations. The COD at each delamination is unknown, but the problem is reduced to the solution of a boundary integral equation formulated for the reference unit-cell. The kernel of the boundary integral equation is evaluated using the relation between exponential series and a Dirac delta function, the integral equation is solved via the Bubnov–Galerkin method.

The comparison normal and tangential component of stiffnesses matrix is performed for periodic and random distributions of interfacial defects of various shapes. Also, the transmission through the damaged interface simulated by the random and periodic distribution of cracks is analysed.

References

- [1] M. V. Golub, O. V. Doroshenko, A. Boström, Effective spring boundary conditions for a damaged interface between dissimilar media in three-dimensional case, *International Journal of Solids and Structures*, **81**, 141–150 (2016).
- [2] M. V. Golub, O. V. Doroshenko, Wave propagation through an interface between dissimilar media with a doubly periodic array of arbitrary shaped planar delaminations, *Mathematics and Mechanics of Solids*, doi: 10.1177/1081286517745122 (2017).
- [3] Ye. V. Glushkov, N. V. Glushkova, Diffraction of elastic waves by three-dimensional cracks of arbitrary shape in a plane *Journal of Applied Mathematics and Mechanics*, **60**, 277–283 (1996).

Polarization characteristics of graphene-containing composite L-band antenna

Dugin N.A.¹, Belyaev G.R.¹, Lobastov V.G.², Zaboronkova T.M.²

¹Lobachevsky State University, 23 Gagarin Ave., Nizhny Novgorod 603950, Russia

²R. E. Alekseev State Technical University, 24 Minin St., Nizhny Novgorod 603950, Russia

e-mail: ndugin@yandex.ru, t.zaboronkova@rambler.ru

The devices based on carbon composite materials have a long operation lifetime, enhanced immunity to corrosion, the record-breaking durability-to-weight ratios, and high stability in a wide range of temperatures [1]. Our recent studies have shown the possibility of using composite materials not only for manufacturing the elements of microwave devices, but also for creating antenna systems [2]. Note, that the graphene-containing material properties depend on the concentration of a binding substance in the composite material, and the conductivity of such a material reaches a value of 10^5 S/m. We studied the polarization properties of the graphene-containing carbon composite material in the microwave range and found that in the case of rotation of the composite-material thin plate by 90° , the polarization coefficient with respect to the reflection signal amplitude may reach a value of 0.3 [3].

The anisotropic properties of the composite material may influence the polarization characteristics of antenna. In the present work, the main attention is paid to the polarization characteristics of a graphene-containing composite L-band horn antenna. The measurements were performed under laboratory conditions without using an anechoic chamber for two prototypes of the L-band horn antennas made of (i) carbon fiber and (ii) carbon fabric, as well as for their metal analogs. The polarization characteristics of antennas were measured using a polarization device made on the basis a circular waveguide. We obtained that the polarization coefficient of the composite antenna lies in the interval 0.35–0.45 and is 1.5–2 times less than that determined for the metal analog. The experimental data is a good agreement with theoretical results. The numerical results will be presented and discussed for some cases of interest.

Acknowledgments. This work was supported by the Russian Foundation for Basic Research (project No. 18-42-520004r-a).

References

- [1] V. V. Rybin, P. A. Kuznetsov, I. V. Ulin, B. V. Farmakovskii, V. E. Bakhareva, *Voprosy Materialovedeniya*, **45**, 169–178 (2006).
- [2] N. A. Dugin, T. M. Zaboronkova, E. N. Myasnikov, *Technical Physics Letters*, **42**, 598–600 (2016).
- [3] N. A. Dugin, T. M. Zaboronkova, E. N. Myasnikov, *Latvian Journal of Physics and Technical Sciences*, **53**, 17–24 (2016).

A spheroidal model for axisymmetric scatterers based on the quasistatic approach

Farafonov V.G.¹, Ustimov V.I.¹, Tulegenov A.P.¹, Sokolovskaya M.V.¹, Il'in V.B.²

¹St. Petersburg State University of Aerospace Instrumentation, Bol. Morskaya 67, St. Petersburg, 190000 Russia

²St. Petersburg State University, Astronomical Institute, Universitetskij pr. 28, St. Petersburg, 198504 Russia

e-mail: far@aanet.ru, v.b.ilin@spbu.ru

The quasistatic approach is a generalization of the Rayleigh–Gans and Rayleigh approximations when the field inside a scatterer is represented by a plane wave taking into account polarizability of the particle [1]. The approach was earlier applied only to the prolate and oblate spheroids. It was found that the approach allowed one to find the main terms of the field asymptotic for small values of the ratio b/a , where a and b are the major and minor semiaxes. It is also clear that the applicability range of the approach increases for more optically soft particles, i.e. when the refractive index m becomes closer to 1. The spheroidal model means the replacement of a non-spherical scatterer with the spheroid whose optical characteristics in the far field zone are close to those of the modelled particle [2]. We combine both approaches, numerically consider the accuracy of the improved spheroidal models in different cases and discuss how it increases with a decrease of $|m - 1|$ and b/a .

References

- [1] B. Posselt, V. G. Farafonov, V. B. Il'in, Light scattering by multi-layered spheroidal particles in the quasistatic approximation, *Measurement Science & Technology*, **13**, 256–262 (2002).
- [2] V. G. Farafonov, V. I. Ustimov, V. B. Il'in, M. V. Sokolovskaya, A spheroidal model for small layered scatterers, *Optics & Spectroscopy*, **124**(2), in press (2018).

Difference equations, uniform quasiclassical asymptotics and Airy functions

Fedotov A.¹, Klopp F.²

¹St. Petersburg State University, Russia

²Université Pierre et Marie Curie, France

e-mail: a.fedotov@spbu.ru, frederic.klopp@imj-prg.fr

Let us consider the difference Schrödinger equation

$$g(z + h) + g(z - h) + v(z)g(z) = Eg(z), \quad (1)$$

where h is a positive parameter, z is a complex variable, and v is an analytic function. In the case of small h , the solutions to (1) have quasiclassical behavior. Buslaev and Fedotov studied the equation with $v(z) = 2 \cos z$, i.e. Harper equation, for small h and developed for this equation an analog the complex WKB method. It was later generalized to a wide class of v , see, for example, [A. A. Fedotov, E. V. Shchetka. Complex WKB method for difference equations in bounded domains. *Journal of Mathematical Sciences (New York)*, 2017, 224(1), 157–169]. The complex WKB method allows to describe the asymptotics of the solutions to (1) in domains of the complex plane, where $\pm 2 + v(z) \neq E$. The points where $\pm 2 + v(z) = E$ play the same role for (1) as the turning points for differential Schrödinger equations. In the framework of the method, we construct solutions that have the asymptotics of the form

$$g(z) = \frac{e^{\frac{i}{h} \int^z p(z) dz + o(1)}}{\sqrt{\sin p(z)}}, \quad (2)$$

where p is an analytic branch of the momentum defined by the equation $2 \cos p + v(z) = E$.

In this talk, we describe the quasiclassical asymptotics of solutions to (1) in a neighborhood (independent of h) of the points, where $\pm 2 + v(z) = E$.

Suppose that z_0 is a branch point of p . Then $\cos p(z_0) \in \{-1, +1\}$ and $\sin p(z_0) = 0$. So, near z_0 the asymptotic formula (2) is no longer applicable. This phenomenon is well known in the case of one-dimensional differential Schrödinger equations: in a vicinity of a turning point, the usual asymptotic formulas of the WKB method must be replaced by more complicated ones: the asymptotic expansions contain Airy functions and their derivatives.

Suppose that $z_0 \in \mathbb{C}$ is a branch point of p such that $\frac{dv}{dz}(z_0) \neq 0$, and that V is a sufficiently small neighborhood of z_0 (independent of h). Then we can define a function ζ analytic in V by the formula

$$\zeta(z) = \left(\frac{3i}{2} \int_{z_0}^z (p(z) - p(z_0)) dz \right)^{2/3},$$

where we integrate from z_0 to z in V . We have proved

Theorem. *Let u be a solution to the Airy equation. There exists a solution f to equation (1) that is analytic in V and admits the asymptotic representation*

$$f(z) = \frac{(\zeta(z))^{1/4}}{(\sin p(z))^{1/2}} h^{1/3} u(h^{-2/3} \zeta(z)) (1 + O(h)) + O(h^{5/3} u'(h^{-2/3} \zeta(z))), \quad z \in V, \quad h \rightarrow 0. \quad (3)$$

This representation is uniform in $z \in V$.

Remark. The function $z \mapsto \frac{(\zeta(z))^{1/4}}{(\sin p(z))^{1/2}}$ is analytic in V .

As equation (3) is not local with respect to z , the proof of this theorem is much more complicated than the proof of the analogous result in the case of differential equations. To construct an Ansatz uniform in $z \in V$, one has to use non-standard techniques. The proof of the existence of solutions with the asymptotics described by this Ansatz requires to study singular integral equations.

Monodromy matrices for Harper equation

Fedotov A.¹, Shchetka E.²

¹St. Petersburg State University, 3, Ulyanovskaya st., St. Petersburg, 198504, Russia

²Chebyshev Laboratory, 14th Line, 29B, Vasilyevsky Island, St. Petersburg, 199178, Russia

e-mail: a.fedotov@spbu.ru, shchetka.ekaterina@mail.ru

Let us consider the difference equations of the form

$$\Psi(z+h) = M(z)\Psi(z), \quad z \in \mathbb{C}, \quad (1)$$

where $M : \mathbb{C} \rightarrow SL(2, \mathbb{C})$ is a given matrix-valued 1-periodic function, and $h > 0$ is a small constant parameter.

One can show that the space of solutions to (1) is a two-dimensional module over the ring of h -periodic functions, i.e., given two linearly independent solutions to this equation, any other solution equals their linear combination with h -periodic coefficients.

Since M is 1-periodic, the space of solutions to (1) is invariant with respect to the shift $z \mapsto z+1$. Being restricted to the space of solutions to (1), the corresponding shift operator can be represented by two-times-two matrices that are h -periodic in z . These matrices are called monodromy matrices, see the review [1] and references to it. In the quasiclassical limit $h \rightarrow 0$, we describe monodromy matrices for an important class of equations arising when studying a well known model (Harper equation) from the solid state physics.

References

- [1] A. A. Fedotov, Monodromization method in the theory of almost-periodic equations, *St. Petersburg Mathematical Journal*, **25**(2), 303–325 (2014).

Interaction of modes near an eigenvalue crossing for the diagonalizable perturbed Hamiltonian

Fialkovsky I.V.¹, Perel M.V.²

¹CMCC-Universidade Federal do ABC, Santo André, S.P., Brazil

²St. Petersburg State University, Russia

e-mail: fialkovsky.i@ufabc.edu.br, m.perel@spbu.ru

We study asymptotic solutions of the equation of the form:

$$\hat{\mathcal{K}}(x, \hbar)\Psi(x, \hbar) = -i\hbar\Gamma\frac{\partial\Psi(x, \hbar)}{\partial x}, \quad \hat{\mathcal{K}}(x, \hbar) \equiv \mathcal{K}(x) + \sqrt{\hbar}\mathcal{B}(x) \quad (1)$$

in the Hilbert space as $\hbar \rightarrow 0$. We assume that $\mathcal{K}(x)$, $\mathcal{B}(x)$, Γ and Γ^{-1} , are operators that are self-adjoint for real x . The latter three of them are assumed to be bounded, as well as $\mathcal{K}(x) - \mathcal{K}(0)$. Operators $\mathcal{K}(x) - \mathcal{K}(0)$ and $\mathcal{B}(x)$ have N derivatives, which are bounded. If Γ is not an identical operator, then $\Gamma^{-1}\hat{\mathcal{K}}$ is the non selfadjoint one and equations (1) include the Dirac equation and elastic equations in the plane elastic waveguide or another waveguide problems, which are described by elliptic equations.

Adiabatic modes as $\hbar \rightarrow 0$ are expressed in terms of eigenvalues and eigenfunctions of the operator $\Gamma^{-1}\hat{\mathcal{K}}$. We study the case, where such adiabatic approximation fails in the neighborhood of $x = 0$ due to the crossing of two eigenvalues β of the following spectral problem

$$\mathcal{K}(x)\varphi(x) = \beta(x)\Gamma\varphi(x). \quad (2)$$

We make specific assumptions concerning the behaviour of β and φ :

1. The eigenvalues of (2), $\beta_1(x)$ and $\beta_2(x)$, are degenerating at a single point $x = 0$ and they stay real on the whole interval. The point $x = 0$ is of a simple crossing type, i.e.,

$$\beta_2(x) - \beta_1(x) \underset{x \rightarrow 0}{\simeq} 2Qx, \quad Q > 0. \quad (3)$$

Here Q does not depend on \hbar , $Q \sim 1$, and both β_1 and β_2 are separated from the rest of the spectrum of (2) (if any) with a gap independent on \hbar .

2. The invariant subspace corresponding to $\beta_1(0) = \beta_2(0)$ is the two-dimensional one and therefore an operator $\Gamma^{-1}\mathcal{K}$ is diagonalizable.

By the method of matched asymptotic expansions, we construct an asymptotic approximation, which satisfies the equation with the discrepancy of order $\mathcal{O}(\hbar^{N+1})$ for any N . Our main result is the transition matrix, which matches the leading terms of adiabatic expansions on both sides of $x = 0$.

Two regimes are highlighted. They depend on the sign of the product N_1N_2 , $N_j = (\varphi_j(x), \Gamma\varphi_j(x))$, $j = 1, 2$. In one regime, $\text{sign}(N_1N_2) > 0$ and the crossing of eigenvalues $\beta_j(x)$ is replaced by the avoided crossing after account of perturbation $\mathcal{B}(x)$. The transition matrix in this case is the Landau–Zener one. In the regime where $\text{sign}(N_1N_2) < 0$, the crossing of eigenvalues leads to two real degeneracy points of the perturbed problem with complex ones between them. Both cases are studied in the literature for different particular problems, and we present a general expression of the transition matrix valid for both cases. Also we give a recipe as how to obtain the result without intermediate considerations if the main terms of expansions of eigenvalues β_j and eigenelements φ_j in x are known.

Author (M.V.P.) is supported by the RFBR grant 17-02-00217 A.

Low-frequency backward waves in an elastic cylindrical shell filled with fluid: comparison of shell theories and 3D theory of elasticity

Filippenko G.V.^{1,2}, **Wilde M.V.**³

¹Institute for Problems in Mechanical Engineering of RAS, Vasilievsky Ostrov, Bolshoy Prospect 61, St. Petersburg, 199178, Russia

²Saint Petersburg State University, 7-9, Universitetskaya nab., St. Petersburg, 199034, Russia

³Saratov State University, 83, Astrakhanskaya str., Saratov, 410012, Russia

e-mail: g.filippenko@gmail.com, g.filippenko@spbu.ru, mv_wilde@mail.ru

A wave with opposite signs of the phase and group velocities (backward wave) is a rare phenomenon appearing at some special combinations of parameters. This fact involves enhanced requirements to the accuracy, when the approximate theories are applied for describing the vibrations of the waveguide under consideration.

In this talk the results of investigation concerning backwards waves in a cylindrical shell filled with fluid, which were presented on the preceding conference [1], are validated by comparison with the solution on the basis of the exact 3D theory of elasticity. Three lowest modes described by Kirchhoff–Love theory of shells are considered. The statement of the problem is similar to that presented in [2]. The ideal compressible fluid is described by acoustical equations. In 3D analysis the shell is modelled as a hollow circular cylinder. Vibrations of this cylinder are described by equations of elasticity in cylindrical coordinate system. For describing the vibrations of the shell the Kirchhoff–Love theory is used as in papers [1, 2]. Beside of it, the refined shell theories are applied to the problem under consideration in order to investigate their possibilities in revealing the backwards waves. These theories are Timoshenko–Reissner-type theory [3] and refined shell theory with the modified inertia [4]. It is shown that the results of [1] concerning the shell with fluid are correct, when the parameters of the problem belong in the range of applicability of Kirchhoff–Love theory. The numerical results illustrating the ranges of parameters for which the backward waves exist are presented for each of the three shell theories and for the 3D theory of elasticity. The limits of applicability of the shell theories in describing the backwards waves when the thickness of the shell is growing are investigated. The problem of existence of backwards waves beyond these limits (i.e. in a thick-walled hollow cylinder), is also considered.

References

- [1] G. V. Filippenko, Asymptotic analysis of the waves with the negative group velocity in cylindrical shell, *Abstracts of “Days on Diffraction 2017”*, St. Petersburg, 56–57 (2017).
- [2] G. V. Filippenko, The energy flux analysis of the “shell” type waves in the infinite cylindrical shell filled with acoustical fluid, *Proc. of “Days on Diffraction 2016”*, St. Petersburg, 54–58 (2016).
- [3] R. M. Cooper, P. M. Naghdi, Propagation of nonaxially symmetric waves in elastic cylindrical shells, *J. Acoust. Soc. Amer.*, **29**, 1365–1373 (1957).
- [4] J. D. Kaplunov, L. Yu. Kossovich, E. V. Nolde, *Dynamics of Thin Walled Elastic Bodies*, Academic Press, San Diego, 1998.

Modelling longitudinal bulk strain waves in elastic waveguides with Boussinesq and Korteweg–de Vries type equations

Garbuzov F.E.¹, **Khusnutdinova K.R.**²

¹Ioffe Institute, 26 Polytechnicheskaya Street, Saint-Petersburg, 194021, Russia

²Loughborough University, Loughborough LE11 3TU, UK

e-mail: fedor.garbuzov@gmail.com, k.khusnutdinova@lboro.ac.uk

In this talk we will revisit the derivations of Boussinesq and Korteweg–de Vries type models for the description of long weakly — nonlinear longitudinal bulk strain waves in elastic waveguides within

the scope of dynamic nonlinear elasticity and Murnaghan’s model for elastic energy, with an emphasis on contributions made by L. A. Ostrovsky and A. M. Sutin [1], A. M. Samsonov [2] and A. V. Porubov [3]. Equations of this type can be successfully used to model the propagation of nonlinear longitudinal bulk strain waves in various inhomogeneous and layered waveguides (e.g. [4–6]).

References

- [1] L. A. Ostrovsky, A. M. Sutin, Nonlinear elastic waves in rods, *PMM*, **41**, 531–537 (1977).
- [2] A. M. Samsonov, *Strain Solitons in Solids and How to Construct Them*, Chapman & Hall/CRC, Boca Raton, 2001.
- [3] A. V. Porubov, *Amplification of Nonlinear Strain Waves in Solids*, World Scientific, New Jersey, 2003.
- [4] K. R. Khusnutdinova, A. M. Samsonov, Fission of a longitudinal strain solitary wave in a delaminated bar, *Phys. Rev. E*, **77**, 066603 (2008).
- [5] A. M. Samsonov, I. V. Semenova, F. E. Garbuzov, Nonlinear guided bulk waves in heterogeneous elastic structural elements, *Int. J. Non-lin. Mech.*, **94**, 343–350 (2017).
- [6] K. R. Khusnutdinova, M. R. Tranter, On radiating solitary waves in bi-layers with delamination and coupled Ostrovsky equations, *Chaos*, **27**, 013112 (2017).

Natural vibrations of some inhomogeneous rod-like systems

Gavrikov A.A.

Ishlinsky Institute for Problems in Mechanics RAS, Prospekt Vernadskogo 101-1, Moscow, Russia
 e-mail: gavrikov@ipmnet.ru

In this study, the results of application of an iterative approach to solution of eigenproblems are presented. The method utilized was developed for solving the scalar and vector Sturm–Liouville problems that are nonlinear in the spectral parameter [1–3], and then was generalized to solve the linear Hamiltonian systems [4]. It is based on the shooting procedure with a Newton-type spectral correction on each iteration step.

In the current report, the proposed method is applied to a number of transverse vibrating rod-like systems, that are both linear and nonlinear in the spectral parameter: a beam with a density defect, for which three vibration models (Euler–Bernoulli, Rayleigh and Timoshenko) are considered; a pipe conveying fluid, that is placed on the Winkler foundation (here, the influence of an elastic substrate on the frequency shift is studied); and a nonhomogeneous tapered beam with a singularity at the end.

As an example, in Fig. 1 the results of computations of two lowest eigenfrequencies ν are shown for the hinged Timoshenko beam with a density defect. Their values are normalized to the frequencies of the homogeneous Euler beam here. The behaviour of the first (curves 1 and 2 corresponding to small and big defects, respectively) and the second (curves 3 and 4, small and big defects, correspondingly) eigenfrequencies is presented while the place of the defect d is varying.

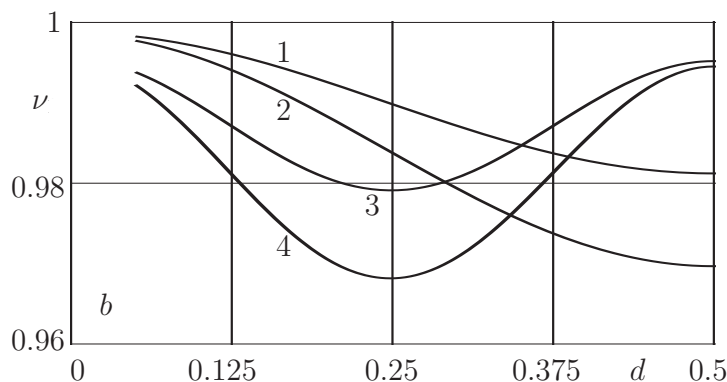


Fig. 1: Two lowest eigenfrequencies ν for the hinged Timoshenko beam with a density defect.

This work was supported by the Russian Foundation for Basic Research (project No. 16-31-60078-mol_a_dk).

References

- [1] L. D. Akulenko, A. A. Gavrikov, S. V. Nesterov, Natural oscillations of multidimensional systems nonlinear in spectral parameter, *Doklady Physics*, **40**(2), 90–94 (2017).
- [2] L. D. Akulenko, A. A. Gavrikov, S. V. Nesterov, Numerical solution of vector Sturm–Liouville problems with Dirichlet conditions and nonlinear dependence on the spectral parameter, *Computational Mathematics and Mathematical Physics*, **57**(9), 1484–1497 (2017).
- [3] L. D. Akulenko, A. A. Gavrikov, S. V. Nesterov, The synthesis of an inhomogeneous elastic system with a boundary load, *Moscow University Mechanics Bulletin*, **72**(5), 113–118 (2017).
- [4] A. A. Gavrikov, Numerical solution of eigenproblems for linear Hamiltonian systems and their application to non-uniform rod-like systems, *Days on Diffraction 2017*, St. Petersburg, 122–127 (2017).

Evolution of a trapped mode of oscillation in a Bernoulli–Euler beam on the Winkler foundation with point inhomogeneity

Gavrilov S.N.^{1,2}, Mochalova Yu.A.¹, Shishkina E.V.¹

¹Institute for Problems in Mechanical Engineering RAS, St. Petersburg, Bolshoy pr. V.O., 61

²Peter the Great St. Petersburg Polytechnic University, St. Petersburg, Polytechnicheskaya str., 29
e-mail: serge@pdm.ras.ru, yumochalova@yandex.ru, shishkina_k@mail.ru

We consider a mechanical system with mixed spectrum of natural oscillations. This is an infinite Bernoulli–Euler beam on the Winkler elastic foundation with point inhomogeneity (the concentrated spring with negative stiffness). The governing equation in the dimensionless form can be written as follows:

$$w_{tt} + w_{xxxx} + w = P(t)\delta(x), \quad (1)$$

$$P(t) = |K|w(0, t) + p(t). \quad (2)$$

Here x and t are the position and the time, respectively; w is the displacement, $P(t)$ is the force on the beam from the point spring, $p(t)$ such that $p(t) \equiv 0$ for $t > t_0 > 0$ is the external force on the inclusion, $-K$ (where $K > 0$) is the concentrated spring stiffness.

It easy to show that for $K = \text{const}$, $p = 0$ this system in a certain domain of the problem parameters can have a mixed spectrum of natural frequencies of oscillation. In the system under consideration, unique trapped mode of oscillation can exist. The corresponding frequency is

$$\Omega_0 = \sqrt{1 - \frac{|K|^{4/3}}{4}}. \quad (3)$$

In the paper, we use asymptotic procedure analogous to the one suggested in [1–3] for different problems concerning the infinite string, and based on the method of multiple scales [4], to construct the solution of (1), (2) together with zero initial conditions $w|_{t<0} \equiv 0$ in the case the spring with slowly varying stiffness $K = K(\epsilon t)$. Here ϵ is a formal small parameter. We show that for the weakly non-stationary system the amplitude of localized oscillation is proportional to

$$W_0 = C_0 \frac{(1 - \Omega_0^2)^{1/8}}{\Omega_0^{1/2}}. \quad (4)$$

The constructed solution is verified by independent numerical calculations. The comparison demonstrates a good mutual agreement.

References

- [1] S. N. Gavrilov, D. A. Indeitsev, *PMM J. Appl. Math. Mech.*, **66**, 825–833 (2002).
- [2] D. A. Indeitsev, S. N. Gavrilov, Yu. A. Mochalova, E. V. Shishkina, *Doklady Physics*, **61**, 620–624 (2016).
- [3] S. N. Gavrilov, Yu. A. Mochalova, E. V. Shishkina, *Proc. Int. Conf. DAYS on DIFFRACTION 2017*, pp. 128–133.
- [4] A. H. Nayfeh, *Perturbation Methods*, Wiley, 1973.

Theoretical and experimental study of resonance Lamb wave scattering by an impact-induced damage

Golub M.V., Eremin A.A., Glushkov E.V., Glushkova N.V.

Institute for Mathematics, Mechanics and Informatics, Kuban State University, Krasnodar, 350040, Russian Federation

e-mail: m_golub@inbox.ru, eremin_a_87@mail.ru, evg@math.kubsu.ru, nvg@math.kubsu.ru

Impact-induced delaminations are common defects in laminate composites occurring during their life-time cycle. Among them, multi-ply delaminations located at and beneath the impact zone are especially challenging for characterization. Since damage detection in thin-walled composite structures could be achieved employing elastic guided waves (GWs), the investigation of their diffraction by this type of defects is of particular interest.

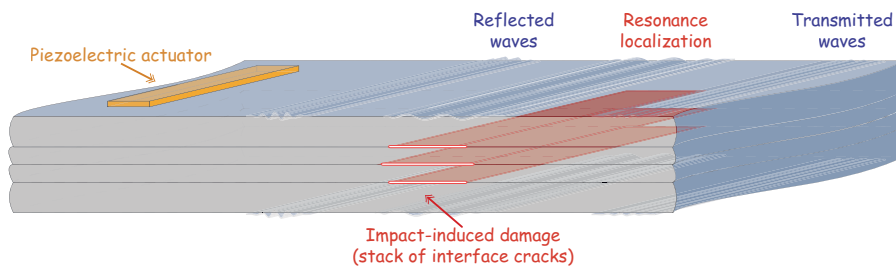


Fig. 1: Geometry of the problem.

In 2D simulation, it has been shown that GW diffraction with delamination-like obstacles could be featured by resonance scattering resulting in prolonged high-amplitude damage localized motion at its eigenfrequencies [1–3]. Whereas these frequencies strongly depend on the obstacle geometry and location within the waveguide thickness, we hope that this phenomenon could have a high potential for the identification of multi-ply delaminations as well.

In the current contribution, theoretical and experimental results for the 3D problem are discussed: GW resonance interaction with a stack of differing in size planar three-dimensional delaminations in an isotropic laminate structure is investigated. Relying on the developed semi-analytical computational model [1, 2], eigenfrequencies and eigenforms are analyzed depending on the geometrical properties of the delamination stack. Experimental studies for aluminium plates with a stack of rectangular cracks have been performed to validate the computational results. An approach for experimental resonance frequency extraction from B-scan and pointwise measurements with scanning Laser Doppler vibrometry has been proposed and implemented. A good agreement between predicted and measured eigenfrequencies and corresponding localization patterns (eigenforms) is observed. The dependence of eigenfrequency detectability on the waveguide side of surface measurements is also illustrated and discussed.

The work is supported by the Russian Science Foundation (Project 17-11-01191).

References

- [1] E. V. Glushkov, N. V. Glushkova, M. V. Golub, Ch. Zhang, Resonance blocking of travelling waves by a system of cracks in an elastic layer, *Acoustical Physics*, **55**, 8–16 (2009).

- [2] E. V. Glushkov, N. V. Glushkova, M. V. Golub, A. A. Eremin, Resonance blocking and passing effects in two-dimensional elastic waveguides with obstacles, *Journal of the Acoustical Society of America*, **130**, 113–121 (2011).
- [3] E. V. Glushkov, N. V. Glushkova, M. V. Golub, J. Moll, C.-P. Fritzen, Wave energy trapping and localization in a plate with a delamination, *Smart Materials and Structures*, **21**, 125001 (2012).

Semi-analytical hybrid approach for modelling wave motion excited by a piezoelectric transducer in periodic layered composite with a crack

Golub M.V.¹, Shpak A.N.¹, **Fomenko S.I.**¹, Zhang Ch.²

¹Institute for Mathematics, Mechanics and Informatics, Kuban State University, Krasnodar, 350040, Russian Federation

²Chair of Structural Mechanics, Department of Civil Engineering, University of Siegen, Paul-Bonatz Strasse 9-11, D-57076, Siegen, Germany

e-mail: m_golub@inbox.ru, alisashpak7@gmail.com, sfom@yandex.ru, c.zhang@uni-siegen.de

This paper presents an efficient semi-analytical hybrid approach for modelling the interaction of a piezoelectric transducer and a layered periodic elastic structure with a crack. This is a hybrid approach that combines the frequency domain spectral element method [1] and the semi-analytical integral approach [2] at the boundary between a waveguide and a transducer. The spectral element method allows simulating a complex-shaped transducer (e.g. curvilinear or with wrapped electrodes). The integral approach can efficiently describe the wave excitation and propagation in layered periodic structures with internal defects. The total wave-field is a sum of the wave-field generated by the piezoelectric transducer and the wave-field scattered by a crack. The boundary integral equation method is applied in order to determine the unknown crack-opening-displacements on the crack-faces.

The authors are grateful to the support by Russian Foundation for Basic Research and German Research Foundation (DFG) under joint grant 18-501-12069 / ZH 15/29-1.

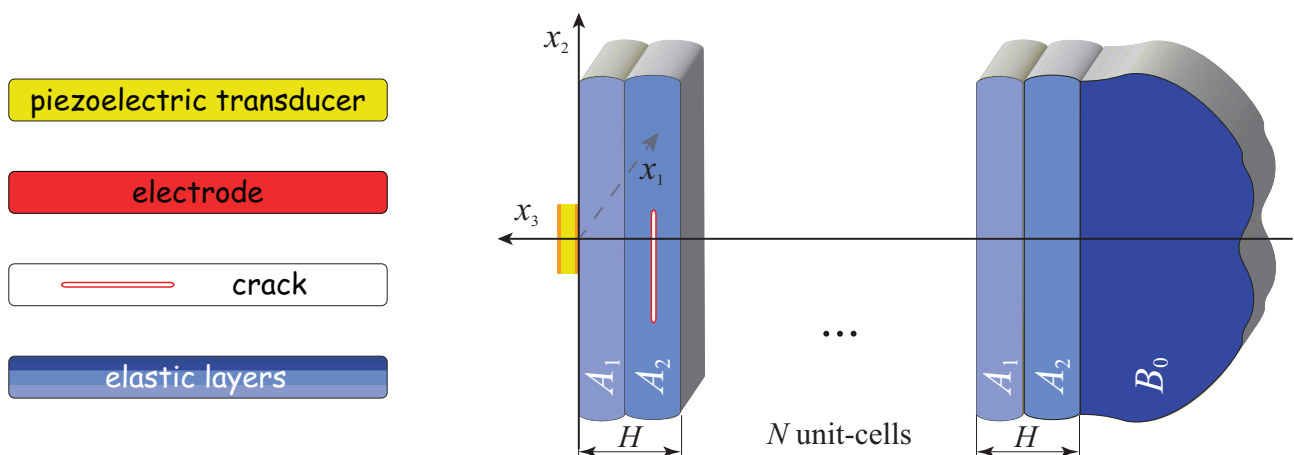


Fig. 1: Geometry of the problem.

References

- [1] D. Komatitsch, J. Tromp, Introduction to the spectral element method for three-dimensional seismic wave propagation, *Geophysical Journal International*, **139**, 806–822 (1999).
- [2] E. V. Glushkov, N. V. Glushkova, *The Integral Transforms and Wave Processes*, Kuban State University Press, Krasnodar, 2017.

High frequencies for some spectral problems in thin structures

Gómez D.

Universidad de Cantabria, Av. de Los Castros s.n. 39005 Santander, SPAIN
e-mail: gomezdel@unican.es

We analyze the behavior of the spectrum of the Laplacian in a planar domain. The thickness of the domain or of one of the components depends on a small parameter ε that we shall make to go to zero. The boundary conditions can be Dirichlet or Neumann depending on the problem. As it is well known, in some of these models, the low frequencies can give rise to vibrations affecting only a part of the structure or ignore, e.g., transverse vibrations (cf. [1, 3–7]). We characterize the asymptotic behavior as $\varepsilon \rightarrow 0$ of the high frequencies, in a certain range which depends on the structure. In particular, we look at the behavior of the high frequencies in a T-like planar structure (cf. [2]).

References

- [1] L. Friedlander, M. Solomyak, On the spectrum of the Dirichlet Laplacian in a narrow strip, *Israel Journal of Mathematics*, **170**, 337–354 (2009).
- [2] A. Gaudiello, D. Gómez, E. Pérez. High frequencies in a T-like structure, *in preparation*.
- [3] A. Gaudiello, A. Sili, Asymptotic analysis of the eigenvalues of a Laplacian problem in a thin multidomain, *Indiana University Mathematics Journal*, **56**, 1675–1710 (2007).
- [4] D. Gómez, S. A. Nazarov, E. Pérez, Spectral stiff problems in domains surrounded by thin stiff and heavy bands: local effects for eigenfunctions, *Networks and Heterogeneous Media*, **6**, 1–35 (2011).
- [5] S. A. Nazarov, Localization effects for eigenfunctions near to the edge of a thin domain, *Mathematica Bohemica*, **127**, 283–292 (2002).
- [6] S. A. Nazarov, E. Pérez, J. Taskinen, Localization effect for Dirichlet eigenfunctions in thin non-smooth domains, *Transactions of the American Mathematical Society*, **368**, 4787–4829 (2016).
- [7] G. P. Panasenko, E. Pérez, Asymptotic partial decomposition of domain for spectral problems in rod structures, *Journal de Mathématiques Pures et Appliquées*, **87**, 1–36 (2007).

Harmonic waves in simplest reduced Kelvin’s and gyrostatic media under external body follower torque

Grekova E.F.

Institute for Problems in Mechanical Engineering, Russian Academy of Sciences, Bolshoy pr. V.O., 61, St. Petersburg, Russia
e-mail: elgreco@pdmi.ras.ru

We consider two types of homogeneous elastic media whose body-points possess finite dynamic spin. One is Kelvin’s medium [1], whose particles have axial symmetry and may freely rotate about their axes not causing any stresses in the medium. Another is gyrostatic medium, consisting of spherical particles containing rotors. In both cases we consider large rotation of rotors (or axisymmetric particles) about their axes. Other rotational ($\boldsymbol{\theta}$) and translational (\mathbf{u}) displacements are infinitesimal. We consider infinitesimal tensors of inertia, but large velocity of proper rotation, resulting in finite dynamic spin. The gyroscopic term prevails in dynamics of both media. In the natural configuration all axes of rotors coincide (with \mathbf{m} the unit vector) and their angular velocities are equal.

We consider *reduced* Kelvin’s medium and *reduced* gyrostatic medium, whose elastic energy does not depend on the gradient of turn. Such a constraint for the linear isotropic Cosserat medium without finite dynamic spin yields the existence of a band gap for shear waves, i.e. this medium is a single negative acoustic metamaterial. In the case of the simplest reduced gyrostatic medium [2] with isotropic strain energy, for zero external loads most of harmonic waves are polarized. If $\mathbf{k} \cdot \mathbf{m} \neq 0$

and $\mathbf{k} \cdot \mathbf{m} \neq \pm 1$, where \mathbf{k} is the wave vector, for each direction of wave propagation $\hat{\mathbf{k}} = \mathbf{k}/|\mathbf{k}|$ there are two shear harmonic waves which are elliptically (frequency-dependent) polarized, one of them has a band gap and another one has not. For $\mathbf{k} \cdot \mathbf{m} = 0$ we have two shear plane waves, one is non-dispersive and another one with a band gap analogously to the reduced Cosserat continuum. For $\mathbf{k} \cdot \mathbf{m} = \pm 1$ both shear waves have circular polarization.

In this work we consider a similar problem for the simplest gyrostatic medium and for Kelvin's medium, both subjected to the external body torque $b\boldsymbol{\theta}$. Equations of Kelvin's medium have an exact analogy with the equations of ferromagnetic insulators in the approximation of quasimagnetostatics [1, 3] in the state close to the magnetic saturation. Such a torque in magnetic materials is caused by constant magnetic field. Considering a reduced Kelvin's medium is analogous to neglect of the exchange interactions taking into account spin-lattice interactions (stresses caused in the material by the change of the direction magnetisation relatively to the surrounding medium). In an artificially made gyrostatic medium we may provide this torque also by means of magnetic induction.

The character of waves in both media is similar to the case considered in [2] for $b > 0$, but we can partially control the band gap, which is present for one branch: when b increases, the band gap also increases and moves to the domain of higher frequencies. An interesting phenomenon is observed for $b < 0$ but sufficiently small in absolute value to provide the stability of the medium. For some domain of parameters b , $\hat{\mathbf{k}} \cdot \mathbf{m}$ and elastic constants both branches have cut-off frequency, and one of them has a band with negative group velocity just above its cut-off frequency. Thus these media are double negative acoustic metamaterials in this domain.

References

- [1] E. F. Grekova, P. A. Zhilin, Basic equations of Kelvin's medium and analogy with ferromagnets, *Journal of Elasticity and the Physical Science of Solids*, **64**(1), 29–70 (2001).
- [2] E. F. Grekova, Simplest linear homogeneous reduced gyrocontinuum as an acoustic metamaterial, in *Generalized Models and Non-classical Approaches in Complex Materials 1*, Altenbach, H., Pouget, J., Rousseau, M., Collet, B., Michelitsch, Th. (Eds.), Springer, 2018.
- [3] G. A. Maugin, *Continuum Mechanics of Electromagnetic Solids*, Elsevier, North Holland series for Applied Mathematics and Mechanics, vol. 33, Amsterdam, 2013.

Electromagnetic field structure of a charge flying out from a vacuum area to bilayer one in a circular waveguide

Grigoreva A.A., Tyukhtin A.V., Vorobev V.V., Galyamin S.N.

Saint Petersburg State University, 7/9 Universitetskaya nab., St. Petersburg 199034, Russia
e-mail: aleksandra.a.grigoreva@gmail.com, a.tyukhtin@spbu.ru

The analysis of electromagnetic field produced by charged particle in a dielectric loaded waveguide is relevant for wakefield acceleration technique development [1]. The influence of the transverse boundary in the waveguide has been considered earlier only in the case of homogeneous filling of the contacting areas [2]. Meanwhile the combination of layer structure and transverse boundary leads to the more complicated problems.

We consider the infinite circular waveguide containing a vacuum area ($z < 0$) and bilayer area ($z > 0$). The latter consists of a dielectric layer with characteristics ε_d , μ_d and a central vacuum channel. Point charge or thin Gaussian bunch moves along the waveguide axis with uniform velocity v and intersects the transverse boundary at time $t = 0$. It is assumed that the condition $\sqrt{\varepsilon_d \mu_d} \beta > 1$ is satisfied, i.e. Cherenkov radiation is generated in the bilayer area. Solution is performed by representation of the total electromagnetic field in each waveguide area as a sum of known "forced" field (i.e., the source field in a regular infinite waveguide) [3] and unknown "free" field (describing the transverse boundary influence). The "free" field is written as a series of corresponding eigenfunctions.

Heavy emphasis is placed on the investigation of the wave field main part (which can be named as “reduced wakefield”) in the bilayer waveguide area.

Fig. 1 presents typical “reduced wakefield” depending on time at the given point. One can see that the field structure is simplified with time.

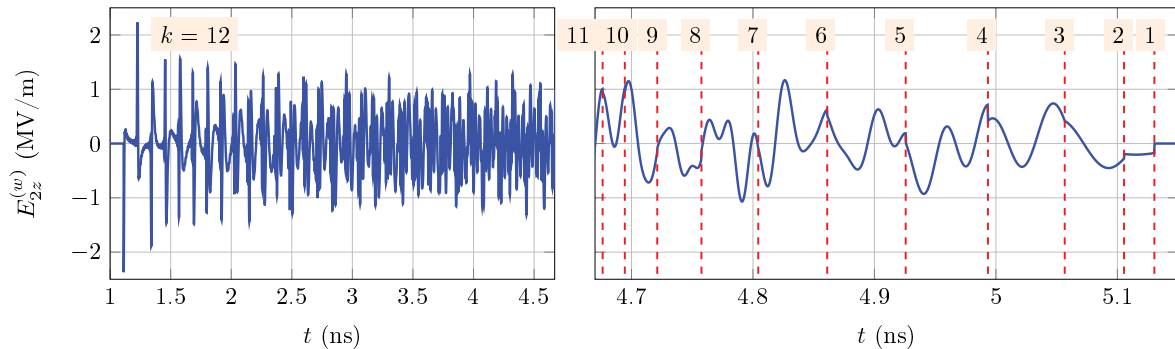


Fig. 1: Time dependence of the “reduced wakefield” longitudinal component $E_{2z}^{(w)}$ at point $r = 0$ cm, $z = 30$ cm. Waveguide and point charge parameters are $a = 1$ cm, $b = 0.2$ cm, $\varepsilon_d = 5.7$, $\mu_d = 1$, $q = 1$ nC, $v = 0.9c$. The number k means the number of modes in corresponding time interval.

References

- [1] M. Rosing, W. Gai, Longitudinal- and transverse-wake-field effects in dielectric structures, *Phys. Rev. D*, **42**, 1829–1834 (1990).
- [2] T. Yu. Alekhina, A. V. Tyukhtin, Radiation of a charge in a waveguide with a boundary between two dielectrics, *J. Phys.: Conf. Ser.*, **357**, 012010 (2012).
- [3] B. M. Bolotovskii, Theory of Cherenkov radiation (iii), *Phys. Usp.*, **4**, 781–811 (1962).

Surface acoustical waves at the boundary of bimodule medium

Gusev V.A.

Lomonosov’s Moscow State University, Physical Faculty, Department of Acoustics, Russia, 119991, Moscow, Leninskie gori
 e-mail: vgusev@bk.ru

It is well known that localized acoustic disturbances such as Rayleigh and other types waves propagate along the interfaces of layered media. These waves have sufficient energy and less geometric divergence compared to bulk waves. The strong dependence of the localization depth of these waves on its length allows its using for diagnostics of medium parameters in the problems of geophysics and nondestructive testing. The greatest interest is associated with the study of inhomogeneous media with complex internal structure. Such media often shows structural and nonclassical inhomogeneities and nonlinearities, which depends on frequency and amplitude of acoustic wave. For example, pores or cracks existing in medium shows such complex dynamics. It is clear that in the presence of cracks, the behavior of medium will be different in phases of expansion and contraction. A small effort is enough to stretch cracks, and, on the contrary, for its compression one need more power. The simplest model of such medium is a bimodule medium with different modules of elasticity in compression and in tension. A more complex analogue of this model is the medium in which the elasticity modulus changes at some critical value of the driving amplitude. This means that, for example, medium contains some internal structure. When exceeding the critical value of the driving amplitude the response of this structure turns on or the destruction of this structure matter that leads to changes in elastic moduli.

The generation of surface acoustic waves on the boundary of an elastic bimodule medium is described. The rheological equation for surface wave propagation in such media is suggested. It

is supposed that elastic moduli depend only on volume change of medium and are different for compression and rarefaction phases. This model allows to formulate equations for different phases and derive their solutions. The temporal profile of the surface wave is built. Different phases propagates with different speeds and have different amplitudes. It is shown that in the bimodule medium wave profile is fundamentally asymmetric. During propagation the shock front is formed so some part of each phase annihilates. This leads to the formation of the unipolar limit profile at large distance. The developed model of medium allows to describe acoustic phenomena with non-classical nonlinearity in shallow sea in the presence of bottom soil with the amplitude-dependent threshold effects, caused by the presence of internal structure such as cracks or polymeric chains.

This work was supported by Russian Foundation For Basic Research (project 16-02-00764).

Appell hypergeometric expansions of the solutions of the general Heun equation

A.M. Ishkhanyan

Institute for Physical Research, NAS of Armenia, 0203 Ashtarak, Armenia

e-mail: aishkhanyan@gmail.com

Starting from a second-order Fuchsian differential equation having five regular singular points, an equation obeyed by a function proportional to the first derivative of the solution of the Heun equation, we construct several expansions of the solutions of the general Heun equation in terms of Appell generalized hypergeometric functions of two variables of the first kind. Several cases when the expansions reduce to those written in terms of simpler mathematical functions such as the incomplete Beta function or the Gauss hypergeometric function are identified. The conditions for deriving finite-sum solutions via termination of the series are discussed.

In general, the coefficients of expansions obey four-term recurrence relations. However, there exist certain choices of parameters for which the recurrence relations involve only two terms, though not necessarily successive. For such cases, the coefficients of expansions are explicitly calculated and the general solution of the Heun equation is constructed in terms of the Gauss hypergeometric functions.

Finally, we show that the four-term recurrence relations for expansion coefficients can always, for arbitrary parameters, be reduced to three-term ones. This is achieved by a “desingularization” through a third-order ordinary differential equation derived from the equation obeyed by the derivative of the solution of the Heun equation.

Generalized confluent hypergeometric solutions of the confluent Heun equation

T.A. Ishkhanyan^{1,2,3}, C. Leroy³, A.M. Ishkhanyan¹

¹Institute for Physical Research, NAS of Armenia, Ashtarak, 0203 Armenia

²Moscow Institute of Physics and Technology, Dolgoprudny, 141700 Russian Federation

³Université de Bourgogne Franche-Comté, Dijon, 21078 France

e-mail: tishkhanyan@gmail.com

We show that the single confluent Heun equation with non-zero ε (this is the parameter characterizing the irregular singularity at the infinity) admits infinitely many solutions in terms of the generalized hypergeometric functions ${}_pF_p$. For each of these solutions a characteristic exponent of a regular singularity of the confluent Heun equation is a non-zero integer and the accessory parameter obeys a polynomial equation. Each solution can be written as a linear combination with constant coefficients of a finite number of the Kummer confluent hypergeometric functions.

Furthermore, we show that for the Ince limit $\varepsilon = 0$ the confluent Heun equation admits infinitely many solutions in terms of the functions ${}_pF_{p+1}$. Here again a characteristic exponent of a regular singularity should be a non-zero integer and the accessory parameter should obey a polynomial

equation. This time, each solution can be written as a linear combination with constant coefficients of a finite number of the Bessel functions.

Transversal connecting orbits of Lagrangian systems with turning points: Newton–Kantorovich method

Ivanov A.V.

Saint-Petersburg State University, 199034, Russian Federation, Saint-Petersburg, Universitetskaya nab. 7/9

e-mail: a.v.ivanov@spbu.ru

We study a time-dependent Lagrangian system with Lagrangian

$$L(q, \dot{q}, t) = \frac{1}{2}|\dot{q}|^2 - f(t)V(q) \tag{1}$$

on a compact Riemannian manifold \mathcal{M} . We assume that the potential V is of class $C^2(\mathcal{M})$ and the factor f satisfies the following conditions:

(A₁) there exists a unique $t_0 \in \mathbb{R}$ such that $f(t_0) = 0$,

(A₂) $|f(t)| \rightarrow +\infty$ as $t \rightarrow \pm\infty$,

(A₃) $f''(t)f(t) < 3/2(f'(t))^2$ for all $t \in \mathbb{R}$.

Systems of this type often arise in different areas of physics. In particular, if $f(t) = (t - t_0)^\kappa$ it can be considered as an approximation of a Lagrangian system with potential $U(q, t)$ in a vicinity of a turning point $t = t_0$. Let $X_c^{+(-)}$ denotes a subset of \mathcal{M} at which $f(t)V(x)$ as a function of x distinguishes its maximum for any fixed positive (negative) t . We assume that

(A₄) X_c^\pm consists of isolated nondegenerate critical points of V .

Under these assumptions it was proved by variational methods that such system possesses infinitely many doubly asymptotic trajectories connecting any two points $x_\pm \in X_c^\pm$ [2]. However, the transversality of such trajectories has not been established. One should note that transversality condition is crucial for the existence of connecting orbits of singularly perturbed time-periodic Lagrangian system with turning points.

In the present work we study the problem of existence of transversal connecting orbits for the system (1) joining any two fixed points x_- and x_+ such that $x_\pm \in X_c^\pm$. It can be shown that such orbits are in one-to-one correspondence with non-singular critical points of the action functional

$$I[q] = \int_{\mathbb{R}} [L(q, \dot{q}, t) + f(t)V(\chi(t))] dt, \quad \chi(t) = \begin{cases} x_+, & t \geq 0, \\ x_-, & t < 0. \end{cases}$$

defined on an infinite-dimensional Hilbert manifold

$$\mathfrak{M} = \left\{ q \in AC(\mathbb{R}, \mathcal{M}) : \int_{\mathbb{R}} (|\dot{q}(t)|^2 + |f(t)| \cdot |q(t) - \chi(t)|^2) dt < \infty \right\}.$$

We adopt the Newton–Kantorovich method [1] for the Riemannian manifold \mathfrak{M} and construct two sequences of expanding intervals $\Omega_k = [-T_k, T_k]$ and non-degenerate solutions $q_k : \Omega_k \rightarrow \mathcal{M}$ satisfying $q_k(\pm T_k) = x_\pm$. For any $k \geq 1$, the solution q_{k-1} obtained on the previous step is used as initial approximation for q_k . While for q_0 a geodesic γ connecting x_- and x_+ is taken as initial approximation. Under additional assumptions on the upper bounds of the potential V and its first and second derivatives, curvature of \mathcal{M} and non-degeneracy of γ , we prove that q_k converges as $k \rightarrow +\infty$ to a transversal connecting orbit q joining x_- and x_+ .

References

[1] O.P. Ferreira, B.F. Svaiter, Kantorovich’s theorem on Newton’s method in Riemannian manifolds, *Journal of Complexity*, **18**(1), 304–329 (2002).

- [2] A. V. Ivanov, Connecting orbits of Lagrangian systems in a nonstationary force field, *Regular & Chaotic Dynamics*, **21**(5), 510–522 (2016).

Variability of the phase and pulse fronts of the sound signal due to horizontal refraction in shallow water waveguide

Boris Katsnelson

University of Haifa, Israel

e-mail: bkatsnels@univ.haifa.ac.il

Variability of the interference pattern of the narrow-band sound signal in horizontal plane in shallow water waveguide in the presence of horizontal stratification, in particular due to linear internal waves, or due to variation of bathymetry in area of coastal wedge is studied. We introduce phase front as line of constant phase and pulse (amplitude) front as a line of constant amplitude/envelope. It is shown that they may have different directions in some spatial vicinity of the point of reception. Angle between these fronts depends on the waveguide's parameters and sound frequency. Similar effects were registered in laser optics for the pico-second pulses passing through the prism or nonlinear media.

Theoretical estimations and data processing methodology for getting mentioned angles from experimental acoustical data recorded by horizontal line array are proposed. On the base of analytical estimations is shown, that in typical situation, if horizontal refraction is due to linear internal waves of small amplitude (~ 1 m) or due to the bottom slope 0.01 then angle of revolution of the phase front (direction of horizontal ray) is about $1^\circ \div 2^\circ$ for an acoustical track of the length 20 km. Angle between horizontal rays, corresponding to different frequencies depends on difference between frequencies, from estimation about 0.01 deg/Hz, we get for narrow-band pulse with the band 10 Hz this angle $\sim 0.1^\circ$. Behavior of mentioned angles, which are obtained using proposed method for two episodes from Shallow Water 2006 experiment, has rather good agreement with the theory presented in the paper.

“Separation of variables” in the model problems of the diffraction theory

A.Ya. Kazakov

SPbUITD, SPbUAI

e-mail: a_kazak@mail.ru

Propagation of the whispering gallery modes in the domain $0 \leq z < \infty$, $-\infty < t < \infty$ is governed by the parabolic equation

$$i\Psi_t(z, t) + \Psi_{zz}(z, t) + zf(t)\Psi(z, t) = 0, \quad (1)$$

where function $f(t)$ describes the effective curvature of the boundary [1, 2]. The waves localized in the vicinity of the ray can be described by equation

$$i\Psi_t(z, t) + \Psi_{zz}(z, t) + z^2f(t)\Psi(z, t) = 0. \quad (2)$$

This equation describes the quantum time-dependent harmonic oscillator too. We propose new integral representations for solutions of the equations (1) and (2), which give the possibility to solve corresponding boundary problems.

References

- [1] V. M. Babich, V. S. Buldyrev, *Short-Wavelength Diffraction Theory. Asymptotic Methods*, Springer, Berlin, 1991.
- [2] V. M. Babich, N. Ya. Kirpichnikova, *The Boundary-Layer Method in Diffraction Theory*, Leningrad University, 1974.

**Asymptotical and numerical investigation of the currents
in a short-wave diffraction problem of a plane incident wave
by smooth prolate bodies of revolution
with Dirichlet and Neumann boundary conditions**

Anna Kirpichnikova¹, Nataliya Kirpichnikova²

¹Liverpool Hope University, Hope Park, Liverpool, L16 9JD, UK

²Saint-Petersburg Department of Steklov's Mathematical Institute, Fontanka, 27, Saint-Petersburg, 191023, Russia

e-mail: kirpica@hope.ac.uk, nkirp@pdmi.ras.ru

The results of numerical comparison of the currents for both boundary conditions are presented. The formulae for the currents were obtained according to the Leontovich–Fock parabolic equation method [1]. We investigated the influence of the expansion term that contains the big parameter which reflects body's elongation on the Fock's current.

Diffraction formulae obtained in [2, 3], give integral representation of the field in some neighbourhood of the point, which is located on the boundary of geometric shadow. These formulae give a continuous transformation from ray field in the lit area to the field in the shadow using Fock's currents.

References

- [1] V. A. Fock, *Electromagnetic Diffraction and Propagation Problems*, International Series of Monograph on Elecromagnetic Waves, **1**, Pergamon Press, 1965.
- [2] N. Ya. Kirpichnikova, M. M. Popov, Leontovich–Fock parabolic equation method in the problems of short-wave diffraction by prolate bodies, *Zap. Nauchn. Sem. POMI*, **409**(42), 55–79 (2012).
- [3] A. S. Kirpichnikova, N. Ya. Kirpichnikova, The Leontovich–Fock parabolic equation method in the Neumann diffraction problem on a prolate body of revolution, *Zap. Nauch. Sem. POMI*, **461**(47), 148–173 (2017).

Astigmatic Gaussian beam: exact solution of the Helmholtz equation

Aleksei P. Kiselev^{1,2,3}, Alexandr B. Plachenov^{4,5}

¹Steklov Mathematical Institute, St. Petersburg Department, Russia

²St. Petersburg State University, St. Petersburg, Russia

³Institute for Problems in Mechanical Engineering RAS, St. Petersburg, Russia

⁴Moscow Technological University (MIREA), Moscow, Russia

⁵Saint Petersburg State University of Aerospace Instrumentation (SUAI), St. Petersburg, Russia e-mail: aleksei.kiselev@gmail.com, a_plachenov@mail.ru

Fundamental mode of astigmatic Gaussian beam is described by the expression (see, e.g., [1, 2])

$$G = \sqrt{\det \mathbf{\Gamma}(z)} \exp ik \left\{ z + \frac{1}{2} \mathbf{r}_{\perp}^T \mathbf{\Gamma}(z) \mathbf{r}_{\perp} \right\}, \quad (1)$$

where $\mathbf{r}_{\perp}^T = (x, y)$, T stands for transposition and $\mathbf{\Gamma}(z)$ is an arbitrary symmetric matrix with positive imaginary part that satisfies the equation $\mathbf{\Gamma}_z + \mathbf{\Gamma}^2 = 0$. Expression (1) is obtained in the framework of paraxial parabolic equation approach [1] and asymptotically satisfies the Helmholtz equation

$$u_{xx} + u_{yy} + u_{zz} + k^2 u = 0 \quad (2)$$

in a neighborhood of the z -axis. It is strongly localized there under the condition

$$kb_{\min} \gg 1, \quad (3)$$

where b_{\min} is a minimal eigenvalue of the matrix $-\Im \mathbf{\Gamma}^{-1}$, which does not depend on z .

We present an exact solution of the equation (2) in free space, dependent on a dimensionless parameter kb_{\min} and asymptotically coinciding with (1) when $kb_{\min} \gg 1$. The construction generalizes that described in [3] for a much simpler axisymmetric case and is based on expansion in plane waves.

References

- [1] V. M. Babič, V. S. Buldyrev, *Asymptotic Methods in Short-Wavelength Diffraction Theory*, Springer, New York, 1991.
- [2] E. Heyman, L. B. Felsen, Gaussian beam and pulsed-beam dynamics: complex-source and complex-spectrum formulations within and beyond paraxial asymptotics, *J. Opt. Soc. Am. A*, **18**(7), 1588–1611 (2001).
- [3] A. P. Kiselev, Time-harmonic Gaussian beams: Exact solutions of the Helmholtz equation in free space, *Opt. Spectr.*, **123**(6), 935–939 (2017). Erratum *Opt. Spectr.*, **124**(3), 450 (2018).

Self-focusing of non-paraxial single cycle optical pulses in nonlinear media

Kislin D.A., Knyazev M.A., Shpolyanskiy Y.A., Kozlov S.A.

ITMO University, St. Petersburg, Russia

e-mail: kislin.dmitriy@gmail.com, knyazev.michael@gmail.com,

yuri.shpolyanskiy@gmail.com, kozlov@mail.ifmo.ru

So far, there are just a few papers on the study of self-action of waves consisting of a small number of oscillations, which are compressed into transverse sizes that are commensurable with the central wavelength of the radiation. In paper [1] it is shown that it is convenient to use the spectral approach in the theoretical analysis of self-action of such waves with an extra-wide temporal and spatial spectra in nonlinear media.

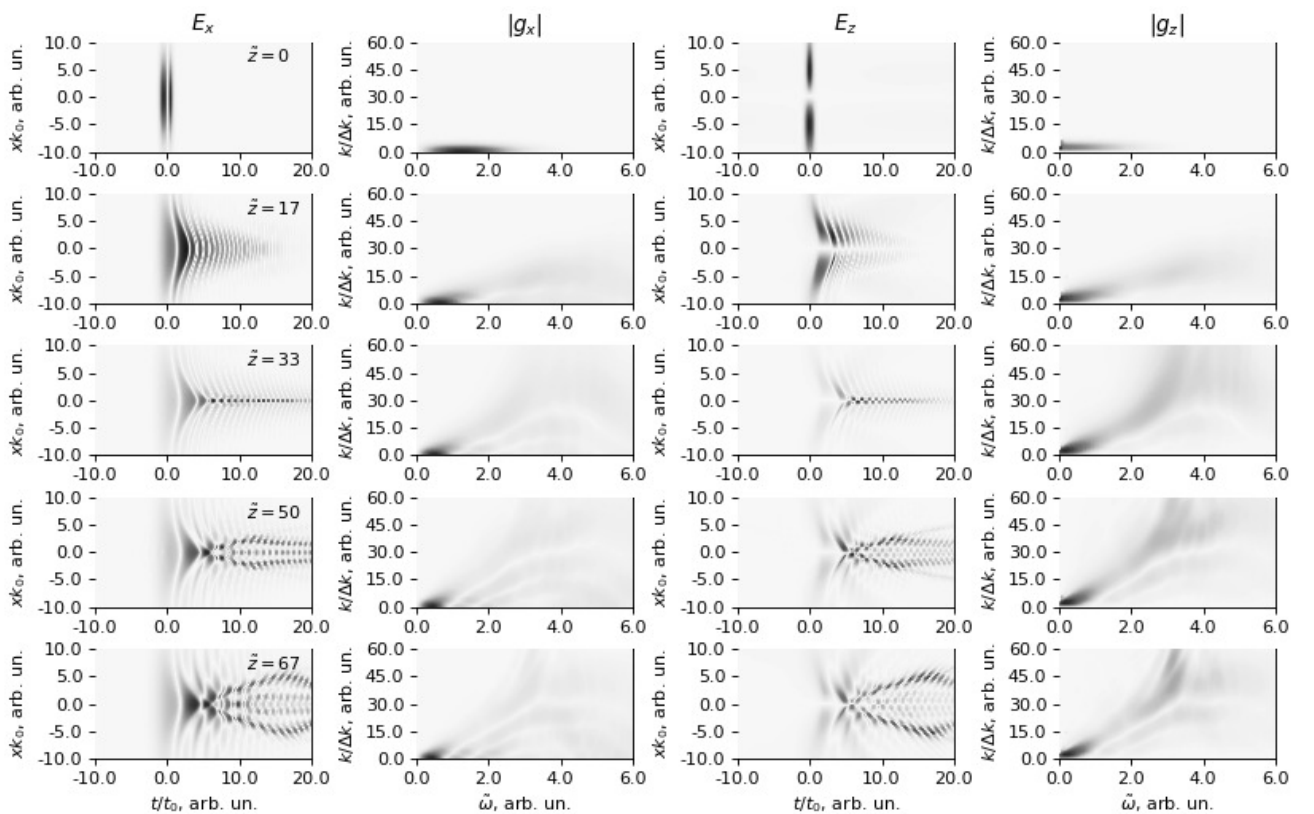


Fig. 1: Typical evolution of the transverse and longitudinal components of the electric field and their spectra in a model nonlinear medium with a nonlinear additive to the refractive index $\Delta n_{nl} = 10^{-2}$.

In this paper, apparently, it is given the analysis of self-action of non-paraxial waves with a small number of oscillations as a continuation of the previous paper. The characteristic evolutions of the transverse and longitudinal components of the electric field are shown. We give the analysis of effects that occur in the process of impulse propagation through the nonlinear medium. Well known and in present work it is shown once again that longitudinal component is asymmetric across a propagation axis. One of the main features that is revealed it is the transfer of energy from the transverse component to the longitudinal one and backward. As a consequence of this, the transverse component becomes asymmetrical too. Moreover, the considerable part of initial energy goes away due to emergence of evanescent waves. At the same time, the energy of the longitudinal component is comparable to the outgoing evanescent energy.

References

- [1] A. Ezerskaya, D. Ivanov, S. Kozlov, Yu. Kivshar, Spectral approach in the analysis of pulsed terahertz radiation, *Journal of Infrared, Millimeter and Terahertz Waves*, **33**(9), 926–942 (2012).
- [2] A. Drozdov, A. Sukhorukov, S. Kozlov, Spatio-temporal dynamics of single-cycle optical pulses and nonlinear frequency conversion, *Int. J. Mod. Phys. B*, **28**, 1442007 (2014).

Inverse problem of tomography of thick layer

Knyazkov D.

Ishlinsky Institute for Problems in Mechanics RAS, Prospekt Vernadskogo 101-1, Moscow, 119526, Russia

e-mail: knyaz@ipmnet.ru

The report considers a problem of diffraction of plane electromagnetic wave on a periodic layer. The layer is bounded by two surfaces. The layer's permittivity is given by a periodic function. The result of diffraction is calculated by the means of Galerkin type method proposed in [1]. The method allows us to reduce the initial diffraction problem to a system of first order differential equations. The layer's irregularities are of the same spatial size as the wavelength of the radiation. Earlier, the method was implemented for the 2-dimensional cases of incidence of H-polarized [2] and E-polarized [3] wave to a cylindrical periodic layer. The developed computer program can be accessed through the internet [4]. This approach was used for the precise modeling of the diffraction for the needs of sea surface radiometry [5] and for estimation of accuracy of the approximate local perturbations method proposed in [6]. The inverse problem of reconstruction of the layer's inner structure can be considered in the scope of the model. For example, a 2-dimensional problem of scattering on a cylinder buried underneath a sinusoidal surface was examined in [3].

The current report considers the 3-dimensional case, i.e. the layer's surface and permittivity distribution are given by arbitrary functions, that are periodic by two dimensions. The plane electromagnetic wave may have arbitrary polarization and may come from any direction. The method from [1] is implemented. The developed computer program is verified by solving some simple examples, that allow analytical solution. An example of reconstruction of the layer's inner structure on the basis of the diffraction image is considered.

The study was supported by the Russian Foundation for Basic Research, project code 16-31-60096.

References

- [1] A. S. Il'inskiy, A method of investigating wave diffraction problems on a periodic structure, *USSR Computational Mathematics and Mathematical Physics*, **14**(4), 242–246 (1974).
- [2] D. Knyazkov, Simulation of diffraction on a layer using the method of projections, *AIP Conference Proceedings*, **1863**, 370006 (2017).
- [3] D. Knyazkov, Simulating diffraction of plane wave on periodic layer with the use of the method of projections, *IEEE Proc. of Days on Diffraction 2017*, Saint-Petersburg, Russia, 180–185 (2017).

- [4] D. Knyazkov, Web-interface for HPC computation of a plane wave diffraction on a periodic layer, *Lobachevskii Journal of Mathematics*, **38**(5), 936–939 (2017).
- [5] A. Gavrikov, D. Knyazkov, A. Romanova, V. Chernik, A. Shamaev, Simulation of influence of the surface disturbance on the ocean self radiation spectrum, *Program Systems: Theory and Applications*, **7**(2), 73–84 (2003) (In Russian).
- [6] D. Yu. Knyaz'kov, A. V. Romanova, A. S. Shamaev, A local perturbation method for the approximate calculation of the acoustic wave diffraction with impedance interface conditions, *Proc. of the Steklov Institute of Mathematics*, **295**(1), 168–178 (2016).

Asymptotics of solutions to non-stationary Maxwell systems in a domain with small cavities

Korikov D.V., Plamenevskii B.A.

St. Petersburg State University, Ul'yanovskaya 1, St. Petersburg, Petrodvorets, 198504, Russia
e-mail: thecakeisalie@list.ru, boris.plamen@gmail.com

The non-stationary Maxwell system is considered, for all times $t \in \mathbb{R}$, in a bounded domain $\Omega(\varepsilon)$ with finitely many small cavities; the cavity diameters are proportional to a small parameter ε . The perfect conductivity conditions or the impedance conditions are given on the boundary. The asymptotics of solutions are derived as ε tends to zero. The cavities are “singular” perturbations of the domain $\Omega(0)$: they are collapsing into points as $\varepsilon \rightarrow 0$. To describe the asymptotics, we use the asymptotics of solutions of the so-called limit problems. One of such problems turns out to be a dynamic problem in a domain with singularities on the boundary. Thus, it is necessary to apply the methods and results of the theory of dynamic problems in domains with a nonsmooth boundary, which were developed in [1–4].

The presented mathematical model describes the electromagnetic field behavior inside a conductive resonator with metallic inclusions of small size. The model can be of use for the diagnostics of plasma filling the resonator and containing such inclusions.

References

- [1] B. A. Plamenevskii, On the Dirichlet problem for the wave equation in a cylinder with edges, *St. Petersburg Math. J.*, **10**(2), 373–397 (1999).
- [2] A. Yu. Kokotov, B. A. Plamenevskii, Asymptotics of the solutions of the Neumann problem for hyperbolic systems in domains with conic points, *St. Petersburg Math. J.*, **16**(3), 477–506 (2005).
- [3] S. I. Matyukevich, Nonstationary Maxwell system in domains with edges, *St. Petersburg Math. J.*, **15**(6), 875–913 (2004).
- [4] S. I. Matyukevich, B. A. Plamenevskii, Elastodynamics in domains with edges, *St. Petersburg Math. J.*, **18**(3), 459–510 (2007).

Non-conventional phase attractors and repellers in weakly coupled autogenerators with hard excitation

Kovaleva M.¹, Manevitch L.I.¹, Pilipchuk V.²

¹N. N. Semenov Institute of Chemical Physics, Kosygin st., 4, 119991, Moscow, Russia

²Wayne State University, 1200 Holden Street, MI 48202, Detroit, USA

e-mail: makovaleva@chph.ras.ru, manevitchleonid3@gmail.com, pilipchuk@wayne.edu

In our earlier studies, we found the effect of non-conventional synchronization, which is a specific type of nonlinear stable beating in the system of two weakly coupled autogenerators with hard excitation given by generalized van der Pol–Duffing characteristics [1–3]. The corresponding synchronized

dynamics are due to a new type of attractor in a reduced phase space of the system in the slow time-scale. In the present work, we show that, as parameter of nonlinear stiffness is changing, the phase portrait undergoes a complicated evolution leading to a quite unexpected appearance of difficult to detect ‘repellers’ separating a stable limit cycle and equilibrium points in the phase plane. In terms of the original variables, the limit cycle associates with nonlinear beatings while the stationary points correspond to the stationary synchronous dynamics with spatial profile corresponding to local nonlinear normal modes.

In the current study, we revealed all possible types of synchronization in quasilinear system of two weakly coupled active oscillators with hard excitation. It was shown that the increase of conservative nonlinearity is accompanied by quite a complicated evolution of possible regimes of synchronization.

We described all the stages of evolution in terms of phase portraits of the asymptotically reduced model. This may provide an adequate tool for controlling the synchronized dynamics of weakly coupled generators through appropriate choice for the system parameters and initial conditions. We found a new type of dynamics of two weakly coupled generators with hard excitation. Namely, a non-stationary repeller in the phase space separates the basins of attraction of two stable synchronization regimes: the non-conventional synchronization with intensive energy exchange and the conventional synchronization without any amplitude modulation. We show for the first time the possibility of existence of two different synchronization regimes under the same parameters magnitudes. The tiny difference in initial conditions can switch the behavior of the system from the intensive beatings to the energy localization and vice versa. It must be noted that such repellers are the non-conventional, as the unstable phase orbits correspond to the intensive beatings in the system. In other words, assuming time-inversion this kind of repeller would become an attractor with periodic energy exchange between two weakly coupled active oscillators.

The reported study was supported by Russian Foundation for Basic Research according to the research project 16-33-60186.

References

- [1] L. I. Manevitch, M. A. Kovaleva, V. N. Pilipchuk, Non-conventional synchronization of weakly coupled active oscillators, *EPL — Europhysics Letters*, **101**, 50002 (2013).
- [2] M. A. Kovaleva, L. I. Manevitch, V. N. Pilipchuk, New type of synchronization of oscillators with hard excitation, *Journal of Experimental and Theoretical Physics — JETP*, **117**(2), 369–377 (2013).
- [3] M. A. Kovaleva, V. N. Pilipchuk, L. I. Manevitch, Nonconventional synchronization and energy localization in weakly coupled autogenerators, *Physical Review E*, **94**(2), 032223 (2016).

Analysis of a mathematical model of oxygen transport in brain

A.E. Kovtanyuk¹, A.Yu. Chebotarev^{2,3}, A.A. Dekalchuk³, N.D. Botkin¹, R. Lampe¹

¹Technische Universität München, Ismaningerstr. 22, 81675 München, Germany

²Institute for Applied Mathematics, FEB RAS, 7 Radio st., 690041 Vladivostok, Russia

³Far Eastern Federal University, 8 Sukhanova st., 690950 Vladivostok, Russia

e-mail: andrey.kovtanyuk@tum.de

Mathematical modeling of oxygen transport in brain is important to predict dangerous situations caused by impaired cerebral circulation. Following to conventional models (cf. [1, 2]), the brain material is considered as a two-compartment (blood and tissue) structure, and the mathematical model consists of coupled equations describing convective and diffusive transports processes of oxygen and its consumption in tissue. Such a promising approach permits to conduct diverse numerical simulations, nevertheless its theoretical investigation is very poor. The current work intends to cover the lack of accurate mathematical analysis for such models.

Let us briefly outline the continuum steady-state model of oxygen transport in brain. It describes the propagation of oxygen in tissue and blood. It is assumed that the tissue and blood fractions occupy the same spatial region $\Omega \subset \mathbb{R}^3$. The equations, look as follows:

$$-\alpha\Delta\varphi + \mathbf{v} \cdot \nabla\varphi = G, \quad -\beta\Delta\theta = -\gamma G - \mu, \quad x \in \Omega. \quad (1)$$

Here, θ is the tissue oxygen concentration, φ the blood oxygen concentration, μ the tissue oxygen metabolic (consumption) rate associated with brain function, G the local exchange at blood-tissue interface, $\gamma = \sigma(1 - \sigma)^{-1}$ with σ being the volume fraction of vessels, \mathbf{v} a given velocity field (in the vessel network), α and β are diffusion coefficients of blood and tissue. The tissue oxygen metabolic rate depends on the tissue oxygen concentration (Michaelis–Menten equation): $\mu = \mu(\theta) := \mu_0\theta/(\theta + \theta_0)$, where μ_0 means the maximum value of the oxygen metabolic rate, θ_0 the value of the tissue oxygen concentration when $\mu = 0.5\mu_0$. The exchange at the blood-tissue interface is given by the formula $G = A(\theta - \psi)$, $\psi = f^{-1}(\varphi)$ with $f := \psi + B\psi^r/(\psi^r + C)$. Here, A , B , C , and r are positive constants.

The following boundary conditions on $\Gamma := \partial\Omega = \Gamma_1 \cup \Gamma_2$ are imposed:

$$\varphi|_{\Gamma_1} = \varphi_b, \quad \theta|_{\Gamma_1} = \theta_b, \quad \partial_n\varphi = \partial_n\theta|_{\Gamma_2} = 0. \quad (2)$$

Here, the boundary functions, φ_b and θ_b , are fixed, and the symbol ∂_n denotes the normal derivative.

In this paper, a priori estimates of the blood and tissue oxygen concentrations in the space L^∞ , ensuring the unique solvability of the problem (1) and (2), are obtained. The convergence of a simple iterative procedure for finding solutions is proven. The theoretical analysis is illustrated by numerical examples.

This work was supported by the Klaus Tschira Stiftung, and Würth Stiftung.

References

- [1] S.-W. Su, S.J. Payne, *Proc. 31st Ann. Int. Conf. IEEE Eng. Med. Bio. Soc. (EMBC 2009)*, 4921–4924 (2009).
- [2] S.-W. Su, *Modelling Blood Flow and Oxygen Transport in the Human Cerebral Cortex*, PhD Thesis, Oxford, Depart. Eng. Sci., 2011.

Dynamic patterns in double-diffusive convection

Kozitskiy S.B.

Il'ichev Pacific Oceanological Institute, 43 Baltiiskaya St., Vladivostok, 690041, Russia
e-mail: skozi@poi.dvo.ru

We study dynamic patterns arising in 3D double-diffusive convection in a layer of an incompressible liquid interacting with horizontal vorticity field in the neighborhood of Hopf bifurcation points. Roll-type one-mode convection with convective rolls placed along the x -axis is considered. We numerically simulate chaotic regimes in this double-diffusive system described by the system of amplitude equations derived in the previous work [1] from the basic hydrodynamic equations:

$$\begin{aligned} U_t &= U + \alpha_0 U_x + \alpha_6 U_{xx} - \alpha_7 U_{yy} + \alpha_9 U \Psi_{xy} + J(\Psi, U) - iU|U|^2, \\ \Omega_t &= \alpha_8 \Delta\Omega + J(\Psi, \Omega) - (|U|^2)_{xy}, \\ \Omega &= \Delta\Psi. \end{aligned} \quad (1)$$

Here α_i are some complex coefficients. The initial-boundary value problem for system (1) is formulated in the square area 15×15 with periodic boundary conditions. We use sinusoidal initial conditions of a small amplitude for convection $U(t, x, y)$ and zero initial conditions for vortex $\Omega(t, x, y)$

and stream function $\Psi(t, x, y)$. Grid 256×256 points is used for each of the variables. For numerical simulation of equations (1), we have developed a few numerical schemes based on pseudospectral methods and created software packages based on these schemes.

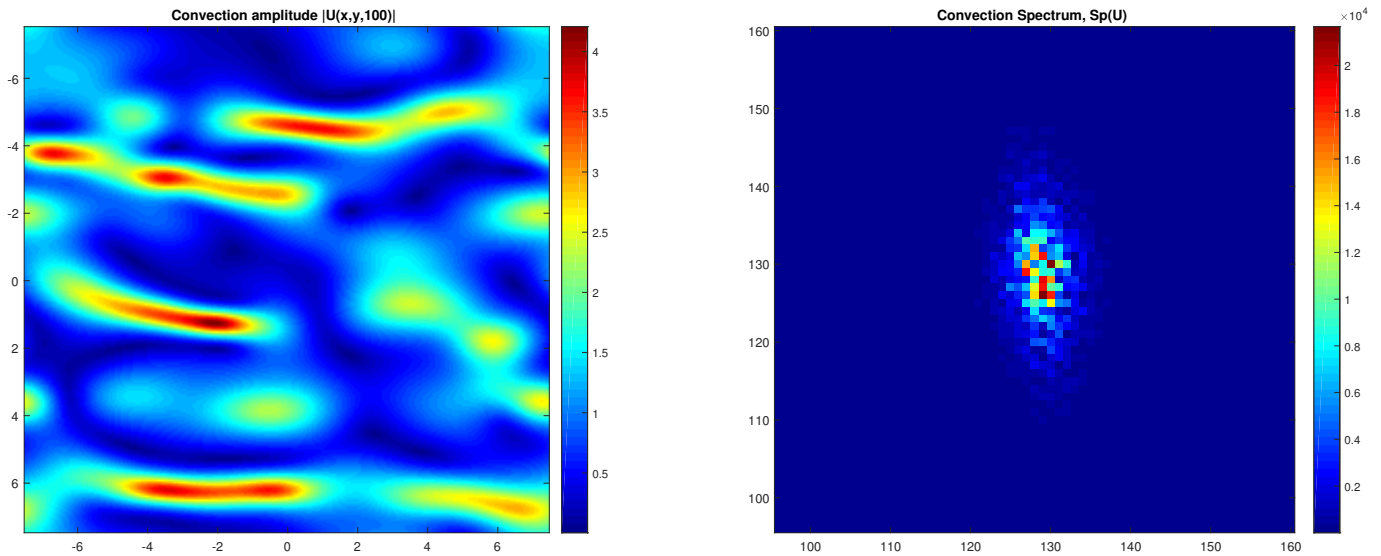


Fig. 1: Numerical solution of equations (1) for $|U(x, y, t)|$ (left) and its spectrum (right).

Simulation has showed that the symmetric initial state given by the initial conditions is destroyed at time $t = 15 - 35$ and the convection becomes irregular. Diffusive chaos state in this case looks like localized dynamic patterns with typical forms depending from the parameters of convection (Fig. 1, left). The spectrum of this state contains a limited number of components located in the oval region (Fig. 1, right). Also, we have developed an approach to the evaluation of Lyapunov’s exponents in the system under study, as a characteristic of the chaotic regime.

The results obtained help to understand the features of convective processes in multi-component media and can be the basis for more advanced models of two-dimensional convective turbulence.

References

- [1] S. B. Kozitskiy, M. Yu. Trofimov, A. D. Zakharenko, Modeling of structures in 3D double-diffusive convection, *Proceedings of the International Conference “Days on Diffraction 2014”*, IEEE, 144–149 (2014).

A comparison theorem for super- and subsolutions of $\nabla^2 u + f(u) = 0$ and its application to water waves with vorticity

V. Kozlov

Department of Mathematics, Linköping University, S-581 83 Linköping, Sweden
 e-mail: vladimir.kozlov@liu.se

A comparison theorem is proved for a pair of solutions that satisfy opposite nonlinear differential inequalities in a weak sense. The nonlinearity is of the form $f(u)$ with f belonging to the class L^p_{loc} and the solutions are assumed to have non-vanishing gradients in the domain, where the inequalities are considered. The comparison theorem is applied to the problem describing steady, periodic water waves with vorticity in the case of arbitrary free-surface profiles including overhanging ones. Bounds for these profiles as well as streamfunctions and admissible values of the total head are obtained.

This is a joint work with N. Kuznetsov, St. Petersburg.

On effective lengths of blood vessels

Vladimir Kozlov¹, Sergei Nazarov^{2,3,4}, German Zavorokhin⁵

¹Department of Mathematics, Linköping University, S-581 83 Linköping, Sweden

²St. Petersburg State University, Universitetskiy pr., 28, Peterhof, St. Petersburg, 198504, Russia

³St. Petersburg State Polytechnical University, Polytechnicheskaya ul., 29, St. Petersburg, 195251, St. Petersburg, Russia

⁴Institute for Problems of Mechanical Engineering RAS, V.O., Bolshoj pr., 61, St. Petersburg, 199178, Russia

⁵St. Petersburg Department of the Steklov Mathematical Institute, Fontanka, 27, 191023, St. Petersburg, Russia

e-mail: vlkoz@mai.liu.se, srgnazarov@yahoo.co.uk, zavorokhin@pdmi.ras.ru

An exponential smallness of the errors in the one-dimensional model of the Stokes flow in a branching thin vessel with rigid walls is achieved by introducing effective lengths of the one-dimensional image of internodal fragments of vessels. Such lengths are evaluated through the pressure-drop matrix at each node describing the boundary-layer phenomenon. The influence of perturbations (e.g., plaques, aneurysms) on the conjugation conditions in the bifurcation node is taken into account by variations in the effective lengths. As a consequence, we can describe further changes in the node while passing blood therethrough.

Wave reduction on a shoaling phenomenon by a porous structure

I.J. Kristianto, I. Magdalena

Industrial & Financial Mathematics Research Group, Faculty of Mathematics & Natural Sciences, Institut Teknologi Bandung, Indonesia, Jalan Ganesha 10, Bandung, West Java, Indonesia

e-mail: ikha.magdalena@math.itb.ac.id, ivanjonathankristianto@gmail.com

Wave shoaling is the phenomenon of wave amplitude increased caused by the changes of the water depth. Small wave amplitude from the deeper area is getting higher when the wave is getting closer to the shallower area. The high wave amplitude can cause damage to the seashore such as erosion. For coastal protection, we can use porous structures, like mangrove tree or an artificial porous media from rock or other material. In this paper, we investigate wave shoaling interaction with an emerged porous medium using a mathematical model. The results are of importance for studying the reduction impact of the porous medium against the shoaling wave. The mathematical model that we use is a Shallow Water-type model with linear friction term. The analytical solution is derived by separation variable method. From the continuity of surface and horizontal flux, we obtain the wave transmission coefficient formulas. We solve the equations numerically using finite volume method on a staggered grid. Next, we compared the solution from the analytical and numerical solution with a different type of porous medium. To ensure the result we have, both analytical and numerical scheme compared with an experiment data.

References

- [1] I. Magdalena, S.R. Pudjaprasetya, L.H. Wiryanto, *Wave Interaction with an Emerged Porous Media*, Cambridge University Press, 2014.
- [2] D. Adytia, S. Husrin, Numerical simulations of nonbreaking solitary wave attenuation by a parameterized mangrove forest model, *Pertanika Journals*, (2016).

Current distribution and input impedance of a circular loop antenna located on the surface of a gyromagnetic cylinder

Kudrin A.V.¹, Zaboronkova T.M.¹, Zaitseva A.S.¹, Krafft C.²

¹University of Nizhny Novgorod, 23 Gagarin Ave., Nizhny Novgorod 603950, Russia

²Laboratoire de Physique des Plasmas, École Polytechnique, 91128 Palaiseau Cedex, France

e-mail: kud@rf.unn.ru, t.zaboronkova@rambler.ru, zaitseva@rf.unn.ru,
catherine.krafft@lpp.polytechnique.fr

Electrodynamic characteristics of strip antennas placed at the interface of isotropic and anisotropic dielectric media have been analyzed for some geometries in [1–3]. In this work, we consider a strip loop antenna located coaxially on the surface of a circular cylinder filled with a lossless gyromagnetic medium described by a scalar dielectric permittivity and a magnetic permeability tensor with nonzero off-diagonal elements. It is assumed that the gyrotropic axis of the medium filling the cylinder is aligned with it. The cylinder is surrounded by an isotropic magnetodielectric medium. The current of the loop antenna is excited by a time-harmonic given voltage that creates an electric field in a narrow angular interval on the surface of the strip conductor of the antenna.

Assuming that the strip is sufficiently narrow, we derive and analytically solve integral equations for the current density on the strip surface in the case where the diagonal elements of the permeability tensor of the gyromagnetic medium have opposite signs. Note that under such conditions, the refractive index surface of one of the normal waves of such a medium possesses an unbounded branch corresponding to magnetostatic waves. It is shown that in the case considered, this fact results in existence of an infinite number of quasi-magnetostatic eigenmodes supported by the cylinder, which significantly affects the antenna characteristics. Under some simplifying assumptions, we obtain closed-form expressions for the current distribution and input impedance of the loop antenna and analyze in what extent they are determined by the parameters of the media inside and outside the cylinder. We have also performed numerical calculations of the current distribution and input impedance of the antenna under consideration, with the emphasis placed on the case where these characteristics turn out to be essentially different from those for operation of the same antenna in the isotropic magnetodielectric medium surrounding the cylinder. The numerical results will be presented and discussed for cases that are of both practical and academic interest.

Acknowledgments. This work was supported by the Ministry of Education and Science of the Russian Federation (project No. 3.1358.2017/4.6).

References

- [1] A. V. Kudrin, A. S. Zaitseva, T. M. Zaboronkova, C. Krafft, G. A. Kyriacou, *PIER B*, **51**, 221–246 (2013).
- [2] A. V. Kudrin, A. S. Zaitseva, T. M. Zaboronkova, S. S. Zilitinkevich, *PIER B*, **55**, 241–256 (2013).
- [3] T. M. Zaboronkova, A. S. Zaitseva, A. V. Kudrin, B. Spagnolo, *Radiophys. Quantum Electron.*, **57**, 795–806 (2014).

Electromagnetic non-polarized symmetric hybrid wave propagation in nonlinear media with saturation

Kurseeva V. Yu.

Department of Mathematics and Supercomputing, Penza State University, Penza, Russia, 440026

e-mail: 79273698109@ya.ru

We consider the propagation of an electromagnetic non-polarized symmetric hybrid wave $\mathbf{E}e^{-i\omega t}$, $\mathbf{H}e^{-i\omega t}$ of the form [1]

$$\mathbf{E} = (E_x(x)e^{i\gamma z}, E_y(x)e^{i\gamma z}, E_z(x)e^{i\gamma z})^\top, \quad \mathbf{H} = (H_x(x)e^{i\gamma z}, H_y(x)e^{i\gamma z}, H_z(x)e^{i\gamma z})^\top, \quad (1)$$

along the boundaries of the dielectric waveguide

$$\Sigma := \{(x, y, z) : 0 \leq x \leq h, (y, z) \in \mathbb{R}^2\},$$

where \mathbf{E} , \mathbf{H} are the complex amplitudes [2]; ω is a circular frequency; $(\cdot)^\top$ is the transposition operation; γ is an unknown real propagation constant; E_x, E_y, E_z, H_x, H_z are unknown functions.

The waveguide Σ is located in the Cartesian coordinate system $Oxyz$. At the boundary $x = 0$ the waveguide Σ has a perfectly conducted wall. The half-space $x > h$ is filled with isotropic medium with constant permittivity $\varepsilon = \varepsilon_0\varepsilon_1$, where $\varepsilon_0 > 0$ is the permittivity of vacuum. We suppose that permittivity inside the waveguide Σ is described by the formula

$$\varepsilon = \varepsilon_0\varepsilon_2 + \frac{\varepsilon_0\alpha |\mathbf{E}e^{-i\omega t}|^2}{1 + \beta |\mathbf{E}e^{-i\omega t}|^2},$$

where $\varepsilon_2, \alpha, \beta > 0$ are real constants. We assume that $\varepsilon_2 > \varepsilon_1 \geq \varepsilon_0$. There are no sources in the entire space. We assume that everywhere $\mu = \mu_0$, where $\mu_0 > 0$ is the permeability of vacuum.

Complex amplitudes (1) satisfy Maxwell's equations

$$\begin{cases} \operatorname{rot} \mathbf{H} = -i\omega\varepsilon\mathbf{E}, \\ \operatorname{rot} \mathbf{E} = i\omega\mu\mathbf{H}; \end{cases} \quad (2)$$

the continuity condition for the tangential field components at the boundary $x = h$; tangential components of \mathbf{E} vanishes on the perfectly conducted wall ($x = 0$); the radiation condition at infinity, where electromagnetic field exponentially decays as $x \rightarrow \infty$ in the domain $x > h$.

The existence of non-polarized symmetric hybrid waves in a dielectric layer is theoretically proved. Numerical results are also presented, comparison with the linear cases is given. An interesting fact is that these waves do not correspond to nonlinear TE and TM polarized waves. Results for similar problems see in [3–5].

References

- [1] J. A. Stretton, *Electromagnetic Theory*, McGraw Hill, New York, 1941.
- [2] P. N. Eleonskii, L. G. Ogan'es'yants, V. P. Silin, Cylindrical nonlinear waveguides, *Soviet Physics JETP*, **35**, 44–47 (1972).
- [3] Yu. G. Smirnov, E. Smolkin, On the existence of non-polarized azimuthal-symmetric electromagnetic waves in circular dielectric waveguide filled with nonlinear isotropic homogeneous medium, *Wave Motion*, **77**, 77–90 (2017).
- [4] E. Smolkin, The azimuthal symmetric hybrid waves in nonlinear cylindrical waveguide, *Progress In Electromagnetics Research Symposium (PIERS)*, 348–353 (2017).
- [5] Yu. Smirnov, E. Smolkin, V. Kurseeva, The new type of non-polarized symmetric electromagnetic waves in planar nonlinear waveguide, *Applicable Analysis*, 1–16 (2017).

An indefinite integral equation without irregular frequencies for the floating-body problem

Nikolay Kuznetsov

Institute for Problems in Mechanical Engineering, Russian Academy of Sciences, V.O., Bol'shoy pr. 61, 199178 St. Petersburg, Russian Federation
e-mail: nikolay.g.kuznetsov@gmail.com

In his paper [1], concerning the floating-body problem (FBP) in a water layer of constant finite depth, located between $\{y = 0\}$ and $\{y = -d\}$, $d > 0$, John used Green's function $G(P, Q)$, $P = (x, y, z)$, $Q = (\xi, \eta, \zeta)$, for reducing the problem to an integral equation (IE) on the wetted part

S of body's surface. A single-layer potential (SLP; see the first term in formula (1) below) satisfies all relations of the FBP except for the non-homogeneous Neumann condition (NC) on S . According to the jump property of the normal derivative of the SLP, the (NC) leads to a Fredholm IE for μ — the density of the SLP. The jump property is applicable if S : (a) has no common points with $\{y = -d\}$; (b) is attached to $\{y = 0\}$ and forms a C^2 -surface with the mirror image of S in $\{y = 0\}$.

The obtained IE has a drawback detected by John himself: for a sequence of *irregular* frequencies (they are related to the spectrum of a problem in the domain confined between $\{y = 0\}$ and S) the IE is solvable not for all right-hand-side terms (RHST) even in the case when the FBP is uniquely solvable for all these terms. In particular, this solvability property holds if S : (c) lies within the vertical cylinder whose generators go through the waterline along which S is attached to the plane $\{y = 0\}$. The question, which IEs are uniquely solvable for all frequencies, was one of the most important in the studies of the FBP (see [2], Sections 3.1.1 and 3.1.2). For the FBP a new IE is proposed so that it is free of irregular frequencies. This IE belongs to the class of indefinite equations introduced by S. G. Krein in the 1950's; see [3], Sections 18 and 20.4.

Assuming that S satisfies conditions (a)–(c), whereas the RHST f in the NC on S belongs to $C^{0,\alpha}(S)$, a solution to the FBP is sought in the form:

$$\int_S \mu(Q) G(P, Q) dS_Q + \int_S \nu(Q) \frac{\partial G(P, Q)}{\partial n_Q} dS_Q. \tag{1}$$

Here n_Q is the unit normal pointing into the water domain at $Q \in S$, and $\mu \in C^{0,\alpha}(S)$ and $\nu \in C^{1,\alpha}(S)$ are unknown densities. Then the normal derivative of the function given by formula (1) exists for $P \in S$, and one arrives at the following IE:

$$-\mu(P) + \frac{1}{2\pi} \int_S \mu(Q) \frac{\partial G(P, Q)}{\partial n_P} dS_Q + \frac{1}{2\pi} \frac{\partial}{\partial n_P} \int_S \nu(Q) \frac{\partial G(P, Q)}{\partial n_Q} dS_Q = f(P) \tag{2}$$

or $(K - I)\mu + T\nu = f$ for short. Here I is the identity operator, K and its adjoint K' are compact operators in $C(S)$, whereas T is self-adjoint.

Equation (2) is solvable for all RHST, if the intersection of the null-spaces of $K' - I$ and T is trivial; see [3], Section 18. To prove this fact we suppose that there exists μ_0 satisfying equations $(K' - I)\mu_0 = 0$ and $T\mu_0 = 0$ simultaneously. The first of them implies that $\mu_0 \in C^{1,\alpha}(S)$, and so the second one means that the double layer potential — see the second term in (1) — solves the homogeneous FBP when $\nu = \mu_0$. Then the uniqueness theorem for the FBP yields that this potential vanishes identically in the water domain. Therefore, the jump formula (as P tends to its limit position on S) implies that $(K' + I)\mu_0 = 0$. Combining this and $(K' - I)\mu_0 = 0$, one obtains that μ_0 vanishes identically on S . Thus, the following theorem is proved.

Let conditions (a)–(c) hold. Then the indefinite equation (2) is solvable for all RHST. Substituting a solution of the IE (2) into the representation formula (1), one obtains a unique solution of the FBP.

References

[1] F. John, *Comm. Pure Appl. Math.*, **3**, 45–101 (1950).
 [2] N. Kuznetsov, V. Maz'ya, B. Vainberg, *Linear Water Waves: A Math. Approach*, CUP, 2002.
 [3] S. G. Krein, *Linear Equations in Banach Spaces*, Birkhäuser, 1982.

Surface waves in a polygonal domain with Robin boundary conditions

M.A. Lyalinov

Saint-Petersburg University

e-mail: lyalinov@yandex.ru, m.lyalinov@spbu.ru

A surface wave propagates from infinity along the boundary of the unbounded polygonal domain. The scattered field satisfies the Helmholtz equation and the impedance boundary conditions as well as

the radiation conditions at infinity. We apply a known modification of the Sommerfeld–Malyuzhinets technique and reduce the problem at hand to that for a system of functional-difference equations on the complex plane. The latter is studied by transformation to a system of integral equations of the second kind. The integral operator analytically depends on the wave number which is the characteristic parameter of the equations. Fredholm property of the system is studied by use of the analytic Fredholm alternative. The far field asymptotics is developed in a standard way from the Sommerfeld integral representation of the wave field. In this way the excitation coefficients of the reflected and transmitted surface waves are deduced as well as the diffraction coefficient of the cylindrical wave propagating at infinity.

Numerical studies for resonant phenomena during wave run-up

I. Magdalena, Kevin

Industrial & Financial Mathematics Research Group, Faculty of Mathematics & Natural Sciences, Institut Teknologi Bandung, Jalan Ganesha 10, Bandung, 40132, Indonesia

e-mail: ikha.magdalena@math.itb.ac.id

In this paper, we investigate the occurrence of resonance phenomena during wave run-up over a sloping beach. Here, we focus on wave run-up within a one-dimensional framework. Most studies on wave run-up do not discuss resonance phenomena, while this phenomenon may arise when the incoming wave frequency is close to natural beach frequency. The occurrence of this phenomena may worsen tsunami impact on beaches. The equation we use here is Shallow Water Equations. The natural frequency of the semi-enclosed beach has been derived analytically using the method of separation variables. We solve the equation numerically using finite volume method on a staggered grid. Implementation of the staggered conservative method to the shallow water equations has provided us with a robust code appropriate for simulating wave oscillation over a sloping beach. Our simulations could predict the amplification of maximum run-up height due to resonance. Moreover, our results have shown a good agreement with other results in literature.

Propagation process of the coupled hyperbolic waves in gas thermoelastic medium

Matias, D.V.

Peter the Great St. Petersburg Polytechnic University, Polytechnicheskaya, 29, St. Petersburg, 195251, Russia

e-mail: dvmatyas@gmail.com

Numerical approach is used to investigate waves propagation due to laser radiation. Thin layer of gas medium is considered, gas is modeled based on ideal gas concept. Aim of research is to examine time relaxation constant's influence on coupled thermoelastic system. Heat flux relaxation according Maxwell–Cattaneo law is studied. Dispersion in waves is introduced due to time relaxation and nonlinearity in acoustics's equations. Spatial description is used in order to describe continuum fields. Density, temperature, heat flux and velocity are evaluated through the system of balance equations: mass, energy and momentum balances are taken in integral form. High speed thermal impact is modeled by defining the distribution of heat sources in the volume for the semitransparent medium with help of Bouguer law. The power of the laser pulse depends on time as the Dirac delta function or as the Heaviside function do.

Number of problems with different time relaxation constant is considered, interaction between thermal and acoustic waves is examined. For numerical calculation explicit technique is applied; moreover, it is shown that numerical solution, which is based on same approach, for similar issue of laser interaction on solid continuum has coincided with analytical one.

Linear and nonlinear aspects of scattering on oscillating potentials

Matveev V.B.

St. Petersburg Department of Steklov Mathematical Institute of Russian Academy of Sciences (PDMI);
St. Petersburg University of Aerospace Instrumentation (SUAI);

Institut de Mathématiques de Bourgogne, (IMB), Université de Bourgogne – Franche Comté, Dijon, France

e-mail: vmatveev@pdmi.ras.ru, vladimir.matveev9@gmail.com, matveev@u-bourgogne.fr

We show that some principal ingredients of the IST method: Jost solutions, reflection and transmission coefficients for 1D Schrödinger equation

$$\psi_{xx} + k^2\psi - u(x)\psi = 0, \quad x \in \mathbb{R}$$

do exist for a wide class of smooth, real, oscillating potentials, not necessarily bounded at infinity. In general, these potentials $u(x)$ are distinguished by some simple integral decay properties.

Let the potential $u(x)$ satisfies the conditions

$$\int_x^{\pm\infty} u(\tau)e^{2ik\tau} d\tau = O(|x|^{-1/2-\epsilon}), \quad \epsilon > 0, \quad k \in \mathbb{R}, \quad |x| \rightarrow \infty,$$

both for some fixed k , $k \neq 0$ and $k = 0$. Then the following statement (Matveev 1973) holds.

Theorem. *There exist the solutions $f(x, k), g(x, k)$ of the Schrödinger equation (called Jost solutions) such that*

$$\lim_{x \rightarrow \infty} f(x, k)e^{-ikx} = 1, \quad \lim_{x \rightarrow -\infty} g(x, k)e^{-ikx} = 1.$$

For some potentials, which we call rapidly oscillating, these conditions are satisfied for all real values of k . Simplest examples of such potentials are

$$u_1 = |x|^\alpha \sin |x|^\beta, \quad \beta > 3/2 + \alpha; \quad u_2 = |x|^\alpha \sin e^{x^2}, \quad \alpha > 0.$$

For other potentials, with periodic or multi-periodic oscillations, modulated by the slowly decaying factors, the same integral decay condition holds for almost all values of k with exception of finite or countable number of points, for which Wigner von Neumann resonances or bound states in the continuous spectrum appear. Location of these points corresponds to the values of k for which the integrals above diverge.

The natural question is as follows: might it be possible to extend the Inverse scattering method for KdV equation, taking these oscillating potentials or a part of them as initial data. Here we will answer this question only partially.

The main message is that in scattering theory local decay conditions to a large extent might be replaced by the integral decay conditions. This provides a very beautiful manifestation of the tunneling effect in quantum mechanics. Its nonlinear manifestations will be also demonstrated in my talk in connection with what I call the super-transparency phenomenon.

Spectral problem for Dirac operator for Y-type splitted chain of nanospheres

Melikhova A.S., Popov I.Y.

ITMO University, 49 Kronverkskiy Pr., St. Petersburg, 197101, Russia

e-mail: alina.s.melikhova@gmail.com, popov1955@gmail.com

Chain structures are widely presented in investigations in nanotechnologies. The dependence of spectral properties on geometry of such systems is rather interesting problem. In this paper

the mathematical model of relativistic electron placed into Y-type splitted chain of nanospheres is presented. As in the case of non-relativistic electron (see, for instance, [1]), the model is constructed in the framework of theory of self-adjoint extensions of symmetric operators.

The splitted chain which consists of identical nanospheres connected through one-dimensional straight wires is considered. Namely, three direct semi-infinite chains of nanospheres are connected via wires to one common sphere with number 0. All contact points on spheres are placed at opposite positions. The one exception is the sphere number 0 with contact points placed at the vertices of an equilateral triangle. An elementary cell of the chain consists of a sphere and a connected wire. The Dirac operator on sphere has the form:

$$H_S = -i\hbar\sigma_1(\partial/\partial\theta + \cot\theta/2) - i\hbar c\sigma_2\partial/\partial\phi(\sin\theta)^{-1} + Mc^2\sigma_3,$$

and on the wire is presented as follows:

$$H_l = ic\,d/dx \otimes \sigma_1 + c^2/2 \otimes \sigma_3,$$

where \hbar is Plank's constant, σ_i ($i = 1, 2, 3$) are the Pauli matrices, c is the speed of light, M is the particle mass. The coupling between parts of any elementary cell is obtained by "restriction-extension" procedure. Specifically, one should firstly restrict the initial operator (on the set of all functions that vanish at the contact points) to obtain the symmetric one and then find the self-adjoint extensions of this operator to get the interacting parts of the cell. To describe the self-adjoint extension of the operator one can employ the Krein formula for resolvents (see, for example, [2, 3]).

Due to the features of the described model, one can use the transfer-matrix's approach for spectral analysis of the system. The solution on the wire is represented as linear combination of exponents and on the sphere is considered as a linear combination of Green's functions for the Dirac operator [4]. By wading through the Krein formula one can obtain the transfer-matrix that stores the necessary information about spectra of the system. More precise study of the sphere number 0 and its neighbours gives one the system for spectral analysis. The solvability condition leads one to sufficient conditions on the existence of the point spectrum.

References

- [1] A. S. Melikhova, I. Y. Popov, Spectral problem for solvable model of bent nano peapod, *Applicable Analysis*, **96**, 215–224 (2017).
- [2] S. Albeverio, F. Gesztesy, R. Hoegh-Krohn, H. Holden, *Solvable Models in Quantum Mechanics: Second Edition*, AMS Chelsea Publishing, Providence, R.I., 2005.
- [3] M. G. Krein, G. K. Langer, Defect subspaces and generalized resolvents of an Hermitian operator in the space Π_η , *Functional Analysis and Its Applications*, **5**, 136–146 (1971).
- [4] E. N. Grishanov, D. A. Eremin, D. A. Ivanov, I. Y. Popov, Dirac operator on the sphere with attached wires, *Chin. Phys. B*, **25**, 047303 (2016).

Leaky wave asymptotics in the case of stationary point and complex pole approaching

Miakisheva O.A., Fomenko S.I.

Institute for Mathematics, Mechanics and Informatics, Kuban State University, Krasnodar, 350040, Russia

e-mail: miakisheva.olga@gmail.com, sfom@yandex.ru

An analytically based computer model for the coupled time-harmonic oscillation generated by a given source in acoustic fluid with an immersed elastic plate has been developed, and explicit integral representations for generated and scattered wave fields have been derived using the Fourier transform

technique. In the far-field, the body and guided waves are described by the asymptotic representations obtained from those integrals using the stationary phase method and residual technique [1]. The comparison with the results of numerical integration has shown that, in some cases, the contributions of stationary points and residues taken separately do not give the correct amplitudes of the reflected and transmitted body waves. Such a discrepancy occurs for those angles of the directivity diagram at which the distance between the stationary point and a near real complex pole becomes less than a certain threshold value.

For these cases, it is necessary to derive asymptotic representations, which remain correct when the stationary point approach the pole, as it was accomplished in the case of embedded tube waveguide [2]. In our talk, such an analytical expression of body waves derived as a superposition of inhomogeneous and leaky waves will be presented and discussed for 2D and 3D diffraction problems. To validate the considered leaky-wave asymptotic representation a comparison with the results of numerical evaluation of path integrals has been carried out. Numerical results show a good agreement between the integral and asymptotic representations at far and even middle distances from the source.

The work is supported by the Russian Science Foundation (Project No. 17-11-01191).

References

- [1] E. V. Glushkov, N. V. Glushkova, O. A. Miakisheva, Guided wave generation and source energy partition in acoustic fluid with an immersed elastic plate, *Proceedings of the International Conference Days on Diffraction 2016*, **90**, 166–170 (2016).
- [2] E. V. Glushkov, N. V. Glushkova, S. I. Fomenko, Wave generation and source energy distribution in cylindrical fluid-filled waveguide structures, *Wave Motion*, **72**, 70–86 (2017).

Dynamic inverse problem for canonical system with smooth positive Hamiltonian

A.S. Mikhaylov^{1,2}, V.S. Mikhaylov^{1,2}

¹St. Petersburg Department of V. A. Steklov Institute of Mathematics of the Russian Academy of Sciences, 7, Fontanka, 191023 St. Petersburg, Russia

²St. Petersburg State University, 7/9 Universitetskaya nab., 199034 St. Petersburg, Russia
e-mail: mikhaylov@pdmi.ras.ru, ftvsm78@gmail.com

We consider the dynamic inverse problem for canonical system with smooth strictly positive Hamiltonian. The problem consists in recovering a Hamiltonian from a response operator (dynamic Dirichlet-to-Neumann map) given on a finite time interval. Transferring canonical system to Dirac-type system, we can use ideas from [1] to derive equations of inverse problem. We also describe recently discovered relationships between dynamic approach and spectral approach by De Branges [2–4] to inverse problems for canonical systems.

References

- [1] M. I. Belishev, V. S. Mikhaylov, Inverse problem for one-dimensional dynamical Dirac system (BC-method), *Inverse Problems*, **26**(4), 045009 (2010).
- [2] A. S. Mikhaylov, V. S. Mikhaylov, Boundary control method and de Branges spaces. Schrödinger equation, Dirac system and discrete Schrödinger operator, *Journal of Mathematical Analysis and Applications*, doi:10.1016/j.jmaa.2017.12.013 (2017).
- [3] A. S. Mikhaylov, V. S. Mikhaylov, Inverse dynamic problems for canonical systems and de Branges spaces, submitted to *Nanosystems: Physics, Chemistry, Mathematics*, (2018).
- [4] R. V. Romanov, Canonical systems and de Branges spaces, *arXiv:1408.6022 [math.SP]*.

On analytical modeling of cold field electron emission from nanotube films in irregular and aperiodic cases

Minenkov D.S.

Ishlinsky Institute for Problems in Mechanics RAS, Prospekt Vernadskogo 101-1, Moscow, Russia
e-mail: minenkov.ds@gmail.com

We consider a nanotube based cathode and cold field electron emission. Physically interesting question is how emission current depends on geometrical characteristics of the cathode, including tubes aspect ratio and intertube distance. Emission current can be calculated using Fowler–Nordheim formula if we know electrostatic field near tube tips. Corresponding mathematical problem is the Dirichlet problem to the Laplace equation for electrostatic potential $u(x, y, z)$:

$$\Delta u = 0, \quad g(x, y) \leq z \leq d, \quad u|_{z=g(x,y)} = 0, \quad u|_{z=d} = U.$$

Here interelectrode distance d and bias U are given positive constants and function $0 \leq g(x, y) \ll d$ describes the cathode surface (see fig. 1).

This problem cannot be extended into area $z \in [0, d]$ because of high aspect ratio of tubes (tube height is much larger than diameter). The problem is nonlinear because of boundary condition at $z = g(x, y)$. Physically this nonlinearity is well known as the screening effect. Exact analytical formulas in integral form are hard to evaluate and numerical simulations are also time-consuming. That is why usually simple cathodes with identical tubes placed in regular lattice are considered.

In [1, 2] we proposed an analytical model that is easy to implement and that can be applied for irregular arrays. Our approach is based on a family of elementary functions that solve considered mathematical problem for some certain surfaces $g(x, y)$. The main idea is to use these solutions to describe approximately the behavior of cathode with given geometrical characteristics. This model seems to describe the screening effect and in the talk we provide comparison of the model with some experimental data that can be found in literature.

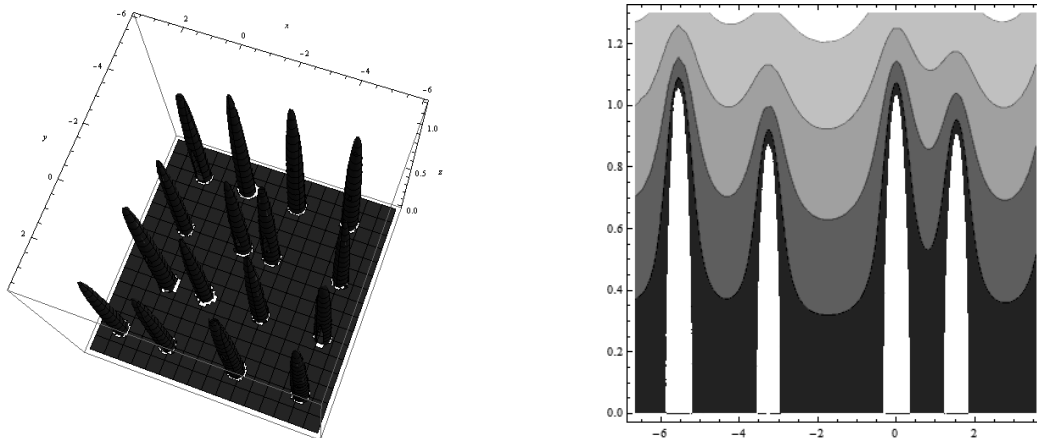


Fig. 1: Irregular array of tubes (left) and density plot of electrostatic potential (right).

The work is done in the frame of government program in IPMech RAS (program number AAAA-A17-117021310377-1).

References

- [1] J. Brüning, S. Y. Dobrokhotov, D. S. Minenkov, Some solutions of the 3D Laplace equation in a layer with oscillating boundary describing an array of nanotubes and an application to cold field emission. I. Regular array, *Russ. J. Math. Phys.*, **18**(4), 400–409 (2011).
- [2] J. Brüning, S. Y. Dobrokhotov, D. S. Minenkov, Some solutions of the 3D Laplace equation in a layer with oscillating boundary describing an array of nanotubes with applications to cold field emission. II. Irregular arrays, *Russ. J. Math. Phys.*, **21**(1), 1–8 (2014).

On evaluation of the confluent Heun functions

Oleg V. Motygin

Institute for Problems in Mechanical Engineering, Russian Academy of Sciences, V.O., Bol'shoy pr. 61, 199178, St. Petersburg, Russia
e-mail: o.v.motygin@gmail.com

In its general form, Heun differential equation — introduced by Karl Heun in 1889 — is a Fuchsian equation with four regular singular points, which are usually chosen to be $z = 0, 1, a,$ and ∞ in the complex z -plane. Confluence of these singularities, when two or more of them merge to an irregular singularity, produce the confluent, double confluent, biconfluent and triconfluent Heun equations. In this work, we deal with the confluent Heun equation being a result of the simplest case of confluence $a \rightarrow \infty$ and having two regular singular points $z = 0, 1$ and an irregular one $z = \infty$.

Solutions of the Heun equations generalize many known mathematical functions and appear in many fields of modern physics, such as general relativity, astrophysics, hydrodynamics, atomic and particle physics, etc. (see, e.g. [1, 2]). However, despite the increasing interest to the Heun equations, it is only Maple amidst known software packages which is able to evaluate the Heun functions numerically and the Maple code is known to be imperfect and vaguely documented.

The purpose of the present work is to develop alternative algorithms. Following [3], for numerical evaluation of the confluent Heun functions we suggest a procedure based on power series, asymptotic expansions and analytic continuation. Program realization is presented in [4] as Octave/Matlab code. Results of numerical tests and comparison with cases when confluent Heun functions reduce to elementary functions are given.

References

- [1] “The Heun project”, <http://theheunproject.org/>.
- [2] M. Hortaçsu, Heun functions and their uses in physics, *arXiv:1101.0471v9 [math-ph]* (2017).
- [3] O.V. Motygin, On numerical evaluation of the Heun functions, *Proceedings of Days on Diffraction 2015*, 222–227 (2015); *arXiv:1506.03848 [math.NA]* (2015).
- [4] O.V. Motygin, Matlab/Octave code for evaluation of the confluent Heun functions, https://github.com/motygin/confluent_Heun_functions/ (2018).

“Blinking and wandering” eigenvalues: Blunted elastic cusps and rounded plasmonic singularities

Sergei A. Nazarov

St. Petersburg State University and Institute for Problems in Mechanical Engineering, Russia
e-mail: srgnazarov@yahoo.co.uk

Describing strange behavior of eigenvalues of several spectral problems in mathematical physics and a new way to form the continuous spectrum from a family of the discrete spectra of perturbed problems, we proceed with two primitive scalar problems, namely the Helmholtz equation with the Robin boundary condition

$$-\Delta u^\varepsilon = \lambda^\varepsilon u^\varepsilon \text{ in } \Omega^\varepsilon, \quad \partial_\nu u^\varepsilon = a u^\varepsilon \text{ on } \partial\Omega^\varepsilon \quad (1)$$

and the Steklov spectral problem

$$-\Delta u^\varepsilon = 0 \text{ in } \Omega^\varepsilon, \quad \partial_\nu u^\varepsilon = \lambda^\varepsilon u^\varepsilon \text{ on } \partial\Omega^\varepsilon. \quad (2)$$

Here, $\Omega^\varepsilon = \{x = (y, z) \in \Omega : z := x_n > \varepsilon\}$, ∂_ν is the outward normal derivative, $\varepsilon > 0$ is a small parameter, and Ω is a domain in \mathbb{R}^n , $n \geq 2$, whose boundary $\partial\Omega$ is smooth everywhere, except at

the coordinate origin \mathcal{O} while in a neighbourhood of \mathcal{O} , the domain Ω coincides with the sharp cusp

$$\Pi = \{x = (y, z) : z \in (0, d), z^{-\gamma}y \in \omega\}, \quad (3)$$

where $\omega \subset \mathbb{R}^{n-1}$ is a domain with smooth boundary and $\gamma = 2$ is the sharpness exponent.

The corresponding limit ($\varepsilon = 0$) problems in the domain Ω with the cusp (3) possess the specific properties:

(i) in the case $a \geq a_{\dagger} > 0$, the residual spectrum of the problem (1) covers the whole complex plane \mathbb{C} , see [1];

(ii) the spectrum of the problem (2) has the continuous component $[\lambda_{\dagger}, +\infty)$ with a cutoff value $\lambda_{\dagger} > 0$, see [2].

The spectra σ_p^{ε} of the problems (p), $p = 1, 2$, in the Lipschitz domain Ω^{ε} are discrete. Certain families of eigenvalues $\{\lambda_{p,m(\varepsilon)}^{\varepsilon}\} \subset \sigma_p^{\varepsilon}$ which depend continuously on $\varepsilon > 0$ and have varying index $m(\varepsilon)$ in the monotone eigenvalue sequences composing the spectrum, are detected with the uncommon behavior as $\varepsilon \rightarrow +0$.

(i) In the case $a \geq a_{\dagger} > 0$, the eigenvalues $\lambda_{1,m(\varepsilon)}^{\varepsilon}$ plummet at the high rate $O(|\ln \varepsilon|)$ along the whole real axis downward while a subset of the spectrum σ_1^{ε} stays almost unchanged periodically in the $|\ln \varepsilon|$ -scale;

(ii) The eigenvalues $\lambda_{2,m(\varepsilon)}^{\varepsilon}$ glide at the rate $O((\lambda^{\varepsilon} - \lambda_{\dagger})|\ln \varepsilon|)$ along the ray $(\lambda_{\dagger}, +\infty)$ downward but have a smooth touchdown at the threshold λ_{\dagger} . A subset of the spectrum σ_2^{ε} stays almost unchanged periodically in the $|\ln \varepsilon|$ -scale.

Some other types of eigenvalue asymptotics are found out in the spectra of these singularly perturbed problems, in particular the “stable” ones which do not leave the very vicinity of a fixed point. Furthermore, each point $\lambda > \lambda_{\dagger}$ implies a “blinking” eigenvalue of the Steklov problems, that is, it becomes a true eigenvalue of the problem (2) in the domain Ω^{ε} for an infinitesimal positive sequence $\{\varepsilon_j(\lambda)\}$ of the parameter ε which is almost periodic in the $|\ln \varepsilon|$ -scale. The latter allows us to construct a singular Weyl sequence of the Steklov problem operator at any point $\lambda \in (\lambda_{\dagger}, \infty)$ and to identify the continuous spectrum in the problem.

Asymptotics of the same type (i) for blunted cuspidal elastic bodies [3] and (ii) for surface plasmonic polaritons (a diffusion operator with sign-changing coefficients) [4] are described as a generalization of the above-mentioned results.

The presented results are obtained in cooperation with J. Taskinen, N. Popoff and L. Chesnel, X. Clays.

References

- [1] S. A. Nazarov, J. Taskinen, Spectral anomalies of the Robin Laplacian in non-Lipschitz domains, *J. Math. Sci. Univ. Tokyo*, **20**, 27–90 (2013).
- [2] S. A. Nazarov, J. Taskinen, On the spectrum of the Steklov problem in a domain with a peak, *Vestnik St. Petersburg Univ. Math.*, **41**(1), 45–52 (2008).
- [3] S. A. Nazarov, “Wandering” eigenfrequencies of a two-dimensional elastic body with a blunted cusp, *Doklady Physics*, **62**(11), 512–516 (2017).
- [4] L. Chesnel, X. Clays, S. A. Nazarov, A curious instability phenomenon for a rounded corner in presence of a negative material, *Asymptotic Analysis*, **88**, 43–74 (2014).

Spectral problems for long and infinite Kirchhoff plates

Sergei A. Nazarov

St. Petersburg State University and Institute for Problems in Mechanical Engineering, Russia

e-mail: srgnazarov@yahoo.co.uk

Asymptotics of eigenvalues and eigenfunctions of the bi-harmonic operator Δ^2 with various boundary conditions related to two-dimensional Kirchhoff plates, are obtained when the relative

width ε of the plate tends to zero. Several series of eigenvalues with stable asymptotics of orders 1, ε^{-2} and ε^{-4} are found in the case of the Neumann conditions (edges of the plate are free) and the Dirichlet conditions (edges of the plate are rigidly fixed) which are described by fourth- and second-order ordinary differential equations in the longitudinal coordinate. Junctions and lattices of such plates are studied as well while new series of eigenvalues appear due to the boundary layer effects near the junction nodes. These eigenvalue series are related to the discrete spectrum of waveguides Ξ composed of clamped infinite Kirchhoff plates, i.e., eigenvalues below the continuous spectrum of the bi-harmonic operator Δ^2 in Ξ with either the Dirichlet conditions on $\partial\Xi$, or the boundary conditions of simple support. Certain results on the spectra of such Kirchhoff infinite waveguides are obtained but many questions on the spectral structures remain open.

The results are derived in cooperation with Fedor Bakharev within the grant 17-11-01003 of Russian Science Foundation.

Operator estimates in homogenization of second-order divergence elliptic equation with coefficient matrix in BMO

Pastukhova S.E.

Moscow Technological University (MIREA), Moscow, Russia

e-mail: pas-se@yandex.ru

Let us consider the Dirichlet problem

$$\begin{aligned} u_\varepsilon &\in H_0^1(\Omega), \quad A^\varepsilon u_\varepsilon = f, \quad f \in L^2(\Omega), \\ A^\varepsilon &= -\operatorname{div} a^\varepsilon(x) \nabla, \quad a^\varepsilon(x) = a(x/\varepsilon), \quad \varepsilon \in (0, 1], \end{aligned} \tag{1}$$

where $\Omega \subset \mathbb{R}^d$ ($d \geq 2$) is a bounded domain with sufficiently smooth boundary. Assuming that the measurable 1-periodic real-valued matrix $a(x)$ is not symmetric, we decompose it into the symmetric and skew-symmetric parts:

$$a(x) = a^s(x) + b(x).$$

We suppose

$$\exists \lambda > 0 : \quad \lambda |\xi|^2 \leq a^s \xi \cdot \xi \leq \lambda^{-1} |\xi|^2 \quad \forall \xi \in \mathbb{R}^d, \tag{2}$$

$$b \in \text{BMO}. \tag{3}$$

We recall that a measurable function g on \mathbb{R}^d lies in the space BMO if $\|g\|_{\text{BMO}} = \sup \frac{1}{|B|} \int_B |g - g_B| dx < \infty$, where $g_B = \frac{1}{|B|} \int_B g dx$ and the supremum is taken over all balls $B \subset \mathbb{R}^d$.

Owing to (2) and (3), the form $(a^\varepsilon \nabla u, \nabla \varphi)$ is bounded and coercive on $H_0^1(\Omega)$, which ensures the unique solvability of the problem (1). Here and hereafter, the simplified notations for the scalar product and the norm in $L^2(\Omega)$ is used: $(\cdot, \cdot) = (\cdot, \cdot)_{L^2(\Omega)}$ and $\|\cdot\| = \|\cdot\|_{L^2(\Omega)}$. We associate with (1) the homogenized problem

$$u_0 \in H_0^1(\Omega), \quad A_0 u_0 = -\operatorname{div} a^0 \nabla u_0 = f.$$

Here a^0 is a constant positive-definite matrix. It is calculated according to the known procedure via solutions to the auxiliary problem, written as follows:

$$N^j \in H_{per}^1(\square), \quad \operatorname{div}[a(x)(e^j + \nabla N^j(x))] = 0, \quad j = 1, \dots, d,$$

where e^1, \dots, e^d is a canonical basis in \mathbb{R}^d , $\square = [-\frac{1}{2}, \frac{1}{2}]^d$ is a unite cube, and $H_{per}^1(\square)$ is the Sobolev space of 1-periodic functions with zero mean value over the cell \square . Under the above assumptions on the matrix $a(x)$, the auxiliary cell problem is well-posed.

Let

$$v_\varepsilon(x) = u_0(x) + \varepsilon N^j(x/\varepsilon) \frac{\partial}{\partial x_j} S^\varepsilon u_0(x),$$

where $S^\varepsilon g(x) = \int_{\square} g(x + \varepsilon\omega) d\omega$ is the Steklov average of the function $g(x)$.

Theorem. *The following estimates hold:*

$$\begin{aligned} \|u_\varepsilon - u_0\| &\leq C\varepsilon\|f\|, \\ \|u_\varepsilon - v_\varepsilon\| + \|\nabla(u_\varepsilon - v_\varepsilon)\| &\leq C\varepsilon^{1/2}\|f\|, \end{aligned} \quad (4)$$

where the constants C depend only on λ , $\|b\|_{\text{BMO}}$, Ω and d .

These estimates admit an operator form. For example, $(4)_1$ means that

$$\|(A_\varepsilon + 1)^{-1} - (A_0 + 1)^{-1}\|_{L^2(\Omega) \rightarrow L^2(\Omega)} \leq C\varepsilon.$$

This result is proved jointly with V. V. Zhikov [1].

References

- [1] V. V. Zhikov, S. E. Pastukhova, Operator estimates in homogenization theory, *Russian Math. Surveys*, **71**(3), 417–511 (2016).

Steady-state oscillations of the volume of liquid on an elastic layer

Pavlova A.V.¹, Rubtsov S.E.¹, Telyatnikov I.S.²

¹Kuban State University, Krasnodar, Russia

²Federal Research Center Southern Scientific Center of the Russian Academy of Sciences, Rostov-on-Don, Russia

e-mail: pavlova@math.kubsu.ru, rub_serg@mail.ru, ilux_t@list.ru

The relevance of research dedicated to the dynamic interaction of a deformable foundation with hydrotechnical structures is determined by the increased requirements for their reliability during exploitation and the degree of forecast reliability concerning the aftereffects of vibrations.

We investigated the problem of oscillations of the limited volume of a perfect compressible fluid on an elastic layer with a rigid bottom edge, the surface of which is subjected to a harmonic load localized in the area Ω_0 . The displacements of the elastic foundation satisfy the Lamé equations. As a characteristic of the wave field in a fluid we consider the velocity potential satisfying the wave equation and the given boundary conditions: there is no hydrodynamic pressure on the upper surface of the fluid, the non-flow condition is given on the vertical boundaries, on the lower surface the fluid is influenced by the elastic foundation, described by the hydrodynamic pressure vector. The interaction of fluid and elastic media is specified by continuous vertical velocity in the contact area.

Assuming that the oscillations of the system are steady, after the time multiplier $\exp(-i\omega t)$ separation, using the integral Fourier transform, the problem was reduced to the integral equation (IE) with respect to the complex amplitude of the unknown hydrodynamic pressure in the contact area $q(x)$. For a plane problem, when the fluid occupies volume $\{0 \leq x \leq d; 0 \leq z \leq h\}$ on a layer $\Omega_0 = \{-l - s \leq x \leq -s\}$ IE has the form [1]

$$\begin{aligned} \sum_{n=-\infty}^{\infty} \left(\int_0^d k(x - 2nd - \xi) q(\xi) d\xi + \int_0^d k(x - 2nd + \xi) q(\xi) d\xi \right) \\ - \rho_0 \omega^2 \int_0^d r(x - \xi) q(\xi) d\xi = f(x), \quad 0 < x < d. \end{aligned}$$

Here kernels k , r depend on the oscillation frequency ω , and also mechanical and geometrical characteristics of a fluid and an elastic foundation, respectively.

IE is reduced to a system of functional equations that can be solved using the integral method of factorization [2]. The resulting representation $q(x)$ allowed us to construct the relations for the velocity potential in fluid $\phi(x, z)$ and the displacement amplitude vector of an elastic foundation.

The authors have studied the behavior of mechanical characteristics of the system depending on frequency, dimensions of the reservoir and thickness of the elastic foundation.

The obtained results make it possible to determine the main parameters of the contact interaction of hydroelastic systems “fluid–soil” taking into account the effect of natural and technogenic vibration loads, to reveal the conditions for occurrence of dangerous for the construction dynamic modes and to estimate their frequency range depending on the defining characteristics of the system.

The work was supported by RFBR (18-01-00124) and administration of Krasnodar region (16-41-230184).

References

- [1] S. E. Rubtsov, A. V. Pavlova, To study of the mixed dynamic problems for a limited volume of fluid on an elastic foundation, *Ecological Bulletin of Research Centers of the Black Sea Economic Cooperation*, **4**, 75–81 (2016).
- [2] V. A. Babeshko, *Generalized Factorization Method in Spatial Dynamical Mixed Problems of Elasticity Theory*, Nauka Press, Moscow, 1984.

Asymptotics for the spectrum in boundary value problems with strongly alternating boundary conditions

Pérez E.

Universidad de Cantabria, Av. de Los Castros s.n. 39005 Santander, SPAIN

e-mail: meperez@unican.es

We consider the homogenization of spectral problems for different operators in a bounded domain of $\mathbb{R}^{n+} \equiv \{x \in \mathbb{R}^n : x_n > 0\}$, $n = 2, 3$. The spectral parameter arises on the boundary conditions in small regions, of size $O(\varepsilon)$, periodically placed along $\{x_n = 0\}$. These boundary conditions are of Steklov type, while a Dirichlet condition is imposed in the rest of the boundary. ε is a small parameter that measures the period of the structure, and we look at the asymptotic behavior of the eigenvalues when $\varepsilon \rightarrow 0$. We provide an overview of some results for the Laplace operator and for the elasticity system (cf. [1, 2, 5, 6]), and also some new challenges (cf. [3, 4]).

References

- [1] D. Gómez, S. A. Nazarov, E. Pérez, Homogenization of Winkler–Steklov spectral conditions in three-dimensional linear elasticity, *Zeitschrift für Angewandte Mathematik und Physik ZAMP*, **69**, article 35 (2018).
- [2] M. Lobo, E. Pérez, Long time approximations for solutions of wave equations associated with the Steklov spectral homogenization problems, *Mathematical Methods in the Applied Sciences*, **33**, 1356–1371 (2010).
- [3] S. A. Nazarov, E. Pérez, New asymptotic effects for the spectrum of problems on concentrated masses near the boundary, *Comptes Rendues de Mecanique*, **337**, 585–590 (2009).
- [4] S. A. Nazarov, E. Pérez, On multi-scale asymptotic structure of eigenfunctions in a boundary value problem with concentrated masses near the boundary, *Revista Matemática Complutense*, **31**, 1–62 (2018).
- [5] E. Pérez, On periodic Steklov type eigenvalue problems on half-bands and the spectral homogenization problem, *Discrete and Continuous Dynamical Systems — Series B*, **7**, 859–883 (2007).
- [6] E. Pérez, Long time approximations for solutions of evolution equations from quasimodes: perturbation problems, *Mathematica Balkanica. New Series*, **25**, 95–130 (2011).

Various options for migration in elastic environments based on the method of Reverse Time Migration

Pestov L.N., Danilin A.N.

Immanuel Kant Baltic Federal University, Kaliningrad, Russia
e-mail: lpestov@kantiana.ru, adanilin@kantiana.ru

We know, that artifacts arise during migration in elastic media because the presence of longitudinal and transverse waves which having different characteristic surfaces [1, 2]. In our research, we did several migration options which were based on the method of Reverse Time Migration [3] for considered to reduce the influence of artifacts.

As a direct dynamic elasticity problem, we consider the Lamé system in the form of a first-order system:

$$\frac{\partial}{\partial t} v^i = \frac{1}{\rho} \sum_{j=1}^2 \frac{\partial \sigma_{ij}}{\partial x^j},$$

$$\frac{\partial}{\partial t} \sigma_{ij}(x, t) = \lambda \delta^{ij} \operatorname{div} v + \mu \left(\frac{\partial v^i}{\partial x^j} + \frac{\partial v^j}{\partial x^i} \right) + f(t) \delta(x - x_0) \delta_{ij},$$

$$v|_{t=0} = 0, \quad \sigma|_{t=0} = 0, \quad \sigma_v|_{\Gamma \times [0, T]} = 0,$$

where $\delta(x - x_0)$ is Dirac function, δ_{ij} is Kronecker symbol, f is Ricker wavelet, $\rho(x)$ is density, and λ, μ are Lamé parameters.

On the basis of the solution of the direct elasticity problem in forward and reverse time, we were constructed some variants of migration. A comparative analysis of the results is carried out.

This work was supported by the Russian Science Foundation under grant 16-11-10027.

References

- [1] V. G. Baidin, Problems of the quality of seismic migration in the reverse time on the example of the model BP2004, *Proceedings of the 54th Scientific Conference MIPT. Management and Applied Mathematics*, **2**, 16–18 (2011).
- [2] V. G. Baidin, Methods of improving seismic images. Development and implementation on high-performance computing systems, *Proceedings of the 53rd Scientific Conference of the Moscow Institute of Physics and Technology. Part VII. Management and Applied Mathematics*, **6**, 7–10 (2010).
- [3] V. M. Filatova, V. V. Nosikova, L. N. Pestov, Application of Reverse Time Migration (RTM) procedure in ultrasound tomography, numerical modeling, *Eurasian Journal of Mathematical and Computer Applications*, **4**(4), 5–13 (2016).

Sound speed determining in weak inclusions degraded by noise in the ultrasound tomography problem

Pestov L.N., Filatova V.M., Nosikova V.V.

Immanuel Kant Baltic Federal University, Kaliningrad, Russia
e-mail: lpestov@kantiana.ru, vifilatova@kantiana.ru, vnosikova@kantiana.ru

Rudnitskii A.G.

Institute of Hydromechanics NASU, Kyiv, Ukraine
e-mail: a.rudnitskii@gmail.com

The problem of early detection of cancer remains relevant despite the existence of a spectrum of non-invasive examination methods such as mammography, computer and magnetic resonance imaging (MRI), ultrasonography. Even with these advanced techniques the diagnosis and detection

of pathologies is difficult problem due to a dense background of the mammary gland and complex structure of breast tissue.

One of the most perspective approaches for solving of this problem is ultrasound tomography. It should be noticed several scientific groups providing modern investigation in ultrasound tomography [1–4].

The work is devoted to the problem of determining small sound speed fluctuations in medical ultrasound tomography problem. The primary aim of the paper is to determine the location of small inclusions, sound speeds in them and also to determine unknown boundary between the fatty and glandular tissues. The sound speeds in these tissues are known.

The approach is based on visualization of unknown inner boundary and inclusions and determination of the sound speeds in inclusions using wave kinematics. The work is the continuation of the work [5], where the problem of visualization by the method of Reverse Time Migration was already solved. For testing of robustness of algorithm the original data (artificial clean image) were damaged by Gaussian and alpha-stable noises with different intensity. The results of numerical modeling are presented.

The numerical simulation is supported by the Russian Science Foundation under grant 16-11-10027. The preparing noisy data is supported by the Volkswagen Foundation project “Modeling, Analysis and Approximation Theory toward Applications in Tomography and Inverse Problems”.

References

- [1] G. Y. Sandhu, C. Li, O. Roy, S. Schmidt, N. Duric, Frequency domain ultrasound waveform tomography: breast imaging using a ring transducer, *Physics in Medicine & Biology*, **60**, 5381–5398 (2015).
- [2] V. A. Burov, D. I. Zotov, O. D. Romyantseva, Reconstruction of the sound velocity and absorption spatial distributions in soft biological tissue phantoms from experimental ultrasound tomography data, *Acoustical Physics*, **61**(2), 231–248 (2015).
- [3] A. V. Goncharsky, S. Y. Romanov, S. Y. Seryozhnikov, A computer simulation study of soft tissue characterization using low-frequency ultrasonic tomography, *Ultrasonics*, **67**, 136–150 (2016).
- [4] N. V. Ruiter, M. Zapf, T. Hopp, R. Dapp, H. Gemmeke, Phantom image results of an optimized full 3DUSCT, *Medical Imaging 2012: Ultrasonic Imaging, Tomography, and Therapy*, **8320**, 832005-1–832005-6 (2012).
- [5] V. M. Filatova, V. V. Nosikova, L. N. Pestov, Application of Reverse Time Migration (RTM) procedure in ultrasound tomography, numerical modeling, *Eurasian Journal of Mathematical and Computer Applications*, **4**(4), 5–13 (2016).

Asymptotic solution of the Helmholtz equation in a three-dimensional layer of variable thickness with a localized right-hand side

Petrov P.N., Dobrokhotov S.Yu.

Moscow Institute of Physics and Technology (State University), 9 Institutskiy per., Dolgoprudny, Moscow Region, 141701, Russian Federation;

Ishlinsky Institute for Problems in Mechanics of the Russian Academy of Sciences, Prospekt Vernadskogo 101-1, Moscow, 119526, Russia

e-mail: petr.petrov@phystech.edu, dobr@ipmnet.ru

We construct the asymptotic solution of the Helmholtz equation in a three-dimensional layer of variable thickness with a localized right-hand side

$$(h^2\Delta + n^2(x, y))u = F\left(\frac{x - \xi_1}{\mu}, \frac{y - \xi_2}{\mu}\right)g\left(\frac{z - z_0}{\mu}\right), \quad u|_{z=hd_1(x,y)} = 0, \quad u|_{z=hd_2(x,y)} = 0.$$

Here coefficient $n^2(x, y)$, and functions $d_1(x, y)$, $d_2(x, y)$, $F(x, y)$, $g(z)$ are smooth functions of their arguments. Functions $d_1(x, y) < d_2(x, y)$ define the boundary of the layer. We suppose that functions $F(x, y)$, $g(z)$ rapidly decay at infinity. Numbers (ξ_1, ξ_2, z_0) define coordinates of the point in the neighborhood of which the source is localized. The positive parameters h and μ are assumed to be small.

Using method of adiabatic dimension reduction [1] and recently developed approach [2], assuming the absence of “trap” states and the fulfillment of radiation conditions at infinity (such as the Sommerfeld condition) we construct the asymptotic solution of the formulated problem under the condition $1 \gg \mu \geq h$. The asymptotic solution can be represented as an decomposition into a finite number of modes, each mode is connected with pair of Lagrangian manifolds. One of the corresponding manifolds defines a localized (“singular”) part of the solution in the neighborhood of the point $(x = \xi_1, y = \xi_2)$. The second manifold defines the oscillating (“wave”) part of the solution over the entire layer (taking into account the possible appearance of caustics and focal points). In the limit $F(x, y)g(z) \rightarrow \delta(x)\delta(y)\delta(z)$ the obtained formulae describe the asymptotics of the Green’s function for the considered Helmholtz equation, but unlike such asymptotics, the obtained formula allows us to describe influence of the source shape on the wave part of the solution quite explicitly.

The research was carried out within the state assignment (theme No. AAAA-A17-117021310377-1), supported in part by RFBR (project No. 17-01-00644).

References

- [1] V. V. Belov, S. Yu. Dobrokhotov, T. Ya. Tudorovskii, Asymptotic solutions of nonrelativistic equations of quantum mechanics in curved nanotubes: I. Reduction to spatially one-dimensional equations, *Theoretical and Mathematical Physics*, **141**(2), 1562–1592 (2004).
- [2] A. Yu. Anikin, S. Yu. Dobrokhotov, V. E. Nazaikinskii, M. Rouleux, The Maslov canonical operator on a pair of Lagrangian manifolds and asymptotic solutions of stationary equations with localized right-hand sides, *Doklady Mathematics*, **96**(1), 406–410 (2017).

Transformation of the modal structure of acoustical field in course of the sound propagation from continental shelf to the deep ocean

Petrov P.S., Burenin A.V., Golov A.A., Morgunov Yu.N.

V.I. Il’ichev Pacific Oceanological Institute, 43 Baltiyskaya str., Vladivostok, 690041, Russia
e-mail: petrov@poi.dvo.ru

The problem of pulse signals propagation from continental shelf to the underwater sound channel (USC) of the deep sea and related physical effects are important for many practical applications of underwater acoustics, including, for instance, acoustical ranging and navigation. A compound waveguide consisting of a shallow-water part, a section with the continental slope and of an underwater sound channel of the deep sea is a strongly range-dependent environment where many interesting propagation effects (such as mode coupling and mudslide effect [1]) can be observed.

The goal of the present study is to investigate the transfer of acoustical energy from shallow-to deep-water area, and to describe related effects in the framework of the ray theory and using the method of normal modes [2]. Our work is based on the data obtained in an *in-situ* experiment conducted in the Sea of Japan by our institution (POI). The measurements in this experiment were performed along an acoustical track beginning near the coast of Primorsky Krai and directed towards the Kita-Yamato Bank in the deep-water area of the Sea of Japan. Pulse signals emitted by a transducer moored near the shore were received at different ranges from the source at the depths from 0 to 1000 m. Performing spectral analysis of the signals received at different depths, we developed a realistic model of the compound waveguide and performed the simulation of sound propagation using the method of wide-angle parabolic equation [2].

The results of the modeling allow us to study the modal structure of acoustical field along the track and the variation of modal amplitudes with range in the transition area between the shelf and the deep-water waveguide. The analysis results are discussed, and the mudslide effect is explained in terms of mode amplitudes variation.

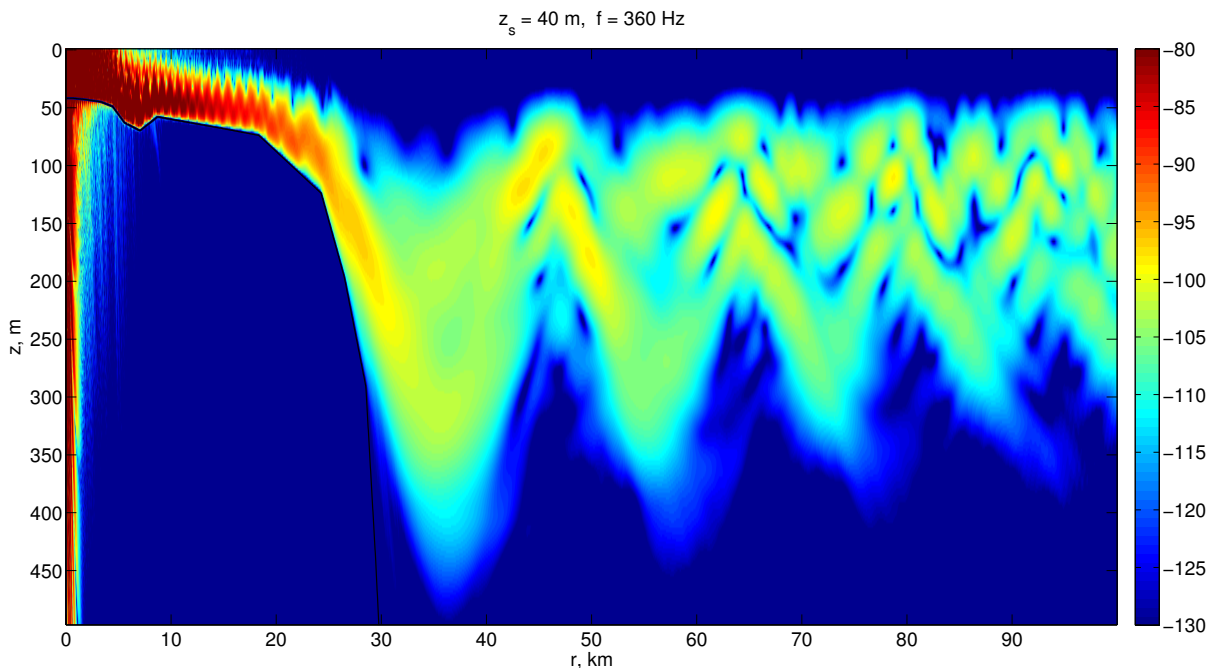


Fig. 1: Sound field in the compound waveguide for the frequency $f = 360$ Hz.

References

- [1] F. D. Tappert, J. L. Spiesberger, M. A. Wolfson, Study of a novel range-dependent propagation effect with application to the axial injection of signals from the Kaneohe source, *JASA*, **111**, 757–762 (2002).
- [2] F. Jensen, W. Kuperman, M. Porter, H. Schmidt, *Computational Ocean Acoustics*, Springer, New York et al., 2011.

Numerical solution of iterative parabolic equations approximating the nonlinear Helmholtz equation

Petrov P.S., Tyshchenko A.G.

V. I. Il'ichev Pacific Oceanological Institute, 43 Baltiyskaya str., 690041, Vladivostok, Russia;
Far Eastern Federal University, 8 Sukhanova str., 690950, Vladivostok, Russia
e-mail: petrov@poi.dvo.ru, ggoldenfeniks@gmail.com

Ehrhardt M.

Bergische Universität Wuppertal, Gaußstraße 20, D-42119 Wuppertal, Germany
e-mail: ehrhardt@uni-wuppertal.de

Nonlinear Helmholtz equation (NHE)

$$\frac{\partial^2}{\partial z^2} E + \frac{\partial^2}{\partial x^2} E + k_0^2 (1 + \epsilon |E|^{2\sigma}) E = 0, \quad (1)$$

(where $E = E(x, z)$ denotes the electric field) is a standard mathematical tool for describing the propagation of electromagnetic waves in Kerr media [1]. Boundary value problems for the nonlinear Helmholtz equation are extremely difficult to solve, and the only direct solution technique known

from the literature is based on some iterative procedure. The iterations start from the solution of nonlinear Schrödinger equation (NSE) that is a paraxial approximation to the NHE.

Recently a new approach to the modeling of one-way wave propagation in Kerr media was proposed [2]. Within this approach, the NHE is replaced by a system of iterative parabolic equations (IPEs) of the form

$$\begin{aligned}
 2ik_0 A_{0z} + A_{0xx} + \epsilon k_0^2 |A_0|^2 A_0 &= 0, \\
 2ik_0 A_{1z} + A_{1xx} + \epsilon k_0^2 (2|A_0|^2 A_1 + A_0^2 A_1^*) + A_{0zz} &= 0, \\
 2ik_0 A_{2z} + A_{2xx} + \epsilon k_0^2 (2|A_0|^2 A_2 + A_0^2 A_2^*) + \epsilon k_0^2 (2|A_1|^2 A_0 + A_1^2 A_0^*) + A_{1zz} &= 0, \\
 \dots,
 \end{aligned} \tag{2}$$

and the solution of the NHE is approximated by a converging series of IPEs solutions. By contrast to the NSE (i.e., the paraxial approximation), IPEs take the nonparaxial propagation effects into account. For example, it was shown that IPEs allow to simulate nonparaxial soliton propagation accurately.

In this study we develop an efficient pseudospectral numerical method for solving the system of IPEs. The method is a generalization of an exponential time differencing (ETD) method for the NSE. A ETD technique is well-suited for the system of IPEs, as it allows to reduce the order of the derivative in the input term.

References

- [1] G. Fibich, *The Nonlinear Schrödinger Equation: Singular Solutions and Optical Collapse*, Springer International Publishing, Cham et al., 2015.
- [2] P. S. Petrov, D. V. Makarov, M. Ehrhardt, Wide-angle parabolic approximations for the nonlinear Helmholtz equation in the Kerr media, *EPL*, **116**, 24004 (2016).

Diffraction of high-frequency hadronic waves

Vladimir Petrov

A. A. Logunov Institute for High Energy Physics of the National Research Center “Kurchatov Institute”

e-mail: vladimir.petrov@ihep.ru

This is a review of the current state of art — both experimental and theoretical — in the field of high-energy hadron diffractive scattering. Latest results from the Large Hadron Collider and related theory problems will be presented.

Averaged equations bi-continuum material in the long-wavelength approximation

Polyanskiy V.A.¹, Belyaev A.K.¹, Tretyakov D.A.¹, Yakovlev Yu.A.¹, Polyanskiy A.M.²

¹Institute for Problems in Mechanical Engineering RAS, V.O., Bolshoj pr., 61, St. Petersburg, 199178 Russia

²RDC Electron and Beam Technology, Ltd., st Bronevaya, 6, St. Petersburg, 198188 Russia

e-mail: vapol@mail.ru, vice.ipme@gmail.com, ampol@electronbeamtech.com

The phenomenon of fatigue failure includes a strong influence of random factors. In our paper [1], we showed that this phenomenon can be described as a parametric resonance associated with the accumulation of hydrogen in a metal. More recent studies [2] have shown that in the case of direct exposure of hydrogen to a metal, resonance phenomena are actually observed experimentally.

In particular, there is a resonant frequency of mechanical loading, in which destruction occurs about a hundred times faster. In this case, a strong influence of the boundary conditions was observed.

It is known that the place of fatigue failure under cyclic loading is largely determined by random factors. To study this feature, we applied the equations of the bi-continual material. In the case of a sufficiently long working part of the test sample of a metal, it can be regarded as a beam of the same cross section. This allows one to obtain one-dimensional equations for a continuous medium.

It is necessary to take into account the periodic nature of mechanical loading. The processes that associated with the diffusion and accumulation of hydrogen have a time constant of the order of tens of hours and more. This allows us to consider displacements under the action of a cyclic load as a fast movement. Then it is possible to separate fast and slow motions with averaging over the period of the load cycle. Such averaging leads to a separate equation for the slow component of the motion.

The equations for the averaged parameters have a maximum fifth order of derivatives, instead of the third order in the original equation. Investigation of their solutions by the Fourier method shows that there are wave solutions resembling a kink. At the same time, it is known that hydrogen inside metals is in traps with dimensions of the order of not more than grain sizes. Consequently, the influence of boundary conditions on the development of hydrogen degradation should not be decisive. This allows us to use the long-wave approximation in the study of averaged equations for a slow variable.

Analysis of dispersion relations shows that we have two stable solutions, one is a constant, the second is slowly damped. The relationship between the frequency and the length of the damped wave depends only on the hydrogen sorption- desorption coefficients in the traps, the temperature of the medium and the generalized cross section of the diffusion channels. Thus, the external cyclic load on these decisions does not affect. On the contrary, perturbations give short wave solutions, which strongly depend on the parameters of external loading. The results obtained are in good agreement with the experimental data.

The support by the Russian Foundation for Basic Research, projects 17-08-00783 and 18-08-00201, is acknowledged.

References

- [1] A. K. Belyaev, et al., Parametric instability in cyclic loading as the cause of fracture of hydrogenous materials, *Mech. Solids*, **47**(5), 533–537 (2012).
- [2] J. Yamabe, et al., Effects of hydrogen pressure, test frequency and test temperature on fatigue crack growth properties of low-carbon steel in gaseous hydrogen, *Procedia Structural Integrity*, **2**, 525–532 (2016).

GPR image deconvolution from antenna current waveform

Popov A.V., Edemsky F.D., Prokopovich I.V.

Pushkov Institute of Terrestrial Magnetism, Ionosphere and Radio Wave Propagation IZMIRAN, Troitsk, Moscow, 108840 Russia

e-mail: popov@izmiran.ru

Monopulse ground penetrating radar (GPR) registers reflections and diffraction response from subsurface interfaces or localized objects. Usually the image is blurred due to inherent oscillations of the probing pulse. This effect can be mitigated by deconvolution of the GPR image from the probing pulse waveform. The difficulty lies in the variability of the transmitter antenna current depending on the unknown ground parameters. We propose a practical solution that consists in comparing the subsurface echo with the primary electromagnetic pulse propagating from the GPR antenna into the air. Having the same origin, both aerial and subsurface signals are convolutions of the antenna current waveform with the corresponding time-domain Green functions [1]. This gives a possibility to find the current from aerial measurements and clear up the subsurface echoes applying

a deconvolution procedure. We illustrate analytical issues with a model example of a line antenna lying on the uniform dielectric half-space [2] and discuss practical aspects of the proposed method.

Work is supported in part by RFBR grant No. 18-02-00185.

References

- [1] J. D. Jackson, *Classical Electrodynamics*, 3rd ed., John Wiley & Sons, Inc., 1999.
- [2] F. Edemsky, A. Popov, S. Zapunidi, A time domain model of GPR antenna radiation pattern, *Internat. Journal of Electronics and Telecommunications*, **57**(3), 407–411 (2011).

On Morse index calculations for geodesic lines on smooth surfaces imbedded in \mathbb{R}^3

Popov M.M.

Saint-Petersburg Department of V. A. Steklov Institute of Mathematics, Fontanka emb., 27
e-mail: mmpopov@gmail.com

Morse index, see [1], appears in problems of mathematical physics devoted to construction and application of quasi-classical asymptotics [2, 3] and short-waves propagation in inhomogeneous media, e.g. in the ray method. In the presentation a new approach for calculation of it is developed for geodesic lines on smooth surfaces imbedded in \mathbb{R}^3 . That topic is of interest in theory of surface waves due to the waves slide along geodesic line of the surfaces. That takes place also in short-wave diffraction by 3D scatterers with smooth boundary surface in the shadowed part of the surface where creeping waves arise.

Approach under discussions is actually based on two ideas and mathematical technique what stem from the recent paper of the author [4]:

1. We consider a beam of geodesic lines in a close vicinity of the separated, central geodesic and derive equations in variation which enable calculating of the geometrical spreading of the beam precisely on the central one. For details see also [5, 6].
2. We construct further a complex-valued function from two linearly independent solutions of the equations in variation which never turn to zero and its argument is monotonic function of arc length of central geodesic. Incremental value of the argument the complex-valued function between two points on the geodesic provides number of focal point on the geodesic between those points.

References

- [1] J. Milnor, *Morse Theory*, Princeton University, Princeton, New Jersey, 1963.
- [2] V. P. Maslov, M. V. Fedoryuk, *Quasiclassical Approximation to the Equations of Quantum Mechanics*, “Nauka”, Moscow, 1976, (in Russian).
- [3] V. I. Arnold, On characteristic class, entering into quantization condition, *Functional Analysis and Application*, **1**, 1–14 (1967), (in Russian).
- [4] M. M. Popov, On calculating the Morse index and continuation of ray formulas beyond caustics, *J. Math. Sci. (N. Y.)*, **224**, 150–156 (2017).
- [5] M. M. Popov, On a method of calculation of geometrical spreading in inhomogeneous medium with interfaces, *Doklady Acad. Sci. SSSR*, **237**, 1059–1062 (1977), (in Russian).
- [6] M. M. Popov, *Ray Theory and Gaussian Beam Method for Geophysicists*, EDUFBA, Salvador-Bahia, 2002.

Two dimensional nonlinear waves in crystalline media

Porubov A.V.

Institute for Problems in Mechanical Engineering, Saint Petersburg, Russia;
Peter the Great St. Petersburg Polytechnic University (SPbPU), Polytechnicheskaya st., 29, Saint Petersburg, Russia

e-mail: alexey.porubov@gmail.com

Various nonlinear two-dimensional lattice models are considered including square lattice model with additional long-range interactions, di-atomic lattice and hexagonal graphene lattice. These models allow us to study both translation and rotation interactions between the elements of the lattice. The models based on an interaction between sub-lattices are also considered. An analysis of the linearized discrete equations reveals the most important intervals of the wave numbers where continuum limits can be obtained. An asymptotic procedure is developed to obtain continuum two-dimensional dispersive nonlinear equations for longitudinal and shear waves. Of primary interest are their plane localized wave solutions and their transverse instability. An influence of the long-range interactions between the elements of the lattice on the sign of the amplitude of the plane localized waves is found.

Preliminary results have been obtained in Refs. [1–3].

The work has been supported by the Russian Foundation for Basic Researches, grant No 17-01-00230-a.

References

- [1] A. V. Porubov, A. M. Krivtsov, A. E. Osokina, Two-dimensional waves in extended square lattice, *Intern. J. Non-linear Mechanics*, **99**, 281–287 (2018).
- [2] A. V. Porubov, I. E. Berinskii, Two-dimensional nonlinear shear waves in materials having hexagonal lattice structure, *Mathematics and Mechanics of Solids*, **21**, 94–103 (2016).
- [3] A. V. Porubov, I. V. Andrianov, B. Markert, Transverse instability of nonlinear longitudinal waves in hexagonal lattices, *Proceedings of the Estonian Academy of Sciences*, **64**, 349–355 (2015).

Mathematical theory of continuum mechanics with angular momentum

Prozorova E.V.

Mathematics & Mechanics Faculty, St. Petersburg State University, University av. 28, Peterhof, 198504, Russia

e-mail: e.prozorova@spbu.ru

The aim of the paper is to eliminate inaccuracies in the mathematical model for describing the mechanics of a continuous medium and to bring it into line with the provisions of classical theoretical mechanics. All conservation laws are based on experimental data obtained for finite elementary volumes. However, when writing conservation laws via delta functions, the same equations are obtained. This indicates that we neglect the processes inside the volume and with the volume and their influence on the conservation laws. Excluded effects can affect critical and near critical operating modes of aircraft, missiles, various devices, building structures, as well as in some natural processes, in astrophysics. The magnitude of the additional force is determined by the value of the gradient of physical quantities (density, velocity, momentum) and the structure of the object under study. The classic theory of continuum mechanics does not preserve the continuity of the environment due to the use of the conditions of equilibrium of forces and the symmetry of the stress tensor. We used many unreasonable mathematical approximations when by the Boltzmann equation is solved to describe the equations of continuum mechanics. The paper presents an analysis of mathematical approximations underlying description in different environments, and new models, to

avoid the resulting misunderstandings. For rarefied gas the self-diffusion and thermo-diffusion which were foretold by S. V. Vallander are obtained from kinetic theory. A new method for calculating the pressure and energy for a multicomponent gas is proposed. In conclusion, we note that in the construction of statistical theories of an equilibrium liquid in the Clausius theory, for pressure,

$$p - nkT = -\frac{1}{6}\rho^2 \int v(\mathbf{r})g(\mathbf{r}) d\mathbf{r},$$

where $v(\mathbf{r})$ is the power of the intermolecular interaction force $\frac{d\varphi(\mathbf{r})}{dn(\mathbf{r})}$, $\varphi(\mathbf{r})$ is potential, and $g(\mathbf{r})$ is the pair distribution function; i.e. the value of the same structure (dimensional) as the term in the equations with allowance for the angular momentum, that is $M = (\mathbf{r}-\mathbf{r}_0) \times \frac{d\varphi(\mathbf{r})}{d(\mathbf{r})}$, \mathbf{r}_0 is position of inertia center. So

$$p - nkT = -\frac{1}{6}\rho^2 \int \left(v(\mathbf{r}) + \mathbf{r} \frac{dM}{d\mathbf{r}} \right) g(\mathbf{r}) d\mathbf{r}.$$

For a viscous gas, the formula for the transition from the integral over the surface to the integral over the volume which we use when deriving the conservation laws must be generalized, that is, the circulation of the velocity must be taken into account. Hence the Stokes formula (Ostrogradsky, Gauss) should be generalized.

References

- [1] E. Prozorova, Effect of mathematical models on experimental data for the gas and liquids, *Journal of Mechanics Engineering and Automation*, **6**, 313–318 (2016).
- [2] E. Prozorova, The role of dispersion effects and delay for continuum mechanics, *Proceedings of 16th International Workshop on New Approaches to High-Tech: Nano-Design, Technology, Computer Simulations. NDTCS-2015*, 136–138.
- [3] E. V. Prozorova, Influence of the delay and dispersion in mechanics, *Journal of Modern Physics*, **5**, 1796–1805 (2014).

Basic multiple-twisted spiral beams

Evgeniya V. Razueva, Eugeny G. Abramochkin

Lebedev Physical Institute, Samara, 443011, Russia

e-mail: dev@fian.smr.ru

We consider paraxial light fields whose intensity distribution rotates during propagation in free space keeping its form. Such beams are named spiral or rotating beams. The angle of total intensity rotation, corresponding the beam propagation from the waist plane to far field, is defined as $\theta\pi/2$, where θ is an arbitrary real, named the rotation parameter.

For the case $\theta = \pm 1$, the theory of spiral beams has been described in [1]. If θ is a nonzero integer, $\theta = \pm N$, then corresponding spiral beams (named *multiple-twisted* or *N-twisted spiral beams*) in the waist plane have the form

$$F(x, y, 0) = \exp(x^2 + y^2) \iint_{\mathbb{R}^2} \exp(-\xi^2 - \eta^2 + 2\sqrt{2}i(x\xi + y\eta)) f(W) d\xi d\eta, \quad (1)$$

where $f(z)$ is an arbitrary entire function such that the field F is of finite energy, and

$$W = \begin{cases} (\xi^2 + \eta^2)^{2N-1}(\xi \mp i\eta)^2, & \text{if } \theta = \pm 2N, \\ (\xi^2 + \eta^2)^N(\xi \mp i\eta), & \text{if } \theta = \pm(2N + 1). \end{cases} \quad (2)$$

This expression provides a way to construct various multiple-twisted spiral beams because $f(z)$ is arbitrary. However, when we need to construct a spiral beam with the intensity distribution of a

predetermined shape, it is not clear how to choose the function. If $\theta = -1$, then the function $f(z)$ is known:

$$f(z) = \exp(ic^*z - cc^*), \quad (3)$$

where c is a complex-valued shift parameter, that leads to a shifted Gaussian beam. The beam shaping technique uses this beam as a light drawing tool. More exactly, the shifted Gaussian beam works as a pencil tip moved along the prescribed curve in the xy -plane because its intensity looks as one and the same Gaussian spot for all values of c [2].

In general case, $\theta = \pm N$, it is more difficult to choose a similar basic beam. Using the shifted Gaussian beam, we construct a *shifted pseudo-Gaussian beam* for each value of $N > 1$. This beam, in contrast with the ordinary shifted Gaussian beam, does not keep its intensity shape when the shift distance from the origin changes. Nevertheless, numerical simulations show that shifted pseudo-Gaussian beams provide a simple way for constructing multi-spot spiral beams. The last ones are an effective tool for localization of single fluorescent molecules in superresolution microscopy [3].

The shifted pseudo-Gaussian beam is not a unique choice for constructing multiple-twisted spiral beams. For the case $\theta = -3$, another kind of a basic beam is a *pseudo-Bessel beam*, depending on the Bessel function $J_0(z)$. We present some examples of 3-twisted spiral beams based on pseudo-Bessel beams.

References

- [1] E. G. Abramochkin, V. G. Volostnikov, Spiral light beams, *Physics–Uspekhi*, **47**, 1177–1203 (2004).
- [2] J. A. Rodrigo, T. Alieva, E. Abramochkin, I. Castro, Shaping of light beams along curves in three dimensions, *Optics Express*, **21**, 20544–20555 (2013).
- [3] S. R. P. Pavani, R. Piestun, High-efficiency rotating point spread functions, *Optics Express*, **16**, 3484–3489 (2008).

Laplacians on periodic graphs with boundary

Ryadovkin K.S.

Saint-Petersburg State University, Universitetskaya nab. 7/9, St. Petersburg, 199034, Russia
e-mail: kryadovkin@gmail.com

It is well known that the spectrum of the Laplacian on a periodic graph consists of a finite number of non-degenerate bands and eigenvalues of infinite multiplicity. We consider the Laplacian on the periodic graph with the periodic boundaries. Under some conditions on the boundary the spectrum of the Laplacian has so-called surface spectrum, i.e. spectrum corresponding to the waves localized near the boundary. The surface spectrum is of particular interest due to its connection with study of the modern crystalline structure, thermal transport, propagation of electromagnetic and acoustic waves. We discuss condition when the part of the surface spectrum is above the spectrum of the Laplacian on the periodic graph without boundary. This part of the surface spectrum has a band structure. Also estimates of the Lebesgue measure and the position of this part of the surface spectrum are given. We consider a number of examples that can be of particular interest for physics. This talk is based on joint work with E. Korotyaev and N. Saburova.

Invariants and spectral estimates for Laplacians on periodic graphs

Saburova N.Yu.

Northern (Arctic) Federal University, Northern Dvina emb. 17, Arkhangelsk, 163002, Russia
e-mail: n.saburova@gmail.com

We consider Laplacians on periodic discrete graphs. The spectrum of the Laplacian consists of a finite number of bands, where degenerate bands are eigenvalues of infinite multiplicity. We obtain

the estimates of the Lebesgue measure of the Laplacian spectrum in terms of geometric invariants for periodic graphs and show that these estimates become identities for specific graphs. The proof is based on a special decomposition of the Laplacian into a direct integral, where fiber Laplacians have the minimal number of coefficients depending on the quasimomentum. Moreover, similar results for Schrödinger operators with periodic potentials on periodic discrete graphs are obtained. This is a joint work with E. L. Korotyaev from St. Petersburg State University.

Nonlinear Fourier transform, nonlinear modes and nonlinear superposition

Pavle Saksida

Faculty of Mathematics and Physics, University of Ljubljana, Jadranska 21, Ljubljana, Slovenia
e-mail: pavle.saksida@fmf.uni-lj.si

One of the principal tools in the analysis of the integrable nonlinear partial differential equations is the theory of the *inverse scattering transform*. This theory is reminiscent of the application of the Fourier analysis in solving the linear partial differential equations. Indeed, the scattering transform is often called the nonlinear Fourier transform. We shall consider the nonlinear Fourier transform associated with the ZS-AKNS systems with periodic boundary conditions. In general, the linear Fourier theory provides solutions of linear initial problems as linear superpositions of the Fourier modes. To some extent, the integrable nonlinear partial differential equations can be analyzed in an analogous way. In the talk I will present a perturbation theoretic approach to the construction of the nonlinear Fourier modes and of their nonlinear superposition in the case of the ZS-AKNS nonlinear Fourier transform with periodic boundary conditions. The key element of this approach is a convergent iterative scheme for the evaluation of the inverse nonlinear Fourier transform of the ZS-AKNS type.

References

- [1] P. Saksida, Nonlinear Fourier transform — towards the construction of nonlinear Fourier modes, *J. Phys. A: Math. Theor.*, **51**, 0152015 (2018).

Light bullets in a planar waveguide with quadratic nonlinearity and normal group velocity dispersion

Sazonov S.V., Kalinovich A.A., Zakharova I.G., Komissarova M.V.

Lomonosov Moscow State University, 119991, Leninskie Gory, Moscow, Russia

e-mail: sazonov.sergey@gmail.com, kalinovich@gmail.com, zaharova@physics.msu.ru,
komissarova@physics.msu.ru

We study solutions to the second-harmonic-generation equations in a 2D waveguide with normal dispersion. An analytical solution is obtained in an approximate form of the planar spatiotemporal two-component soliton by means of the averaged Lagrangian method [1]. It is demonstrated that waveguide geometry plays the fundamental role for light bullets existence provided that the normal dispersion is at both frequencies.

The system of second-harmonic generation for the envelopes of the fundamental and second harmonics in a focusing planar waveguide with parabolic profile of the refractive index, taking into account the mutual influence of nonlinearity, second-order diffraction and dispersion in dimensionless form is written as:

$$i \left[\frac{\partial B_1}{\partial z} - D_{a1} x^2 \frac{\partial B_1}{\partial \tau} \right] + D_\tau \frac{\partial^2 B_1}{\partial \tau^2} - B_1^* B_2 = -D_{q1} x^2 B_1 + \frac{1}{2} D_x \frac{\partial^2 B_1}{\partial x^2}, \quad (1)$$

$$i \left[\frac{\partial B_2}{\partial z} - D_{a2} x^2 \frac{\partial B_2}{\partial \tau} \right] + 2D_\tau \frac{\partial^2 B_2}{\partial \tau^2} - \frac{1}{2} B_1^2 = -D_{q2} x^2 B_1 + \frac{1}{4} D_x \frac{\partial^2 B_2}{\partial x^2}. \quad (2)$$

Under normal dispersion, and the absence of waveguide, the pulse is unstable. Distribution in the form of bullets is observed only in the presence of waveguide. In computations we set the initial pulse in the form of the trial solutions $B_{1,2} = E_{1,2} \operatorname{sech}(x/a_{1,2}) \operatorname{sech}(\tau/\tau_{1,2})$. Numerical solution of the system (1)–(2) presented in Fig. 1 (a,b) is close to a two-component soliton forming at defocusing nonlinearity and focusing waveguide.

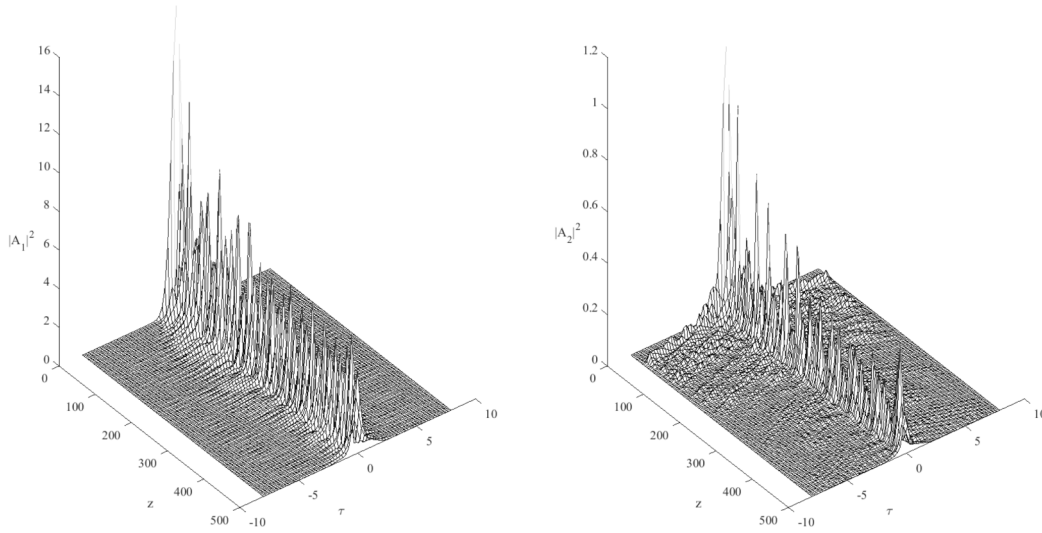


Fig. 1: Intensity distribution at the cross-sections tz showing the two-component soliton formation and spreading in a focusing waveguide with defocusing nonlinearity. (a) — fundamental frequency, (b) — second harmonic. $D_\tau = 0.01$, $\delta = 0$, $D_{a1,2} = 10^{-5}$, $\gamma_1 = 1$, $\gamma_2 = 0.5$, $D_{q1,2} = 5$, $D_x = 1$, $E_1 = 4$, $E_2 = 0.15$, $a_1 = 0.33$, $a_2 = 0.24$, $\tau_1 = 0.78$, $\tau_2 = 1.16$.

The investigation was made using support of the Russian Science Foundation (Grant № 17-11-01157).

References

[1] S. V. Sazonov, M. S. Mamaikin, I. G. Zakharova, M. V. Komissarova, Planar light bullets under conditions of second-harmonic generation, *Physical Review E*, **96**(2), 022208 (2017).

Simulation of the optical components surface quality influence on the propagation of high-power laser radiation

Schadko A.O., Zaytsev K.I., Chernomyrdin N.V., Nosov P.A.

Bauman Moscow State Technical University, Moscow 105005, Russia

e-mail: pan@bmstu.ru

The problem is solved on the basis of the numerical solution of the Maxwell equations by the finite-difference time-domain (FDTD) method [1]. The mathematical model describes the physical process of radiation interaction with the boundary between two media taking into account the random character of the surface shape. This allows obtaining a result for certain parameters of surface treatment that does not depend on the specific shape of the surface.

The initial data for the simulation are the parameters of the incident wave and the permittivity distribution. The incident wave was set as a plane one using the Total Field / Scattered Field method [2]. To model the region of the air-glass surface, the boundaries perpendicular to the separation plane have periodic boundary conditions, and the other two boundaries are the absorbing boundary conditions.

The developed model is implemented in the form of a program that uses the capabilities of GPUs. For each value of the described parameters, a series of simulations with independently generated surface forms was performed and for the region near the surface the parameter of interest was calculated, after which the data were averaged for all calculations of this series. The figure shows the results of calculating the maximum intensity for different values of the characteristic dimensions of surface elements. Calculation of the radiation intensity distribution was carried out for the range of the maximum height of surface microroughness $0.1\lambda \leq R \leq 5\lambda$ with 0.3λ increment, where λ is the radiation wavelength. Also, calculations were carried out for several values of the characteristic dimensions of the surface elements $\sigma = 0.6\lambda$, $\sigma = 1.1\lambda$, and $\sigma = 1.6\lambda$, that also allowed to determine this parameter influence on the simulation results (see Fig. 1).

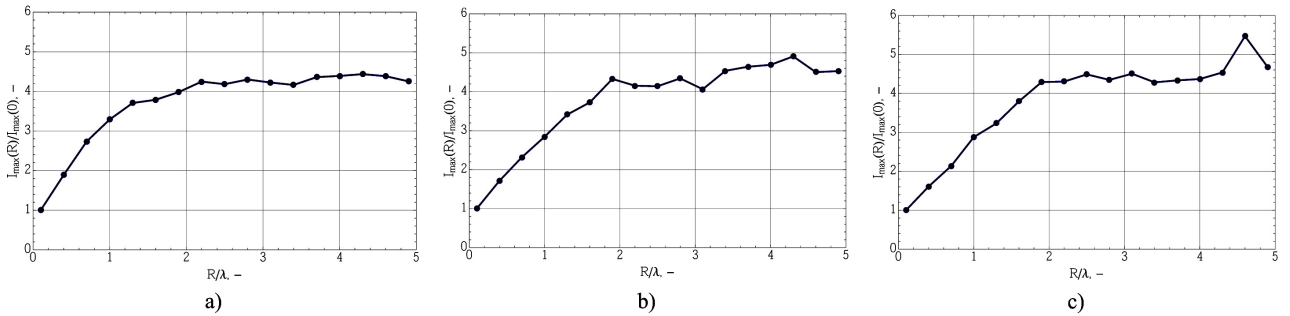


Fig. 1: Maximum radiation intensity normalized to the value for an ideal surface ($R = 0$) vs. maximum height of surface microroughness for different values of surface elements characteristic dimensions: $\sigma = 0.6\lambda$ (a), $\sigma = 1.1\lambda$ (b), $\sigma = 1.6\lambda$ (c).

Another important task is to investigate the effect of volume inclusions on the propagation of high-power laser radiation in transparent optical components. The system model is based on a linear dielectric material, without absorption. The inhomogeneities are characterized by their size and density and are described by a local change in the refractive index with a step profile. The position of the centers of inhomogeneities are determined by a random distribution with a uniform probability density.

The reported study was partially supported by RFBR, research project No. 16-08-00936 a.

References

- [1] J. B. Schneider, *Understanding the Finite-Difference Time-Domain Method*, School of Electrical Engineering and Computer Science, Washington State University, www.eecs.wsu.edu/~schneidj/ufdtd, 2010.
- [2] J. B. Schneider, Plane waves in FDTD simulations and a nearly perfect total-field/scattered-field boundary, *IEEE Transactions on Antennas and Propagation*, **52**, 3280–3287 (2004).

On homogenization for strongly elliptic operators with “Hölder continuous” locally periodic coefficients

Nikita N. Senik

St. Petersburg State University, Universitetskaya nab. 7/9, St. Petersburg 199034, Russia
e-mail: nnsenik@gmail.com

In homogenization theory, one is interested in studying asymptotic properties of solutions to differential equations with rapidly oscillating coefficients. We will consider such a problem for a matrix strongly elliptic operator $\mathcal{A}^\varepsilon = -\operatorname{div} A(x, x/\varepsilon)\nabla$ on \mathbb{R}^d , where A is Hölder continuous of order $s \in [0, 1]$ in the first variable and periodic in the second. We do not require that $A^* = A$, so \mathcal{A}^ε need not be self-adjoint. It is well known that the resolvent $(\mathcal{A}^\varepsilon - \mu)^{-1}$ converges, in some sense, as $\varepsilon \rightarrow 0$. In this talk, we will discuss results regarding convergence in the uniform operator

topology on $L_2(\mathbb{R}^d)^n$, i.e., the strongest type of operator convergence. We present the first two terms of an approximation for $(\mathcal{A}^\varepsilon - \mu)^{-1}$ and the first term of an approximation for $(-\Delta)^{s/2}(\mathcal{A}^\varepsilon - \mu)^{-1}$. Particular attention will be paid to the rates of approximation.

Maslov's canonical operator in the problem of acoustic pulse signal propagation in a shallow sea with penetrable bottom

Sergeev S.A., Tolchennikov A.A.

Institute for Problems in Mechanics of the Russian Academy of Sciences, Moscow, Russia;
Moscow Institute for Physics and Technology (State University), Dolgoprudny, Russia
e-mail: sergeevse1@yandex.ru, tolchennikovaa@gmail.com

Petrov P.S.

V.I. Il'ichev Pacific Oceanological Institute, Vladivostok;
Far Eastern Federal University, Vladivostok
e-mail: petrov@poi.dvo.ru

In the paper [1] the problem of modelling of the pulse acoustic signals in the deep ocean with the help of the Maslov's canonical operator was considered. In this talk we continue implementing the ideas of [1, 2] to the construction of the time series of pulse acoustic signal in the shallow sea [3].

In the mathematical language this problem can be formulated as the Cauchy problem for the inhomogeneous wave equation with zero initial functions.

$$\frac{1}{c_0^2} p_{tt} - \Delta_x p = Q(x, t), \quad x = (x_1, x_2, x_3) \in B, \quad (1)$$

$$B = \{(x_1, x_2) \in \mathbb{R}^2, x_3 \in [0, H]\}, \quad c_0 = \text{const.}$$

with the initial conditions

$$p|_{t=0} = p_t|_{t=0} = 0.$$

The variable x_3 describes the depth of the sea near the shore and here we set $H = \text{const}$. Equation $x_3 = 0$ describes the surface of the sea and the boundary condition on it has the standard form of the Dirichlet condition. The bottom is described by $x_3 = H$ and we assume it is penetrable for sound waves and at the bottom some part of the sound wave transmitted into the bottom. Therefore we pose the special reflection conditions [3].

The right-hand function $Q(x, t)$ depends on parameters λ, l :

$$Q(x, t) = \lambda^2 g'_0(\lambda t) \frac{1}{l^3} V\left(\frac{x - x^0}{l}\right)$$

with some fast decaying at infinity real functions $V(x)$, $g_0(\tau)$ and parameters $l \ll 1$, $\omega = \frac{c_0}{\lambda l} < \omega_0$. While the parameter $\lambda \rightarrow \infty$ function $\lambda^2 g'_0(\lambda t)$ tends to δ' -function, and we pose in our calculations λ is sufficiently big. Parameter l describes radius of the source function and we seek the asymptotic solution of the posed problem (1) while $l \rightarrow 0$.

Using [1, 2] we describe the procedure based on the modified Maslov's canonical operator for the asymptotic solution. We simulate with this procedure the propagation of the acoustic waves in the shallow sea near the shore. The asymptotic solution is built in the point where located the receiver.

This work was supported by grant RFBR-18-31-00148 mol_a.

References

- [1] P. S. Petrov, S. A. Sergeev, A. A. Tolchennikov, *Doklady Akademii Nauk*, **473**(2), 142–145 (2017) (in Russian).
- [2] S. Yu. Dobrokhotov, D. A. Minenkov, V. E. Nazaikinskii, B. Tirozzi, *Oper. Theory Adv. Appl.*, **228**, 95–125 (2013).
- [3] L. M. Brekhovskikh, *Waves in Stratified Media*, Moscow, Nauka, 1973 (in Russian).

Numerical method for solving the problem of electromagnetic wave scattering by a perfectly conducting object of small thickness

Setukha A.V.¹, Fetisov S.N.²

¹Lomonosov Moscow State University, Moscow, Leninskie gory, 1

²Institute of Numerical Mathematics RAS, Moscow, Gubkina, 8

e-mail: setuhaav@rambler.ru, sereja.fit@gmail.com

A three dimensional problem of monochromatic electromagnetic wave scattering by perfectly conducting objects of small thickness (one of the overall dimensions is much smaller than the others) is considered. Often, to reduce computational complexity of this problem, the original objects are replaced by thin screen, but it leads to incorrect results. The numerical method for the solution of this problem, based on relocation of the boundary condition to the median surface is developed. In this method we state a new boundary value problem at the domain outside this surface. The original shape of the body is taken into account due to the boundary conditions. The resulting problem is reduced to the system of two integro-differential equations at the median surface. The numerical scheme for solving these equations is developed. The quadrature formulas [1] has been used for the approximation of integral operators. Unlike boundary integral equation method (BIE) [2], developed numerical scheme does not degenerate when the body thickness tends to zero.

To test the developed method, there were obtained numerical solutions for the problem of the plane electromagnetic wave scattering by the rectangular wing with the symmetrical airfoil NACA0012 and aspect ratio (ratio of the maximum thickness to the chord) $t/c = 5\%$. The results of proposed method were compared with experimental data and results obtained by the BIE method in the cases $t/c = 5\%$ and 0% (thin screen). Solution results are presented as radar cross section (RCS) diagram (Fig. 1).

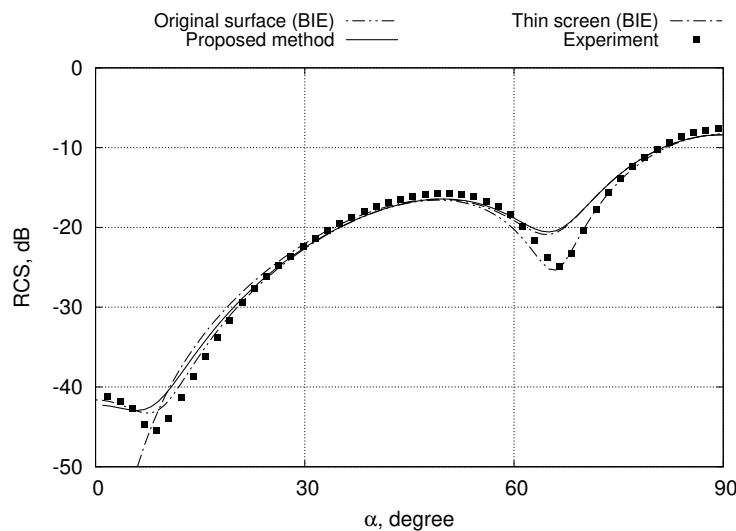


Fig. 1: Part of the RCS diagram for rectangular wing, obtained by different methods, $t/c = 5\%$, $\lambda = c$.

The main conclusions of testing:

1. The results of numerical solutions, obtained by proposed method, are in good agreement with experimental data;
2. Using thin screen instead original object lead to mismatch numerical solution by the BIE method with experimental data at an angle of observation at leading edge ($0^\circ \pm 10^\circ$).

References

- [1] E. V. Zakharov, A. V. Setukha, E. N. Bezobrazova, Method of hypersingular integral equations in a three-dimensional problem of diffraction of electromagnetic waves on a piecewise homogeneous dielectric body, *Differential Equations*, **51**(9), 1197–1210 (2015).

- [2] E. V. Zakharov, G. V. Ryzhakov, A. V. Setukha, Numerical solution of 3D problems of electromagnetic wave diffraction on a system of ideally conducting surfaces by the method of hypersingular integral equations, *Differential Equations*, **50**(9), 1240–1251 (2014).

Method of parabolic equation in diffraction theory. When it is applicable?

Shanin A.V., Korolkov A.I.

Moscow State University, Moscow, 119992 Russia

e-mail: a.v.shanin@gmail.com, korolkov@physics.msu.ru

The method of parabolic equation is used in diffraction theory to describe waves having a narrow angular spectrum [1]. Namely, the parabolic approximation can be applied to the wide range of problems: the problem of diffraction by a strip [2], by a body of revolution [3, 4], and to some waveguide problems [5]. Some of these problems can be solved explicitly in the parabolic approximation. Moreover, numerous numerical experiments show that the parabolic approximation works well even in the case when the diffraction process cannot be treated as paraxial. In the current work authors try to understand why it works better than expected. The problem of diffraction by a half-plane is considered. First, a problem for the parabolic equation with appropriate boundary conditions is introduced. Second, the problem is reduced to the boundary integral equation. The same procedure is repeated for the initial (Helmholtz) problem and the Wiener–Hopf equation is derived. It is found out that the kernel of the “parabolic” equation is one of the factors of the factorization of the “Helmholtz” equation kernel. This fact explains why the parabolic equation works well for the half-plane problem (even near the edge of the half-plane). Possible generalizations of this result is discussed.

The work is supported by the RSF grant 14-22-00042.

References

- [1] V. M. Babich, V. S. Buldyrev, *Asymptotic Methods in Short-Wave Diffraction Problems*, Vol. I, “Nauka”, Moscow, 1972 (in Russian).
- [2] A. I. Korolkov, A. V. Shanin, High-frequency plane wave diffraction by an ideal strip at oblique incidence: parabolic equation approach, *Acoust. Phys.*, **62**(4), 405–413 (2016).
- [3] A. V. Shanin, A. I. Korolkov, Diffraction by a thin cone in the parabolic approximation. Method of the boundary integral equation, *Proceedings of 2017 International Conference on Electromagnetics in Advanced Applications (ICEAA)*, IEEE, 696–699 (2017).
- [4] A. V. Shanin, A. I. Korolkov, Method of the boundary integral equation for the parabolic equation on a curved surface, *Proceedings of PIERS*, St. Petersburg, Russia, 1454–1459 (2017).
- [5] A. V. Shanin, A. I. Korolkov, Diffraction of a mode close to its cut-off by a transversal screen in a planar waveguide, *Wave Motion*, **68**(1), 218–241 (2017).

Experimental study of diffraction by a thin cone

Shanin A.V., Korolkov A.I., Belous A.A.

Moscow State University, 119992 Russia

e-mail: artem.belous@gmail.com, korolkov@physics.msu.ru, andrey_shanin@mail.ru

Diffraction by a thin cone attracts considerable attention of researchers. Several different approaches exist to developing both asymptotics of the diffracted field and the diffracted field itself. First, there is a traditional asymptotic approach based on ray representation [1]. Second, there is an approach based on the parabolic equation method [2]. Third, there is an approach based on the boundary integral equation method for the parabolic equation in Cartesian coordinates [3]. Also,

there is an approach based on the Smyshlyaev's formula [4], and an approach based on Kontorovich–Lebedev integral representation [5]. All these methods are mathematically complicated, and the question about which one works better is still open.

In this work, a direct diffraction experiment is used to measure the diffracted field on the surface of a thin cone and in its penumbral zone. The experiment is performed using MLS (Maximum Length Sequence) method. The results of the experiment are compared with those calculated using the existing methods.

The work is supported by the RSF grant 14-22-00042.

References

- [1] A. Popov, A. Ladyzhensky, S. Khozioski, Uniform asymptotics of the wave diffracted by a cone of arbitrary cross section, *Russ. J. Math. Phys.*, **16**(2), 296–299 (2009).
- [2] I. V. Andronov, Diffraction by a strongly elongated body of revolution, *Acoust. Phys.*, **57**, 147–152 (2011).
- [3] A. V. Shanin, A. I. Korolkov, Diffraction by a thin cone in the parabolic approximation. Method of the boundary integral equation, *ICEAA Proceedings 2017*, doi: 10.1109/ICEAA.2017.8065342.
- [4] V. M. Babich, D. B. Dement'ev, B. A. Samokish, V. P. Smychlyaev, On evaluation of the diffraction coefficient for arbitrary “nonsingular” directions of a smooth convex cone, *SIAM J. Appl. Math.*, **60**(2), 536–573 (2000).
- [5] M. A. Lyalinov, N. Y. Zhu, Acoustic scattering by a circular semitransparent conical surface, *J. Eng. Math.*, **59**(4), 385–398 (2007).

Scattering of quasi-electrostatic waves on the conducting bodies of revolution in media with dielectric anisotropy

Shirokov E.A.

Institute of Applied Physics of the Russian Academy of Sciences, Nizhny Novgorod, Russia
e-mail: evshirok@gmail.com

In this paper, scattering of quasi-electrostatic waves on the conducting bodies of revolution in media with dielectric anisotropy is investigated. The typical examples of such media are anisotropic plasmas (magnetoplasmas) [1] and hyperbolic metamaterials [2]. In these media, the refractive index surface has asymptotes if the diagonal (with respect to the anisotropy axis) dielectric tensor components have opposite signs. These asymptotes define the so-called resonance cone. The quasi-electrostatic waves propagate close to the resonance cone direction so their wave numbers can be quite large.

The problem is investigated both theoretically and numerically. The theoretical approach is based on the analytical methods of solution of the partial differential equation (for the complex amplitude of electrostatic potential) and the integral equation (for the charge density distribution on the conductor surface) that follow from Maxwell's equations. Much attention is paid to the Green's function of the partial differential equation because it is singular not only at the source point but on the resonance surface too [3]. The numerical approach is based primarily on the method of moments for solution of the integral equation.

The bodies of revolution used in this research are a metal circular cylinder and a metal sphere. The corresponding scattering characteristics (e.g., scattered fields and cross sections) are found and analyzed. The results can be important for the theory of antennas in plasmas and metamaterials.

References

- [1] T. H. Stix, *Waves in Plasmas*, Springer, New York, 1992.
- [2] N. Engheta, R. W. Ziolkowski, *Metamaterials: Physics and Engineering Explorations*, Wiley-IEEE Press, Hoboken, 2006.

- [3] A. A. Andronov, Yu. V. Chugunov, Quasisteady-state electric fields of sources in a dilute plasma, *Sov. Phys. Usp.*, **18**, 343–360 (1975).

Inverse scattering technique for deep water waves

Slunyaev A. V.

Institute of Applied Physics, Nizhny Novgorod, 46 Ulyanova Street;
 N. Novgorod State Technical University n. a. R. E. Alekseev, Nizhny Novgorod, 24 Minina Street
 e-mail: slunyaev@appl.sci-nnov.ru

We develop approaches for the application of the Inverse Scattering Technique (IST) to the analysis of the surface water waves (see e.g. [1]). The general idea is to interpret the nonlinear wave groups in terms of the soliton-like structures (envelope solitons in the framework of the integrable nonlinear Schrödinger equation), what could improve understanding of the nonlinear wave group dynamics, and in particular, could help to elaborate tools for short-term wave forecasting as suggested in [2, 3]. There is a number of significant difficulties in application of the IST to the practically important case of sea waves: wave directionality, phase-locked bound wave components, insufficiently narrow (or simply broad) wave spectrum, uncertainty in the choice of the carrier wavenumber. These problems are absent or greatly reduced in the application to optical fibers.

Based on the original idea of applying the IST to samples of waves in a sliding window [2] (see the left part in the figure below), a thorough study of various approaches was performed recently [4]; in particular, a feedback procedure was suggested with the purpose to stabilize the values of the calculated spectral data. In the right part of the figure the relative errors in evaluation of the soliton amplitude are shown for different actual amplitudes of the soliton-like structure simulated in the primitive equations of hydrodynamics. The quantity $k_p A_{env} = k_p (A_{cr} - A_{tr})/2$ stands for the dimensionless amplitude of the envelope, where k_p is the peak wavenumber and $A_{cr} = \max \eta$ and $A_{tr} = -\min \eta$ are the maximum crest and trough amplitudes. A few most efficient approaches are represented by different symbols. The best approaches typically provide accuracy within 10%.

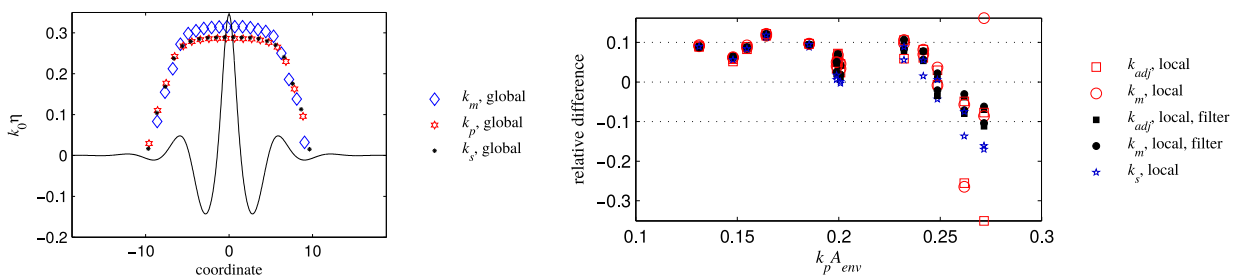


Fig. 1: Left: A steep envelope soliton (line) and soliton’s amplitudes (symbols) estimated with the help of the windowed IST method. Right: The relative difference between the estimated and actual amplitudes of envelope solitons versus the normalized amplitude.

Support from RSF Grant No. 16-17-00041 (development of the stable IST procedure) and RFBR Grant No. 16-55-52019 (numerical simulations of irregular sea waves) is acknowledged.

References

- [1] A. R. Osborne, *Nonlinear Ocean Waves and the Inverse Scattering Transform*, Academic Press, 2010.
 [2] A. V. Slunyaev, Nonlinear analysis and simulations of measured freak wave time series, *Eur. J. Mech. B / Fluids*, **25**, 621–635 (2006).
 [3] A. V. Slunyaev, Predicting rogue waves, *Moscow Univ. Phys. Bulletin*, **72**, 236–249 (2017).
 [4] A. V. Slunyaev, Analysis of the nonlinear spectrum of intense sea waves with the purpose of extreme wave forecasting, *Radiophys. Quantum Electronics*, (2018, in press).

Numerical study of the electromagnetic wave propagation problem in an anisotropic waveguide

Eugene Smolkin, Maxim Snegur

Penza State University, Penza, Russia

e-mail: e.g.smolkin@hotmail.com, snegur.max15@gmail.com

The propagation of monochromatic electromagnetic waves in a cylindrical waveguide filled with inhomogeneous anisotropic media is considered. The surface waves propagating along the axis Oz of the waveguide have the form [1]

$$\begin{aligned} E_\rho &= E_\rho(\rho)e^{im\varphi+i\gamma z}, & E_\varphi &= E_\varphi(\rho)e^{im\varphi+i\gamma z}, & E_z &= E_z(\rho)e^{im\varphi+i\gamma z}, \\ H_\rho &= H_\rho(\rho)e^{im\varphi+i\gamma z}, & H_\varphi &= H_\varphi(\rho)e^{im\varphi+i\gamma z}, & H_z &= H_z(\rho)e^{im\varphi+i\gamma z}, \end{aligned} \quad (1)$$

where γ is the real propagation constant (spectral parameter of the problem) and m is an angular integer parameter (which assumed to be known).

The permittivity inside the waveguide specified by the expression $\varepsilon = \hat{\varepsilon}\varepsilon_0$, where

$$\hat{\varepsilon} = \begin{bmatrix} \varepsilon_\rho & 0 & 0 \\ 0 & \varepsilon_\rho & 0 \\ 0 & 0 & \varepsilon_z \end{bmatrix},$$

and ε_ρ and ε_z are sufficiently smooth functions which depend on the radial coordinate ρ . For $m = 0$ this problem splits into two independent wave propagation problems: TE and TM.

The physical problem is reduced to solving a transmission eigenvalue problem for a system of ordinary differential equations. Spectral parameters of the problem are propagation constants of the waveguide. Numerical results are found with the modification of the projecting methods. The method [2, 3] allows us to determine approximate eigenvalues with any prescribed accuracy. The comparison with known exact solutions (for particular values of parameters) are made. The approach described in this paper can be applied to other problems, e.g., to multilayered opened anisotropic magnetic waveguides.

References

- [1] A. W. Snyder, J. Love, *Optical Waveguide Theory*, Springer, London, 1983.
- [2] E. Smolkin, Numerical method for electromagnetic wave propagation problem in a cylindrical inhomogeneous metal dielectric waveguiding structures, *Mathematical Modelling and Analysis*, **22**(3), 271–282 (2017).
- [3] E. Smolkin, M. Snegur, Yu. Shestopalov, Numerical method for electromagnetic wave propagation problem in a cylindrical anisotropic inhomogeneous waveguide with longitudinal magnetization, *2017 Progress In Electromagnetics Research Symposium – Fall (PIERS – FALL)*, 299–305 (2017).

The effect of curvature and torsion of inclusions on effective permittivity

Starkov I.A.¹, Starkov A.S.²

¹Nanotechnology Center, St. Petersburg National Research Academic University RAS, Khlopin st. 8/3, 194021 St. Petersburg, Russia

²Department of Advanced Mathematics, University ITMO, Kronverksky pr. 49, 197101 St. Petersburg, Russia

e-mail: starkov@spbau.ru, ferroelectrics@ya.ru

One of the simplest and physically vivid techniques for finding the effective dielectric constant of composite media is the Maxwell–Garnett (MG) approximation. The composite consists of two

(or more) dielectric components, of which one is treated as a matrix with dielectric constant ε_m and the other as the inclusion phase with dielectric constant ε_i . In the MG approach, the effective permittivity ε_{eff} is determined through the solutions of the model problem of a single inclusion located in an unbounded medium (matrix) and a homogeneous electric field. Since the electric field inside the inclusion is determined by its geometric parameters, in the general case ε_{eff} depends on its volume, surface area, edge length, and the curvature of the surface. For fiber composites, one should add to these characteristics a torsion of the curve that defines fiber. In this study, we investigate the effect of only curvature and torsion. In the planar case, it is feasible to obtain explicit expressions for ε_{eff} . Thus, for a set of rings (see Fig. 1a), we have

$$\varepsilon_{\text{eff}} = \varepsilon_m \left[1 + \frac{2f(\varepsilon_i - \varepsilon_m)}{\varepsilon_i + \varepsilon_m + (\varepsilon_m - \varepsilon_i)(f + \lambda - \lambda f)} \right]. \quad (1)$$

Here f is the volume fraction of inclusions, $\lambda = \frac{R_1^2(\varepsilon_m - \varepsilon_i)}{R_2^2(\varepsilon_m + \varepsilon_i)}$, and $R_{1,2}$ is the inner and outer radius of the ring, respectively. For $\lambda = 0$ we obtain the standard MG formula.

The situation is much more complicated in the three-dimensional case because of the necessity to take into account the torsion. If the intensity of the electric field is directed along the tangent to the fiber (see Fig. 1b), then the solution of the electrostatic problem of single inclusion cannot be explicitly constructed. It is possible only to find an asymptotics of this solution under the assumption that the thickness of the fiber is small in comparison with its radii of curvature and torsion. The problem of inclusions in the form of a torus is chosen as a reference. In general, its solution reduces to a system of difference equations. However, there exists as well an asymptotics of the solution of this system for thin toruses. As a result, we derive a formula for the effective dielectric constant of a composite medium, which takes into account the curvature and torsion of the fiber as an inclusion.

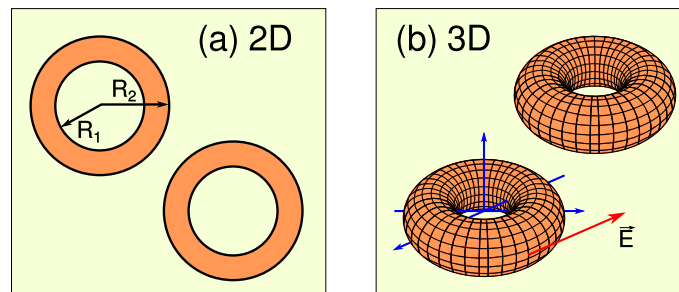


Fig. 1: The types of inclusions under consideration.

The reported study was funded by RFBR, according to the research project No. 16-32-60189 mol_a_dk.

Low-rank matrices with a hierarchical basis in an electromagnetic problem of diffraction

Stavtsev S.L.

Institute of Numerical Mathematics Russian Academy of Sciences, Moscow, Russia
e-mail: sstass2000@mail.ru

The parallel algorithms combined with low-rank approximations of dense matrices to solve problems of the electromagnetic wave diffraction on perfectly conducting objects with a complex shape are presented. If the problem is solved on a large object with a small wave length, this yields a large dense matrix.

Iterative methods, for example, General Minimal RESidual method (GMRES), are used routinely for the solution of linear systems of algebraic equations with large dense matrices. GMRES employs only multiplication of a low-rank matrix by a vector and does not involve any other operations with

the low-rank matrix. Since the parallel matrix-vector multiplication with a matrix in the mosaic-skeleton format scales well, the whole algorithm of the linear system solution with a matrix in the mosaic-skeleton format is also well scalable [1, 2].

However, the number of GMRES iterations increases rapidly with the large object. Therefore, for small wave length GMRES requires a lot of memory or a lot of time. Even more memory or time demanding is the problem of solving the linear system with many right-hand sides, which arises in the computation of the monostatic Radar Cross Section (RCS) characteristic.

To reduce the number of GMRES iterations one can use preconditioners. For example, in [3] an effective preconditioner is constructed, but its parallel version is poorly scalable. Moreover, experiments of applying this preconditioner to the electrodynamics problem have shown that the number of iterations can be reduced only if the inverse matrix is approximated very accurately.

The new well scalable parallel algorithm for calculating the low-rank matrices with a hierarchical basis is developed. The low-rank matrix with a hierarchical basis approach results in a better matrix compression rate than mosaic-skeleton matrix. The new algorithm is a kernel-independent MultiLevel Fast Multipole Algorithm (MLFMA).

A parallel solver for a low-rank matrix with a hierarchical basis that arises from the electrodynamics problem is constructed. The new method solver system with tens of millions of unknowns.

The new methods solve electromagnetic problem of diffraction (monostatic RCS) on the object with size of several tens of wave lengths.

The work was supported by the Russian Science Foundation, grant 14-11-00806.

References

- [1] S. L. Stavtsev, Application of mosaic-skeleton approximations for solving EFIE. *Progress in Electromagnetics Research Symposium (PIERS 2009 Moscow)*, 1752–1755 (2009).
- [2] A. A. Aparinov, A. V. Setukha, S. L. Stavtsev, Supercomputer modelling of electromagnetic wave scattering with boundary integral equation method, *Communications in Computer and Information Science*, **793**, 325 – 336 (2017).
- [3] S. L. Stavtsev, Block LU preconditioner for the electric field integral equation. *Progress in Electromagnetics Research Symposium*, 1523–1527 (2015).

Supercar model for dielectric equilateral triangle microresonators validated by the integral equation method

I.O. Sukharevsky¹, M. Lebental², B. Dietz³, C. Lafargue², S. Bittner²

¹Chair of High-Frequency Engineering, Department of Electrical and Computer Engineering, Technical University of Munich, 80333 Munich, Arcisstr. 21, Germany

²Laboratoire de Photonique Quantique et Moléculaire, CNRS UMR 8537, Institut d'Alembert FR 3242, Centrale Supélec, Ecole Normale Supérieure de Paris-Saclay, F-94235 Cachan, France

³School of Physical Science and Technology, and Key Laboratory for Magnetism and Magnetic Materials of MOE, Lanzhou University, Lanzhou, Gansu 730000, China

e-mail: i.sukharevsky@gmail.com

Dielectric microresonators have found a wide range of applications in optics and photonics during the last decade. We investigate in detail the resonant properties of a 2D dielectric cavity with an equilateral triangle shape for both transverse electric and transverse magnetic polarization. We complement a numerical approach based on the integral equations with a ray-based (semiclassical) approach by treating the resonator as a photon billiard. The billiard problem for a cavity with equilateral triangle shape is more challenging than for other integrable billiard geometries since it is not separable.

The homogeneous Muller boundary equation is used to calculate the resonant modes of a dielectric triangle in a wide range of frequencies. Though most of the results are valid for arbitrary

refractive index, we concentrate on the case of $n = 1.5$ which corresponds to the important case of polymer microlasers [2]. The method is validated and verified by the comparison of numerical results with exact solutions for canonical problems. Comparison with Weyl's law furthermore confirms the completeness of the calculated spectra.

The equilateral triangle exhibits two degenerate and two non-degenerate symmetry classes of resonances, and taking into account their symmetries helps to reduce the computational time significantly.

The numerical results obtained allowed us to clarify the nature of triangular resonator modes and the precision and validity of semiclassical approximations. It is shown that the modes of dielectric triangles are often localized on families of periodic orbits. These modes can be well described in terms of a semiclassical superscar model. Special attention is given to the resonances of quasi Fabry–Perot and inscribed triangle types.

I.S. is supported by the Alexander von Humboldt Foundation.

References

- [1] I. O. Sukharevskiy, M. Lebental, B. Dietz, C. Lafargue, S. Bittner, Dielectric equilateral triangle microresonators: integral equations and semi-classical physics approaches, *Laser Resonators, Microresonators, and Beam Control XX. — International Society for Optics and Photonics*, no. 105181U, 1–14 (2018).
- [2] C. Lafargue, M. Lebental, A. Grigis, C. Ulysse, I. Gozhyk, N. Djellali, J. Zyss, S. Bittner, Localized lasing modes of triangular organic microlasers, *Physical Review E*, **90**(5), 052922 (2014).

Spectral geometry of surfaces with curved conic singularities

Suleymanova A.

Max Planck Institut for Mathematics, Vivatsgasse 7, Bonn, Germany
e-mail: aasuleimanova@gmail.com

Consider the heat kernel of the Laplace–Beltrami operator on a Riemannian manifold. On a manifold with conic singularities we derived a detailed asymptotic expansion of the heat trace using the Singular Asymptotics Lemma of Jochen Brüning and Robert T. Seeley, see [1]. Then we investigated how the terms in the expansion reflect the geometry of the manifold, see [2]. In the two-dimensional case, we expand the results to a conic singularity such that the metric of the cross-section (link) depends on the radial coordinate. We see how the curvature near the tip of the cone enters the expansion.

References

- [1] A. Suleymanova, Heat trace expansion on manifolds with conic singularities, *arXiv:1701.01874 [math.SP]* (2017).
- [2] A. Suleymanova, On the spectral geometry of manifolds with conic singularities, *arXiv:1710.05355 [math.SP]* (2017).

Focusing of the seabottom images

Sushchenko A.A.^{1,2}, Kovalenko E.O.^{1,2}, Kan V.A.^{1,2}

¹Institute for Applied Mathematics, FEB RAS, Vladivostok, Russia

²Far Eastern Federal University, Vladivostok, Russia

e-mail: sushchenko.aa@dvvfu.ru, kovalenko.eo@dvvfu.ru, kan_va@dvvfu.ru

The kinetic model describing sound propagation in the ocean with diffuse reflection by Lambert's cosine law on the bottom surface is considered. The inverse problem of the bottom scattering

reconstruction is formulated. The inverse problem is reduced to the Fredholm integral equation of the first kind. Authors develop a generalized algorithm of object focusing for the reconstruction of seabed scattering coefficient based on the received echosignal by SSS equipped by the widely directivity pattern. Thus, a solution of the Fredholm integral equation of the first kind is reduced to the solving of SLE by an iterative method combined with the regularization.

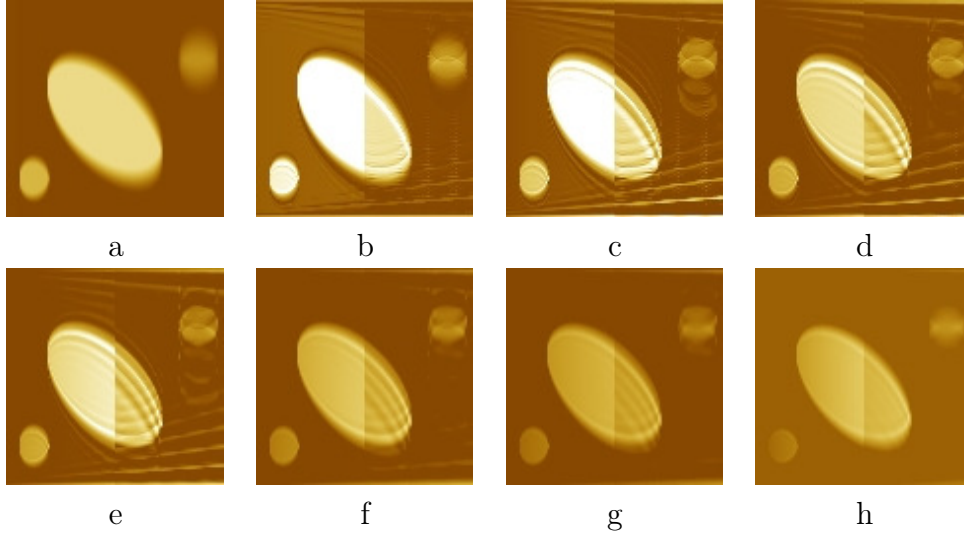


Fig. 1: Seabottom reconstruction with aperture of receiving antenna $\varepsilon = 8^\circ$.

Figure 1 shows the seabottom surface $20 \text{ m} \times 20 \text{ m}$. The sonar moves from the top left corner downwards. Each line of the image corresponds to the new probing interval. From the physical point of view, the coefficient of the seabottom scattering is part of the reflected signal and is limited by the range $[0, 1]$. Real experiments show that a part of the reflected signal does not exceed 35%. In Fig. 1 black color corresponds to 0, whereas white color to 0.35. Letters corresponds to the number of an iteration in the Seidel algorithm.

The RMS error decreases to the certain threshold value, but after it is increased. Thereby, the instability of the iterative method is confirmed. However, the visual representation of the image improves in further iterations.

References

- [1] I. V. Prokhorov, A. A. Sushchenko, Studying the problem of acoustic sounding of the seabed using methods of radiative transfer theory, *Acoustical Physics*, **61**(3), 368–375 (2015).
- [2] E. O. Kovalenko, I. V. Prokhorov, A. A. Sushchenko, Processing of the information from side-scan sonar *Proceedings of SPIE – The International Society for Optical Engineering*, **10035**, Art. No. 100352C (2016).

On spectral approach to homogenization of elliptic operators in a perforated space

Suslina T.A.

St. Petersburg State University, Universitetskaya nab. 7/9, 199034, Russia
e-mail: t.suslina@spbu.ru

Let $\Gamma \subset \mathbb{R}^d$ be a lattice. For $\varepsilon > 0$, we consider the perforated space $\Pi_\varepsilon \subset \mathbb{R}^d$ which is an $(\varepsilon\Gamma)$ -periodic open connected set with Lipschitz boundary.

In $L_2(\Pi_\varepsilon; \mathbb{C}^n)$, we consider a selfadjoint strongly elliptic second order differential operator A_ε . It is assumed that A_ε is given by the differential expression $b(\mathbf{D})^*g(\mathbf{x}/\varepsilon)b(\mathbf{D})$ with the Neumann (natural) boundary condition. Here $b(\mathbf{D}) = \sum_{l=1}^d b_l D_l$ is the $(m \times n)$ -matrix first order differential

operator. We assume that $m \geq n$ and that the symbol $b(\boldsymbol{\xi}) = \sum_{l=1}^d b_l \xi_l$ has maximal rank for any $0 \neq \boldsymbol{\xi} \in \mathbb{C}^d$. A matrix-valued function $g(\mathbf{x})$ of size $m \times m$ is assumed to be Γ -periodic and such that $g(\mathbf{x}) > 0$; $g, g^{-1} \in L_\infty$.

We study the behavior of the resolvent $(A_\varepsilon + I)^{-1}$ for small ε . We show that

$$\|(A_\varepsilon + I)^{-1} - (A^0(\varepsilon) + I)^{-1}\|_{L_2(\Pi_\varepsilon) \rightarrow L_2(\Pi_\varepsilon)} \leq C\varepsilon. \tag{1}$$

Here $A^0(\varepsilon)$ is the effective operator acting in $L_2(\Pi_\varepsilon)$ and given by $b(\mathbf{D})^* g^0 b(\mathbf{D})$ with the Neumann boundary condition; g^0 is a constant positive effective matrix.

Also, we obtain more accurate approximation:

$$\|(A_\varepsilon + I)^{-1} - (A^0(\varepsilon) + I)^{-1} - \varepsilon K_\varepsilon\|_{L_2(\Pi_\varepsilon) \rightarrow L_2(\Pi_\varepsilon)} \leq C\varepsilon^2. \tag{2}$$

Finally, we find approximation for the resolvent in the energy norm:

$$\|(A_\varepsilon + I)^{-1} - (A^0(\varepsilon) + I)^{-1} - \varepsilon K_\varepsilon^{(1)}\|_{L_2(\Pi_\varepsilon) \rightarrow H^1(\Pi_\varepsilon)} \leq C\varepsilon. \tag{3}$$

The corrector $K_\varepsilon^{(1)}$ is similar to the standard corrector; it contains the rapidly oscillating factor. The corrector K_ε is the sum of three terms: $K_\varepsilon = K_\varepsilon^{(1)} + (K_\varepsilon^{(1)})^* + K_\varepsilon^{(3)}$; the term $K_\varepsilon^{(3)}$ does not contain oscillating factors.

Estimates (1)–(3) are order-sharp. The general results are applied to the acoustics operator, the elasticity operator, and the Schrödinger operator with a singular periodic potential.

We apply the operator-theoretic approach which was suggested and developed by Birman and Suslina. It is based on the scaling transformation, the Floquet–Bloch theory, and the analytic perturbation theory. Before, this method was used for homogenization problems in the whole \mathbb{R}^d . We show that the method can be adapted also for homogenization problems in a perforated space.

Note that homogenization problems in a perforated space for the acoustics and elasticity operators have been studied by Zhikov and Pastukhova [1] with the help of the shift method (the modified method of the first-order approximation); estimates (1) and (3) were obtained.

We study more general class of operators. Our main goal is to adapt the operator-theoretic method to the problems in a perforated space. Also, we obtain estimate (2) which is new for the case of a perforated space. The results will appear in [2].

References

[1] V.V. Zhikov, S.E. Pastukhova, On operator estimates for some problems in homogenization theory, *Russ. J. Math. Phys.*, **12**(4), 515–524 (2005).
 [2] T. A. Suslina, Spectral approach to homogenization of elliptic operators in a perforated space, In: *Ludvig Faddeev Memorial Volume*, World Scientific, Singapore, 2018 (to appear).

On the method of the block element in the problem of vibration of an elastic medium with a composite coating

Telyatnikov I.S.

Federal Research Center Southern Scientific Center of the Russian Academy of Sciences, Rostov-on-Don, Russia

e-mail: ilux_t@list.ru

Dynamic interaction problems for coatings with deformable foundation have numerous applications in materials science, engineering, using composite thin-walled structures and seismology.

We consider the problem of harmonic oscillations of two extended plates contacting along a straight line, rigidly adhered to an elastically deformable substrate. It is proposed to use a simplified version of the block element method [1] for solving problems of vibration of different plate types with averaged thickness parameters on the surface of the elastic layer. In the adopted model, the

$x_1 O x_2$ plane coincides with the middle surface of the coating. Displacements of plates for the case of steady-state oscillations satisfy two-dimensional equations in the corresponding half-planes [2]

$$\mathbf{R}_j \mathbf{u}_j - \mathbf{E} \mathbf{g}_j = \mathbf{b}_j, \text{ for } j = 1, \quad x_1 > 0, \text{ for } j = 2, \quad x_1 < 0, \quad -\infty < x_2 < +\infty.$$

Here $\mathbf{u}_j = \{u_{kj}\}$, $j = 1, 2$, $k = 1, 2, 3$, displacement vector of plate $\mathbf{g}_j = \{g_{kj}\}$ vector of stresses acting from the side of the substrate to the lower boundary of the plate, the elements of the matrix differential operator \mathbf{R}_j and the diagonal matrix \mathbf{E}_j depend on the mechanical and geometrical characteristics of the plates. Vectors \mathbf{b}_j describe the effects on the upper surfaces of the coating plates.

For an elastic foundation with the use of the Green's matrix-function, we formulate integral relations on its surface that connect the amplitudes of stresses and displacements obtained from the solution of the boundary problem of steady-state oscillations of an elastic foundation. For media models with complex properties, these relationships, also called influence functions, can be obtained experimentally. It is assumed that the plates are rigidly adhered to the substrate. Various boundary conditions can be set at the connection of plates.

The application of the Fourier transform to the equations for plate displacements leads to a system of ordinary differential equations solution of which, together with the functional relationships for the substrate and the conditions of its interface with the coating, makes it possible to construct functional equations with respect to the Fourier transforms of the amplitudes for contact stresses between the coating and the substrate \mathbf{G}_j , solved by the Wiener–Hopf method. An algorithm for constructing systems allowing to find unknown values of Fourier transforms \mathbf{G}_j , included in the loaded Wiener–Hopf equations, is proposed.

The approach to the construction of model for multilayer extended plates, taking into account the features of the transition from three-dimensional to two-dimensional elasticity theory for plates and shells, leads to a single-layer plate model with reduced mechanical characteristics.

The work was prepared as part of the SA SSC RAS 2018 (pr. 01201354241) and support by RFBR and administration of Krasnodar region (16-41-230184).

References

- [1] V. A. Babeshko, O. V. Evdokimova, O. M. Babeshko, Block elements and analytical solutions of boundary-value problems for sets of differential equations, *Doklady Physics*, **59**(1), 30–34 (2014).
- [2] A. S. Volmir, *Nonlinear Dynamics of Plates and Shells*, Nauka Press, Moscow, 1972.

Propagation of electromagnetic waves in a shielded dielectric layer with cubic nonlinearity

Tikhov S.V., Valovik D.V.

Department of Mathematics and Supercomputing, Penza State University, Penza, Russia, 440026
e-mail: tik.stanislav2015@yandex.ru, dvalovik@mail.ru

We consider the propagation of a monochromatic transverse-magnetic (TM) wave along the dielectric layer $\Sigma := \{(x, y, z) : 0 \leq x \leq h, (y, z) \in \mathbb{R}^2\}$ with perfectly conducted walls [1]. The TM wave has the form $(\mathbf{E}, \mathbf{H})e^{-i\omega t}$, where

$$\mathbf{E} = (E_x(x)e^{i\gamma z}, 0, E_z(x)e^{i\gamma z})^\top, \quad \mathbf{H} = (0, H_y(x)e^{i\gamma z}, 0)^\top, \quad (1)$$

are the complex amplitudes; ω is the circular frequency; $(\cdot)^\top$ is the transposition operation; γ is an unknown (real) spectral parameter (propagation constant of a guided wave); E_x, E_z, H_y are unknown functions [2, 3].

The waveguide Σ is located in the Cartesian coordinates $Oxyz$. At the boundaries $x = 0, x = h$ the waveguide has perfectly conductive walls [1]. Inside the waveguide Σ the permittivity is described

by the formula

$$\epsilon = \epsilon_l + a|\mathbf{E}|^2, \quad (2)$$

where ϵ_l , $a > 0$ are real constants. Everywhere $\mu = \mu_0$, where μ_0 is the magnetic permeability of free space [2, 3].

Complex amplitudes (1) satisfy Maxwell's equations

$$\text{rot } \mathbf{H} = -i\omega\epsilon\mathbf{E}, \quad \text{rot } \mathbf{E} = i\omega\mu\mathbf{H}; \quad (3)$$

tangential components of the electric field \mathbf{E} vanish on the perfectly conductive walls. It is natural to suppose that the x -th component of an electric field has a fixed value at the $x = 0$ [1].

A rigorous analytical approach is suggested [1]. It is proved that even for small values of the nonlinearity coefficients a , the nonlinear problem has infinitely many nonperturbative solutions (propagation constants and eigenmodes), whereas the corresponding linear problem always has a finite number of solutions. Asymptotic distribution of the propagation constants is found, periodicity of the eigenmodes is proved and exact formula for the period is found, zeros of the eigenmodes are determined. Similar results for an open plane waveguide with cubic nonlinearity are presented in [4].

References

- [1] D. V. Valovik, S. V. Tikhov, On the existence of infinitely many eigenvalues in a nonlinear waveguiding theory problem, *Computational Mathematics and Mathematical Physics*, accepted.
- [2] P. N. Eleonskii, L. G. Ogan'es'yants, V. P. Silin, Cylindrical nonlinear waveguides, *Soviet Physics JETP*, 44–47 (1972).
- [3] A. D. Boardman, P. Egan, F. Lederer, U. Langbein, D. Mihalache, *Third-Order Nonlinear Electromagnetic TE and TM Guided Waves*, Elsevier Sci. Publ. North-Holland, Amsterdam, London, New York, Tokyo, 1991.
- [4] Yu. G. Smirnov, D. V. Valovik, On the infinitely many nonperturbative solutions in a transmission eigenvalue problem for Maxwell's equations with cubic nonlinearity, *Journal of Mathematical Physics*, **57**, art. no. 103504, 15 pages (2016).

Nonlinear waves: theory, computer simulation, experiment

M.D. Todorov

Faculty of Applied Mathematics and Computer Science, Technical University of Sofia, Bulgaria
e-mail: mditod@gmail.com

The Boussinesq equation is the first model of surface waves in shallow water, that considers the nonlinearity and the dispersion and their interaction as a reason for wave stability known as Boussinesq Paradigm. This balance bears solitary waves that behave like quasi-particles. At present there are some Boussinesq-like equations. The prevalent part of the known analytical and numerical solutions, however, relates to 1d case while for multidimensional cases almost nothing is known so far. An exclusion are the solutions of Kadomtsev–Petviashvili equation. The difficulties originate from the lack of known analytic initial conditions and the nonintegrability in the multidimensional case. Another problem is which kind of nonlinearity will keep the temporal stability of localized solutions.

The system of coupled nonlinear Schrödinger equations known as well as Vector Schrödinger equation is a soliton supporting dynamical system. It is considered as a model of light propagation in Kerr isotropic media. Along with that the phenomenology of the equation opens a prospect of investigating the quasi-particle behavior of the interacting solitons. The initial polarization of the Vector Schrödinger equation and its evolution evolves from the vector nature of the model. The existence of exact (analytical) solutions usually is rendered to the more simple models while for the Vector Schrödinger equation such solutions are not known. This determines the role of the numerical

schemes and approaches. Vector Schrödinger equation is a spring-board for combining of the reduced integrability and conservation laws in a discrete level.

The experimental observation and measurement of ultrashort pulses in waveguides is a hard job and this is the reason and stimulus to create mathematical models for computer simulations as well as reliable algorithms for treating the governing equations. Along with the nonintegrability here appears one more problem — about the multidimensionality and necessity to split and linearize the operators in appropriate way.

Distribution of the spectrum of symmetrically deformed unitary invariant random matrix ensemble

Vasilchuk V.

St. Petersburg State University of Architecture and Civil Engineering, 4, 2nd Krasnoarmeiskaya Str., St. Petersburg, 190005, Russia;

Peter the Great St. Petersburg Polytechnic University, 29, Polytechnicheskaya Str., St. Petersburg, 195251, Russia

e-mail: vvyu@yahoo.com

We consider the ensemble of $n \times n$ random matrices

$$H_n = A_n + F^*(A_n)U_n^*B_nU_nF(A_n),$$

where A_n and B_n are hermitian random (or non-random), having the limiting Normalized Counting Measure (NCM) of eigenvalues, $F(A_n)$ is some smooth function of A_n , U_n is unitary, uniformly distributed over $U(n)$, and A_n , B_n and U_n are mutually independent. By using the technic described in [1], we establish the convergence of NCM of ensemble H_n to the non-random limit then $n \rightarrow \infty$ and find the limiting NCM via its Stieltjes transform. The later is the unique solution of some system of functional equations written in terms of functions having the integral representations via the limiting NCMs of A_n and B_n . We also study the limiting NCM of H_n using an approach of [2].

References

- [1] L. Pastur, M. Shcherbina, *Eigenvalue Distribution of Random Matrices*, Math. Surv. Monogr., **171**, RI:(AMS), 2011.
- [2] V. Vasilchuk, On the asymptotic distribution of the commutator and anticommutator of random matrices, *J. Math. Phys.*, **44**, 1882–1908 (2003).

Hamilton–Jacobi method in non-Hamiltonian situation and Boltzmann extremals

Vedenyapin V.V.

Keldysh Institute of Applied Mathematics

e-mail: vicveden@yahoo.com

The hydrodynamic substitution, which is well-known in the theory of the Vlasov equation [1–3], has recently been applied to the Liouville equation and Hamiltonian mechanics [4–8]. In [4–6], Kozlov outlined the simplest derivation of the Hamilton–Jacobi(HJ) equation, and the hydrodynamic substitution simply related this derivation to the Liouville equation [7, 8]. The hydrodynamic substitution also solves the interesting geometric problem of how a surface of any dimension subject to an arbitrary system of nonlinear ordinary differential equations moves in Euler coordinates (in Lagrangian coordinates, the answer is obvious). This has created prerequisites for generalizing the HJ method to the non-Hamiltonian situation. The H-theorem is proved for generalized equations of chemical kinetics, and important physical examples of such generalizations are considered: a discrete

model of the quantum kinetic equations (the Uehling–Uhlenbeck equations) and a quantum Markov process (a quantum random walk). The time means are shown to coincide with the Boltzmann extremes for these equations and for the Liouville equation [9]. This give possibility to prove existence of analogues of action-angles variables in non-Hamiltonian situation.

References

- [1] A. A. Vlasov, *Statistical Distribution Functions*, Nauka, Moscow, 1966 [in Russian].
- [2] D. Bom, *General Theory of Collective Coordinates*, Wiley, New York, 1959; Mir, Moscow, 1964.
- [3] V. V. Vedenyapin, A. V. Synitsyn, E. I. Dulov, *Kinetic Boltzmann, Vlasov, and Related Equations*, Elsevier, Amsterdam, 2011.
- [4] V. V. Kozlov, The hydrodynamics of Hamiltonian systems, *Mosc. Univ. Mech. Bull.*, **38**(6), 9–23 (1983).
- [5] V. V. Kozlov, *Symmetry, Topology, and Resonances in Hamiltonian Mechanics*, Udmurt. Gos. Univ., Izhevsk, 1995 [in Russian].
- [6] V. V. Kozlov, *General Vortex Theory*, Udmurt. Gos. Univ., Izhevsk, 1998 [in Russian].
- [7] V. V. Vedenyapin, N. N. Fimin, Liouville equation, hydrodynamic substitution and Hamilton–Jacobi method, *Dokl. Math.*, **86**, 697–699 (2012).
- [8] V. V. Vedenyapin, M. A. Negmatov, On the topology of steady-state solutions of hydrodynamic and vortex consequences of the Vlasov equation and the Hamilton–Jacobi method, *Dokl. Math.*, **87**, 240–244 (2013).
- [9] V. V. Vedenyapin, S. Z. Adzhiev, Entropy in the sense of Boltzmann and Poincare, *Russian Math. Surveys*, **69**(6), 995–1029; *Uspekhi Mat. Nauk*, **69**(6), 45–80 (2014).

Numerical simulation of nonlinear wave propagation in symmetric cross-ply laminates with hyperelastic material behavior

Ngoc Nguyen Vu, Rolf Lammering

Institute of Mechanics, Helmut-Schmidt-University / University of the Federal Armed Forces Hamburg, Holstenhofweg 85, 22043 Hamburg, Germany

e-mail: n.vn@hsu-hh.de

Due to microstructural damages in composite structures, e.g. caused by cyclic loads, material degradation may occur, changing material properties. Over time these damages are likely to accumulate and can lead to an abrupt structural failure. Therefore, it is necessary to investigate or detect material degradation as a result of cyclic loading at an early stage.

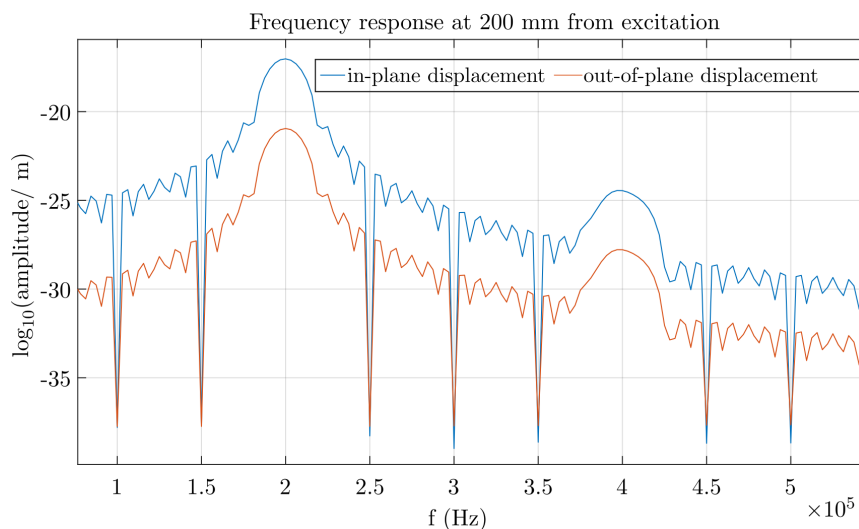


Fig. 1: An example for second harmonic wave modes in CPL.

In a thin-walled, large-scale composite structure damaged by microstructural defects, guided waves (Lamb waves) propagate nonlinearly. By means of the wave analysis, a statement about the degree of degradation of the structure should be made. Meanwhile, the generation of so-called cumulative second harmonic modes [1] is employed. In order to map the nonlinear behavior of wave propagation for material reasons numerically, hyperelastic material models are used. Based on existing work in this area for isotropic and unidirectional materials [2], the numerical investigation is extended to symmetric cross-ply laminates (CPL). The aspects of material stability as well as of conditions of existence regarding cumulative second harmonic generation in CPL will be investigated and discussed.

References

- [1] M. Deng, Cumulative second-harmonic generation of Lamb-mode propagation in a solid plate, *Journal of Applied Physics*, **85**(6), 3051–3058 (1999).
- [2] R. Lammering, N. Rauter, Nonlinear elastic waves for evaluation of composite material deterioration, *Engineering Transactions*, **64**(4), 597–604 (2016).

Analysis of longitudinal impact waves in a thin viscoelastic rod on the basis of 3D equations for a Rabotnov's hereditary elastic body

Wilde M.V., Sergeeva N.V.

Saratov State University, 83, Astrakhanskaya str., 410012, Saratov, Russia
e-mail: mv_wilde@mail.ru, sergeevanv@info.sgu.ru

In the practical applications the longitudinal wave motion in a thin rod is usually described by an approximate theory based on “strength-of-materials” considerations. For a semi-infinite viscoelastic rod subjected to a step pressure pulse on its end, this theory yields (see [1] and references therein) two characteristic wave speeds $c_0 = \sqrt{E/\rho}$ and $c_\infty = \sqrt{E_\infty/\rho}$, where E and E_∞ are instantaneous and long-time values of the Young's modulus, respectively. The former is the velocity of the wave-front while the latter represents the wave velocity at the large values of time. A rapid growing of the stress arises in the vicinity of the ray $x = c_\infty t$ which is often called “quasi-front”. On the other hand, from the studies of the waves in an elastic rod on the basis of a refined rod theory and the exact theory of elasticity (see, e.g., [2]) it is known, that the front propagating with the thin-rod velocity c_0 is itself a quasi-front characterized by a smoothed step. This phenomenon can be considered as an effect of the geometrical dispersion while the quasi-front of the former type is an effect of the physical one. The goal of this talk is to compare these two effects by studying the longitudinal waves in a rod on the basis of 3D theory of viscoelasticity describing both of them.

The propagation of non-stationary waves in a semi-infinite viscoelastic solid circular cylinder is considered. The properties of material are described by Rabotnov's hereditarily elastic rheological model. The dynamic stress-strain state of the cylinder is described by the three-dimensional equations of motion in stresses and displacements in the cylindrical coordinate system (r, φ, z) . The constitutive equations are written in the integral form [3]. The integral operators are defined by formulae

$$\tilde{E} = E(1 - \Gamma^*), \quad \tilde{\nu} = \nu + \frac{1 - 2\nu}{2}\Gamma^*, \quad \Gamma^* f(t) = k \int_{-\infty}^t \mathfrak{D}_\alpha(-\beta, t - \tau) f(\tau) d\tau,$$

were ν is instantaneous value of Poisson's ratio, k, β are parameters of the material, α is a rational singularity parameter ($-1 < \alpha \leq 0$), $\mathfrak{D}_\alpha(-\beta, t)$ is the fractional exponential Rabotnov's function [1]. At the initial moment of time, the step pressure pulse is applied to the end $z = 0$. An axisymmetrical problem is considered, for the sake of simplicity the end is assumed to be fixed in the radial direction. On the surface the homogeneous boundary conditions for the stresses are imposed. The initial conditions assume that the body was at rest and unloaded before applying of the load. The solution of the problem is obtained by using Laplace and Fourier transforms technique. The qualitative

analysis of the problem is based on low-frequency asymptotic obtained in [3]. It is shown that the different situations are possible depending on the ratio of relaxation time and the characteristic time of elastic wave propagation. If the former is much greater than the latter we can see the elastic quasi-front degrading to a viscoelastic one at the large times. If the ratio is of the order of unity there is no quasi-front with the instantaneous thin-rod velocity $c_0 = \sqrt{E/\rho}$.

The results were obtained within the framework of the state assignments of the Ministry of Education and Science of Russia No. 9.8570.2017/8.9.

References

- [1] Yu. N. Rabotnov, *Elements of Hereditary Solid Mechanics*, Nauka, Moscow, 1977; Engl. transl. by Mir Publishers, Moscow, 1980.
- [2] K. F. Graff, *Wave Motion in Elastic Solids*, Clarendon Press, Oxford, 1975.
- [3] M. V. Wilde, N. V. Sergeeva, Development of asymptotic methods for the analysis of dispersion relations for a viscoelastic solid cylinder, *Izv. Saratov Univ. (N. S.), Ser. Math. Mech. Inform.*, **17**(2), 183–195 (2017) (in Russian).

Gradient method for detecting sites of local hydrogen embrittlement of metals

Yakovlev Yu.A., Belyaev A.K., Polyanskiy V.A., Tretyakov D.A.

Institute for Problems in Mechanical Engineering RAS, V.O., Bolshoj pr., 61, St. Petersburg, 199178
Russia

e-mail: yura.yakovlev@gmail.com, vice.ipme@gmail.com

Arseniev D.G.

Saint-Petersburg University, 7-9, Universitetskaya nab., St. Petersburg, 199034, Russia

e-mail: vicerektor.int@spbstu.ru

The destruction of parts of machines and structural elements from high-strength steels is, in most cases, accompanied by the formation of sites of hydrogen embrittlement at fractures.

This indicates the critical effect of local hydrogen brittleness on the process of destruction of high-strength metals. The problem is exacerbated by the fact that in the modern high-strength steels widely used in industry, the hydrogen content leading to brittle fracture lies at the concentration level, that are more smaller than in the case of ordinary steels.

The correlation between the distributions of the values of the relative difference in the velocities of transverse ultrasonic waves of mutually perpendicular polarization-and the spatial distribution of hydrogen concentrations in samples from commercial rolled metal was discovered by us and was repeatedly confirmed experimentally [1, 2].

Measurements of the fields of the values of the relative difference in the velocities of transverse ultrasonic waves of mutually perpendicular polarization on real objects is a laborious task. Minimization of the number of these measurements is possible due to the application of the search procedure type s^2 method. This method is actually gradient.

Studies of the distribution of the propagation velocities of transverse ultrasonic waves of different polarizations and the relative difference in the surface of corset specimens from them were carried out in parallel with the study of their microcracking and the distribution of the concentrations of diffusion mobile hydrogen.

Estimates of the propagation velocity of transverse ultrasonic waves of different polarization with the help of a bi-continual model containing hydrogen were made.

Non-destructive testing is particularly important for working constructs and machines. The use for the nondestructive testing of the megnotostriptive effect does not allow to separate the local hydrogen fragility from other less critical violations of the metal structure. During ultrasonic testing, waves reflected from defects are not formed. There are no other widely used methods for volumetric control of constructional materials.

On the contrary, based on a comparison of the data obtained, it was shown that the zones of local hydrogen micro-cracking can be detected by analyzing information on the distribution of sound velocities.

The results are of great importance for the development of new methods of non-destructive testing hydrogen embrittlement.

The support by the Russian Foundation for Basic Research, projects 17-08-00783 and 18-08-00201, is acknowledged.

References

- [1] E. L. Alekseeva, A. K. Belyaev, A. I. Grishchenko, D. E. Mansyrev, V. A. Polyanskiy, D. A. Tretyakov, O. V. Shvetsov, The initiation mechanism of plastic strain localization bands and acoustic anisotropy, *Procedia Structural Integrity*, **6**, 128–133 (2017).
- [2] A. K. Belyaev, A. I. Grishchenko, V. A. Polyanskiy, A. S. Semenov, D. A. Tretyakov, L. V. Shtukin, D. G. Arseniev, Yu. A. Yakovlev, Acoustic anisotropy and dissolved hydrogen as an indicator of waves of plastic deformation, Days on Diffraction (DD) 2017 – IEEE, 39–44 (2017).

Interaction of nonsymmetric electromagnetic waves guided by cylindrical duct with enhanced density in magnetoactive plasma

Yashina N.F., Zaboronkova T.M.

R. E. Alekseev State Technical University, 24 Minin St., Nizhny Novgorod 603950, Russia
e-mail: gematityash@mail.ru, t.zaboronkova@rambler.ru

Krafft C.

Laboratoire de Physique des Plasmas, École Polytechnique, 91128 Palaiseau Cedex, France
e-mail: catherine.krafft@lpp.polytechnique.fr

Electromagnetic waves guided by plasma structures aligned with an external static magnetic field play an important role in many physical phenomena occurring in laboratory and space plasma [1]. Nonlinear interaction of waves guided by an anisotropic cylinder in free space have been considered in [2, 3]. Here we study the resonance parametric instability of nonsymmetric whistler waves guided by cylindrical density ducts with enhanced plasma density surrounded by homogeneous background magnetized plasma. The anisotropic media both inside or outside duct are described by dielectric tensor with nonzero off-diagonal elements. The main attention is paid to the case of a cold resonant magnetoplasma when the diagonal elements of the tensors have opposite signs. Note that under such conditions, the refractive index surface of propagating normal wave of magnetoactive plasma possesses unbounded branch corresponding to electrostatic waves.

In the linear approximation the dispersion characteristics and structures of the fields for the nonsymmetric whistler modes are analyzed for conditions typical of modeling laboratory experiments [4] when the frequency of the waves belongs to the interval between the lower hybrid frequency and the electron-cyclotron frequency. We show that the presence of the external time-harmonic electromagnetic field in magnetoplasma can lead to interaction of waves guided by enhanced-density plasma duct if a space-time synchronism of the external field and the guided waves takes place. The frequency interval of guided waves when three-wave interaction can occur is determined. In the approximation of a weak nonlinearity the instability increment of guided waves and the threshold of the external electric field intensity are found. The results of the numerical calculations will be presented and discussed for cases that are of both practical and academic interest.

Acknowledgments. This work was supported by the Centre national de la recherche scientifique.

References

- [1] I. G. Kondrat'ev, A. V. Kudrin, T. M. Zaboronkova, *Electrodynamics of Density Ducts in Magnetized Plasmas*, Gordon and Breach, Amsterdam, 1999.

- [2] N. F. Yashina, T. M. Zaboronkova, *Proceedings of the International Conference Days on Diffraction 2009*, 202–205 (2009).
- [3] N. F. Yashina, T. M. Zaboronkova, C. Krafft, *Proceedings of the International Conference Days on Diffraction 2016*, 277–280 (2016).
- [4] T. M. Zaboronkova, A. V. Kudrin, M. Yu. Lyakh, L. L. Popova, *Radiophysics and Quantum Electronics*, **46**, 452–471 (2003).

Low frequency spectra of layered plates and their parametrical study

D.D. Zakharov

Russian University of Transport (RUT-MIIT), 127994 Moscow, Obraztsova str. 9-9

e-mail: dd_zakh@mail.ru

New method based on the combination of asymptotical and numerical approaches is suggested for evaluating the complex dispersion curves for coated elastic plates.

At the first step, the dispersion equation and its limit formulation for statics are deduced in the explicit form. The asymptotics of static roots are obtained assuming the wavenumber modulus as a large parameter. Based on the asymptotic error analysis, the iterative method is suggested for calculating the exact roots in statics. The influence of the geometrical and elastic parameters is studied. The existence of critical value of geometrical parameters providing the changeover of the root asymptotics is shown.

At the second step, the long wave asymptotics for the complex dispersion curves are derived. It is proved that each dispersion curve has a flat segment at low frequency. The larger is the wavenumber and the dispersion curve index, the longer is the validity interval of the deduced asymptotics.

The exact complex curves are calculated using another iterative procedure. The analysis of fundamental mode with its pure imaginary analogue is performed together with other possible pure imaginary curves. The numerical procedure and its results for the subcritical, critical and supercritical value of the geometrical parameter are presented with the respective efficiency estimation.

The parametrical analysis is discussed together with the possible generalization of suggested method for more complicated waveguides.

Electromagnetic resonance structures made of thin metallic wires

V. Zalipaev, S. Kosulnikov, S. Glybovski

ITMO University, Birzhevaya line V.O. 14, 199034, St. Petersburg, Russia

e-mail: v.zalipaev1@metalab.ifmo.ru

In the paper we study two different examples of electromagnetic open resonators made of thin metallic wires. In the first problem a Fabry–Perot resonator formed by two perfectly conducting (PEC) and infinitely thin, parallel, circular disks in 3D space is considered. It is excited by PEC vertical vibrator (VV). It is a thin wire, comparing to the wavelength, which radius is much smaller than its length and the wavelength (longwave approximation), located at the exact center of cylindrical space between the two horizontal disks. Thus, the vibrator excites the whole resonator space. The problem is considered in the high-frequency approximation, i.e., the diameter of the disks is much greater than the wavelength [1]. In this diffraction problem we observe infinitely many multiply diffracted fields. Firstly, a radial waveguide modes excited by VV and travelling towards to the circular open end due to diffraction partially radiate into the outer space and partially reflect back. This process of multiple diffractions continues up to infinity. We apply Geometrical Theory of Diffraction (GTD) [1] with the help of uniform stationary method to construct uniform asymptotic expansions for directivity of field scattered into the far field zone of the outer space as well as the field representation inside the resonator. This GTD asymptotic analysis is based on the exact solution to the corresponding canonical problem — radiation of the open end of a waveguide formed by

two parallel half-planes and obtained in [2] by means of the method of factorization (Wiener–Hopf method). The case of excitation of the resonant antenna formed by two metallic parallel disks by point Hertz dipole was studied in [4]. Thus, the key point of the paper is taking into account the effect of interaction of all the multiply diffracted fields, propagating from the disks edges back inside the cylindrical space of the resonator, with VV in the longwave approximation. It is computed on the basis of the famous in radio science and antenna theory Pocklington integral equation (see, for example, [3]). It is also shown that the maxima of the total radiating power takes place when the frequency of excitation VV coincides with the real part of one of the complex resonance eigen-frequency. A comparison to test our GTD asymptotic formulas by means of finite element method is discussed.

For the second example we study guided electromagnetic waves propagating along infinite 1D periodic array of thin PEC wires suspended over PEC infinite screen. The approach makes extensive use of a well-known numerical analysis of method of integral equations in two different forms of Pocklington and Hallen integral formulations to make a comparison between results. An approximation being used in the analysis is based on the assumption of presence of low parameter, i.e. that the ratio wires radius to wavelength is much less than one. The quasi-periodic wave field is constructed as a superposition of wave fields generated by linear electric currents that satisfies the boundary conditions on the surfaces of the conductors leading to an infinite system of real linear algebraic equations. The vanishing of the determinant of the associated matrix provides the condition for localized guided waves to exist and the corresponding dispersion curves are determined numerically. Our analysis is based on the accurate and efficient computation of lattice sums. The problem is a natural extension of the equivalent electromagnetic problem [5]. The modes that we seek have frequencies below this cut-off and decay exponentially as one moves away from the array.

We also study resonance properties of excitation of a finite array of parallel thin wires suspended over PEC infinite screen. Again we apply numerical analysis of method of integral equations in two different forms of Pocklington and Hallen integral formulations. We compare numerical results obtained on the basis of this integral formulations with data computed using CST Microwave studio numerical simulations. The key point of the analysis for the finite array of thin wires is to show that the frequencies of localized modes belong to the passbands evaluated for the case of the corresponding infinite array.

References

- [1] V. A. Borovikov, B. E. Kinber, *Geometrical Theory of Diffraction*, IEEE Electromagnetic Waves Series, Institution of Electrical Engineers, 1994.
- [2] L. A. Weinstein, *The Theory of Diffraction and Method of Factorization*, Golem Press, Boulder, CO, 1969.
- [3] R. Mittra, *Computer Techniques for Electromagnetics*, Pergamon Press, 1973.
- [4] V. V. Zalipaev, S. B. Glybovski, A. Yu. Andreev, High frequency asymptotic description of resonant antenna formed by two metallic parallel disks, *IEEE Transactions on Antennas and Propagation*, PP(99), 12 (2016).
- [5] C. M. Linton, V. V. Zalipaev, I. Thompson. Electromagnetic guided waves on linear arrays of spheres, *Wave Motion*, **50**(1), 29–40 (2013).

Ice-coupled surface water waves near a vertical barrier

Zhuchkova M.G.

Institute for Problems in Mechanical Engineering of the Russian Academy of Sciences, V.O., Bolshoy pr., 61, St. Petersburg, 199178
e-mail: m.zhuchkova@list.ru

Exact analytical solution is provided for the scattering of incident flexural-gravity waves in water of finite depth against a junction of a floating elastic plate with a vertical slope of a hydraulic

structure. The floating plate is considered to be attached with the vertical barrier in different ways, giving rise to edge conditions: free edge, clamped edge, sliding with friction edge condition. Important physical quantities such as strain in the plate, shear force and vertical displacement of the plate are determined. Infinitely deep fluid and thin fluid layer approximation are also under consideration.

References

- [1] M. G. Zhuchkova, D. P. Kouzov, The transmission of a flexural-gravitational wave through a rigid end-stop in a floating plate, *Journal of Applied Mathematics and Mechanics*, **66**(3), 447–454 (2002).
- [2] L. A. Tkacheva, Interaction of surface and flexural-gravity waves in ice cover with a vertical wall, *Journal of Applied Mechanics and Technical Physics*, **4**(54), 651–661 (2013).
- [3] I. V. Sturova, L. A. Tkacheva, Wave motion in a fluid under an inhomogeneous ice cover, *Journal of Physics: Conference Series*, **894**(1), 012092 (2017).
- [4] P. Brocklehurst, A. A. Korobkin, E. I. Parau, Interaction of hydro-elastic waves with a vertical wall, *Journal of Engineering Mathematics*, **68**, 215–231 (2010).

High-frequency diffraction by a contour with a jump of curvature

Ekaterina A. Zlobina¹, Aleksei P. Kiselev^{1,2,3}

¹St. Petersburg State University, St. Petersburg, Russia

²Steklov Mathematical Institute, St. Petersburg Department, Russia

³Institute for Problems in Mechanical Engineering RAS, St. Petersburg, Russia

e-mail: ezlobina2@yandex.ru, aleksei.kiselev@gmail.com

We address high-frequency diffraction of a plane wave by a contour having a jump of curvature, aiming at explicit construction of asymptotic formulas. In contrast to earlier research (see, e.g., [1–4]) based on the Kirchhoff method, we apply a rigorous version of the boundary layer approach. The technique can be adapted to several related problems such as diffraction by a contour with a Hölder discontinuity of curvature. According to the Keller geometrical theory of diffraction [5], wavefield at the illuminated region is given by a sum of incident, geometrically reflected and diffracted waves; in transition zone, diffracted and reflected waves merge and must be described by some special function. We present expressions for diffracted wave and for wavefield in transition zone.

References

- [1] J. B. Keller, L. Kaminetzky, Diffraction coefficients for higher order edges and vertices, *SIAM J. Appl. Math.*, **22**, 109–134 (1972).
- [2] A. V. Popov, Backscattering from the line of discontinuity of curvature, *Proc. 5th All-Union Symposium on Wave Diffraction and Propagation*, 171–175 (1971).
- [3] N. Ya. Kirpichnikova, V. B. Philippov, Diffraction of creeping waves by a jump of curvature of a boundary of a conducting body, *Proc. Days on Diffraction 1997*, 53–58 (1997).
- [4] Z. M. Rogoff, A. P. Kiselev, Diffraction at jump of curvature on an impedance boundary, *Wave Motion*, **33**, 183–208 (2001).
- [5] J. B. Keller, Geometrical theory of diffraction, *J. Opt. Soc. Amer.*, **52**, 116–130 (1962).

Workshop on Nanophotonics and Metamaterials

M-Cube project: objectives and some results

Redha Abdeddaim, Stefan Enoch

Aix Marseille Univ, CNRS, Centrale Marseille, Institut Fresnel, Marseille, France

e-mail: stefan.enoch@fresnel.fr

We will present the main challenges in the development of routine clinical use of ultra-high field MRI and opportunities for metamaterials for ultra-high field MRI. Then results obtained by the M-Cube project consortium will be presented. Ultra-High Field (UHF) Magnetic Resonant Imaging (MRI) clinical applications are limited by lack of homogeneity of the radio-frequency fields with classical antennas. Several solutions have been proposed to control the radiofrequency (RF) electromagnetic fields in MRI, passive shimming using high permittivity materials [1] and parallel transmit [2] are probably the most promising routes that have been studied.

Since the beginning of the millennium researchers have proposed a new way to control electromagnetic fields from RF to optical wavelength range based on composite media designed by metamaterials. These metamaterials provide us a completely new avenue to control RF fields in UHF MRI and to circumvent homogeneity issues in MRI.

Thus, M-Cube project (MetaMaterials for ultra-high field MRI) [3] gathers 8 academic actors and 2 SMEs and aims at changing the paradigm of High-Field and Ultra High-Field MRI antennas to offer much better insight of the human body and enable earlier detection of diseases and conditions. The main objective of the project is to go beyond the limits of existing clinical imaging using an MRI scanner and radically improve spatial and temporal resolutions on image quality. The M-Cube solution relies on innovative systems using passive metamaterial structures to avoid or at least reduce the number of active elements. These systems are expected to make High-Field MRI fully diagnostically relevant for physicians.

We will show how several examples of applications of metamaterials in UHF MRI systems in order to illustrate the approaches that the consortium is developing.

Acknowledgement. This project has received Union's Horizon 2020 research and innovation program under grant agreement No. 736937.

References

- [1] W. M. Teeuwisse, W. M. Brink, A. G. Webb, Quantitative assessment of the effects of high-permittivity pads in 7 tesla MRI of the brain, *Magnetic Resonance in Medicine*, **67**(5), 1285–1293 (2012).
- [2] W. Grissom, C. Y. Yip, Z. Zhang, V. A. Stenger, J. A. Fessler, D. C. Noll, Spatial domain method for the design of RF pulses in multicoil parallel excitation, *Magnetic Resonance in Medicine*, **56**(3), 620–629 (2006).
- [3] <http://www.mcube-project.eu/>

A metasurface-based beam-steering solution for microstrip patch arrays

Muhammad U. Afzal, **Karu P. Esselle**

Macquarie University, Sydney, Australia

e-mail: muhammad.afzal@mq.edu.au, karu@ieee.org

Ali Lalbakhsh, Mst Nishat Yasmin Koli

Macquarie University, Sydney, Australia

A phased-array antenna, comprising microstrip patch array feed and phase shifters, is perceived as a solution in several medium-gain beam-steering antenna applications [1]. In a typical phased array, the array creates the medium-gain beam and phase combinations (through phase shifters) steer the beam. One of the biggest challenges with such solution is that the state-of-the-art phase shifters become exceedingly expensive and lossy at millimeter frequencies. Due to these limitations, researchers have been investigating alternative low-cost solutions for steering beam of large arrays. Our research on medium-to-high gain beam-steering antennas has been focused on the development of low-profile, totally passive, and simple beam-steering mechanism. We have recently demonstrated a working prototype at X band using resonant cavity antenna (RCA) and a pair of near-field phase transforming metasurfaces [2]. The method is very simple to implement and can be applied to any type of antenna or array. It basically requires an electromagnetic illuminator, referred to as base antenna, and a pair of flat and thin phase transforming metasurfaces — we refer to these metasurfaces to as turning metasurfaces (TMs).

This paper presents a hybrid of patch array and our beam-steering method in a configuration depicted in Fig. 1. The microstrip array radiates a medium-gain beam at the operating frequency of 11 GHz and the metasurface (or turning metasurface) placed on its aperture steers the beam to an offset angle. By simple rotation of this metasurface, the beam can be steered in azimuthal plane and the rotation of two such metasurfaces moves the beam in both azimuth and elevation planes. In comparison to a phased array, this method alleviates the need of active devices or components and presents a very simple beam-steering solution.

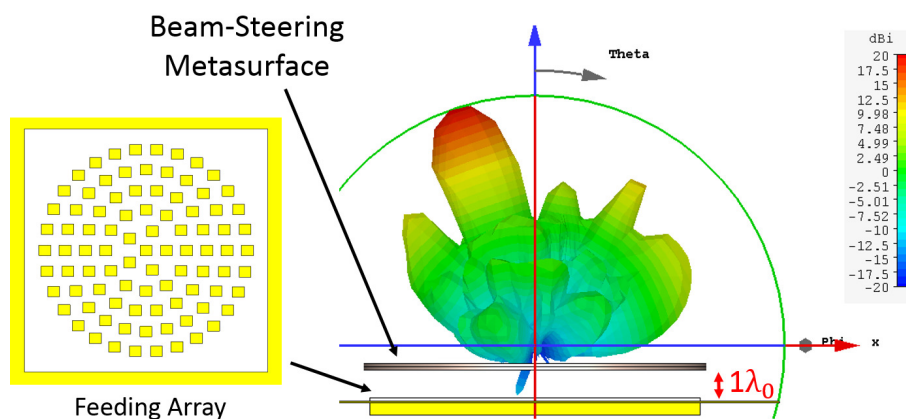


Fig. 1: Microstrip antenna array of 89 radiating elements with a beam-steering metasurface.

References

- [1] Y. I. Chong, D. O. U. Wenbin, Microstrip series fed antenna array for millimeter wave automotive radar applications, *2012 IEEE MTT-S International Microwave Workshop Series on Millimeter Wave Wireless Technology and Applications*, 1–3 (2012).
- [2] M. U. Afzal, K. P. Esselle, Steering the beam of medium-to-high gain antennas using near-field phase transformation, *IEEE Transactions on Antennas and Propagation*, **65**, 1680–1690 (2017).

Charge transport in a semiconductor multilayer heterostructures driven by a high-frequency acoustic wave

A.G. Balanov^{1,2}, A. Apostolakis¹, K.N. Alekseev¹, F.V. Kusmartsev¹, F. Wang^{1,3}, C.L. Poyser³, A.V. Akimov³, A.J. Kent³, M.T. Greenaway¹, T.M. Fromhold³

¹Department of Physics, Loughborough University, Loughborough LE11 3TU, United Kingdom

²Yuri Gagarin State Technical University of Saratov, Politechnicheskaja 77, Saratov 410054, Russia

³School of Physics and Astronomy, University of Nottingham, Nottingham NG7 2RD, United Kingdom

e-mail: a.balanov@lboro.ac.uk

We investigate charge transport induced in semiconductor multilayer heterostructures (superlattices) by hypersonic (GHz) acoustic stimuli. An acoustic wave packet propagating along the axis of the superlattice influences the electron tunneling, and thus affects the dynamics of charge in the device. However, in contrast to electromagnetic waves, the propagation time of the acoustic pulses cannot be neglected [1, 2]. In our calculations, we employed a nonperturbative kinetic description of the directed transport in a superlattice by utilizing the exact path-integral solutions of the semi-classical transport equation. This approach allows us to understand the dynamic regimes and instabilities governing the electron transport [2]. Our results suggest that a GHz (hypersonic) acoustic wave can create fast electron dynamics in a superlattice, thus generating sub-millimeter electromagnetic waves, even when no static electric field is applied. These findings were supported by direct quantum simulations, which have very good agreement with experimental measurements of the current-voltage characteristics [3] and the current pulse shape in superlattices under action of a high-frequency strain pulse train. In addition, our quantum simulations predict current oscillations with a frequency much higher than the frequency of the acoustic pulses, confirmed by our semi-classical calculations. We believe that our results are applicable to other systems with spatially periodic quantum potentials such as cold atoms, acoustic crystals and quantum metamaterials.

References

- [1] M. T. Greenaway, A. G. Balanov, D. Fowler, A. J. Kent, T. M. Fromhold, *Phys. Rev. B*, **81**, 235313 (2010).
- [2] A. Apostolakis, M. K. Awodele, K. N. Alekseev, F. V. Kusmartsev, A. G. Balanov, *Phys. Rev. E*, **95**, 062203 (2017).
- [3] C. L. Poyser, A. V. Akimov, A. G. Balanov, R. P. Campion, A. J. Kent, *New J. Phys.*, **17**, 083064 (2015).

Embedded photonic topological insulators

Miguel A. Bandres, Mordechai Segev

Physics Department and Solid State Institute, Technion, Haifa 32000, Israel

e-mail: bandres@gmail.com, msegev@technion.ac.il

We show that it is possible to control the properties of photonic topological insulators by tailoring defects. Although photonic topological insulators are robust to defects and imperfections, as counterintuitive as it may seem, we show that even a single defect placed in the right place can interact just with the edge states that resonate at a specific frequency. Moreover, by creating a line of defects in the photonic topological insulator we show that it is possible to deflect and filter a specific frequency range of edge states from a topological transmission line. In the extreme case, we show that a lattice of defects embedded in a topological insulator creates a totally new topological insulator. Our results allow to manipulate the current and future photonic topological insulator in new nontrivial ways which open the doors to new applications.

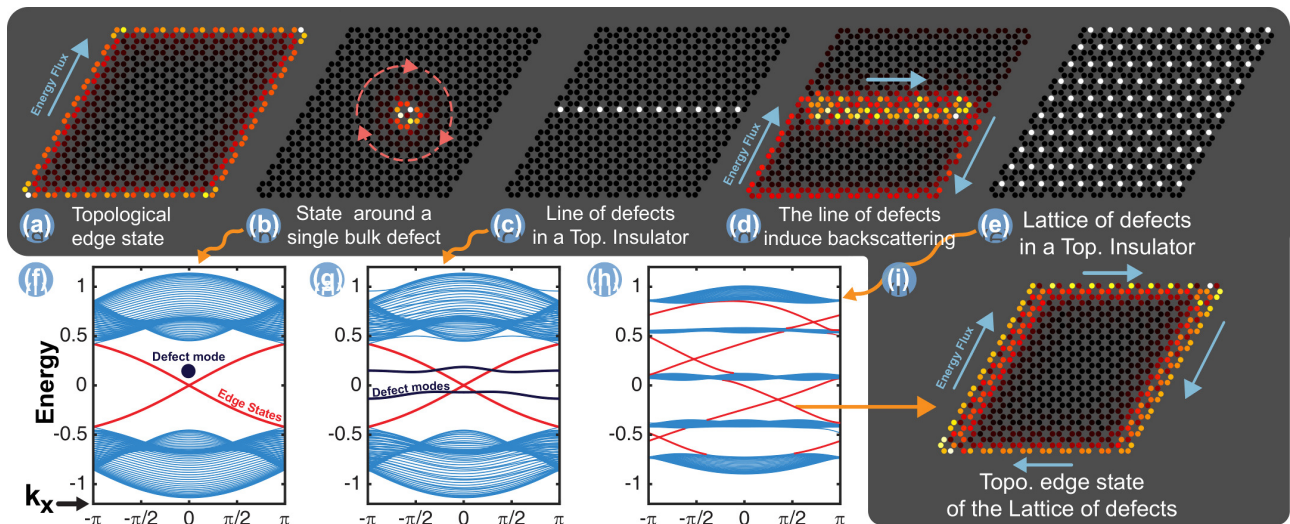


Fig. 1: (a) Topological edge state and (f) band structure of a Floquet Photonic topological insulator. Each site represents a helical waveguide or a microresonator which are coupled evanescently. The topological edge state is confined to the perimeter of the lattice and its energy flux, depicted by a blue arrow, is unidirectional. (b) A topological defect state created in the topological insulator by changing the onsite energy (index of refraction or resonator frequency) of a single site. The mode is confined around the defect and rotates around it, as shown by the red arrows. In frequency space - this mode lives inside the topological band gap, as shown in (f). (c) A line of defects in a topological insulator and (g) the corresponding band structure. (d) A line of defects that halts the upward propagation of specific edge states by deflecting them to the other side of the lattice, where they turn downwards in the lattice without ever reaching the top end of it. (e) Lattice of defects embedded in a topological insulator and its corresponding (h) band structure and one of its (i) topological edge modes.

Coherent control of light for virtual absorption and wireless power transfer

Baranov, D.G.

Department of Physics, Chalmers University of Technology, 412 96 Gothenburg, Sweden
e-mail: denisb@chalmers.se

Li, S.

ITMO University, St. Petersburg 197101, Russia

Generalov, A.

Department of Electronics and Nanoengineering, Aalto University, 02150 Espoo, Finland

Krasnok, A., Alù, A.

Department of Electrical and Computer Engineering, The University of Texas at Austin, Austin, Texas 78712, USA

Recent studies have shown that absorption and scattering of electromagnetic waves may be effectively controlled via coherent spatial and temporal modulation of the incident electromagnetic field. For instance, a coherent perfect absorber is a linear electromagnetic system, in which perfect absorption of radiation is achieved with two or more incident coherent waves, creating constructive interference inside an absorbing structure [1]. Similar principles enable engineering linear logic gates and recognition setups.

For perfect absorption of a harmonic incident wave the structure must exhibit some Joule losses, otherwise the system conserves energy and any incident radiation is scattered. On the other hand,

even lossless systems have scattering zeros in the complex frequency plane that mathematically correspond to “absorbing” solutions with no scattered fields.

We show that it is possible to generalize the notion of perfect absorption to lossless (Hermitian) structures and achieve virtual absorption in a transparent system with the use of a complex scattering zero [2]. Instead of adding absorption to the system, we tailor the temporal profile of the incident field, such that it matches the exponentially growing time dependence associated with the complex scattering zero. Remarkably, during this transient excitation the scattering from the structure totally vanishes, as if the system was perfectly absorbing despite the absence of actual dissipation. Instead, all incident energy is getting locked inside the cavity as long as the exponentially growing incident field is sustained.

As another example of a coherently assisted effect, we introduce the concept of coherently enhanced wireless power transfer (WPT). For an efficient WPT, a receiving antenna must be resonant and has to have an equal coupling with free space and the load, which is known as the critical coupling. However, this condition is not always easily implemented. To bypass this difficulty and achieve efficient operation with an antenna that is not critically coupled, we propose an approach that relies on coherent excitation of the receiving antenna with a backward propagating wave [3]. Given a correct amplitude and phase of this coherent wave, it induces a proper interference pattern in the system, which in turn restores the critical coupling condition and results in a largely increased amount of transferred energy.

The two effects reported here suggest that coherent manipulation of light with light may lead to counter-intuitive electromagnetic effects even in rather simple systems and may be used to improve performance of energy harvesting devices.

References

- [1] D. G. Baranov, A. Krasnok, T. Shegai, A. Alù, Y. D. Chong, Coherent perfect absorbers: linear control of light with light, *Nat. Rev. Mater.*, **2**, 17064 (2017).
- [2] D. G. Baranov, A. Krasnok, A. Alù, Coherent virtual absorption based on complex zero excitation for ideal light capturing, *Optica*, **4**, 1457 (2017).
- [3] A. Krasnok, D. G. Baranov, S. Li, A. Generalov, A. Alù, Coherently enhanced wireless power transfer, accepted to *Phys. Rev. Lett.*

Enhanced Raman emission by non-scattering anapole state of a silicon nanodisk

Baranov, D.G., Verre, R., Karpinski, P., Käll, M.

Department of Physics, Chalmers University of Technology, 412 96 Gothenburg, Sweden

e-mail: denisb@chalmers.se

Enhancement of inelastic light scattering, such as photoluminescence or Raman scattering, by a nanostructure is associated with optical resonances of the structure. For the particular case of Raman scattering by molecules this results in the famous $(E/E_0)^4$ rule that describes enhancement of Raman emission [1]. It is therefore often accepted that elastic scattering by a nanostructure and Raman enhancement are two correlated processes. An intriguing question that arises at this point is whether it is possible to challenge this naive picture and attain enhanced Raman scattering along with suppressed elastic scattering.

Recently, a considerable progress has been made in enhancement of Raman scattering from high-index nanostructures made of silicon that support Mie resonances. Similarly to plasmonic particles, Raman enhancement in these systems matches their elastic scattering spectra [2]. An especially intriguing regime of light scattering found in dielectric nanoparticles is the anapole mode [3]. When light is scattered by a dielectric nanodisk with a large diameter/height aspect ratio, there is a

particular wavelength, at which the intensity of elastic scattering is almost completely suppressed, despite resonant enhancement of electromagnetic field inside the disk and local density of states.

Here, we report enhancement of Raman scattering from silicon nanodisks supporting the anapole mode, as sketched in Fig. 1a. Compared to an unstructured film, we found a two orders of magnitude enhancement of Raman scattering for nanodisks, which present an anapole state at the excitation wavelength. Our results demonstrate that while the particle is non-scattering, the Raman signal originating within the particle itself is largely enhanced, as depicted in spectra in Fig. 1(b). This enhancement is possible due to inelastic and incoherent transfer of energy to Raman polarization via emission of a phonon. Enhanced Raman emission can thus be observed due to the enhanced electromagnetic energy within the nanoparticle and due to incoherent nature of Raman emission. Our results demonstrate unusual relation between resonances in elastic and inelastic scattering and suggest a way toward background free frequency conversion devices.

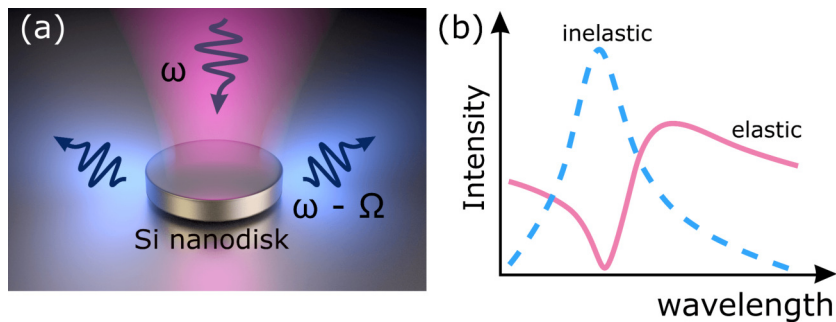


Fig. 1: Schematic illustration of Raman scattering enhancement by the anapole mode. Incident field at excitation frequency ω excites the anapole mode in a Si nanodisk, which results in enhanced scattering at Stokes frequency $\omega - \Omega$ and at the same time suppressed elastic scattering.

References

- [1] P. L. Stiles, Surface-enhanced Raman spectroscopy, *Annu. Rev. Anal. Chem.*, **1**, 601–626 (2008).
- [2] P. Dmitriev et al, Resonant Raman scattering from silicon nanoparticles enhanced by magnetic response, *Nanoscale*, **8**, 9721–9726 (2016).
- [3] A. E. Miroschnichenko, Nonradiating anapole modes in dielectric nanoparticles, *Nat. Commun.*, **6**, 8069 (2015).

Optomechanical manipulation and optical properties of vaterites

Hani Barhom¹, Andrey Machnev¹, Ivan I. Shishkin¹, Roman Noskov¹, **Pavel Ginzburg**^{1,2}

¹School of Electrical Engineering, Tel Aviv University, Tel Aviv, 69978, Israel

²ITMO University, Saint Petersburg, 197101, Russia

e-mail: pginzburg@post.tau.ac.il

Vaterite is the metastable phase of Calcium carbonate (CaCO_3), which forms porous spherical particles with sizes of several microns. Vaterite platform is highly important for a range of biomedical applications, where it is used as a cargo for targeted drug delivery. In this contribution we will review our recent progress in studies of optical properties of pure and doped vaterite particles, concentrating on peculiar electromagnetic interactions mediated by complex permittivity tensors of mesoporous compounds. Furthermore, being dissolvable in fluid solutions, vaterite cargoes can be subject to flexible optomechanical manipulations, including linear translations and rotations. Flexible optomechanical manipulation of cargos opens new opportunities in light-driven targeted drug delivery applications.

Enhanced Faraday effect in hybrid metasurfaces

Barsukova M.G.¹, Shorokhov A.S.¹, Musorin A.I.¹, Luk'yanchuk B.S.^{1,2}, Fedyanin A.A.¹

¹Faculty of Physics, Lomonosov Moscow State University, Moscow 119991, Russia

²Data Storage Institute, Agency for Science, Technology and Research, Singapore 138634, Singapore

e-mail: barsukova@nanolab.phys.msu.ru, shorokhov@nanolab.phys.msu.ru,

musorin@nanolab.phys.msu.ru, boris_l@dsi.a-star.edu.sg,

fedyanin@nanolab.phys.msu.ru

Control of light with the magnetic field is one of the important methods for modulation of its intensity and polarisation [1]. Faraday effect is a base of optical isolators and magneto-optical modulators. The nanostructuring of the materials allows one to enhance the effect in several times. High-index nanostructures have been studied extensively in the recent years [2]. They can strongly localize both electric and magnetic fields when Mie resonances are excited [3]. The concept of metamaterials allows one to design artificial subwavelength meta-atoms that support a excitation of dipole magnetic modes, termed as *optical magnetism*, even when they are made of nonmagnetic materials. We aim to study magneto-optical effects in hybrid metal-dielectric metasurfaces that combine all advantages of all-dielectric high-refractive-index structured materials with the properties of magnetic metallic inclusions, thereby providing a new opportunity for light control with metasurfaces.

The important direction in this field is a combination of Mie resonances with magnetophotonics. Here we study the interplay of all-dielectric resonant nanostructures and magnetic materials for developing compact active magneto-optical metadevices and demonstrate the enhancement of the magneto-optical effects by Mie-resonant surfaces.

We study magneto-optical effects in magnetophotonic nanostructures [4, 5]. Figure 1 shows numerical simulations of transmittance and magneto-optical response spectra in a hybrid metasurface. A square lattice of Si disks with 140-nm-diameter and 225-nm-height and lattice constant of 400 nm is covered by 5-nm-thick Ni film. There are two dips in the transmittance spectrum: the dip at the wavelength of 680 nm corresponds to the electric dipole Mie resonance and the other one at the wavelength of 780 nm relates to the magnetic dipole Mie resonance of a Si nanodisk.

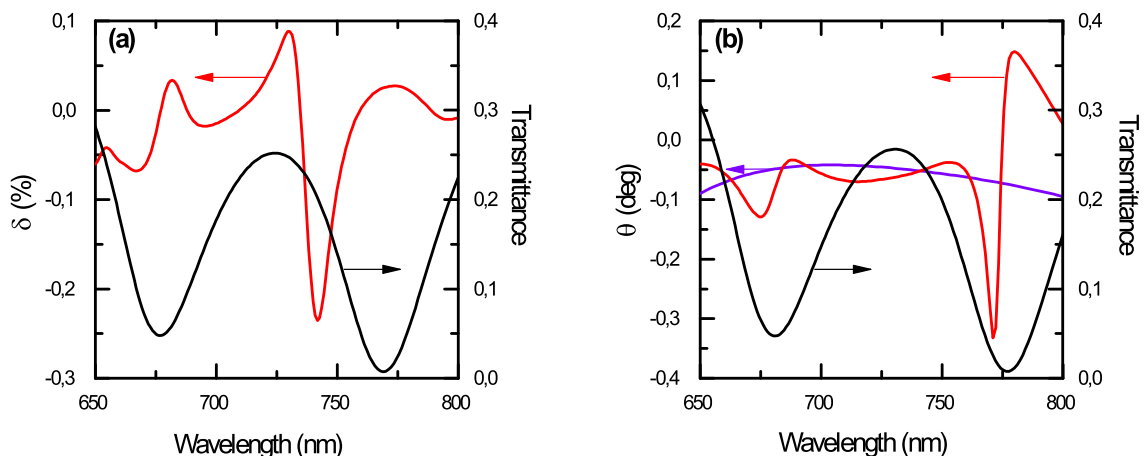


Fig. 1: Numerically calculated (a) transmittance spectra (black curve) and magneto-optical response spectra in Voigt geometry (red curve); (b) transmittance spectra (black curve) and Faraday rotation (red curve) spectra of the sample. Purple curve corresponds to the numerically calculated Faraday rotation effect of an unstructured Ni film.

The spectrum of the Faraday rotation (see Fig. 1b) and magneto-optical response in Voigt geometry (see Fig. 1a) show resonant enhancement in the vicinity of magnetic dipole Mie resonance of the Si nanodisks, while a reference flat Ni film (purple curve) does not have any peculiarities. Thus, we can easily trace correlations between the magneto-optical enhancement and magnetic dipole resonance in the hybrid metasurface.

To conclude, we have numerically demonstrated the multifold enhancement of the magneto-optical response both in Voigt and Faraday configurations near the magnetic dipole Mie resonance of Si nanoparticles covered with a thin magnetic film. Our results offer a novel approach for magnetic-field-controlled metadevices.

The work has been supported by the Ministry of Education and Science of the Russian Federation (grant N14.W03.31.0008, No 14.W02.18.6862-NSH), Russian Foundation for Basic Research (grant N17-02-01286, N17-52-560011, N18-52-50021). The authors are grateful to D. N. Neshev and Y. S. Kivshar for fruitful discussions.

References

- [1] M. Inoue, et al., Magnetophotonic crystals, *J. Phys. D: Appl. Phys.*, **39**, R151 (2006).
- [2] N. Zheludev, Y. Kivshar, From metamaterials to metadevices, *Nature Materials*, **11**, 917 (2012).
- [3] A. Kuznetsov, et al., Optically resonant dielectric nanostructures, *Science*, **354**, 2472 (2016).
- [4] M. Barsukova, et al., Magneto-optical response enhanced by Mie resonances in nanoantennas, *ACS Photon.*, **4**, 2390 (2017).
- [5] A. Musorin, et al., Manipulating the light intensity by magnetophotonic metasurfaces, *J. Magn. Magn. Mater.*, doi.org/10.1016/j.jmmm.2017.11.049 (2017).

Stronger, faster, and more powerful artificial muscle yarns and fibers

Ray H. Baughman, Alan G. MacDiarmid

NanoTech Institute, the University of Texas at Dallas

e-mail: ray.baughman@utdallas.edu

Successive generations of artificial muscle yarns and fibers have provided the understanding needed to progressively increase muscle performance. While our original electrochemical muscles based on carbon nanotube (CNT) sheets provided only about 0.1% tensile strokes, our present coiled yarn electrochemical CNT muscles provide tensile strokes as high as 12%, and 65 times the work capacity per cycle and 100 times the load-lifting capability as the same size natural muscle. Our polymer muscles made from fishing line or sewing thread, which are thermally, electrothermally, or chemically powered, can rotate at 100,000 rpm, contract 49%, generate 5 times the gravimetric power of a car engine, lift 100 times heavier loads than the same length and weight human muscle, or actuate at 7.5 cycles/s for millions of cycles. The strokes of these polymer muscles has been increased to a remarkable 9000% for applications as diverse as thermal energy harvesting and comfort-adjusting clothing. We have very recently shown that our CNT muscles can be operated in reverse to generate a gravimetric electrical power output that is higher than for any reported mechanical energy harvester for few Hz to 600 Hz frequencies. These “twistron” harvesters were used in the ocean to harvest wave energy, combined with thermally-driven artificial muscles to convert temperature fluctuations to electrical energy, sewn into textiles for use as self-powered respiration sensors, and used to power a LED and to charge a storage capacitor.

Strain engineering in MoSe₂ monolayers

Benimetskiy F.A.¹, Alekseev P.A.², Sinev I.S.¹, Mukhin I.S.^{1,3}, Samusev A.K.¹

¹ITMO University, St. Petersburg 197101, Russia

²Ioffe Institute RAS, St. Petersburg 194021, Russia

³St. Petersburg Academic University, St. Petersburg 194021, Russia

e-mail: fedor.benimetskiy@metalab.ifmo.ru

Over the last decade, the field of physics which dealing with the two-dimensional layered materials is undergoing rapid development. The most promising non-graphene layered materials are

the transition-metal dichalcogenides such as MoS₂, WSe₂, MoSe₂ and others. The ability to control optical properties of two-dimensional crystals using strain engineering opens the way for a broad range of applications such as optoelectronic and MEMS devices, sensors, etc.

In this work, we study how photoluminescence (PL) spectrum of MoSe₂ monolayer is influenced by its local deformation by means of an atomic force microscopy (AFM) tip. The monolayers were produced by mechanical exfoliation. In the experiment, the samples were pumped from the substrate side by 633 nm (HeNe CW laser) focused with a 0.7 NA objective. PL signal was collected by the same objective and analyzed by a spectrometer in confocal arrangement. The scanning performed by the objective allowed to map PL spectra in horizontal plane before and after deformation (Fig. 1).

The observed PL spectra possess peak at the energies of ≈ 1.58 eV. During the deformation of the MoSe₂ monolayer by the AFM tip (from 0 to 0.7 μm), PL peaks shifted towards higher energy and their intensity decreased (Fig. 1a,b). The maximum displacement of the PL peak due to the deformation per 0.7 micrometre was about 6 meV, the value was determined by subtracting the initial image (before deformation) from the final (after deformation) (Fig. 1c). The observed phenomena correspond to the stretching of a monolayer. Our experimental results are consistent with theoretical predictions[1] and other experimental works, in which the stretching of a TMD monolayer was carried out by means of other methods [2].

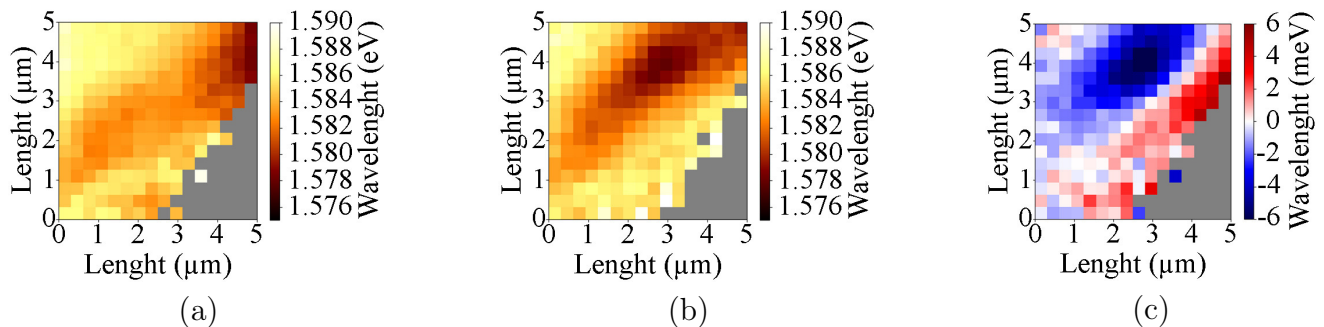


Fig. 1: PL wavelength map of the MoSe₂ monolayer (a) before and (b) after deformation. The displacement of the PL peak due to the deformation was about 6 meV, the value was determined by (c) subtracting the image (a) from the image (b)

The present study was funded by the Megagrant No. 14.Y26.31.0015 of the Ministry of Education and Science of Russian Federation.

References

- [1] P. Johari, V.B. Shenoy, Tuning the electronic properties of semiconducting transition metal dichalcogenides by applying mechanical strains, *ACS Nano*, **6**(6), 5449–5456 (2012).
- [2] R. Roldán, et al., Strain engineering in semiconducting two-dimensional crystals, *Journal of Physics: Condensed Matter*, **27**(31), 313201 (2015).

Optical properties of spatially dispersive Mie-resonant halide perovskite nanoparticles

Berestennikov A.S., Tiguntseva E.Y., Iorsh I.V., Makarov S.V.

Department of Nanophotonics and Metamaterials, ITMO University, Russia

e-mail: a.berestennikov@metalab.ifmo.ru

Metal halide perovskite materials have attracted great scientific and technological interest in recent years, due to their excellent properties including bandgap tunability, long charge diffusion length, outstanding optoelectronic merits combined with low cost and solution processability, which greatly contribute to their high potential for optoelectronic devices [1]. The materials based on

perovskite quantum dots (QDs) have a favourable combination of quantum-size effects, improving their optical properties in comparison with bulk analogues, Mie resonances and the ability to disperse in a variety of solvents and matrices, which allows them to be introduced into various devices. In order to create effective light-emitting devices, it is necessary to be able to change the optical properties of nanoparticles, such as the wavelength of the luminescence, the absorption/scattering cross-sections and the radiation direction [2]. In some works [3, 4] it was found that in nanocrystals of perovskites with a size of less than 80 nm, the photoluminescence peak is blue-shifted. The origin of this phenomenon was not explained, and the curve of the dependence of the peak shift on the particle sizes was interpolated by the empirical formula. In this work we proposed a possible mechanism responsible for the shift of the photoluminescence peak in perovskite nanoparticles. It may be related with the effect of nonlocality of excitons in such nanoparticles.

The Mie theory explains the optical properties of spheres of arbitrary diameters, consisting of an isotropic material, which is characterized by a local dielectric constant, which depends only on the frequency. However, metallic and dielectric spheres can have interesting optical effects, which cannot be explained by the classical local model. In this case, the observed effects can be explained by using a modified Mie theory, in which spatial dispersion is included by adding a nonlocal term to the equation of the classical local dielectric function [5]:

$$\varepsilon(\omega, \mathbf{k}) = \varepsilon_0 + \frac{\omega_p^2}{\omega_T^2 + Dk^2 - \omega^2 - i\gamma\omega}, \quad (1)$$

where ε_0 is background dielectric constant, ω_p is the dipole oscillator strength, Dk^2 is the spatial dispersion term, γ is the damping term and ω_T is the excitonic transition frequency.

In order to explain the blue-shift of the photoluminescence we applied the generalized Mie theory to the calculation of the optical properties of the $\text{CH}_3\text{NH}_3\text{PbI}_3$ (or MAPI) nanoparticles. The local and nonlocal absorption cross-sections of the MAPI nanoparticles with different radii were calculated. In the classical (local) case, the shift of the absorption peak is not observed. For nonlocal case with decreasing of the nanoparticle radius, the main peak shifts to lower wavelengths. This shift is due to the fact that the exciton is not stationary, but has kinetic energy, so it emits and absorbs at a higher frequency

We proposed that a mechanism with which the blueshift of the luminescence peak in perovskite nanoparticles is associated with nonlocality of material around exciton. We performed numerical calculations of the absorption and scattering cross-sections of incident light in such nanoparticles in the local and nonlocal cases. Using this results, we plotted the spectral and radii dependences of the in both cases. Our investigations showed that the possible mechanism of blue shift of the photoluminescence peak in perovskite nanoparticles is associated with the nonlocality of excitons.

References

- [1] He Huang, L. Polavarapu, J. A. Sichert, A. S. Susa, A. S. Urban, A. L. Rogach, *NPG Asia Materials*, **8**, e328 (2016).
- [2] M. V. Kovalenko, L. Protesescu, M. I. Bodnarchuk, *Science*, **358**(6364), 745–750 (2017).
- [3] D. Di, K. P. Musselman, G. Li, A. Sadhanala, Y. Ievskaya, Q. Song, Z.-K. Tan, M. L. Lai, J. L. MacManus-Driscoll, N. C. Greenham, R. H. Friend, *J. Phys. Chem. Lett.*, **6**(3), 446–450 (2015).
- [4] V. D’Innocenzo, A. R. S. Kandada, M. De Bastiani, M. Gandini, A. Petrozza, *J. Am. Chem. Soc.*, **136**(51), 17730–17733 (2014).
- [5] R. Ruppin, *J. Opt. Soc. Am.*, **71**(6), 755–758 (1981).

The role of leaky waves in extraordinary transmission hole arrays and corrugated antennas

M. Beruete

Department of Electrical and Electronic Engineering, Universidad Pública de Navarra, Edificio Los Tejos Planta 1, Campus Arrosadia, 31006, Pamplona, Spain

e-mail: miguel.beruete@unavarra.es

The discovery of extraordinary transmission through subwavelength hole arrays revitalized the research on plasmonic structures [1, 2]. This phenomenon consists in high transmission peaks that appear in the cutoff region of periodic matrices of apertures and was explained as a result of the interaction of the incident light with the surface plasmons supported by the metal-air interface and excited thanks to the high-order modes of the periodic structure. This result opened the way towards the investigation of similar resonances in periodic metallic structures, being of especial interest the case of a subwavelength aperture flanked by grooves [3]. This last geometry gave rise to an enhanced transmission along with a strong beaming in the normal direction. Although all the previous results were found in the infrared range of the electromagnetic spectrum, soon after they were replicated at longer wavelengths such as millimeter-waves and terahertz [4–6], generalizing the results beyond pure surface plasmons excitation. Indeed, at those frequencies the waves responsible for the strong enhancement are leaky-wave modes supported by the periodic structure, as discussed in [7]. In this talk, I will overview our latest results related with extraordinary transmission structures, putting the emphasis in the leaky-wave interpretation of the experimental results. I will present several antennas developed following the guidelines of the narrow aperture flanked by periodic grooves, a topic that has given rise to a new family of competitive antennas at microwaves and millimeter-waves [8–14]. Additionally, I will present a recent result where we demonstrate experimentally extraordinary transmission with a reduced number of directly illuminated holes, in contrast with typical experiments and analyses where this number is relatively big. As it will be discussed, the enhancement of transmission is mainly due to the excitation of the $n = -1$ leaky-wave mode supported by the periodic structure, similarly to the case of the antennas. All these results will serve to clarify the exact role of leaky-waves in this type of structures.

References

- [1] T. W. Ebbesen, H. J. Lezec, H. F. Ghaemi, T. Thio, P. A. Wolff, Extraordinary optical transmission through sub-wavelength hole arrays, *Nature*, **391**, 667–669 (1998).
- [2] Editorial, Surface plasmon resurrection, *Nat. Photonics*, **6**, 707 (2012).
- [3] H. J. Lezec, et al., Beaming light from a subwavelength aperture, *Science*, **297**(5582), 820–822 (2002).
- [4] M. Beruete, et al., Enhanced millimeter-wave transmission through subwavelength hole arrays, *Opt. Lett.*, **29**(21), 2500–2502 (2004).
- [5] M. Beruete, M. Sorolla, I. Campillo, J. S. Dolado, Subwavelength slotted corrugated plate with enhanced quasi-optical millimeter wave transmission, *IEEE Microw. Wirel. Components Lett.*, **15**(4), 286–288 (2005).
- [6] S. A. Kuznetsov, et al., Regular and anomalous extraordinary optical transmission at the THz-gap, *Opt. Express*, **17**(14), 11730–11738 (2009).
- [7] D. R. Jackson, et al., The fundamental physics of directive beaming at microwave and optical frequencies and the role of leaky waves, *Proc. IEEE*, **99**(10), 1780–1805 (2011).
- [8] M. Beruete, et al., Very low-profile ‘bull’s eye’ feeder antenna, *IEEE Antennas Wirel. Propag. Lett.*, **4**(1), 365–368 (2005).
- [9] M. Beruete, et al., Dual-band low-profile corrugated feeder antenna, *IEEE Trans. Antennas Propag.*, **54**(2), 340–350 (2006).

- [10] M. Beruete, et al., Terahertz corrugated and bull's-eye antennas, *IEEE Trans. Terahertz Sci. Technol.*, **3**(6), 740–747 (2013).
- [11] U. Beaskoetxea, et al., 77-GHz high-gain bull's-eye antenna with sinusoidal profile, *IEEE Antennas Wirel. Propag. Lett.*, **14**, 205–208 (2015).
- [12] U. Beaskoetxea, M. Navarro-Cía, M. Beruete, Broadband frequency and angular response of a sinusoidal bull's eye antenna, *J. Phys. D. Appl. Phys.*, **49**(26), 265103 (2016).
- [13] U. Beaskoetxea, S. Maci, M. Navarro-Cía, M. Beruete, 3D-printed 96 GHz bull's-eye antenna with off-axis beaming, *IEEE Trans. Antennas Propag.*, **65**(1), 17–25 (2017).
- [14] U. Beaskoetxea, M. Beruete, High aperture efficiency wide corrugations bull's-eye antenna working at 60 GHz, *IEEE Trans. Antennas Propag.*, **65**(6), 3226–3230 (2017).

Topological polaritonics

Bleu O., Malpuech G., Solnyshkov D.D.

Institut Pascal, PHOTON-N2, University Clermont Auvergne, CNRS, 4 avenue Blaise Pascal, 63178 Aubiere Cedex, France

e-mail: dmitry.solnyshkov@uca.fr

We discuss the possibilities offered by the polariton platform to study fundamental topological effects and their applications [1, 2]. We begin with the anomalous Hall effect arising from the TE-TM spin-orbit coupling and Zeeman splitting [3]. We compare the behavior of the surface states in the quantum anomalous Hall effect and the interface states in the quantum valley Hall effect [4].

We analyze the behavior of a polariton condensate as a quantum fluid in staggered polariton graphene lattice, showing that an analog of quantum spin Hall effect can be observed for quantum vortices [5]. We demonstrate the existence of a coupling between the vortex winding and the valley of the bulk Bloch band. This leads to chiral vortex propagation on each side of the zigzag interface between two regions of inverted staggering. The topological protection provided by the vortex winding prevents valley pseudospin mixing and resonant backscattering, allowing a truly topologically protected valley pseudospin transport.

Finally, we study the properties of a topological optical isolator [6], as an integrated optical device based on the chiral surface states of polariton graphene in the quantum anomalous Hall regime. We study the practical properties of such device and optimize its parameters. We obtain an isolation ratio of 49 dB at 783 nm wavelength for a device of 40 microns with maximal signal modulation frequency of 300 GHz, operating at temperatures up to 50 K.

References

- [1] D. Solnyshkov, G. Malpuech, Chirality in photonic systems, *Comptes Rendus Physique*, **17**, 920 (2016).
- [2] T. Ozawa, et al., Topological Photonics, *arXiv:1802.04173* (2018).
- [3] O. Bleu, G. Malpuech, D. Solnyshkov, Effective theory of non-adiabatic quantum evolution based on the quantum geometric tensor, *arXiv:1612.02998* (2016).
- [4] O. Bleu, D. D. Solnyshkov, G. Malpuech, Quantum valley Hall effect and perfect valley filter based on photonic analogs of transitional metal dichalcogenides, *Phys. Rev. B*, **95**, 235431 (2017).
- [5] O. Bleu, G. Malpuech, D. D. Solnyshkov, \mathbb{Z}_2 topological insulator analog for vortices in an interacting bosonic quantum fluid, *arXiv:1709.01830* (2017).
- [6] D. D. Solnyshkov, O. Bleu, G. Malpuech, Topological optical isolator based on polariton graphene, *Appl. Phys. Lett.*, **112**, 031106 (2018).

Optical momentum and angular momentum in complex media

Bliokh K.Y.^{1,2}, **Bekshaev A.Y.**³, **Nori F.**¹

¹RIKEN, Wako-shi, Saitama 351-0198, Japan

²Nonlinear Physics Centre, RSPE, The Australian National University, Canberra, Australia

³I.I. Mechnikov National University, Dvorianska 2, Odessa, 65082, Ukraine

e-mail: k.bliokh@gmail.com

We examine the momentum, spin, and orbital angular momentum of structured monochromatic optical fields in dispersive inhomogeneous isotropic media. There are two bifurcations in this general problem: the Abraham–Minkowski dilemma and the kinetic (Poynting-like) versus canonical (spin-orbital) pictures. We show that the kinetic Abraham momentum describes the energy flux and group velocity of the wave in the medium. At the same time, we introduce novel canonical Minkowsky-type momentum, spin, and orbital angular momentum densities of the field. These quantities exhibit fairly natural forms, analogous to the Brillouin energy density, as well as multiple advantages as compared with previously considered formalisms. We apply this general theory to inhomogeneous surface plasmon-polariton (SPP) waves at a metal-vacuum interface and show that SPPs carry a “super-momentum”, proportional to the wave vector $k_p > \omega/c$, and a transverse spin, which can change its sign depending on the frequency ω .

References

- [1] K. Y. Bliokh, A. Y. Bekshaev, F. Nori, Optical momentum, spin, and angular momentum in dispersive media, *Phys. Rev. Lett.*, **119**, 073901 (2017).
- [2] K. Y. Bliokh, A. Y. Bekshaev, F. Nori, Optical momentum and angular momentum in complex media: from the Abraham–Minkowski debate to unusual properties of surface plasmon-polaritons, *New J. Phys.*, **19**, 123014 (2017).

High-Q modes in subwavelength dielectric resonators

A.A. Bogdanov^{1,2}, **M.V. Rybin**^{1,2}, **K.L. Koshelev**^{1,3}, **Z.F. Sadrieva**¹, **K.B. Samusev**^{1,2}, **M.F. Limonov**^{1,2}, **Yu.S. Kivshar**^{1,3}

¹ITMO University, St. Petersburg 197101, Russia

²Ioffe Institute, St. Petersburg 194021, Russia

³Australian National University, Canberra ACT 2601, Australia

e-mail: a.bogdanov@metalab.ifmo.ru

Recent progress in nanoscale optical physics is associated with the development of a new branch of nanophotonics exploring strong Mie resonances in dielectric nanoparticles with a high refractive index. The high-index resonant dielectric nanostructures form building blocks for novel photonic metadevices with low losses and advanced functionalities. However, unlike extensively studied cavities in photonic crystals, such dielectric resonators demonstrate low quality factors (Q factors). We uncover a novel mechanism for achieving giant Q factors of subwavelength nanoscale resonators by realizing the regime of bound states in the continuum. In contrast to the previously suggested multilayer structures with zero permittivity, we reveal strong mode coupling and Fano resonances in homogeneous high-index dielectric finite-length nanorods resulting in high-Q factors at the nanoscale. Thus, high-index dielectric resonators represent the simplest example of nanophotonic supercavities, expanding substantially the range of applications of all-dielectric resonant nanophotonics and meta-optics.

Adjustable metasurface-based resonator for in vivo MRI

Bruï E.A., Shchelokova A.V., Zubkov M.A., Melchakova I.V., Glybovski S.B., Andreychenko A.E., Slobozhanyuk A.P.

Nanophotonics and Metamaterials, ITMO University, Saint-Petersburg, Russian Federation
e-mail: e.bruï@metalab.ifmo.ru

In this work a novel subwavelength metasurface-inspired resonator which enhances the sensitivity of existing coils for 1.5 T MRI is proposed. The meta-resonator was formed by an array of capacitively loaded wires. The capacitive loads allowed to achieve a high level of miniaturization of the electrical length of the structure and made it resonant, while its length was much shorter than half of the operating wavelength.

Methods and materials. The developed prototype of metasurface-based resonator consisted of an array of 10 parallel telescopic, subwavelength brass wires (Figure 1(a)). Each wire connected at both ends to capacitive loads, implemented as rectangular copper patches on a common grounded dielectric substrate (Arlon AD1000, Arlon Microwave Materials). The length (L) of the wires and dimensions of copper patches (width w and length l) were optimized by means of 3D electromagnetic full-wave simulations (CST Microwave Studio 2017). The resulting geometric parameters that tuned the resonator's eigenmode with the highest penetration depth of field to the proton Larmor frequency at 1.5 T ($f = 63.8$ MHz) were used for fabrication of the prototype. T1-weighted turbo-spin echo coronal images of the wrist joint of a healthy volunteer were acquired in "superman" position for three set-ups: body coil birdcage (BC) in transmit mode (Tx-mode) and 4-channel flexible coil in receive mode (Rx-mode), i.e. conventional setup for wrist MRI; BC TxRx-mode with and without the resonator placed below the hand. Signal-to-noise (SNR) ratio was measured for a ROI located in a capitate bone. The standard deviation of noise was measured in a signal free area of the images.

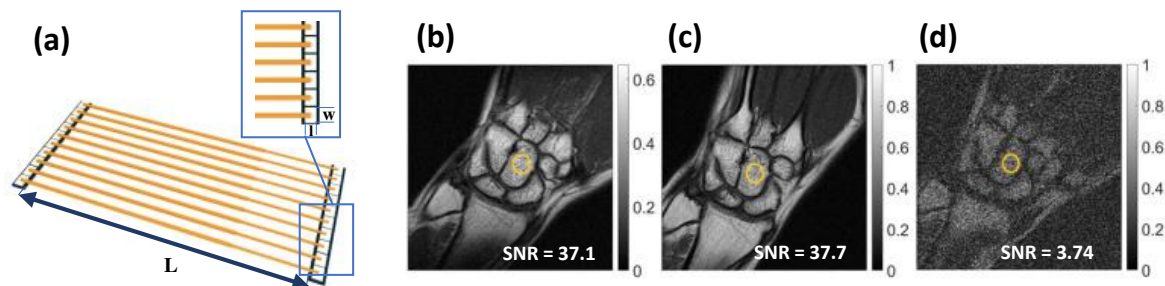


Fig. 1: (a) Artist's view of the meta-resonator (final parameters were: $L = 291$ mm, $l = 11$ mm, $w = 18$ mm). In vivo T1-weighted turbo-spin echo coronal images: (b) BC Tx and 4-channel flexible coil Rx; BC Tx and Rx with (c) and without (d) the resonator placed below the hand.

Results and Discussion. MR-imaging of the wrist in a presence of created resonator allowed to obtain almost the same SNR in a ROI located in a capitate bone as the Rx-only 4-channel coil and 10-fold enhancement of SNR when compare with BC-only RxTx image (Figure 1(b, c, d)). The proposed meta-resonator may be used as a pad (local wireless coil) and placed close to the area of interest, due to its compact and cordless design. It provides the same SNR efficiency as a 4-channel receive-only coil but with 32-fold less power that significantly improves RF-safety of MRI and could be used to reduce acquisition time of clinical MR-sequences containing power intensive RF pulses.

References

- [1] A. V. Shchelokova, et al., Locally enhanced image quality with tunable hybrid metasurfaces, *Phys. Rev. Appl.*, **9**, 14020 (2017).
- [2] E. A. Bruï, et al., Adjustable subwavelength metasurface-inspired resonator for magnetic resonance imaging, *Phys. Status Solidi A*, **215**(5), 1700788 (2018).

Engineering Weyl semimetals and anyons

Hrvoje Buljan

Department of Physics, Faculty of Science, University of Zagreb, Bijenicka c. 32 10000 Zagreb, Croatia

e-mail: hbuljan@phy.hr

I will present two topics of research in our group related to synthetic topological quantum matter [1]: (i) topological phases in 3D optical lattices, more specifically a proposal for experimental realization of Weyl semimetals in ultracold atomic gases [2], and (ii) anyons [3, 4]. I will present one possible route to engineer anyons in a 2D electron gas in a strong magnetic field sandwiched between *metamaterials with high magnetic permeability*, which induce electron-electron vector interactions to engineer charged flux-tube composites [3]. I will also discuss intriguing concepts related to extracting observables from anyonic wavefunctions [4]: one can show that the momentum distribution is not a proper observable for a system of anyons [4], even though this observable was crucial for the experimental demonstration of Bose–Einstein condensation or ultracold fermions in time of flight measurements. I will show how time of flight measurements can be used to extract anyonic statistics [4].

References

- [1] N. Goldman, G. Juzeliunas, P. Ohberg, I. B. Spielman, *Rep. Prog. Phys.*, **77**, 126401 (2014).
- [2] T. Dubček, C. J. Kennedy, L. Lu, W. Ketterle, M. Soljačić, H. Buljan, Weyl points in three-dimensional optical lattices: Synthetic magnetic monopoles in momentum space, *Phys. Rev. Lett.*, **114**, 225301 (2015).
- [3] M. Todorčić, D. Jukić, D. Radić, M. Soljačić, H. Buljan, The Quantum Hall Effect with Wilczek’s charged magnetic flux tubes instead of electrons, *arXiv:1710.10108* [cond-mat.str-el].
- [4] T. Dubček, B. Klajn, R. Pezer, H. Buljan, D. Jukić, Quasimomentum distribution and expansion of an anyonic gas, *Phys. Rev. A*, **97**, 011601(R) (2018).

One-dimensional optical Tamm plasmons

Chestnov I. Yu.

Vladimir State University, 87 Gorkii Street, 600000 Vladimir, Russia

e-mail: igor_chestnov@mail.ru

Sedov E.S., Kavokin A.V.

University of Southampton, Highfield, Southampton SO17 1BJ, United Kingdom

Tamm plasmons are confined optical states at the interface of a metal and a dielectric Bragg mirror. Unlike conventional surface plasmons, Tamm plasmons may be directly excited by an external light source in both TE and TM polarizations [1]. Here we consider the one-dimensional propagation of Tamm plasmons under long and narrow metallic stripes deposited on top of a semiconductor Bragg mirror, see Fig. 1. The spatial confinement of the field imposed by the stripe and its impact on the structure and energy of Tamm modes are investigated. We show that the Tamm modes are coupled to surface plasmons arising at the stripe edges. These plasmons form an interference pattern close to the bottom surface of the stripe that involves modification of both the energy and loss rate for the Tamm mode. This phenomenon is pronounced only in the case of TE polarization of the Tamm mode. These findings pave the way to application of laterally confined Tamm plasmons in optical integrated circuits as well as to engineering potential traps for both Tamm modes and hybrid modes of Tamm plasmons and exciton polaritons with meV depth [2].

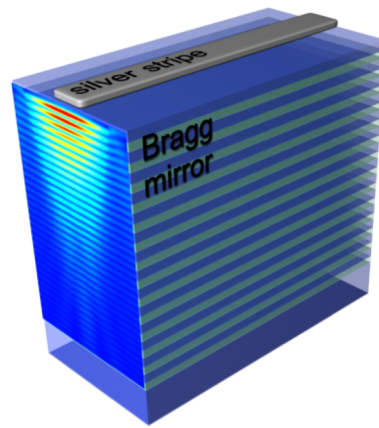


Fig. 1: Sketch of the Bragg mirror with the metal stripe deposited on the top surface. The distribution of the electric field of the tamm plasmon mode is sketched in the front side.

References

- [1] M. Kaliteevski, I. Iorsh, S. Brand, R. A. Abram, J. M. Chamberlain, A. V. Kavokin, I. A. Shelykh, *Phys. Rev. B*, **76**, 165415 (2007).
- [2] SK. S.-U. Rahman, T. Klein, S. Klemmt, J. Gutowski, D. Hommel, K. Sebald, *Sci. Rep.*, **6**, 34392 (2016).

Transmission properties of a chain of plasmonic nanoparticles beyond the point dipole approximation

Chubchev E.D.

Dukhov Research Institute of Automatics (VNIIA), 22 Suchevskaya, Moscow 120755, Russia
e-mail: chubchev.evgeniy@physics.msu.ru

Dorofeenko A.V., Vinogradov A.P.

Institute for Theoretical and Applied Electromagnetics, Russian Academy of Science, 13 Izhorskaya, Moscow 125412, Russia

Recently, it has been shown in [1, 2] that surface plasmons travelling along a chain of metal nanospheroids have both nanosized transverse localization length comparable to the interparticle distance and macroscopic propagation length up to 15 μm . However, these results has been obtained in [1, 2] by the point dipole approximation. The applicability of this approximation seems questionable if the interparticle distance is comparable to the nanoparticle size.

We study the propagation of surface plasmons along a chain of metal nanospheroids taking into account their finite size. We have shown that the finite size of spheroids leads to a significant change in the transmission characteristics of the nanoparticle chain, in particular, the propagation length of the surface plasmon drastically decreases.

References

- [1] A. A. Govyadinov, V. A. Markel, From slow to superluminal propagation: Dispersive properties of surface plasmon polaritons in linear chains of metallic nanospheroids, *Physical Review B*, **78**, 035403 (2008).
- [2] I. L. Rasskazov, S. V. Karpov, V. A. Markel, Nondecaying surface plasmon polaritons in linear chains of silver nanospheroids, *Optics Letters*, **38**, 4743–4746 (2013).

Potential to improve performance of state-of-the-art receive arrays with high-permittivity materials

Christopher M. Collins, Giuseppe Carluccio, Gillian Haemer

New York University School of Medicine, Dept. of Radiology; 660 First Ave; New York, NY 10016, USA

In recent years, a number of works have demonstrated the potential to improve the safety and efficacy of MRI in humans with strategic placement of materials having a high electric permittivity [1, 2]. Until now, all successful demonstrations of this have been attributed to improvements in the RF fields from large volume coils, or the transmit field in experiments having separate transmit and receive coil. To do this, the high-permittivity material (HPM) needs only to enhance the RF magnetic field in a small, nearby region within a large excitation coil. Thus, the transmit efficiency (B_1^+/\sqrt{P}) in the region near the HPM can generally be improved with a range of choices of electric permittivity in the HPM. In the case where the same large coil is used in reception, the reception efficiency or receive efficiency (B_1^-/\sqrt{P}) of the coil is proportional to Signal-to-Noise Ratio (SNR), and is generally also enhanced by the HPM. In these equations, B_1^+ and B_1^- are the counter-rotating circularly-polarized components of the RF magnetic field pertinent to excitation and reception at a given location of interest, while P indicates the total power dissipated in the entire subject. Fig. 1 shows simulations of an example where the transmit and receive efficiency of a large volume coil are enhanced in a relatively small region with placement of a nearby HPM. The situation for a state-of-the-art receive array is quite different. Rather than a single, large coil, there are several small coils positioned very near the Region of Interest (ROI). From prior work, it is not immediately intuitive what advantages HPMs may have in this situation.

To investigate potential advantages within a state-of-the-art receive array, we performed numerical simulations of many-element receive arrays designed for imaging the head and examined the associated array SNR for cases with and without a thin shell of HPM between the coils and the head. SNR for a receive array can be calculated [3]:

$$\text{SNR} \propto \sqrt{(B_1^- * R^{-1} B_1^-)}$$

where, for an array of N-coils, B_1^- is an N-element array of receptivity fields at the location of interest and R is an N by N noise resistance matrix with elements calculated as

$$R_{ij} = \int \sigma E_i \cdot E_j dv$$

where E_i and E_j are local electric fields from coils i and j and, s is local tissue conductivity, and the integration is performed over the entire subject.

Figure 2 shows a representative HPM helmet geometry inside a 28-channel close-fitting head array, as well as the array SNR calculated with and without the helmet present. Figure 3 shows dramatic improvements in array SNR with addition of the HPM helmet.

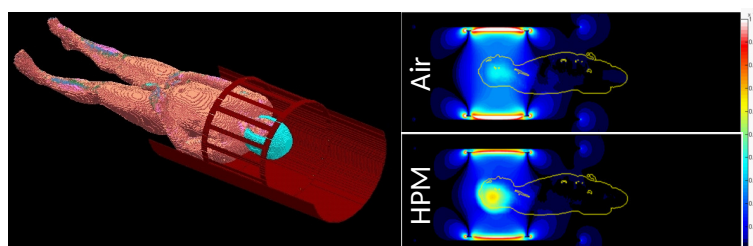


Fig. 1: Geometry of numerical model (left) in 28-coil head array (green) and calculated SNR distribution at 7 T (right) with and without HPM helmet (colored blue on left) present. Linear color scale from 0 to 1 a.u. for sagittal and 0 to 2 a.u. on axial and coronal planes.

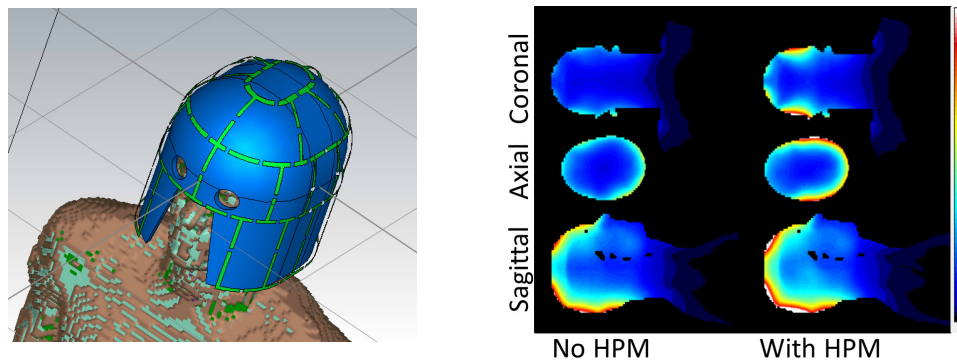


Fig. 2: Geometry of numerical model (left) and calculated transmit or receive efficiency distribution for a large 3 T body coil both without (top right) and with (bottom right) an HPM helmet (colored blue on left) placed around the head. Linear color scale from 0 to $1 \mu\text{T}/\sqrt{\text{W}}$.

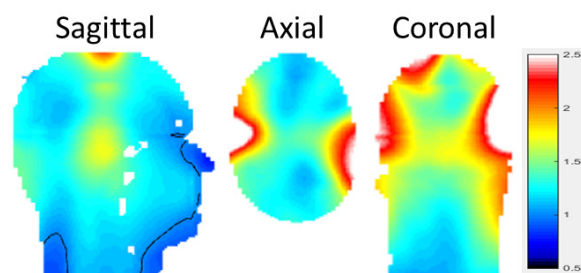


Fig. 3: Ratio of SNR with HPM to without HPM for close-fitting head array of Figure 2. SNR is increased everywhere in brain, by more than 40% on average and in some places by more than 200%. Linear color scale from 0 to 2.5.

References

- [1] Q. Y. Yang, et al., *J. Magn. Reson. Imaging*, **24**, 197 (2006).
- [2] A. G. Webb, *Concepts in Magn. Reson.*, **38A**, 148 (2011).
- [3] C. M. Collins, et al., *Proc. 2014 ISMRM*, 6645 (2014).

Dispersive shock waves in optical fibers

M. Conforti, G. Xu, C. Mas Arabí, T. Marest, A. Bendahmane, A. Kudlinski, A. Mussot

Univ. Lille, CNRS, UMR 8523-PhLAM-Physique des Lasers Atomes et Molécules, F-59000 Lille, France

e-mail: matteo.conforti@univ-lille1.fr

S. Trillo

Department of Engineering, University of Ferrara, Via Saragat 1, 44122 Ferrara, Italy

e-mail: trlsfn@unife.it

Dispersive shock waves are strongly oscillating wave trains that spontaneously form and expand thanks to the action of weak dispersion, which contrasts the tendency, driven by the nonlinearity, to develop a gradient catastrophe [1]. In this talk we review the basic concepts and our recent progresses made in the description of such nonlinear waves, both in terms of experimental results and modelling. After a brief introduction on the generating mechanisms of dispersive shocks in optical fibers [2], we report the experimental observation of the rupture of a photonic dam [3], as well as the theory [4] and some experiments on the generation of resonant radiation from shocks in fibers [5, 6] and resonators [7].

References

- [1] G. A. El, M. A. Hoefler, Dispersive shock waves and modulation theory, *Phys. D Nonlinear Phenom.*, **333**, 11–65 (2016).
- [2] G. Xu, A. Mussot, A. Kudlinski, S. Trillo, F. Copie, M. Conforti, Shock wave generation triggered by a weak background in optical fibers, *Opt. Lett.*, **41**, 2656 (2016).
- [3] G. Xu, M. Conforti, A. Kudlinski, A. Mussot, S. Trillo, Dispersive dam-break flow of a photon fluid, *Phys. Rev. Lett.*, **118**, 254101 (2017).
- [4] M. Conforti, F. Baronio, S. Trillo, Resonant radiation shed by dispersive shock waves, *Phys. Rev. A*, **89**, 13807 (2014).
- [5] M. Conforti, S. Trillo, A. Mussot, A. Kudlinski, Parametric excitation of multiple resonant radiations from localized wavepackets, *Sci. Rep.*, **5**, 9433 (2015).
- [6] T. Marest, C. Mas Arabí, M. Conforti, A. Mussot, C. Milián, D. V. Skryabin, A. Kudlinski, Emission of dispersive waves from a train of dark solitons in optical fibers, *Opt. Lett.*, **41**, 2454 (2016).
- [7] S. Malaguti, M. Conforti, S. Trillo, Dispersive radiation induced by shock waves in passive resonators, *Opt. Lett.*, **39**, 5626 (2014).

Multi-periodic one-dimensional photonic crystals

Dadoenkova N.N.^{1,2}, Dadoenkova Yu.S.^{1,2}, Panyaev I.S.¹, Sannikov D.G.¹, Lyubchanskii I.L.^{2,3}

¹Ulyanovsk State University, Ulyanovsk, Russia

²Donetsk Physical and Technical Institute of the NAS of Ukraine, Ukraine

³V. N. Karazin Kharkiv National University, Kharkiv, Ukraine

e-mail: dadoenkova@yahoo.com, yulidad@gmail.com, sannikov-dg@yandex.ru,
panyaev.ivan@rambler.ru, ilyubchanskii@gmail.com

In this communication, we present the results of theoretical and numerical investigation of complex 1D photonic structures based on particularly ordered thin layers forming multi-periodic photonic crystals (PCs). This research is development of our previous study of photonic-magnonic crystals [1, 2] and dielectric bi-periodic PCs [3]. We concentrate our attention on calculations of transmittivity spectra of electromagnetic waves for the finite 1D systems $(ABCD)^K$, $[(ABC)^N D]^K$ and $[(AB)^N (CD)^M]^K$, which are single-, two- and three-periodic 1D PCs composed of four different layers with the corresponding thicknesses d_i , ($i = A, B, C, D$), where N and M are the sub-period numbers and K is the super-period number. The unit cells of the structures under consideration are depicted in Figs. 1 (a), (b), (c). The structure $[(AB)^N (CD)^M]^K$ possesses two sub-periods $D_1 = d_A + d_B$, $D_2 = d_C + d_D$, characterizing the PC subsystems $(AB)^N$ and $(CD)^M$, respectively, and the super-period $D_{03} = ND_1 + MD_2$ [see Figs. 1 (c), (d)].

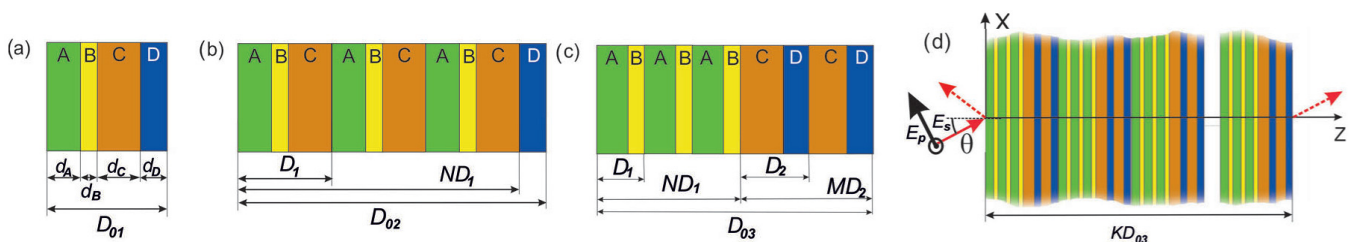


Fig. 1: The unit cells of a single- (a), two- (b) and three-periodic PCs (c). Schematic of the three-periodic 1D PC (d).

We calculated the transmittivity spectra of the electromagnetic waves for the structures above composed of the dielectric oxide layers (SiO_2 , TiO_2 , Al_2O_3 and ZrO_2) which are transparent in the visible and near IR regimes. We examine the modifications of both TE- and TM-modes spectra within the first photonic band gap (PBG) and its vicinity with the change of N , M , and K , incidence

angle θ , the layers thicknesses and their order in the structure. The PBG spectra are polarization-dependent and exhibit the set of complex defect modes (DMs). The number and positions of the DMs are correlated with the sub- and super-period numbers and strongly depend on d_i . The change of θ allows to govern the positions of both PBG edges and DMs. Modifying d_i , one can reach the significant shift of the DMs towards the PBG edges, as well it is possible to increase the DMs number and to obtain the satellite PBGs.

References

- [1] J. W. Kłos, M. Krawczyk, Yu. S. Dadoenkova, N. N. Dadoenkova, I. L. Lyubchanskii, *J. Appl. Phys.*, **115**, 174311 (2014).
- [2] Yu. S. Dadoenkova, N. N. Dadoenkova, I. L. Lyubchanskii, J. W. Kłos, M. Krawczyk, *J. Appl. Phys.*, **120**, 073903 (2016).
- [3] N. N. Dadoenkova, Yu. S. Dadoenkova, I. S. Panyaev, D. G. Sannikov, I. L. Lyubchanskii, *J. Appl. Phys.* **123**, 043101 (2018).

Antenna approach for calculating dynamic polarizability of carbon nanotubes

V.I. Demidchik, R.V. Kornev

Belarusian State University, Minsk, Belarus

e-mail: demidvi@bsu.by

Polymeric composites that contain carbon nanotubes (CNT) are the materials that are used in different spheres of radio engineering, instrument engineering, for synthesizing radio-absorbing coatings. Electrodynamics properties of such composites depend on the properties of separate CNT and their concentration. Together with other factors, the properties of CNT depend on their geometry as well. It is known [1], that in the process of synthesizing CNTs using different methods, along with rectilinear tubes there exist a significant amount of curved CNT and CNT in the form of helices with different coil steps and diameter. To estimate the electrodynamic properties of a singular CNT and for further analysis of composite materials on their basis, it is necessary to know the dipole moments and polarizability coefficients (PC). The values of electrical and dipole moments are determined using current distribution in CNT [2].

It is possible to define the influence of geometry on current distribution using Pocklington integral equation for conductors of arbitrary shape, which is widely used to solve antenna tasks. At the same time, it is necessary to consider surface impedance of CNT similarly to [4]. PC can be determined by solving matrix equation, which describes the connection between dipole moment of particles and the electromagnetic field, that excites them.

In compliance with the proposed algorithm, the investigation of frequency dependence of PC for the case of rectilinear CNT and CNT in the form of few-coil helices was carried out. The influence of coil step of a helical CNT and coil number on the values of electric and magnetic polarizability coefficients, on cross-polarization coefficients was estimated. Known value of PC of a single CNT allows to perform analysis of the composites, that consist of a large set of CNT, embedded into a dielectric matrix.

References

- [1] A. V. Eletsii, Carbon nanotubes, *UFN*, **167**(9), 945–972 (1997).
- [2] A. P. Vinogradov, *Electrodynamics of Composite Materials*, URSS, Moscow, 2001.
- [3] V. I. Demidchik, A. V. Runov, N. V. Kalashnikov, The algorithm of current distribution calculation of long curved wire, *Izvestiya Vuzov, Radioelektronika*, **26**(3), 82–84 (1983).
- [4] G. W. Hanson, Fundamental transmitting properties of carbon nanotube antennas, *IEEE Transactions on Antennas and Propagation*, **53**(11), 3426–3435 (2005).

2D materials for mesoscopic perovskite photovoltaics

Aldo Di Carlo

CHOSE – Centre for Hybrid and Organic Solar Energy, University of Rome Tor Vergata, Roma, Italy

e-mail: aldo.dicarlo@uniroma2.it

In the energy field, the use of hybrid organic-inorganic perovskite materials such as $\text{CH}_3\text{NH}_3\text{PbI}_3$ (MAPI) has opened up new directions to fabricate cost effective and high efficient photovoltaic (PV) devices. Many factors can influence the efficiency and stability characteristics of Perovskite Solar Cells (PSCs). In this perspective, bidimensional (2D) nanomaterials, such as graphene and related materials can play a primary role owing to their 2D nature and the large variety of 2D crystals, whose complementary opto/electronic properties, can be on-demand tuned by chemical functionalization and edge modification. Here, we demonstrate the use of graphene and 2D materials as an effective way to control the morphology [1] and to stabilize the device's interfaces. Several strategies have been used to master interface properties both at the anode and cathode parts of the cell. By dispersing graphene flakes into the mesoporous TiO_2 layer and by inserting graphene oxide (GO) as interlayer between perovskite and Spiro-OMeTAD layers, we demonstrate a PCE exceeding 18% with a two-step MAPI deposition, carried out in air [2]. Further optimization of the 2D interface layers could promote the efficiency above 20% with a strong improvement of the stability. The proposed approach has been exploited for the fabrication of state-of-the-art large area perovskite modules with a PCE of 13.7% on a monolithic (active area exceeding 100 cm^2). The use of 2D materials permitted to increase the PCE by more than 10% with respect to “conventional” modules [3]. Additional results will be shown for other 2D materials such as MoS_2 and Li-GO and for module with active regions $> 100\text{ cm}^2$ where a proper laser patterning was used to reduce interconnection dead area of a module below $400\text{ }\mu\text{m}$ making an aperture ratio of 95% [4].

References

- [1] F. Biccari, et al., *Adv. Energy Mat.*, **7**, 1701349 (2017).
- [2] A. Agresti, et al., *ChemSusChem*, **9**, 2609 (2016).
- [3] A. Agresti, et al., *ACS Energy Lett.*, **2**, 279–287 (2017).
- [4] A. Palma, et al., *IEEE J. Photovoltaics*, **7**, 1674 (2017).

Two-body physics in topological models

Marco Di Liberto

Université Libre de Bruxelles, CP 231 Campus Plaine, 1050 Bruxelles (Belgium)

e-mail: mar.diliberto@gmail.com

Recent advances in different experimental platforms have made possible to realize and explore several single-particle topological models and phenomena. However, interactions can play a major role in enriching the possibilities of new physics, as for the case of the Fractional Quantum Hall effect. I will present theoretical results for two interacting particles in topological models and possible implementation schemes with optical waveguides, polariton pillars and cold atomic systems. In particular, I will focus on the Su-Schrieffer-Heeger model and the Haldane model.

Coupling regimes of high-index dimer

Alexey A. Dmitriev¹, Mikhail V. Rybin^{1,2}

¹Department of Physics and Engineering, ITMO University, St. Petersburg 197101, Russia

²Ioffe Institute, St. Petersburg 194021, Russia

e-mail: alexey.dmitriev@metalab.ifmo.ru

Metamaterials, oligomers and other photonic structures operate due to resonances in their constituent elements [1]. The electric and magnetic dipole resonances are of high importance because of several reasons including strength and robustness of effects. The structure properties are influenced by the coupling between the dipole modes supported by the constituent elements. The coupling strength determines whether the photonic mode would be local or not. Each type of coupling has its own advantages and disadvantages for specific applications. Thus, it is crucial to reveal conditions for the transition between the weak and strong coupling regimes.

Here we investigate these conditions in the simplest system that is a dimer of rods with a high dielectric index. We calculate the scattering on the dimer by means of the multiple-scattering theory that is a rigorous coupled-multipole method, which takes the interaction between all scatterers into consideration. The computation yields the multipole amplitudes $a_{j,l}$ excited by the entire electromagnetic field being a sum of the incident wave and scattered fields from all rods.

We investigate the peaks related to the dipole resonance in scattering spectra. We exploit the optical theorem to obtain the scattering cross-section. It allows us to calculate the spectra without having to integrate the scattered fields. Following Jackson [2], we perform a derivation of two-dimensional (2D) optical theorem, which is based on the analysis of the far-field asymptotic and the Kirchoff's integral. The optical theorem reads

$$C_{\text{ext}} = 2\sqrt{\frac{\pi}{k}} (\text{Im}\{F_0\} - \text{Re}\{F_0\}), \quad (1)$$

where C_{ext} is the extinction cross-section, k is the wavenumber, and F_0 is the forward scattering amplitude. We notice that the optical theorem for 2D case differs significantly from 3D case.

We demonstrate that for an oligomer of N dielectric rods located at \mathbf{r}_j , the forward scattering amplitude can be expressed in terms of the multipole amplitudes $a_{j,l}$:

$$F_0 = \sqrt{\frac{2}{\pi k}} \sum_{j=1}^N \sum_{l=-\infty}^{\infty} [i^{-l} e^{-i\frac{\pi}{4}} e^{-i\mathbf{k}\cdot\mathbf{r}_j}] a_{j,l}, \quad (2)$$

which allows us to obtain the extinction cross-section after the coupled-multipoles equation is solved.

By using our approach we analyze the spectra of extinction cross-section for a dimer of identical non-absorbing dielectric rods of radius R and dielectric constant ε . We set the x axis along the incidence direction of plane wave to distinguish the longitudinal and transverse geometries where the rods are placed either along x axis or y axis. Also we study the system in TE and TM polarizations both. The variable parameters are the distance d between the rods ($2R < d \leq 10^6 \cdot R$) and their dielectric constant ($1 < \varepsilon \leq 100$). We track the evolution of the resonance in spectra in dependence on these parameters, looking for the the peaks splitting, which indicates the strong coupling regime.

In summary, we have derived 2D optical theorem. The coupled-multipoles equation has been solved to simulate extinction spectra. We have shown that the analysis of the dipole peak in spectra makes it possible to obtain the conditions for the weak-to-strong coupling regime transition.

References

- [1] S. Kruk, Y. Kivshar, Functional meta-optics and nanophotonics governed by Mie resonances, *ACS Photon.*, **4**(11), 2638–2649 (2017).
- [2] J. D. Jackson, *Classical Electrodynamics*, 3rd ed., John Wiley & Sons, Inc., New York, 1999.

Peculiarities of the photonic density of states in liquid-crystalline photonic crystals

Dolganov P.V.

Institute of Solid State Physics RAS, 142432 Academician Ossipyan Street, Chernogolovka, Moscow Region, Russia

e-mail: pauldol@issp.ac.ru

Liquid crystals composed by anisotropic molecules form a number of photonic crystals with unique optical properties. Photonic density of states is one of the primary characteristics of photonic crystals. Determination of the photonic density of states is important both from the fundamental point of view and for various applications.

We report studies of optical properties of liquid-crystalline photonic crystals with photonic stop bands in the visible light range. Photonic properties were investigated employing different approaches [1, 2]. Complex experimental methods were used to analyze the photonic structure. Diffraction, reflection and transmission spectra, rotation of the plane of polarization of light were measured. Polarized fluorescence measurements in the range of photonic bands were performed on samples doped with organic dyes. The density of states was determined from measurements of the rotation of the plane of polarization of light, from fluorescence spectra and calculated using material parameters determined from independent reflection and transmission measurements. Fluorescence spectra were modeled on the basis of approach which takes into account the orientational ordering of fluorescent molecules and the properties of the eigenmodes of light in the periodic structure of the photonic crystal [3]. Calculated spectra well agree with experiment both in the spectral range of the photonic band and outside it. Transformation of the photonic properties with sample thickness and temperature was studied. Optical properties of different liquid-crystalline photonic crystals are compared and analyzed on the basis of their photonic density of states.

This work was supported in part by RFBR, grant No. 17-02-00246.

References

- [1] P. V. Dolganov, G. S. Ksyonz, V. E. Dmitrienko, V. K. Dolganov, *Phys. Rev. E*, **87**, 032506 (2013).
- [2] P. V. Dolganov, *Phys. Rev. E*, **91**, 042509 (2015).
- [3] P. V. Dolganov, *JETP Lett.*, **106**, 657–660 (2017).

Structures and optical properties of smectic liquid crystals with multilayer periodicity

Dolganov P.V., Shuravin N.S., Dolganov V.K.

Institute of Solid State Physics RAS, 142432 Academician Ossipyan Street, Chernogolovka, Moscow Region, Russia

e-mail: pauldol@issp.ac.ru, shuravin@issp.ac.ru, dolganov@issp.ac.ru

Polar smectic liquid crystals form a variety of unusual phases whose period can be equal to a large number of molecular layers [1, 2]. In this work we report studies of a smectic liquid crystal with sequence of ferroelectric, antiferroelectric and ferrielectric phases. Selective reflection spectra are measured on bulk samples in the optical wavelength range. Temperature dependence of the spectral position of the selective reflection band was determined in the ferroelectric and antiferroelectric phases. Behavior of large-period structures in confined geometry of thin films and their optical properties attract essential interest. Surface ordering and symmetry breaking near the surface in thin films can induce structures not observed in bulk samples. Appearance of nontrivial structures could be expected when thickness of the films is commensurate with the periodicity of the phases of the bulk sample. Optical methods were used to investigate superthin free-standing films with

thickness equal to several molecular layers. Number of structures observed in the films increases with film thickness. Transitions between structures with different direction of polarization with respect to molecular tilt plane were observed. Electrooptical properties of the structures were studied. In relatively thick films at high temperature the film can be switched by electric field from the state with polarization parallel to the molecular tilt plane into the state with polarization perpendicular to the molecular tilt plane.

Structures in the films and in bulk samples were calculated in the framework of Landau theory of phase transitions with two-component order parameter [3, 4]. Comparison of the results of calculations with experiment allows us to estimate the values of interlayer interactions responsible for appearance of different phases.

This work was supported in part by RFBR, grant No. 17-02-00246.

References

- [1] S. Wang, L. Pan, R. Pindak, Z. Q. Liu, H. T. Nguyen, C. C. Huang, *Phys. Rev. Lett.*, **104**, 027801 (2010).
- [2] A. Iida, I. Nishiyama, Y. Takanishi, *Phys. Rev. E*, **89**, 032503 (2014).
- [3] P. V. Dolganov, V. K. Dolganov, V. M. Zhilin, E. I. Kats, *Phys. Rev. E*, **83**, 061705 (2011).
- [4] P. V. Dolganov, E. I. Kats, *Liquid Crystals Reviews*, **1**, 127–149 (2013).

All-dielectric valley photonic crystals: Paving the way to topological nanophotonics

Jian-Wen Dong

School of Physics & State Key Laboratory of Optoelectronic Materials and Technologies, Sun Yat-sen University, Guangzhou 510275, China
e-mail: dongjwen@mail.sysu.edu.cn

Nanophotonic devices in silicon-on-insulator (SOI) platform can potentially improve the capabilities of modern information-processing systems by replacing some of their electrical counterparts [1]. The discovery of topological photonics provides a new degree of freedom to control the flow of light, enabling novel optoelectronic functionalities and devices [2]. However, the subwavelength strategy at micro-nano scale remains challenge. Recent developments of valley photonic crystals pave an alternative way to achieve SOI topological nanophotonic devices with high performance [3–5]. Last year, we have a proposal on all-dielectric valley photonic crystals (VPCs) with nonzero valley Chern number by employing valley degree of freedom [5]. Valley bulk state with chiral phase vortex is exploited, and it leads to the unidirectional excitation of light flow. Valley dependent edge states and the resultant broadband robust transport are found. In our microwave experiment, we consider the TM_0 waveguide mode in hexagonal ceramic array sandwiched by two parallel metallic plates. Excited by a homemade chiral source with phase vortex, unidirectional bulk state transport can be observed. By mapping propagating electromagnetic fields and measuring transmission spectra, robust transport of edge state around Z-bend is also demonstrated. Recently, we develop a VPC in a standard 220-nm-thickness silicon wafer on the top of SiO_2 substrate. The valley-dependent topological edge states operate below the light cone so that the photonic crystal slab can strongly confine the propagating waves in the plane of chip. Benefit from $\lambda/4$ periodicity, our VPC can develop a high-performance topological photonic device with a compact feature size ($< 10 \mu\text{m}$). We have fabricated flat-, Z- and ω -shape topological channels with footprint $9 \times 9.2 \mu\text{m}^2$. The measured results of these three devices show the flat-top high-transmittance spectra with relatively large bandwidth, even for sharp-bend geometry. Such phenomena give evidences for the observation of topologically robust transport at near-infrared wavelength. These works show a prototype of on-chip photonic devices, with promising applications for optical isolation, lasing, wavelength division multiplexing,

directional antennas, single photon sources, and photonic analog of quantum information processing based on topological nanophotonic modes.

References

- [1] H. J. Caulfield, S. Dolev, Why future supercomputing requires optics, *Nature Photonics*, **4**, 261–263 (2010).
- [2] T. Ozawa, H. M. Price, A. Amo, N. Goldman, M. Hafezi, L. Lu, M. Rechtsman, D. Schuster, J. Simon, O. Zilberberg, Topological photonics, *arXiv:1802.04173* (2018).
- [3] J.-W. Dong, X.-D. Chen, H. Zhu, Y. Wang, X. Zhang, Valley photonic crystals for control of spin and topology, *Nature Materials*, **16**, 298–302 (2016).
- [4] T. Ma, G. Shvets, All-Si valley-Hall photonic topological insulator, *New Journal Physics*, **18**, 82–84 (1983).
- [5] X.-D. Chen, F.-L. Zhao, M. Chen, J.-W. Dong, Valley-contrasting physics in all-dielectric photonic crystals: Orbital angular momentum and topological propagation, *Physical Rev. B*, **96**, 020202 (2017).

Second-order autocorrelation function for amplified spontaneous emission

I.V. Doronin^{1,2}, E.S. Andrianov^{1,2}, A.A. Zyablovsky^{1,2}, A.P. Vinogradov^{1,2,3}, A.A. Lisyansky^{4,5}

¹Dukhov Research Institute of Automatics, Russia, 127055, Moscow

²Moscow Institute of Physics and Technology, Russia, 141700, Moscow region

³Institute for Theoretical and Applied Electromagnetics, Russia, 125412, Moscow

⁴Department of Physics, Queens College of the City University of New York, Queens, New York, 11367, USA

⁵The Graduate Center of the City University of New York, New York, 10016, USA

e-mail: ildoron2@gmail.com

Amplified spontaneous emission (ASE) is a phenomenon that is observed in both cavity and cavity-free structures when spontaneously emitted electromagnetic pulse is amplified while propagating through an active medium with positive population inversion. The output intensity of ASE is much greater than the one of usual spontaneous emission (SE), and the transition from SE to ASE is accompanied by the abrupt increase of slope of the output-input curve at a specific pump rate, called pumping threshold, and gradual narrowing of the radiation line [1]. Such a behavior is similar for both ASE and lasing, which makes it difficult to distinguish between these phenomena. Cavity-free structures that exhibit ASE features are even called single-pass lasers. In this work we show that these two phenomena can be distinguished by comparison of second-order autocorrelation function $g^{(2)}(0)$. We consider nanowire waveguide, partially filled with pumped quantum dots, as the system exhibiting ASE. We use Maxwell–Bloch equations with noise terms to describe dynamics of such a system. Relaxation rates and noise correlations are derived from fluctuation-dissipation theorem [2]. We show via numerical simulation that transition from SE to ASE does not affect second-order autocorrelation function of emitted light, i.e. $g^{(2)}(0)$ remains constant for all pumping rates and is greater than 1. On the other hand, it is established fact that above threshold $g^{(2)}(0)$ of laser emission gradually decreases to 1 with the increase of pumping rate. Thus, ASE cannot be considered as lasing.

References

- [1] K. J. Kim, Three-dimensional analysis of coherent amplification and self-amplified spontaneous emission in free-electron lasers, *Physical Review Letters*, **57**(15), 1871 (1986).
- [2] H. Carmichael, *An Open Systems Approach to Quantum Optics*, Springer-Verlag, Berlin, 1991.

High-Q resonances and bound states in the continuum in photonic elements integrated into a slab waveguide

Doskolovich L.L.^{1,2}, Bezus E.A.^{1,2}, Bykov D.A.^{1,2}

¹Image Processing Systems Institute — Branch of the Federal Scientific Research Centre “Crystallography and Photonics” of Russian Academy of Sciences, 151 Molodogvardeyskaya st., Samara 443001, Russian Federation

²Samara National Research University, 34 Moskovskoe shosse, Samara, 443086, Russian Federation
e-mail: leonid@smr.ru

Over the last decades, investigation of resonant properties of nanophotonic structures has attracted considerable research attention. This is not only due to fundamental interest, but also due to the potential applications of resonant structures for spectral and spatial filtering, enhancing light-matter interaction, and analog optical computing, to name a few.

In a wide class of planar (integrated) optoelectronic systems, spectral or spatial filtering is performed in a slab waveguide [1, 2]. In this case, the processed optical signal corresponds to a superposition of guided modes with different propagation directions (spatial filtering) or with different frequencies (spectral filtering). In this regard, the design and investigation of resonant nanophotonic structures integrated in a slab waveguide is of great interest.

In the present work, we consider two simple planar resonant structures consisting of grooves and ridges on the surface of a slab waveguide. The first structure is the planar counterpart of the so-called W-type waveguide and comprises two grooves on the waveguide surface and a ridge separating them [3]. Resonant effects in this structure are associated with the excitation of leaky modes localized at the ridge. The location and width of the resonant transmittance peak (reflectance dip) can be efficiently tuned by changing the widths of the grooves and of the ridge between them, respectively.

The second considered structure consists of a single subwavelength or near-subwavelength ridge located on the surface of the waveguide. The resonances in this structure are associated with the excitation of a cross-polarized eigenmode of the ridge. We propose a simple analytical coupled-wave model, which describes these resonances and predicts the existence of bound states in the continuum in the studied structure. The presented model is found to be in excellent agreement with the rigorous numerical simulation results.

We discuss several practical applications of the proposed structures including spectral and spatial filtering as well as optical differentiation and integration of an optical signal propagating in the waveguide [3, 4].

This work was funded by the Russian Science Foundation grant 14-19-00796.

References

- [1] G. Calafiore, A. Koshelev, S. Dhuey, A. Goltsov, P. Sasorov, S. Babin, V. Yankov, S. Cabrini, C. Peroz, Holographic planar lightwave circuit for on-chip spectroscopy, *Light Sci. Appl.*, **3**, e203 (2014).
- [2] T. W. Mossberg, Planar holographic optical processing devices, *Opt. Lett.*, **26**, 414–416 (2001).
- [3] L. L. Doskolovich, E. A. Bezus, D. A. Bykov, Two-groove narrowband transmission filter integrated into a slab waveguide, *Photon. Res.*, **6**, 61–65 (2018).
- [4] L. L. Doskolovich, E. A. Bezus, N. V. Golovastikov, D. A. Bykov, V. A. Soifer, Planar two-groove optical differentiator in a slab waveguide, *Opt. Express*, **25**, 22328–22340 (2017).

Bloch oscillations and related phenomena in multidimensional nonlinear settings

R. Driben¹, **V.V. Konotop**², **A.V. Yulin**³, **T. Meier**⁴

¹Department of Physics & CeOPP, University of Paderborn, Warburger Str. 100, D-33098 Paderborn, Germany

²Centro de Física Teórica e Computacional and Departamento de Física Faculdade de Ciências, Universidade de Lisboa, Av. Prof. Gama Pinto 2, Lisboa Portugal

³ITMO University, 49 Kronverskii Ave., St. Petersburg 197101, Russian Federation

⁴Department of Physics & CeOPP, University of Paderborn, Warburger Str. 100, D-33098 Paderborn, Germany

e-mail: driben@mail.uni-paderborn.de

Bloch oscillations is one of the most fundamental physical phenomena which is intensively discussed in the literature over the last eight decades, since it was predicted in the seminal works by Bloch and Zener in the theory of electrons in lattice potentials [1, 2]. In the early 1990s Bloch oscillations (BOs) were first observed experimentally in electrically-biased semiconductor superlattices using optical interband excitation with femtosecond laser pulses [3]. A few years later, also for atoms in optical lattices[4] and for coupled waveguides [5] BOs have been realized. By its nature BO is a linear phenomenon and it is common belief that nonlinearity plays a destructive role which makes it impossible to observe BOs at long times (or propagation distances, depending on the particular physical context) even with without dephasing processes. This was first reported in [6] and later on confirmed experimentally in optics using arrays of Kerr-type waveguides [7] and furthermore in Bose–Einstein condensates (BECs) loaded in optical lattices [8], where only a few oscillations were detected.

However, balance between the linear and nonlinear effects can be achieved in systems that contain an additional continuous dimension besides the one corresponding to the direction of the linear gradient. This balance results in very stable oscillatory motion of discrete-continuous hybrid BO-breather nonlinear waves [9, 10]. Such oscillations can be observed even for moderate nonlinearities and large enough values of linear potential, when the band-gap picture of the underlying linear lattice is not applicable anymore. We will demonstrate that there exists an optimal relation between nonlinearity and linear gradient strengths allowing for extremely long lived BOs. Also we will demonstrate a constructive role of nonlinearity in another famous phenomenon related to BOs—the dynamic localization [11] and also discuss the possibility to launch wave packets experiencing BOs with dark solitons and dark-bright light bullets as carriers.

References

- [1] F. Bloch, Über die Quantenmechanik der Elektronen in Kristallgittern, *Z. Phys.*, **52**, 555 (1928).
- [2] C. Zener, A theory of the electrical breakdown of solid dielectrics, *Proc. R. Soc. A*, **145**, 523 (1934).
- [3] J. Feldmann, K. Leo, J. Shah, D.B.A. Miller, J.E. Cunningham, S. Schmitt-Rink, T. Meier, G. von Plessen, A. Schulze, P. Thomas, Optical investigation of Bloch oscillations in a semiconductor superlattice, *Phys. Rev. B*, **46**, 7252 (1992).
- [4] M. B. Dahan, E. Peik, J. Reichel, Y. Castin, C. Salomon, Bloch oscillations of atoms in an optical potential, *Phys. Rev. Lett.*, **76**, 4508 (1996).
- [5] U. Peschel, T. Pertsch, F. Lederer, Optical Bloch oscillations in waveguide arrays, *Opt. Lett.*, **23**, 1701 (1998).
- [6] D. Cai, A. R. Bishop, N. Gronbech-Jensen, M. Salerno, Electric-field-induced nonlinear Bloch oscillations and dynamical localization, *Phys. Rev. Lett.*, **74**, 1186 (1995).
- [7] R. Morandotti, U. Peschel, J. S. Aitchison, H. S. Eisenberg, Y. Silberberg, Experimental observation of linear and nonlinear optical Bloch oscillations, *Phys. Rev. Lett.*, **83**, 4756 (1999).

- [8] O. Morsch, J. H. Muller, M. Cristiani, D. Ciampini, E. Arimondo, Bloch oscillations and mean-field effects of Bose–Einstein condensates in 1D optical lattices, *Phys. Rev. Lett.*, **87**, 140402 (2001).
- [9] R. Driben, V. V. Konotop, T. Meier, A. V. Yulin, Bloch oscillations sustained by nonlinearity, *Scientific Reports*, **7** (2017).
- [10] A. Yulin, R. Driben, T. Meier, Bloch oscillations and resonant radiation of light propagating in arrays of nonlinear fibers with high-order dispersion, *Physical Review A*, **96**, 033827 (2017).
- [11] R. Driben, V. V. Konotop, B. A. Malomed, T. Meier, A. V. Yulin, Nonlinearity-induced localization in a periodically-driven semi-discrete system, *arXiv:1801.04220* (2018).

Disappearance of self-focusing phenomena for few-cycle pulses

Drozdov A.A., Knyazev M.A., Kozlov S.A.

ITMO University, 49 Kronverskiy pr., Saint-Petersburg, Russia, 197101

e-mail: arkadiy.drozdov@gmail.com, knyazev.michael@gmail.com, kozlov@mail.ifmo.ru

Boyd R.W.

The Institute of Optics, University of Rochester, Rochester, NY 14627-0186, USA

e-mail: boydrw@mac.com

Self-focusing is a fundamental self-action effect in which a light beam comes to a focus as a consequence of the lens it induces in the nonlinear optical medium. The concept of a critical power is a key feature of conventional theories of self-focusing; the critical power determines when the self-induced focusing begins to dominate over diffractive spreading of the light beam. A large number of papers and books have been devoted to this nonlinear phenomenon from 1962 (see, for example, review [1] and references therein). In the present work, we demonstrate that, for few-cycle wave packets with longitudinal dimension less the transverse size, the concept of critical power of self-focusing can lose its physical meaning because of the dominance of dispersion over diffraction.

The normalized equation describing the paraxial propagation of a quasi-monochromatic wave through a nonlinear media has well-known form [2]

$$\frac{\partial \tilde{\mathcal{E}}}{\partial \tilde{z}} + \frac{1}{L_w} \frac{\partial \tilde{\mathcal{E}}}{\partial \tilde{t}} + \frac{i}{L_{D1}} \frac{\partial^2 \tilde{\mathcal{E}}}{\partial \tilde{t}^2} - \frac{1}{L_{D2}} \frac{\partial^3 \tilde{\mathcal{E}}}{\partial \tilde{t}^3} - \frac{i}{L_{NL1}} |\tilde{\mathcal{E}}|^2 \tilde{\mathcal{E}} + \frac{1}{L_{NL2}} \frac{\partial}{\partial \tilde{t}} \left(|\tilde{\mathcal{E}}|^2 \tilde{\mathcal{E}} \right) = \frac{i}{L_{\text{diff}}} \tilde{\Delta}_{\perp} \tilde{\mathcal{E}}, \quad (1)$$

where $\tilde{\Delta}_{\perp} = \frac{\partial^2}{\partial \tilde{x}^2} + \frac{\partial^2}{\partial \tilde{y}^2}$, $L_w = V\tau_0$. Nonlinear lengths $L_{NL1} = \frac{1}{\gamma_1 \mathcal{E}_0^2} = \frac{2c}{\omega_0 (n'_2 \mathcal{E}_0^2)} = \frac{c}{\omega_0 (\Delta n_{NL})}$, $L_{NL2} = \frac{\tau_0}{\gamma_2 \mathcal{E}_0^2} = \frac{2c\tau_0}{(n'_2 \mathcal{E}_0^2)} = \frac{c\tau_0}{\Delta n_{NL}}$; dispersion lengths $L_{D1} = \frac{2\tau_0^2}{\beta_2}$, $L_{D2} = \frac{6\tau_0^3}{\beta_3}$ and diffraction length $L_{\text{diff}} = 2k_0 r_0^2$ characterize the influence on the character of light propagation on various physical phenomena: nonlinearity, dispersion, diffraction. Here $k_0 = k(\omega_0)$, $\Delta n_{NL} = (0.5) \cdot n_2 \mathcal{E}_0^2 = n'_2 I$, n_2 and n'_2 are coefficients of nonlinear refractive index and I is the input intensity.

In the case $L_{NL1} = L_{\text{diff}}$, it is natural to introduce an expression for the self-focusing critical power $P_{cr} = (\pi r_0^2) \cdot I$, which is trivially deduced for this case and takes the form:

$$P_{cr} = c^2 \pi / 2 \omega_0^2 n_0 n'_2 = \lambda_0^2 / 8 \pi n_0 n'_2, \quad (2)$$

where $n_0 = n(\omega_0)$. This naively deduced expression for the critical power (2) coincides with the well-known expression [1] to within a constant factor.

We note that for $L_{D1} < L_{\text{diff}}$ nonlinearity will compete not with diffraction but with dispersion. Under these conditions, the concept of P_{cr} will begin to lose its original meaning. This inequality can be expressed in terms of laboratory parameters as

$$l_0 / D_0 < \sqrt{c \omega_0 n(\omega_0) \beta_2}, \quad (3)$$

where $l_0 = c\tau_0$ is longitudinal size of the wave packet and $D_0 = 2r_0$ is its transverse size. For example, for optical radiation with a central wavelength of 800 nm propagating through fused silica we find that this condition becomes $l_0/D_0 < 0.18$.

By means of numerical calculations, we have observed changes in the nature of self-focusing of light pulses when we reduce the dispersion length to a value smaller than the diffraction length.

References

- [1] R. W. Boyd, S. G. Lukishova, Y. Shen, *Self-focusing: Past and Present*, Springer, New York, 2009.
- [2] G. P. Agrawal, *Nonlinear Fiber Optics*, 3rd. ed., Academic Press, Boston, 2001.

Shaping electromagnetic fields with meta atom for ultra-high field MRI

M. Dubois, R. Abdeddaim, S. Enoch

Aix Marseille Univ, CNRS, Centrale Marseille, Institut Fresnel, Marseille, France

e-mail: marc.dubois@fresnel.fr

L. Leroi, Z. Raolison, A. Vignaud

CEA, DRF, JOLIOT, NeuroSpin, UNIRS, Gif-sur-Yvette, France

Since its discovery in the early 70s, MRI scanners have become one of the most efficient diagnostic tools available for physicians. Also, over time, their magnetic field strength (B_0) has been steadily increased to enhance Signal to Noise Ratio (SNR) [1]. This increasing B_0 induces an increasing Larmor or precessional frequency and thus a decreasing corresponding wavelength of the radio-frequency (RF) excitation field. Consequently, the typical human body size becomes non negligible compared with the wavelength and interferences can occur with bright and dark zones. This induces locally major losses in contrast or shadowing on the images depending on the MR acquisition strategy.

One way to address the RF inhomogeneities is the use of relative High-Dielectric Constant (HDC) materials [2]. Their high displacement current alters the global RF distribution in the transmit coil and generates a secondary localized field used to compensate for inhomogeneities. However, HDC pads add a significant bulk in the coil, reduce patient's comfort and can present ecotoxic effect.

In this work, we propose a new passive shimming method based on metamaterial resonator to improve the field inhomogeneity in UHF volume coils. We demonstrate that the RF field distribution of a birdcage coil inside the coil could be improved by inserting metamaterial resonators between the sample and the coil. The metamaterial resonator is based on a set of four hybridized resonant metallic wires (HMA). We use an analytic approach based on impedance matrices in order to characterize the hybridization mechanism. This model is used to describe the interaction between the hybridized metamaterial resonator and a plane wave excitation as well as near field excitation which is more relevant to study its interaction in the case of MRI application.

The designed HMA supports two modes in the frequency domain of interest that are obtained by hybridizing electric dipolar resonant modes of the four dipoles. It has been shown previously that for proper wire length over wavelength ratio, an electric dipole-like mode and a magnetic dipole-like mode are obtained [3]. We will show that interactions of electric and magnetic modes help to gain control over the electromagnetic fields. Moreover, we will show that the behavior of the HMA is controlled by its length and can be used to enhance the RF field locally by 3-fold or as a local RF shield in order to protect over exposed body areas.

This project has received funding from the European Union's Horizon 2020 Research and Innovation program under Grant Agreement No 736937.

References

- [1] R. Pohmann, et al., Signal-to-noise ratio and MR tissue parameters in human brain imaging at 3, 7, and 9.4 Tesla using current receive coil arrays, *Magnetic Resonance in Medicine*, **75**, 801–809 (2016).

- [2] W. M. Teeuwisse, et al., Quantitative assessment of the effects of high-permittivity pads in 7 Tesla MRI of the brain, *Magnetic Resonance in Medicine*, **67**, 1285–1293 (2012).
- [3] C. Jouvaud, et al., Volume coil based on hybridized resonators for magnetic resonance imaging, *Applied Physics Letters*, **108**, 023503 (2016).

Engineering of resonances in modulated structures

Dyakov, S.V., Gippius, N.A.

Skolkovo Institute of Science and Technology, Nobelya, 3, Moscow, Russia 121205

e-mail: n.gippius@skoltech.ru

Optical properties of the periodical structures are investigated during more than a century and their applications are well known. Broad class of these structures are photonic crystal slabs - layered periodical systems, widely used in modern photonics. Important phenomena of photonic crystal slabs is formation of the resonant quasi-guided modes [1]. The rich spectra of reflection, diffraction and transmission of light in these systems are controlled by the strong redistribution of the electromagnetic fields near the resonances. The relative intensities of the resonant diffraction channels can be tuned by the design of the photonic unit cell and the surrounding layered structures [2]. We show that based on the parameters of the resonances (energies, wave-vectors and resonants field distributions) the resonance parameters of combined structures can be obtained with high accuracy. We discuss several examples of the application of this approach for the modelling and optimisation of the passive elements of integrated photonics.

References

- [1] S. G. Tikhodeev, A. L. Yablonskii, E. A. Muljarov, N. A. Gippius, T. Ishihara, *Phys. Rev. B*, **66**, 45102 (2002).
- [2] N. A. Gippius, S. G. Tikhodeev, T. Ishihara, *Phys. Rev. B*, **72**, 45138 (2005).

Frequency comb generation in a exciton-polariton microring resonator

Egorov, O.A.

Technische Physik, Universität Würzburg, Am Hubland, D-97074 Würzburg, Germany

e-mail: oleg.egorov@uni-jena.de

Skryabin, D.V.

Department of Physics, University of Bath, Bath BA2 7AY, UK

Generation of a regular sequence of narrow spectral lines (optical frequency comb) in micro-ring resonators is an active research area aiming to develop micro-comb sources for precision spectroscopy and other applications, see, e.g., [1, 2]. Here we propose to use advantages of exciton-polaritons, which are mixed states between the microcavity photons and quantum-well excitons, and develop scheme for low-threshold optical frequency comb generation in microcavity wires [3]. Advantage of using polaritons is their strong nonlinearity.

For our analysis we assume a ring resonator etched through the upper Bragg mirror of the planar microcavity with embedded quantum well Fig. 1(a). The light is coupled in through a evanescently coupled waveguide serving as an input/output. To compensate the losses we use a coherent pump field with a pump momentum to be above the inflection point of polariton dispersion relation and tune the pump frequency above the polariton line. This fulfils bistability conditions. In order to excite the pulse train we use a seed pulse of the duration of several Rabi oscillations (≈ 2.5 ps), which excites a stable pulse circling around the ring and coupling out every round-trip through the bus waveguide. The pulse shape is well defined with the spatial extend being $6.3 \mu\text{m}$ and temporal

duration $\simeq 1.7$ ps, see Figs. 1(b,c). Fig. 1(d) shows the spectral content of the stable pulse train representing a frequency comb of 9 modes. The comb lines are up shifted with respect to linear resonances indicated in grey, as it is expected due to repulsive inter-polariton interaction. The comb FSR is 0.3 THz, which also matches the pulse repetition rate.

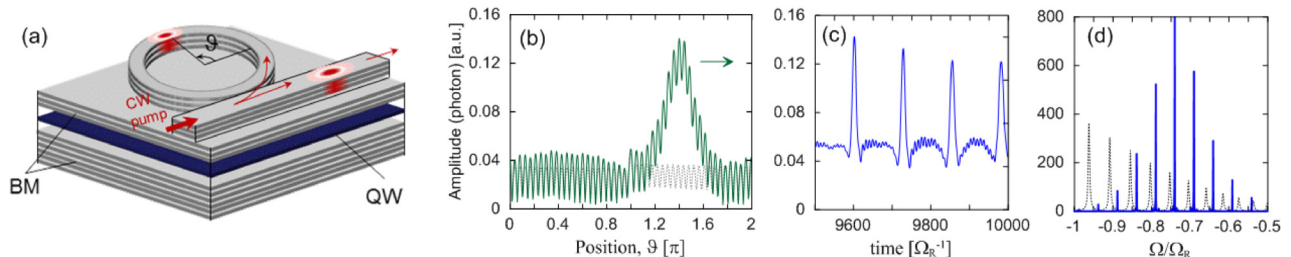


Fig. 1: (a) Sketch of polariton microring resonator with typical radius 10–20 μm . (b) A snapshot of the soliton profile in the ring resonator under a CW pump. (c) Temporal dynamics on the output of the resonator. (d) Fourier transformation of temporal dynamics on the output of resonator showing the frequency-comb with equally-spaced spectral lines. Rabi frequency is $\hbar\Omega_R \simeq 4$ meV.

In conclusion we demonstrated visibility of using microcavity polaritons for the purposes of generation of GHz to THz combs and trains of pulses duration of 1–2 ps that can be used in future all-polariton information processing schemes.

References

- [1] T. J. Kippenberg, R. Holzwarth, S. A. Diddams, Microresonator-based optical frequency combs, *Science*, **332**, 555 (2011).
- [2] T. Herr, *et al.*, Temporal solitons in optical microresonators, *Nature Photon.*, **8**, 145 (2014).
- [3] E. Wertz, *et al.*, Propagation and Amplification Dynamics of 1D Polariton Condensates, *Phys. Rev. Lett.*, **109**, 216404 (2012).

3D-topological — vortex, knotted, and tangled — dissipative optical solitons

S.V. Fedorov¹, N.N. Rozanov^{1,2,3}, N.A. Veretenov^{1,2}

¹ITMO University, Kronverkskiy prospect 49, Saint-Petersburg 197101, Russia

²Vavilov State Optical Institute, Kadetskaya liniya V. O., 14/2, Saint-Petersburg 199053, Russia

³Ioffe Physical-Technical Institute, Politekhnicheskaya str. 26, Saint-Petersburg 194021, Russia

e-mail: nnrosanov@mail.ru

Multidimensional topological solitons, including knotted ones pioneered by L. D. Faddeev [1], become now an object of deep interest in nonlinear science. Important is the feature of conservation of topological characteristics even for not small perturbations. Since the beginning and up to now, these investigations deal with conservative solitons. Exploiting the feature of increased stability of dissipative solitons with the balance of energy input and output, one gets topological dissipative optical solitons with increased stability. In the talk, we present a new wide class of three-dimensional (3D) dissipative optical solitons including those predicted in [2, 3].

The scheme is a homogeneous medium with fast saturation of laser gain and losses. The quasi-optical governing equation for the slowly varying electric field envelope takes into account for diffraction, non-resonance and resonance frequency dispersion, saturable gain and absorption, and weak medium dichroism. As the initial condition at the medium input, we use result of rotation around some axis of the field of 2D-laser soliton or solitons' complex; additionally, we twist the 2D-structure and introduce vorticity along the rotation angle with some topological index (charge).

Important feature of 3D-topological solitons found is existing of vortex lines where the field vanishes and phase changes by 2π along the contour around the line. The solitons are characterized by their “skeletons” — the array of closed and unclosed vortex lines; such skeletons are termed in topology as tangles. More detail characterization of these solitons is provided by the distribution of lines of energy flow, or Poynting vector. We present a number of stable solitons with complicated “skeletons” consisting of some number of vortex lines of the two types. These lines have unit topological charge; its sign gives the line direction. Examples of skeletons include 1, 2, and 3 unclosed vortex lines forming “the spine”, or skeleton axis, and 0, 1, and 2 closed vortex lines engirdling the axis. A topologically simple asymmetric “precession” has only one unclosed vortex line, whereas “apple solitons” are axially symmetric ones with one unclosed and one closed (a circle) vortex lines. Topologically equivalent, but axially asymmetric solitons with deformed closed and/or unclosed vortex lines are also stable. A soliton with 3 unclosed vortex lines and 2 closed unlinked vortex lines passing with increase of propagation distance periodically one through the other, is also presented, as well as a soliton with 3 unclosed vortex lines and one unknot closed vortex line, a soliton with 3 unclosed vortex lines and knotted (trefoil) closed vortex line, a soliton with two unclosed vortex lines and a Solomon’s knot — two linked closed vortex lines.

All the solitons found coexist with the non-lasing mode (zero field), and they are stable inside overlapping domains in the parameters’ space; correspondingly, a slow variation of the parameters results in various bifurcations accompanied by vortex lines’ reconnections, and in hysteretic phenomena. Orientation of the skeleton axis is arbitrary in the special case and generally has some preferable orientation determined by the relations of the dissipative factors.

The variety of stable topological dissipative solitons presented provides a rich alphabet for optical information coding.

References

- [1] L. D. Faddeev, *Quantization of Solitons*, Princeton preprint IAS-75-QS70, Institute for Advanced Study, Princeton, 1975.
- [2] N. A. Veretenov, N. N. Rosanov, S. V. Fedorov, Rotating and precessing dissipative-optical-topological-3D solitons, *Phys. Rev. Lett.*, **117**, 183901 (2016).
- [3] N. A. Veretenov, S. V. Fedorov, N. N. Rosanov, Topological vortex and knotted dissipative optical 3D-solitons generated by 2D-vortex solitons, *Phys. Rev. Lett.*, **119**, 63901 (2017).

Picosecond photo-elastic effect in a VO₂ thin film in insulating and metallic phases

Fedyanin A.E.^{1,2}, Mogunov Ia.A.², Scherbakov A.V.², Lysenko S.³, Akimov A.V.⁴, Kalashnikova A.M.²

¹ITMO University, 197101 St. Petersburg, Russia

²Ioffe Institute, 194021 St. Petersburg, Russia

³Department of Physics, University of Puerto Rico, Mayaguez, Puerto Rico 00681, USA

⁴School of Physics and Astronomy, Nottingham University, Nottingham, UK

e-mail: fedyanin.a.e@mail.ru

Coherent acoustic phonons provide a powerful tool to access and control the properties of the media [1]. However, little is known about effect picosecond strain pulses may have on materials demonstrating insulator-to-metal phase transitions (IMT). Understanding the response of such media to picosecond strain pulses would open an intriguing yet unexplored opportunity to realize ultrafast strain-mediated control of electronic and optical properties of media. In the present work we, therefore, aim at revealing response of a model IMT material VO₂ to picosecond strain pulses.

VO₂ undergoes insulator-to-metal and structural phase transition at $T = 340$ K. At this temperature, the 0.6 eV band gap collapses, which is followed by abrupt change of electrical conductivity and optical properties [2]. Here we report on the experimental and theoretical studies of the picosecond

photo-elastic effect at in thin films of VO₂ in insulating (at room temperature) and metallic (at T > 340 K) phases. In experiments we study the dynamics of the reflectivity of VO₂ under the action of picosecond strain pulses.

The sample was a 145 nm thick VO₂ film epitaxially grown on c-cut of the Al₂O₃ substrates. In order to create strain pulses and inject them into the VO₂ film we used the method developed in picoseconds acoustics. 140 nm thick Al film was sputtered at the back side of the substrate. Upon its excitation by a femtosecond laser pulse, strain pulse with amplitude of $\sim 10^{-4}$ and duration of ~ 10 ps is generated and is injected into Al₂O₃ substrate. Using the pump-probe techniques, we monitor transient changes of the reflectivity of the VO₂ when the strain pulse reaches it.

We have obtained the strain-pulse induced evolution of the VO₂ film reflectivity in both insulating and metallic phases. To model the propagation of the acoustic pulses in the VO₂/Al₂O₃ structure, we used a finite difference method to solve the Korteweg–de Vries equation, and calculated the corresponding photo-elastic response. As a result we were able to obtain estimates of the sound velocity and photo-elastic constants of VO₂ in both phases. To the best of our knowledge, these parameters are obtained experimentally for VO₂ epitaxial films for the first time.

Furthermore, we have studied the strain-induced transient reflectivity when the metallic phase was induced by femtosecond laser pulse [3]. This enabled us to obtain the acoustical and photo-elastic parameters of the metastable laser-induced metallic phase of VO₂ and to compare them with those in the thermodynamically stable metallic phase.

References

- [1] O. Matsuda, M. C. Larciprete, R. L. Voti, O. B. Wright, *Ultrasonics*, **56**, 3 (2015).
- [2] M. Imada, A. Fujimori, Y. Tokura, *Rev. Mod. Phys.*, **70**, 1039 (1998).
- [3] D. Wegkamp, J. Stähler, *Prog. Surf. Sci.*, **90**, 464–502 (2015).

Metamaterial-based super-scatterers

Dmitry Filonov^{1,2}, **Pavel Ginzburg**^{1,2}

¹School of Electrical Engineering, Tel Aviv University, Tel Aviv, 69978, Israel

²ITMO University, Saint Petersburg, 197101, Russia

e-mail: dimfilonov@gmail.com

The interaction between electromagnetic waves and objects is strongly affected by the shape and material composition of the latter. Artificially created materials, formed by a subwavelength structuring of their unit cells, namely metamaterials, can exhibit peculiar responses to electromagnetic radiation and provide additional powerful degrees of freedom to the scatterer design. In particular, negative material susceptibilities give rise to strong resonant interactions with deeply subwavelength particles. In this contribution, we discuss the concept of artificial magnon and plasmon resonances in subwavelength objects with effective negative permeability and/or permittivity, designed based on the metamaterial approach. Strong localized oscillations of the magnetic and electric fields within an array of resonators, forming a sphere, hybridize in a collective mode of the structure. As a result, extremely high scattering cross sections, exceeding that of a steel sphere with the same radius by four orders of magnitude, were demonstrated experimentally. Super scatterers, based on tunable resonances within artificially created materials, can find use in a broad range of electromagnetic applications, including wireless communications, radars, RFID, internet of things hardware and many others.

Polarization effects in second-harmonic generation from inorganic BaTiO₃ perovskite resonant nanoparticles

Frizyuk K.S.^{1,2}, Zograf G.P.¹, Tarasov M.G.¹, Makarov S.V.¹, Grange R.³, Petrov M.I.^{1,2}

¹ITMO University, St. Petersburg, Russia

²St. Petersburg Academic University, Russia

³ETH Zürich, Switzerland

e-mail: g.zograf@metalab.ifmo.ru, m.petrov@metalab.ifmo.ru

Second-harmonic generation (SHG) from nanoscale structures is highly important for applications in optical communication, biosensing, bioimaging and control of laser beams. As the nonlinear effects are normally weak and depend strongly on volume, methods to enhance the conversion efficiency are highly desirable. For instance, silicon polycrystalline resonant nanoantennas are proposed to enhance the nonlinear response [1]. However, bulk second order susceptibility in centro-symmetric materials, such as silicon, is zero, which limits the efficiency of the SHG. Therefore, nanoantennas based on dielectric high-refractive index materials with high intrinsic nonlinear properties are of particular interest in nonlinear nanophotonics. Inorganic resonant perovskite BaTiO₃ nanoparticles already have been studied in terms of SHG efficiency and demonstrated outstanding performance [2].

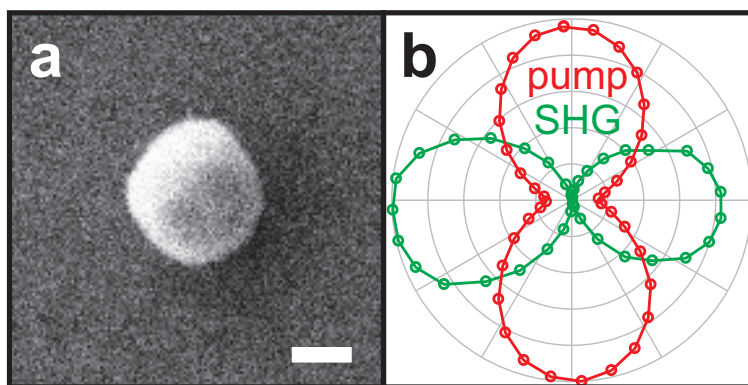


Fig. 1: a) SEM image of BaTiO₃ nanoparticle. Scale bar is 200 nm. b) Sketch for angular dependence of second-harmonic generation intensity from single BaTiO₃ nanoparticle with given femtosecond 1050 nm pump. Intensities are in arbitrary units.

But still effects related to polarization of SHG from BaTiO₃ nanoparticles were not described. In this work we reveal both peculiarities regarding different pump polarization and polarization of the SHG signal for a given pump with experimental and theoretical approaches. Fig. 1(a) shows SEM image of BaTiO₃ nanoparticle, which was studied and Fig. 1(b) discloses results on dependence of SHG signal from laser pump. Polarization effects in SHG are of great interest due to the necessity of advanced light manipulation for modern applications including biosensing, nanosources of light and many others.

References

- [1] S. V. Makarov, *et al.*, Efficient second-harmonic generation in nanocrystalline silicon nanoparticles, *Nano Letters*, **17**(5), 3047–3053 (2017).
- [2] F. Timpu, Enhanced second-harmonic generation from sequential capillarity-assisted particle assembly of hybrid nanodimers, *Nano Letters*, **17**(9), 5381–5388 (2017).

Silicon nanoantennas in perovskite photovoltaics

Furasova A.D.¹, Zakhidov A.A.^{1,2}, Di Carlo A.³, Makarov S.V.¹

¹ITMO University, St. Petersburg 197101, Russia

²University of Texas at Dallas, Richardson, Texas 75080, United States

³Tor Vergata University, Rome, Italy

e-mail: aleksandra.furasova@metalab.ifmo.ru

Nowadays halide perovskite based solar cells (SC) is an extremely prospective class of energy sources due to high power conversion efficiency, low cost of materials and simple solution processing for their fabrication [1]. A lot of attempts have been made to improve perovskite devices by plasmonic nanoparticles made of noble metals to increase their photocurrent and efficiency via increase of nonradiative decay of excitons improving charge separation. However, this approach allowed to achieve efficiency up to 18.2% and fill factor up to 75.5% for record device based on the most popular and well-studied methyl ammonium lead iodide perovskite (MAPbI₃). Moreover, noble metals are expensive and chemically unstable in halide perovskites.

Resonant silicon nanoparticles were recently proposed for a number of applications [2, 3], where its optical losses as compared with plasmonic counterparts and strong Mie resonances were employed for local field enhancement and effective scattering power pattern manipulation. Regarding implementation of silicon nanoparticles for perovskites based devices, high enough optical contrast of silicon ($n = 3.5$) with halide perovskite ($n = 2.2$) would enable the excitation of Mie resonances in visible range resulting in effective light trapping at nanoscale.

Here we present experimentally, for the first time to the best of our knowledge, that the resonant silicon nanoparticles can be introduced to perovskite based SCs. We choose well-studied material (MAPbI₃) to avoid any influence of material's composition to provide the most rigorous comparison of silicon nanoparticles with previously reported plasmonics based approaches. We have achieved the perovskite SC enhancement of efficiency up to 18.8% at the fill factor 79% by incorporation of Mie resonance silicon nanoparticles into devices that now is a record number among previous results with any type of resonant nanoparticles in a MAPbI₃ based perovskite SC. Moreover, we observed even improving photovoltaic characteristics of SCs after incorporation of the silicon nanoparticles. We provide additional theoretical analysis showing that silicon nanoparticles improve the power conversion efficiency by near-field enhancement in the active medium.

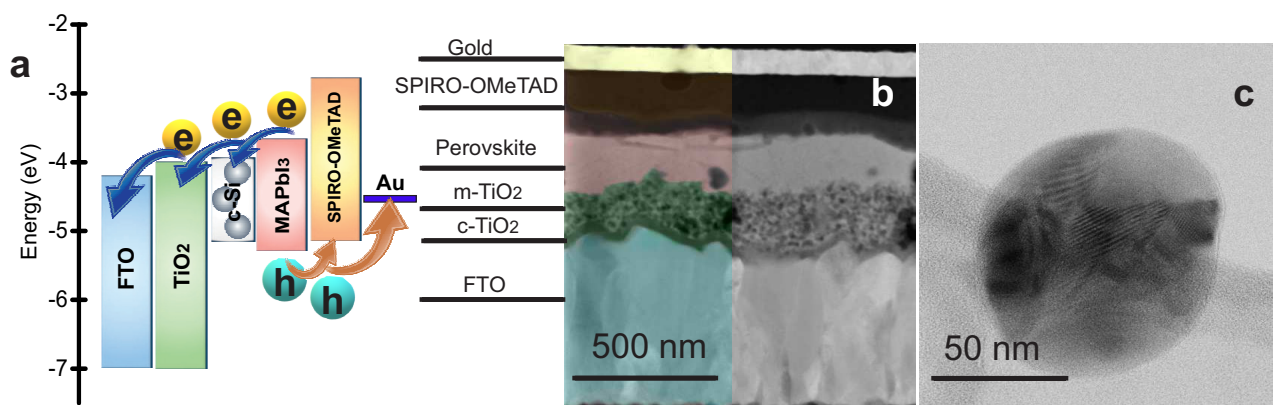


Fig. 1: a) Energy band diagram of the device. b) Color-enhanced and annotated cross-sectional STEM-BF image of a complete solar cell. Dark spot showing Si-NP at the interface with m-TiO₂. c) TEM of a polycrystalline Si nanoparticle fabricated by laser ablation in liquid.

References

- [1] M. M. Lee, et al., *Science*, **345**, (2014).
- [2] A. Kuznetsov, et al., *Science*, **354**, (2016).
- [3] I. Staude, et al., *Nat. Photonics*, **11**, (2017).

Optical vortices and polarization Möbius strips on all-dielectric optical antennas

Aitzol García-Etxarri

Donostia International Physics Center (DIPC), Paseo Manuel de Lardizabal 4, Donostia-San Sebastian 20018, Spain

e-mail: aitzolgarcia@dipc.org

The study of the optical response of high refractive index nano-particles has revealed that these resonant structures are capable of controlling different degrees of freedom of light fields with unprecedented versatility [1]. The ability of these particles to control the intensity, phase and polarization of light has unveiled a plethora of new physical effects and applications. To mention a few, these particles have allowed controlling the directionality of optical antennas in an unprecedented manner [2], they have shown promise in enhancing molecular circular dichroism spectroscopy [3] and all-optical chiral separation methods based on enantioselective photo-excitation of chiral molecules [4].

In this letter, we unveil a new phenomenon that to the best of our knowledge was not reported up to date; the natural emergence of an optical vortex in the back scattering of cylindrically symmetric high index resonators when illuminated at their first Kerker condition of anomalous scattering. Firstly, based on singular optics arguments [5], we deduce the emergence of the vortex for a high index nano-particle illuminated by circularly polarized light at the first Kerker condition. Secondly, using the recently developed helicity and angular momentum conservation framework, we prove that the modulus of the topological charge of the vortex has to be equal to 2. Lastly, we verify our predictions through analytic and numerical calculations.

Moreover, we analyze the emergence of polarization singularities (C lines and L surfaces) in the scattering of optical resonators excited by linearly polarized light. We demonstrate both analytically and numerically that high refractive index spherical resonators present such topologically protected features and calculating the polarization structure of light around the generated C lines, we unveil a Möbius strip structure in the main axis of the polarization ellipse when calculated on a closed path around the generated lines of circular polarization.

References

- [1] A. García-Etxarri, et al., Strong magnetic response of submicron silicon particles in the infrared, *Optics Express*, **19**, 4815–4826 (2011).
- [2] J.-M. Geffrin, et al., Magnetic and electric coherence in forward-and back-scattered electromagnetic waves by a single dielectric subwavelength sphere, *Nature Communications*, **3**, 1171 (2012).
- [3] A. García-Etxarri, J. Dionne, Surface-enhanced circular dichroism spectroscopy mediated by nonchiral nanoantennas, *Physical Review B*, **87**, 235409 (2013).
- [4] C. Ho, A. García-Etxarri, Y. Zhao, J. Dionne, Enhancing enantioselective absorption using dielectric nanospheres *ACS Photonics*, **4**(2), 197–203 (2017).
- [5] A. García-Etxarri, Optical polarization Möbius strips on all-dielectric optical scatterers, *ACS Photonics*, **4**(5), 1159–1164 (2017).

Switchable light emitting perovskite solar cells

Gets D.S.¹, Ishteev A.R.¹, Liashenko T.G.¹, Saranin D.S.², Makarov S.V.¹, Zakhidov A.A.^{1,3}

¹Department of Nanophotonics and Metamaterials, ITMO University, Russia

²National University of Science and Technology, NUST “MISIS”, Russia

³The University of Texas at Dallas, USA

e-mail: dmitry.gets@metalab.ifmo.ru

Solar cell (SC) and light emitting diode (LED) share similar designs, but both devices designed to perform the primary function and their reciprocal function is greatly suppressed. Therefore, the

realization of SC and LED in a monolithic device is very complicated. However, several attempts were made previously. Organic-inorganic metal halide perovskites are recently emerged materials capable of producing high efficient SC and LED. Now, perovskite SCs and LEDs efficiencies are comparable with well-established semiconductor SCs and LEDs [1]. Nevertheless, devices capable of working as a LED and as a SC with relatively high efficiencies do not exist yet. There were attempts to make such device capable of exhibiting SC and LED functions based on silicon SC. It demonstrated 2.1% SC efficiency, but it emitted light in the IR region [2]. Also some attempts were made to realize such device with organic-inorganic metal halide perovskite. For this purpose the authors of work [3] used bromine perovskite (MAPbBr_3) and achieved $\sim 1\%$ SC efficiency and $\sim 0.12\%$ LED efficiency. Low SC performance was attributed to the high band gap energy of MAPbBr_3 (~ 2.3 eV). On the other, hand SCs based on MAPbI_3 demonstrate superior efficiencies, but they emit light in the IR (~ 1.5 eV). Therefore, the practical interest is the realization of the optoelectronic device based on mixed halide perovskites with intermediate composition of Br and I ($\text{MAPbBr}_x\text{I}_{3-x}$ ($0 < x < 3$)), and, thus, to achieve relatively high SC efficiencies and, at the same time, emission in the visible wavelength range with relatively high quantum yield.

But mixed halide perovskites demonstrate one unwanted and crucial effect that affects performance of perovskite based optoelectronic devices. This effect is segregation [3]. The segregation occurs under visible light soaking and high charge carriers injection [4] and results in the reversible movement of halide ions and their vacancies due to generation of photoexcited charge carriers density gradient [5, 6]. As a result, the regions enriched with photoexcited ions that can be easily seen in photoluminescence (PL) and electroluminescence (EL). In $\text{MAPbBr}_x\text{I}_{3-x}$ ($0 < x < 3$), perovskite segregation is manifested in the formation of Br- and I-rich phases due to the movement of Br-, I-ions and their vacancies under white light illumination. The formation of these regions negatively affects performance of SCs and LEDs regardless its temporal character. After removal of external light soaking, perovskite attains its previous characteristics.

Here we propose that the mixed halide perovskite optoelectronic device is able to demonstrate high-efficient dual functionality and thus to work in LED and SC regimes. In this case, segregation, which usually negatively affects device performance, aids to dual functionality. Cycling working regimes by handling the segregation process is a key point in the development of the efficient dual functional devices.

References

- [1] M. A. Green, et al., *Nature Photonics*, **8**, 506–514 (2014).
- [2] D. M. Zhigunov, et al., *Technical Physics Letters*, **43**, 496–498 (2017).
- [3] H.-B. Kim, et al., *Energy & Environmental Science*, **10**, 1950–1957 (2017).
- [4] E. T. Hoke, et al., *Chemical Science*, **6**, 613–617 (2015).
- [5] I. L. Braly, et al., *ACS Energy Letters*, **2**, 1841–1847 (2017).
- [6] S. J. Yoon, et al., *ACS Energy Letters*, **1**, 290–296 (2016).

Visible guided-mode resonances of FIB-nanopatterned mono-c-Si chiral metasurface

Gorkunov M.V., Kondratov A.V., Rogov O.Y., Artemov V.V., Gainutdinov R.V.

Shubnikov Institute of Crystallography, FSRC “Crystallography and Photonics”, Russian Academy of Sciences, 119333 Moscow, Russia

e-mail: gorkunov@crys.ras.ru

Ezhov A.A.

Faculty of Physics, Lomonosov Moscow State University, 119991 Moscow, Russia

High refractive index makes silicon the optimal platform for dielectric metasurfaces capable of versatile control of light. Focused ion beam (FIB) followed by annealing with oxidation allows to

create silicon nanostructures of truly 3D shapes transparent in the visible range [1]. We pattern a chiral metasurface in a 300 nm monocrystalline silicon (mono-c-Si) layer on sapphire (see Fig. 1a), and anneal it at 1100°C to transform the damaged Si layer into a glass coating. By means of the FIB assisted 3D-reconstruction (see Fig. 1b) we resolve the shape of the air/SiO₂/mono-c-Si/Al₂O₃ interfaces and create the average unit cell 3D-model shown in Fig. 1c. The optical measurements demonstrate that the metasurface combines high (50–80%) transmittance with the circular dichroism of up to 0.5 and the optical activity of up to 20° in the visible range (see Figs. 1, d–f) [2]. FDTD simulations performed for the reconstructed 3D-model reproduce the observed sharp spectral features which we attribute to the guided-mode resonances occurring when the incident plane wave diffracts into the modes guided by the thin mono-c-Si layer. In terms of the semi-phenomenological chiral coupled mode model we explain the observed strong optical chirality as a result of a chiral difference in the coupling of the resonances with the incoming and outgoing plane circularly polarized waves.

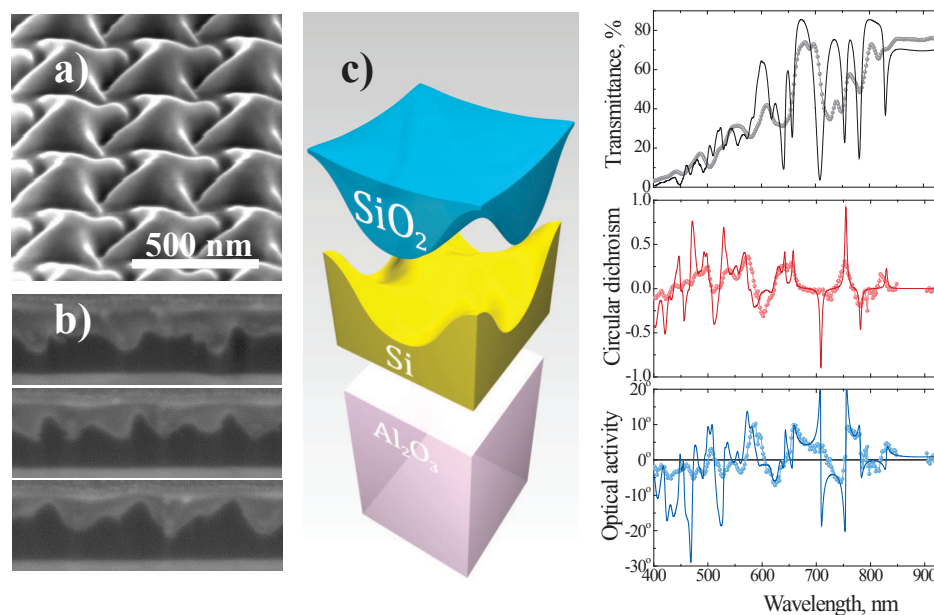


Fig. 1: Chiral mono-c-Si metasurface: patterning produced by digitally controlled FIB (a); exemplary consecutive cross section cuts used for the 3D-reconstruction after annealing (b); 3D model of the reconstructed unit cell (c); measured (dots) and simulated (solid) spectra of the transmittance (d), circular dichroism (e) and optical activity (f).

References

- [1] O. Y. Rogov, V. V. Artemov, M. V. Gorkunov, A. A. Ezhov, D. N. Khmelenin, *J. Microsc.*, **268**, 254–258 (2017).
- [2] M. V. Gorkunov, O. Y. Rogov, A. V. Kondratov, V. V. Artemov, R. V. Gainutdinov, A. A. Ezhov, *Adv. Opt. Mat.*, in press (2018).

Valley Zak topological states in all-dielectric structures

Gorlach A.A.¹, Zhirihin D.V.², Slobozhanyuk A.P.^{2,3}, Gorlach M.A.², Khanikaev A.B.^{2,4,5}

¹Belarusian State University, Minsk 220030, Belarus

²ITMO University, Saint Petersburg 197101, Russia

³Nonlinear Physics Centre, Australian National University, Canberra ACT 2601, Australia

⁴The City College of the City University of New York, New York 10031, USA

⁵Graduate Center of the City University of New York, New York, 10016, USA

e-mail: alexey.gorlach@gmail.com

Photonic topological insulators offer unprecedented opportunities in photonics, making possible low-loss disorder-robust manipulation by light flows at the nanoscale. All-dielectric design provides

especially attractive platform for topological photonics featuring low losses and a great potential for further minituarization. Recently, all-dielectric photonic topological insulators have been realized experimentally in three [1] and two [2] dimensions following the theoretical proposal [3].

In this work, we investigate theoretically and experimentally a 1D array of dielectric disks depicted in Fig. 1(a). The domain wall is realized by turning over half of the disks in the array, so that the bianisotropy parameter μ has different signs for the two halves of the array. We demonstrate that for nonzero bianisotropy the bulk spectrum of the system has a bandgap, and there are four interface states localized inside it. The interface states are grouped into two pseudospin-degenerate doublets [Fig. 1(d)] and characterized by the distributions of electric and magnetic dipole moments depicted schematically in Fig. 1(b,c). As we prove, the system is characterized by the nonzero valley Zak phase which is a direct analogue of valley Chern number in two-dimensional systems. Additionally, we verify the disorder-robust nature of the interface states by numerical calculation.

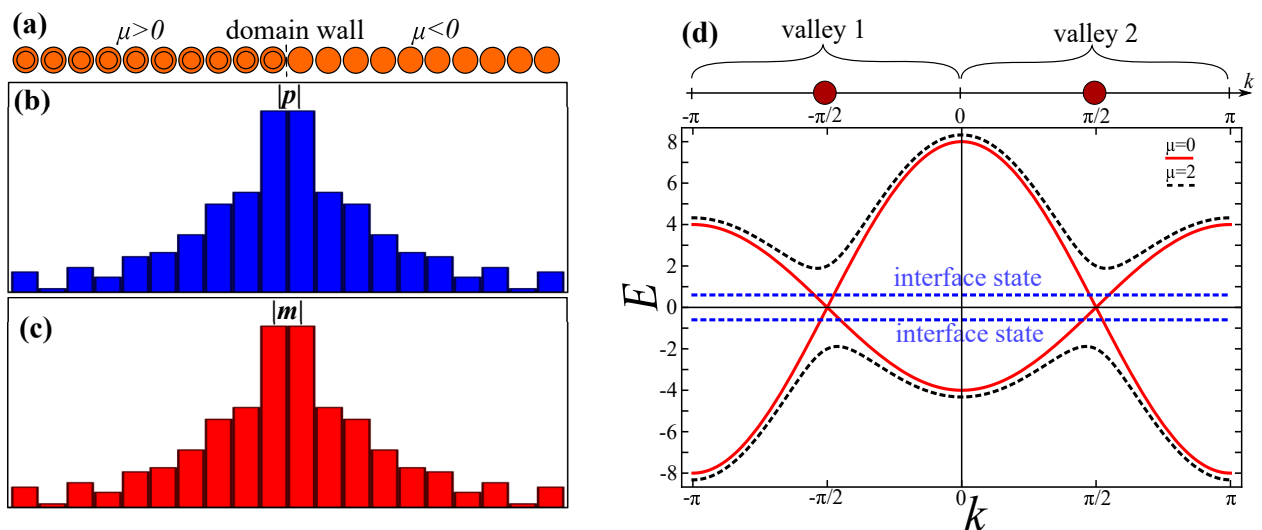


Fig. 1: (a) Array of dielectric disks with broken mirror symmetry. (b,c) Distribution of (b) electric and (c) magnetic dipole moments in the array for interface states. (d) Bulk energy spectrum of the system with and without bianisotropy (black and red lines, respectively). Blue dashed lines indicate the energy of the interface states.

References

- [1] A. Slobozhanyuk, S. H. Mousavi, X. Ni, D. Smirnova, Y. S. Kivshar, A. B. Khanikaev, Three-dimensional all-dielectric photonic topological insulator, *Nature Photonics*, **11**, 130–136 (2017).
- [2] A. Slobozhanyuk, A. V. Shchelokova, X. Ni, S. H. Mousavi, D. A. Smirnova, P. A. Belov, A. Alú, Y. S. Kivshar, A. B. Khanikaev, Near-field imaging of spin-locked edge states in all-dielectric topological metasurfaces, *arXiv*: 1705.07841 (2017).
- [3] A. B. Khanikaev, S. H. Mousavi, W.-K. Tse, M. Kargarian, A. H. MacDonald, G. Shvets, Photonic topological insulators, *Nature Materials*, **12**, 233–239 (2013).

Topological transition due to spontaneous symmetry breaking

Gorlach M.A.¹, **Savelev R.S.**¹, **Poddubny A.N.**^{1,2}

¹ITMO University, Saint Petersburg, 197101, Russia

²Ioffe Physical-Technical Institute, Saint Petersburg, 194021, Russia

e-mail: m.gorlach@metalab.ifmo.ru

Spontaneous symmetry breaking is one of the cornerstone concepts in various fields of science ranging from high-energy physics to nonlinear optics. In condensed matter systems, spontaneous symmetry breaking accompanies second-order phase transitions, for instance, the transition from paramagnetic to the ferromagnetic state [1].

The fundamental question is whether spontaneous symmetry breaking can cause the *topological transition* from trivial to the nontrivial phase with the gapped spectrum of excitations. In this work, we investigate the spontaneous formation of interface excitations in the linearized spectrum of the array consisting of anharmonic oscillators with anharmonic couplings between them. We demonstrate that an initially disordered system can form metastable topologically distinct domains with the interface states at the boundaries. Employing the technique based on the calculation of mean chiral displacement [2] we prove that the in-gap interface state is topological and has a clear analogy with that in the Su–Schrieffer–Heeger model [3].

Our findings thus uncover a fundamental link between the spontaneous symmetry breaking and topological interface states. We believe that the results demonstrated here on a toy model of mechanical system are much more general being applicable to a variety of nonlinear microwave, photonic and polaritonic systems.

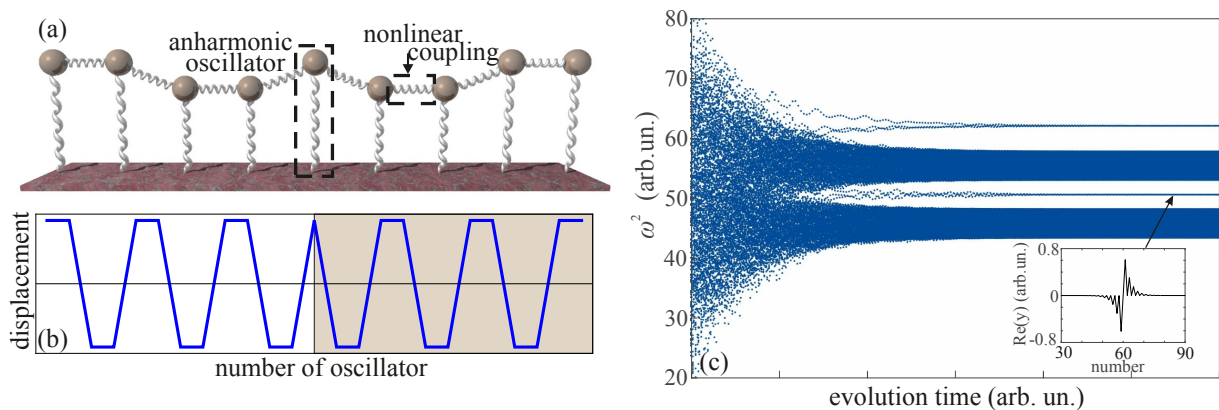


Fig. 1: Illustration of the emergence of the topological interface states in the array of anharmonic oscillators. (a) Schematics of the array. (b) Stationary oscillators displacements after the sufficiently long evolution time. (c) The spectrum of linearized excitations versus the evolution time.

References

- [1] L. D. Landau, E. M. Lifshitz, *Statistical Physics, Part I*, Butterworth-Heinemann, Heidelberg, 1980.
- [2] F. Cardano, A. D’Errico, A. Dauphin, M. Maffei, B. Piccirillo, C. De Lisio, G. De Filippis, V. Cataudella, E. Santamato, L. Marrucci, M. Lewenstein, P. Massignan, *Nature Communications*, **8**, 15516 (2017).
- [3] A. Blanco-Redondo, I. Andonegui, M. J. Collins, G. Harari, Y. Lumer, M. J. Rechtsman, B. J. Eggleton, M. Segev, *Physical Review Letters*, **116**, 163901 (2016).

Quantum directions in topological photonics

Mohammad Hafezi

Joint Quantum Institute, University of Maryland, College Park, MD 20742, USA

e-mail: hafezi@umd.edu

The application of topology in optics has led to a new paradigm in developing photonic devices with robust properties against disorder. Although significant progress on topological phenomena has been achieved in the classical domain, the quantum regime has remains unexplored. In this talk, I discuss in recent developments in the quantum regime:

- (1) We demonstrate a strong interface between single quantum emitters and topological photonic states. Our approach creates robust counter-propagating edge states at the boundary of two distinct topological photonic crystals. We demonstrate the chiral emission of a quantum emitter into these modes and establish their robustness against sharp bends. This approach may enable the development

of quantum optics devices with built-in protection, with potential applications in quantum simulation and sensing.

(2) Spontaneous parametric processes such as down-conversion (SPDC) and four-wave mixing (SFWM) have long been the common sources of quantum light, for instance, correlated photon pairs and heralded single photon. These spontaneous processes are mediated by vacuum fluctuations of the electromagnetic field. Therefore, by manipulating the electromagnetic mode structure, for example, using nanophotonic systems, one can engineer the spectrum of generated photons. However, such manipulations are susceptible to fabrication disorders which are ubiquitously present in nanophotonic systems.

We demonstrate a topological source of correlated photon pairs where the spectrum of generated photons is robust against fabrication disorder. Specifically, we use the topological edge states to achieve an enhanced and robust generation of photons using SFWM and show that they outperform their topologically-trivial counterparts. We show the non-classical nature of intensity correlations between generated photons and the anti-bunching of photons using conditional measurements. Our results could pave the way for topologically robust quantum photonic devices.

References

- [1] S. Barik, A. Karasahin, C. Flower, T. Cai, H. Miyake, W. DeGottardi, M. Hafezi, E. Waks, A topological quantum optics interface, *Science*, **359**, 666–668 (2018).
- [2] S. Barik, H. Miyake, W. DeGottardi, E. Waks, M. Hafezi, Two-dimensionally confined topological edge states in photonic crystals, *New Journal of Physics*, **18**(11), 113013 (2016).
- [3] S. Mittal, M. Hafezi, Topologically robust generation of correlated photon pairs, *arXiv:1709.09984* (2017).

Precise localization of multiple non-cooperative objects in a disordered cavity by wavefront shaping

P. del Hougne^{1,2}, M.F. Imani², M. Fink¹, D.R. Smith², G. Lerosey³

¹Institut Langevin, CNRS UMR 7587, ESPCI Paris, PSL Research University, 1 rue Jussieu, 75005 Paris, France

²Center for Metamaterials and Integrated Plasmonics, Duke University, Department of Electrical and Computer Engineering, Durham, North Carolina 27708, USA

³Greenerwave, PC'Up, 1 rue Jussieu, 75005 Paris, France

e-mail: philipp.delhougne@gmail.com

Wave propagation in a disordered cavity is known to yield a completely scrambled, speckle-like wave field. Typical indoor environments constitute (low quality factor) disordered cavities for microwaves due to the presence of many reflecting and scattering objects. Therefore, probing an indoor scene to localize objects with waves in combination with traditional ray-tracing tools is (almost) unfeasible. Nonetheless, it is well known that information about the object position is encoded in the Green's function. This enabled uniquely identifying the location of a source in a disordered cavity after a dictionary of the Green's functions for different source locations had been established [1]. The process of correlating the measured Green's function with the dictionary entries may be interpreted as a simulated Time Reversal experiment.

Here, we start off by tackling the case of passive (i.e. non-emitting) objects inside a cavity. Indeed, the scattering contribution of such passive objects to the Green's function between two arbitrary points in the cavity also uniquely encodes the object position. Borrowing the assumptions of DRAWS (Diffusive Reverberant Acoustic Wave Spectroscopy [2]), we can decompose the spectrum of the transmission between two arbitrary antennas into the static cavity contribution and the contribution from each object. We demonstrate in the microwave domain that the object contributions are unique. The ability to unravel this interplay permits us to localize multiple passive objects in a disordered cavity.

Next, we replace the temporal degrees of freedom (DoF) of the broadband transmission measurement with spatial DoF obtained by Wavefront Shaping [3, 4]. Using simple electronically reconfigurable reflect arrays partially covering the cavity walls, we measure the single-frequency transmission between two arbitrary points for a series of random configurations of the cavity boundaries. We show that this, too, yields unique signatures. We demonstrate the localization of multiple passive objects with single-frequency measurements by wavefront shaping.

Finally, we discuss the minimum number of DoF needed to successfully localize multiple objects.

References

- [1] R. K. Ing, et al., In solid localization of finger impacts using acoustic time-reversal process, *Appl. Phys. Lett.*, **87**, 204104 (2005).
- [2] J. de Rosny, et al., Field fluctuation spectroscopy in a reverberant cavity with moving scatterers, *Phys. Rev. Lett.*, **90**, 094302 (2003).
- [3] P. del Hougne, et al., Dynamic metasurface aperture as smart around-the-corner motion detector, *Sci. Rep.*, **8**, 6536 (2018).
- [4] P. del Hougne, et al., Spatiotemporal wave front shaping in a microwave cavity, *Phys. Rev. Lett.*, **117**, 134302 (2016).

Coupled wave propagation and nanotrap lattice in hollow fiber filled with Raman-active gas

Husakou A.¹, Alharbi, M.², Chafer, M.², Debord, B.², Gerome, F.², Benabid, F.²

¹Max Born Institute, Max-Born-Str. 2a, D-12489 Berlin, Germany

²GPPMM Group, XLIM Research Institute, CNRS UMR 7252, University of Limoges, Limoges 87410, France

e-mail: gusakov@mbi-berlin.de, f.benabid@xlim.fr

Trapping of molecules has attracted a significant attention due to its impact in exploring new frontiers in physics. In a recent paper [1] we have demonstrated that such a trapping is facilitated by a particularly simple system of Raman-active gas in a hollow-core photonic fiber which is pumped by a continuous wave. Due to the nonlinear Raman amplification of light by the gas and reflection from the fiber ends, a self-consistent configuration of forward- and backward-propagating Stokes waves is formed, as schematically depicted in Fig. 1.

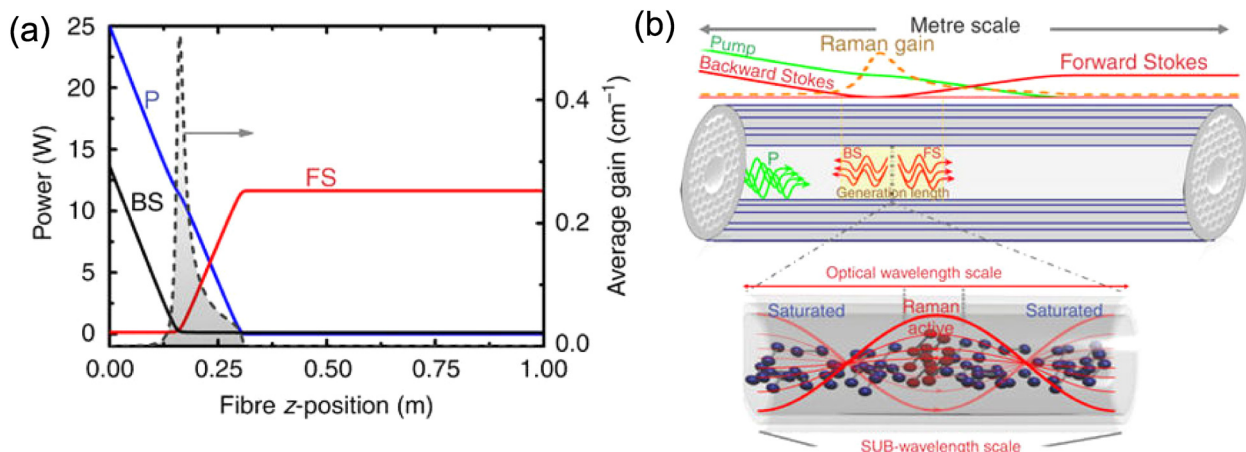


Fig. 1: (a) The distribution of the pump (P), forward Stokes (FS), and backward Stokes (BS) beams along the fiber lengths. By dashed line the Raman gain is presented. In (b), the scheme of the standing wave formation and the microscopic-scale trapping configuration are shown.

The corresponding standing wave pattern yields periodic ultra-deep potential caused by a spatially modulated Raman saturation, where Raman-active molecules are strongly localized in a one-dimensional array of nm-wide sections. Only these trapped molecules participate in stimulated Raman scattering, generating high-power forward and backward Stokes cw laser radiation in the Lamb–Dicke regime with sub-Doppler (14 kHz) emission spectrum, five orders of magnitude narrower than conventional-Raman pressure-broadened linewidth.

The theoretical description of the radiation propagation in fiber is provided by the coupled highly nonlinear propagation equations for forward and backward waves. The description of coupling is based on the microscopic picture of the Raman population modulation within the trap lattice. The solution is obtained by nonlinear shooting methods. The numerical predictions regarding the parameters of the emitted radiation are compared to the experimental data, showing very good agreement. In addition, perspectives of further applications of this novel configuration, such as all-optical cavity formed by two counter-propagating pump beams, are discussed, and the corresponding self-consistent configuration of the waves is calculated numerically.

References

- [1] M. Alharbi, A. Husakou, M. Chafer, B. Debord, F. Gerome, F. Benabid, Raman gas self-organizing into deep nano-trap lattice, *Nature Communications*, **7**, 12779 (2016).

Tunable color bright LED tandems with nanostructured perovskite-polymer composites

Artur Ishteev^{1,2}, Ross Haroldson¹, Masoud Alahbakhshi¹, Alisha Whitehead¹, Sergey Makarov^{1,2}, Anvar Zakhidov^{1,2}

Physics Department and Nanotech Institute, University of Texas at Dallas, USA
ITMO University, Saint Petersburg, Russia
e-mail: zakhidov@utdallas.edu

Organic inorganic perovskites such as $\text{CH}_3\text{NH}_3\text{PbX}_3$ ($X = \text{Cl}, \text{Br}, \text{I}$) have recently attracted great interest as LED emissive materials due to their and high photoluminescence quantum efficiency and narrow pure colors emission. However, very few tandems have been created using perovskite and organic LEDs. Here, we demonstrate a parallel tandem of two pero-LED single layer sub-cells, with CsPbBr_3 /PEO/PVP composite films interconnected with transparent carbon nanotube layers with depositing a hydrophilic and insulating polyvinyl pyrrolidone polymer (PPV) and poly ethoxy oxide (PEO) ionically conductive polymer atop the charge collecting layers. We obtained color tunable tandem light-emitting diodes and compare the performance of conventional in-series LED tandem with more functional parallel tandem, exhibiting a high brightness, high current efficiency and a high external quantum efficiency using a mixed-halide perovskite CsPbBr_2I as the bottom emitting layer and CsPbBr_3 as top emitting layer. To the best of our knowledge, this is the brightest color tunable and efficient perovskite light-emitting tandem reported to date. We discuss the mechanisms of current self-balancing in the composites of pero-nanocrystals embedded into ionic polymer (PEO) matrix as due to electronic barrier function of PEO sequentially working with Coulomb lowering of hole injection interfaces, which results in low, sub-band gap turn on voltage.

Photogalvanic effects in gyrotropic Weyl semimetals

E.L. Ivchenko

Ioffe Institute, 194021 St. Petersburg, Russia
e-mail: ivchenko@coherent.ioffe.ru

The current decade is marked by the discovery of two new classes of solid materials, namely, topological insulators and Weyl semimetals (WSMs). After establishing neutrino mass hierarchy,

the Weyl fermions in condensed matter systems remained the only particles with a massless linear energy dispersion and a definite chirality. The dispersion cones can be tilted or even overtilted which is realized, respectively, in type I and type II WSMs. The topological properties of WSMs manifest themselves in the chiral anomaly, Fermi arcs and topological charges in the reciprocal (momentum) space.

The discovery of WSMs has been followed by theoretical and experimental studies of their transport and optical properties, both linear and nonlinear. In particular, it has been shown that the interaction of circularly-polarized light with chiral fermions is governed by the Berry curvature of the Weyl node. This allows a new look at the Circular PhotoGalvanic Effect (CPGE), an appearance of a helicity-dependent electric photocurrent upon illumination of the sample by circularly polarized light [1]. The CPGE is allowed by the symmetry of gyrotropic (or optically active) media, and many WSMs belong to the family of gyrotropic crystals. It has been demonstrated that, in each Weyl node, the CPGE has universal features independent of details of the material. However, the corresponding CPGE current has the opposite polarity in the Weyl node of opposite chirality. As a result, the net CPGE current induced within two Weyl nodes of opposite chirality becomes nonvanishing only in tilted WSMs where it, however, loses its universality and depends on the tilt.

In Refs. [2, 3] we have developed a theory of the circular photogalvanic effect in Weyl semimetals with the point groups containing improper symmetry operations and proposed minimal models which allow for the CPGE. In semimetals of the C_{2v} symmetry with the linear energy dispersion, the net CPGE photocurrent becomes nonzero taking into account a spin-independent tilt term in the electron effective Hamiltonian. However, this is insufficient for the crystal class C_{4v} , like the TaAs Weyl semimetal. In this case one needs to add to the Hamiltonian not only the tilt but also spin-dependent terms of the second or third order in the electron quasi-momentum. We have complementarily investigated the magneto-gyrotropic photogalvanic effect, i.e. an appearance of a photocurrent under unpolarized excitation in a magnetic field. In quantized magnetic fields, the photocurrent is caused by optical transitions between the one-dimensional magnetic subbands. A value of the photocurrent is particularly high if one of the photocarriers, an electron or a hole, is excited to the chiral subband with the energy below the cyclotron energy.

References

- [1] E. L. Ivchenko, *Optical Spectroscopy of Semiconductor Nanostructures*, Alpha Science Int., Harrow, UK, 2005.
- [2] L. E. Golub, E. L. Ivchenko, B. Z. Spivak, *JETP Lett.*, **105**, 782 (2017).
- [3] L. E. Golub, E. L. Ivchenko, *arXiv:1803.02850* (2018).

Semi-periodic nanostructures: an apt solution to broadband optical applications

Jalali M.¹, Erni D.¹, Nadgaran H.²

¹General and Theoretical Electrical Engineering (ATE), Faculty of Engineering, University of Duisburg-Essen, and CENIDE — Center for Nanointegration Duisburg-Essen, 47057 Duisburg, Germany

²Department of Physics, Shiraz University, Shiraz, Iran

e-mail: mandana.jalali@uni-due.de, daniel.erni@uni-due.de, nadgaran@shirazu.ac.ir

Fully periodic structures are capable of supporting well-defined modes and mode groups at a specific frequency range. On the other hand, random structures excite weak broadband modes that do not have an influential effect on the system performance. Accordingly, researchers proposed semi-periodic structures which can support modes that are not as weak as the random structures modes and meanwhile are broader than fully periodic ones and therefore are an apt solution to broadband optical applications such as solar cells [1, 2]. However, defining semi-periodicity is a challenging task. The main idea is to add defects to a fully periodic structure to move toward randomness.

Such defects can be added based on defined mathematical semi-periodic sequences [3]. In this paper, we have propose defining semi-periodicity based on an optimization procedure through breeding evolutionary algorithm where the position of defects are defined based on the optimization using performance as the figure of merit. A periodic plasmonic Ag back-grating is added to a thin-film c-Si solar cell while some defects are added to the grating based on the optimization procedure.

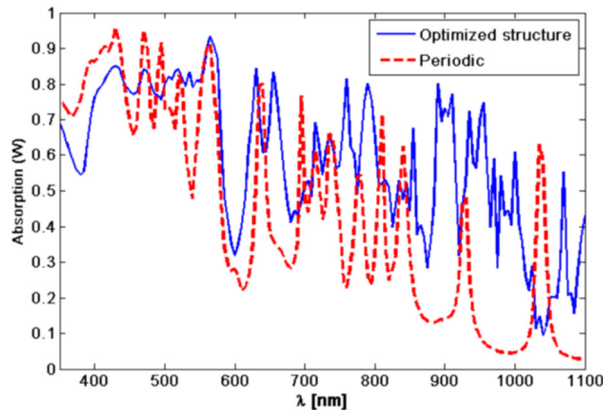


Fig. 1: Simulated spectral responses of the active layer's optical absorption for the optimized semi-periodic topology and periodic structure.

In Figure 1, the spectral response of the active layer's optical absorption for the optimized semi-periodic topology and periodic structure are depicted which confirms that semi-periodicity improved the integrated active layer's optical absorption up to 34.6% compared to fully periodic structure.

References

- [1] R. A. Pala, J. S. Liu, E. S. Barnard, D. Askarov, E. Garnett, S. Fan, M. L. Brongersma, Optimization of non-periodic plasmonic light-trapping layers for thin-film solar cells, *Nature Communications*, **4**, 2095 (2013).
- [2] M. Jalali, H. Nadgaran, D. Erni, Semiperiodicity versus periodicity for ultra broadband optical absorption in thin-film solar cells, *Journal of Nanophotonics*, **10**, 036018 (2016).
- [3] B. I. Berg, The algebra of semiperiodic sequences, *The Michigan Mathematical Journal*, **10**, 237–239 (1963).

Combining chirality and Parity-Time symmetry in metamaterials

Kafesaki M., Katsantonis I., Economou E.N.

Foundation for Research and Technology Hellas (FORTH), Institute of Electronic Structure and Laser (IESL), Heraklion, Greece, and University of Crete, Greece

e-mail: kafesaki@iesl.forth.gr, katsantonis@iesl.forth.gr, economou@admin.forth.gr

Droulias S.

FORTH, IESL, Heraklion, Greece

e-mail: sdroulias@iesl.forth.gr

Soukoulis C.M.

FORTH, IESL, Heraklion, Greece, and Ames Lab and Dept. of Physics and Astronomy, Iowa State University, Ames, Iowa, USA

e-mail: soukoulis@ameslab.gov

The quite new concept of Parity-Time (PT) symmetry, which was first discussed in connection with quantum physics (denoting systems with non-hermitian hamiltonian but commuting with the PT operator and thus presenting the possibility for real eigenvalues) was quite quickly transferred in optics, where the PT-symmetry is quite easily realizable by properly combining loss and gain

systems. In the context of PT-symmetric optical systems and metamaterials novel and fascinating phenomena were demonstrated (see e.g. the reviews [1, 2]), like unidirectional invisibility, coherent perfect absorption and lasing, anisotropic transmission resonances etc.

In this work we investigate the role and the effects of PT-symmetry in chiral metamaterials. Chiral metamaterials, i.e. metamaterials lacking any mirror symmetry plane, are associated with unique effects and possibilities concerning the polarization control of an electromagnetic wave, such as large and thickness independent optical activity and circular dichroism, negative refractive index etc. Combining PT-symmetry and chirality, one expects to merge two different worlds of peculiar propagation characteristics creating unique polarization control possibilities.

In this context, in the present work we (a) investigate and derive the conditions to achieve PT-symmetry in chiral metamaterials, (b) discuss scattering and transmission by PT-symmetric chiral systems and the new associated phenomena, and (c) properly combine chiral metamaterials with PT-symmetric non-chiral systems as to achieve novel propagation characteristics, like direction-dependent optical activity and/or wave ellipticity, offering thus direction-dependent polarization control of an electromagnetic wave.

References

- [1] L. Feng, R. El-Ganainy, L. Ge, Non-Hermitian photonics based on parity-time symmetry, *Nat. Photon.*, **11**, 752 (2017).
- [2] R. El-Ganainy, K. G. Makris, M. Khajavikhan, et. al., Non-Hermitian physics and PT symmetry, *Nat. Phys.*, **14**, 11 (2018).

Purcell factor in periodic metal-dielectric structures

Kaliteevski M.A.^{1,2,3}, Ivanov K.A.¹, Gubaydullin A.R.²

¹ITMO University, 49 Kronverksky pr., St. Petersburg, 197101, Russia

²St. Petersburg Academic University, 8/3 Khlopina st., St. Petersburg, 194021, Russia

³A. F. Ioffe Physico-Technical Institute 26 Politekhnikeskaya, St. Petersburg, 194021, Russia

e-mail: m.kaliteevski@mail.com

A lot of attention has recently been drawn towards studies of metal-dielectric structures and their ability to provide high Purcell factors i.e. to increase the probability of a spontaneous emission. Experimental studies backed by theoretical models have recently shown notable values of amplification in multilayer QD structure with metal coating [1]. Interestingly, one of the recent articles [2] suggests extremely high values of the Purcell factor (up to 10^5) in periodic metal-dielectric structures. However, an important issue worthy of investigation is that of light absorption in metals that can severely diminish the overall gain in the emission increase [3].

We have analysed an infinite structure lacking any absorption. The structure used was after [2], that is, 15 nm metal layers, whose dielectric constant is approximated by the Drude model:

$$\varepsilon = \varepsilon_\infty - \omega_p^2 / \omega(\omega + i\gamma) \quad (1)$$

alternate with 15 nm vacuum slabs. If γ in (1) is non-zero then an infinite system will not be able to hold electromagnetic field due to absorption, contrary to [2]. Other parameters, however, can be taken after [2]: $\varepsilon_\infty = 4.96$, $\omega_p = 8.98$ eV. This produces photonic band structure shown in Fig. 1a and a Purcell factor of a magnitude of 10^4 , which is shown in Fig. 1b. The value is smaller than in [2] because we have taken uneven distribution of the density of states into account. The highest value is obtained when an emitting dipole is placed right at the interface between metal and vacuum.

The value $\tilde{\varepsilon} = \varepsilon + \omega d\varepsilon/d\omega$ describes the relation between density of energy and field amplitude in dispersive media, and the difference between this value for Drude model (1) and real silver is shown in Fig. 2a. We have shown that taking this difference into account further decreases the calculated value of Purcell factor (on a single interface), as shown in Fig. 2b.

We have shown that basic metal-dielectric periodic structures can be used to achieve only fairly modest values of the Purcell factor. Taking real metallic absorption into account leads to a drop of about hundred times in Purcell factor value, keeping its order of magnitude around 10.

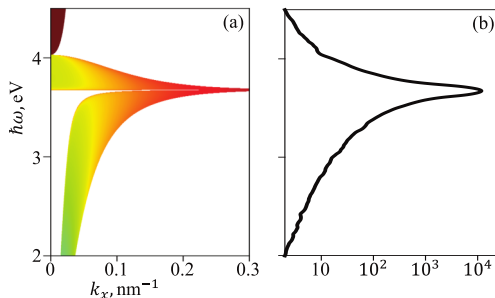


Fig. 1: Periodic structure, dipole directed along the layers and placed at the interface: (a) emission probability density and band structure; (b) integral Purcell factor.

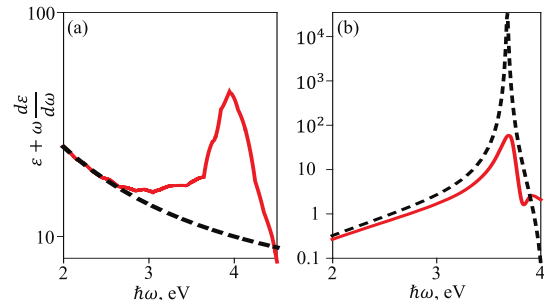


Fig. 2: (a) Energy density factor in metal; (b) integral Purcell factor for a single interface. Dielectric constant is after experiment (solid line) and after the Drude model (dash line). Dipole directed along the interface.

References

- [1] A. R. Gubaydullin, *et al.*, *Scientific Reports*, **7**, 9014 (2017).
- [2] I. Iorsh, *et al.*, *Phys. Lett. A*, **376**, 185 (2012).
- [3] J. B. Khurgin, *Nature Nanotechnology*, **10**(1), 2 (2015).

Ultrastrong coupling of electrons and 2D polaritons

Ido Kaminer

Department of Electrical Engineering, Technion, Israel Institute of Technology, Haifa 32000, Israel
e-mail: kaminer@technion.ac.il

The diversity of light-matter interactions accessible to a system is significantly limited by both the small size of an atom relative to the wavelength of the light it emits, and the small value of the fine-structure constant. Overcoming these limitations is a long-standing challenge. Recent theoretical and experimental breakthroughs have shown that systems such as graphene, boron nitride, and other 2D van der Waals materials can support strongly confined light in the form of plasmon/phonon polaritons. Due to their strong confinement, these polariton force us to recast the main assumptions for light-matter interactions. We identify cases in which the rate of two-photon spontaneous emission can compete with the rate conventional spontaneous emission, suggesting a new way of creating entangled photon pairs. Our findings also offer a potential testing ground for quantum electrodynamics in the ultrastrong coupling regime, and more generally, offer the ability to take advantage of the full electronic spectrum of an emitter, or to modify it. Finally, the seminar will touch upon several examples of such ultrastrong interactions in different systems, revealing connections to the Cherenkov effect and to a new kind of electron-polariton Compton effect.

References

- [1] N. Rivera, I. Kaminer, B. Zhen, J. D. Joannopoulos, M. Soljačić, Shrinking light to allow forbidden transitions on the atomic scale, *Science*, **353**, 263 (2016).
- [2] I. Kaminer, Y. Tenenbaum Katan, H. Buljan, Y. Shen, O. Ilic, J. J. Lopez, L. J. Wong, J. D. Joannopoulos, M. Soljačić, Efficient plasmonic emission by the quantum Čerenkov effect from hot carriers in graphene, *Nature Comm.*, **7**, 11880 (2016).
- [3] N. Rivera, G. Rosolen, J. D. Joannopoulos, I. Kaminer, M. Soljačić, Making two-photon processes dominate one-photon processes using mid-IR phonon polaritons, *PNAS*, **114**, 13607 (2017).

- [4] Y. Kurman, N. Rivera, T. Christensen, S. Tsesses, M. Orenstein, M. Soljačić, J. D. Joannopoulos, I. Kaminer, Control of semiconductor emitter frequency by increasing polariton momenta, *Nature Photonics*, (2018), accepted.
- [5] C. Roques-Carmes, N. Rivera, J. D. Joannopoulos, M. Soljačić, I. Kaminer, The Cherenkov effect beyond the perturbative regime, under review.

Nonlinear wave dynamics in anti-resonant hollow-core fibers

D. Kartashov¹, R. Sollapur¹, M. Zürich¹, M. Chemnitz², M. Schmidt^{2,3}, C. Spielmann¹

¹Institute of Optics and Quantum Electronics, Friedrich Schiller University Jena, Max-Wien-Platz 1, 07743 Jena, Germany

²Leibniz Institute of Photonic Technology e.V., Albert Einstein Strasse 9, 07745 Jena, Germany

³Otto Schott Institute of Material Research, Friedrich Schiller University Jena, Fraunhofer Str. 6, 07743 Jena, Germany

e-mail: daniil.kartashov@uni-jena.de, rudrakant.sollapur@uni-jena.de,
 michael.zuerch@uni-jena.de, mario.chemnitz@leibniz-ipht.de,
 markus.schmidt@leibniz-ipht.de, christian.spielmann@uni-jena.de

In this contribution, we report the results on numerical simulations and experiments with novel types of nanostructured hollow-core photonic crystal fibers (HCPCF), so called anti-resonant hollow-core fibers (ARHCF), which provide an additional degree of freedom in dispersion management and open up new regimes in nonlinear spectral and temporal dynamics of light waveforms. Nanoscale thickness strands within a hollow central core enable single or multi-mode broadband guiding of light with dramatically reduced, in comparison to conventional capillaries, losses. In fact, ARHCF combine advantages of Kagome HCPCF and antiresonant optical waveguides (ARROW) providing additional tuning of the net dispersion via strand geometry and thickness. Grazing incidence reflection from the thin strands enables low loss propagation of light in a broad spectral range except of narrow resonances at wavelengths which are close to the strand thickness and which can effectively tunnel through the strands. The spectral positions of these resonances are determined as $\lambda_m = \frac{2d\sqrt{n^2-1}}{m}$ where d is the strand thickness and m is the resonance order.

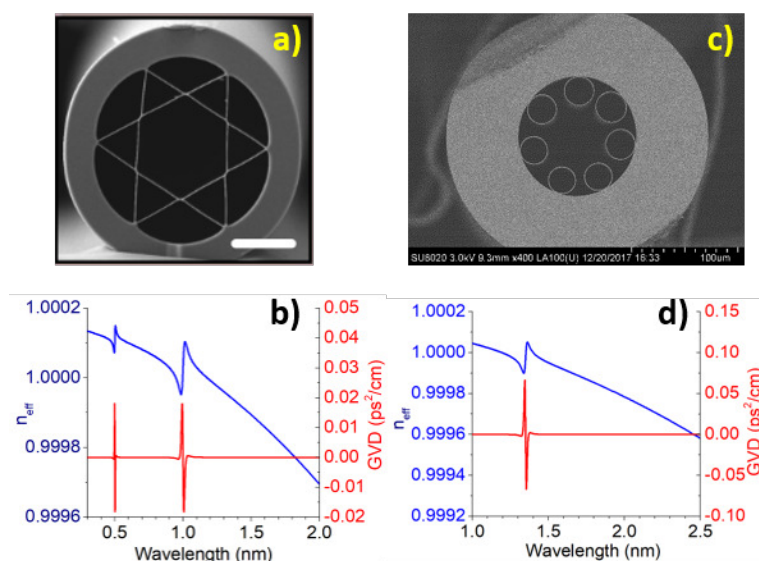


Fig. 1: a) SEM image of the David-star geometry ARHCF and b) its dispersion; c) revolver-type ARHCF and d) its dispersion.

The ARHCF with the David-star geometry of strands shown in Fig. 1a) allows several broad transmission bands in the near-IR-UV spectral range separated by the resonances, whereas the fiber shown in Fig. 1c) and having the revolver-type geometry has only one broad mid-IR (1.3–3 μm)

transmission band. Far from resonances, the dispersion in ARHCF can be well modeled by the dispersion of the gas-filled capillary. In the vicinity of the resonances the effective modal index of refraction experience abrupt changes, causing several orders in magnitude variations in the group-velocity dispersion (Fig. 1b,d)). We show that the abrupt change in the dispersion caused by the resonances triggers new types of nonlinear spectral and temporal dynamics of intense, ultrashort laser pulses propagating through the fiber, leading to explosion-like generation of multi-octave spectral continuum, massive emission of dispersive waves, complex multi-soliton dynamics etc.

All-dielectric topological photonics

A.B. Khanikaev

Department of Electrical Engineering, The City College of the City University of New York, New York, NY 10031, USA;

Advanced Science Research Center, Graduate Center of the City University of New York, New York, NY 10016, USA;

Department of Nanophotonics and Metamaterials, ITMO University, St. Petersburg 197101, Russia
e-mail: akhanikaev@ccny.cuny.edu

The experimental realization of photonic topological systems has proven fascinating properties of their electromagnetic modes [1–3]. Unfortunately, many of these original proposals have been based on metamaterials containing metals, whose functionality cannot be extended into IR and visible domains [4, 5]. In this regard all-dielectric metamaterials and metasurfaces [6] recently emerged in the field represent a well-suited platform to realize compact topological photonic insulators. Based on this concept, I will report on the experimental realization of two-dimensional all-dielectric topological metasurfaces. Such properties unique to topological systems as of the robustness of topological edge states and their spin-locking are confirmed via the direct visualization near and far-field by spectroscopic methods in microwave and near-IR frequency domains [7].

References

- [1] L. Lu, J. D. Joannopoulos, M. Soljačić, *Nat. Photon.*, **8**, 821 (2014).
- [2] M. C. Rechtsman, J. M. Zeuner, Y. Plotnik, et al., *Nature*, **496**, 196 (2013).
- [3] M. Hafezi, S. Mittal, J. Fan, et al., *Nat. Photon.*, **7**, 1001 (2013).
- [4] W.-J. Chen, S.-J. Jiang, X.-D. Chen, et al., *Nat. Commun.*, **5**, 6782 (2014).
- [5] A. P. Slobozhanyuk, A. B. Khanikaev, D. S. Filonov, et al., *Sci. Rep.*, **6**, 22270 (2016).
- [6] A. I. Kuznetsov, A. E. Miroschnichenko, M. L. Brongersma, et al., *Science*, **354**, 846 (2016).
- [7] M. A. Gorlach, X. Ni, D. A. Smirnova, et al., *Nat. Comm.*, **9**, 909 (2018).

Waveguide modes of biaxially anisotropic fiber and electro-optics of porous films filled with nematic liquid crystals

Kiselev A.D.

St. Petersburg National Research University of Information Technologies, Mechanics and Optics, Kronverskiy Prospekt, 49, 197101 St. Petersburg, Russia

e-mail: alexei.d.kiselev@gmail.com

Pasechnik S.V., Shmeliova D.V., Dubtsov A.V.

Moscow Technological University (MIREA), Vernadskiy Prospekt 78, 119454 Moscow, Russia

e-mail: pasechnik@mirea.ru

Liquid crystals are characterized by orientational structures that appear to be extremely sensitive to both external fields and boundary (anchoring) conditions at the bounding surfaces (substrates).

Generally, this sensitivity underlies all well-established modern liquid crystal technologies behind numerous exciting and successful applications of liquid crystal materials. In particular, it lies at the heart of the technologically important electro-optic properties of liquid crystal (LC) fibers [1] and porous films filled with LCs [2].

In this work we theoretically study the waveguide modes of a radially anisotropic LC fiber depending on the effective electrically controlled optical anisotropy of the LC material. For the general case of biaxial anisotropy, we derive the analytical expressions for the transverse and longitudinal components of the electromagnetic field and compute both the dispersion characteristics and the spatial distributions of wavefields for the hybrid TM and TE waveguide modes. We apply our results to go beyond the limitations of the previous work on the light scattering by radially anisotropic cylinders [3] and discuss the experimental data on the electric field dependence of the light transmission through porous films filled with LCs.

This work is supported by the Ministry of Education and Science of the Russian Federation (project No. RFMEFI58316X0058).

References

- [1] A. Corella-Madueno, J. A. Reyes, *Optics Communications*, **264**, 148 (2006).
- [2] A. Chopik, S. Pasechnik, D. Semerenko, D. Shmeliova, A. Dubtsov, A. K. Srivastava, V. Chigrinov, *Optics Letters*, **39**, 1453 (2014).
- [3] H. L. Chen, L. Gao, *Physical Review A*, **86**, 033825 (2012).

Meta-optics and Mie-resonant nanophotonics

Kivshar Yu.S.

Nonlinear Physics Center, Australian National University, Canberra ACT 2601, Australia;
ITMO University, St. Petersburg 197101, Russia
e-mail: ysk@internode.on.net

Metamaterials, artificial electromagnetic media that are structured on the subwavelength scale, were initially suggested for the negative-index media, and later became a paradigm for engineering electromagnetic space and controlling propagation of waves. Recently, we observe the emergence of a new branch of metamaterials and nanophotonics aiming at the manipulation of strong optically-induced electric and magnetic Mie-type resonances in dielectric nanostructures with high refractive index. Unique advantages of dielectric resonant nanostructures over their metallic counterparts are low dissipative losses and the enhancement of both electric and magnetic fields that provide competitive alternatives for metal-based plasmonic structures including nanoantennas, nanoparticle sensors, and metasurfaces. This talk will summarize the recent research on meta-optics and metadevices driven by Mie-resonant nanoparticles.

References

- [1] S. Kruk, Y. S. Kivshar, *ACS Photonics*, **4**, 2638 (2017).

Breaking of bulk-surface correspondence in topological photonics

Vasily V. Klimov

Dukhov Research Institute of Automatics (VNIIA), Moscow, Russia;
P. N. Lebedev Physical Institute, Russian Academy of Sciences, Moscow, Russia
e-mail: klimov256@gmail.com

Development of chip to chip optical interconnects is of great importance for reducing the energy consumption of heavy computations. Now it is widely believed that optical nanowaveguides with

topologically protected surface states can help to achieve this goal. This is rather complicated from physical point of view and most of researchers deal with simplified geometries of waveguides, which are far from practical.

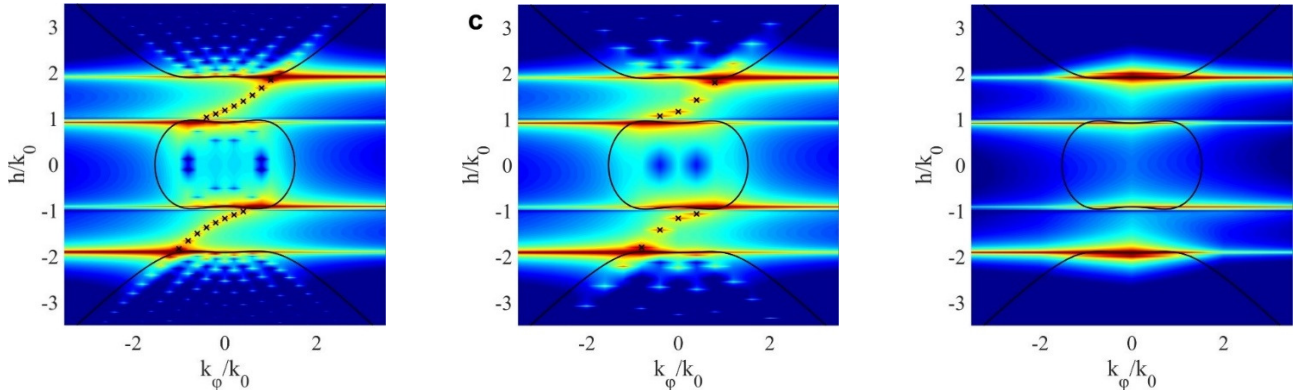


Fig. 1: TPSS positions for the bi-anisotropic waveguides with different radii R (black crosses) together with equifrequency curves of bulk bi-anisotropic medium (solid black lines). (a) $k_0 R = 5$, (b) $k_0 R = 2.5$, (c) $k_0 R = 0.5$. Note that when $k_0 R \leq 0.5$ there are no TPSS at all.

We study the optical properties of 3D bi-anisotropic optical waveguides with nontrivial topological structure in reciprocal space, placed in an ordinary dielectric matrix. We derive an exact analytical description of the eigenmodes of the systems with arbitrary parameters that allows us to investigate topologically protected surface states (TPSS) in details. In particular, we have found that the TPSS on the waveguides would disappear if their radius is smaller than a critical radius due to the dimensional quantization of azimuthal wavenumber (see Fig. 1), and also if the permittivity of the host-medium exceeds a critical value. Interestingly, we also find that the TPSS in the waveguides have negative refraction for some geometries. We have found a TPSS phase diagram that will pave the way for development of the topological waveguides for optical interconnects and devices. Our results rise the general question about domains of applicability of topological protection and bulk-surface correspondence in topological photonics.

Noncollinear interaction features of optical waves with wide spectrum in nonlinear dielectric medium

Knyazev M.A., Kozlov S.A.

ITMO University, St. Petersburg 197101, Russia

e-mail: knyazev.michael@gmail.com, kozlov@mail.ifmo.ru

Analysis of the interaction of intense light waves propagating in an optical media at an angle to each other is a classical problem of nonlinear optics. This problem has been already thoroughly studied in the last century for quasimonochromatic waves [1]. In the present work regularities of the interaction between intense few-cycle waves with wide spectrum propagating at an angle to each other in transparent dielectric medium with an instantaneous nonlinearity were studied. Usually such analysis is performed in the approximation of a given refractive index inhomogeneity induced in the medium by the other wave [2]. We, in contrast, have analysed the interaction strictly as a self-consistent wave problem with boundary conditions of two femtosecond optical beams without introduction of the artificial concept of induced nonlinear refractive index. Spectral approach was used to describe few-cycle wave packets dynamics [3]:

$$\frac{\partial^2 g}{\partial z^2} + [k(\omega)^2 - k_x^2] g = -\frac{\omega^2 \epsilon_{nl}}{c^2} \frac{1}{(2\pi)^4} \iiint \int_{-\infty}^{\infty} g(\omega - \omega', k_x - k'_x, z) \times g(\omega' - \omega'', k'_x - k''_x, z) g(\omega'', k''_x, z) d\omega' dk'_x d\omega'' dk''_x. \quad (1)$$

where g is a spectral density of the radiation, ω and k_x are the temporal and spatial frequencies, respectively, $k(\omega)$ is the wave number, $n(\omega) = N_0 + a\omega^2$ is the refractive index, ϵ_{nl} is the dielectric permittivity, c is the speed of light in vacuum, z is the spatial coordinate along which one of the waves propagates.

It is shown that the interaction between the wave packets may lead to a significant increase in the third-harmonic generation efficiency. In case of presence of a considerable linear refractive index dispersion, the interaction may also lead to significant changes in the spectrum at fundamental frequencies.

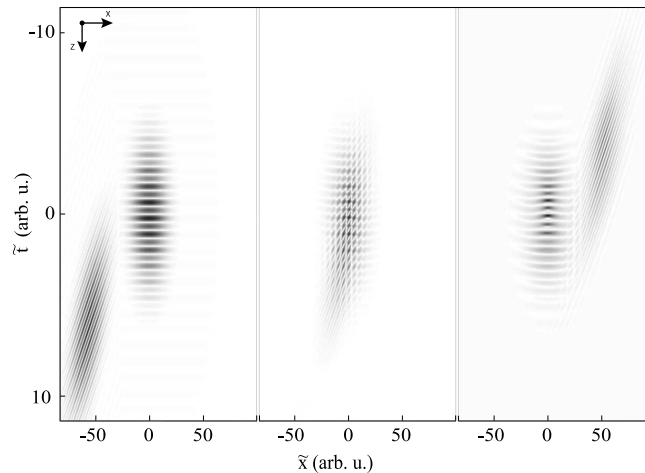


Fig. 1: Space-time distribution of the electric field of waves before, during and after their interaction.

References

- [1] R. W. Boyd, *Nonlinear Optics*, 3rd ed., Academic Press, 2008.
- [2] A. P. Sukhorukov, et al., *Izv. Akad. Nauk, Ser. Fiz.*, **76**, 350 (2012).
- [3] A. A. Ezerskaya, D. V. Ivanov, S. A. Kozlov, et al., *J. Infrared Milli Terahz Waves*, **33**, 926 (2012).

Resonant excitation of TMOKE-based spin waves in hybrid nanostructures via frequency comb

Kolodny S.A., Yudin D.I., Iorsh I.V.

ITMO University, Birzhevaya line V.O., 14, Saint Petersburg, Russia, 199034

e-mail: s.kolodny@metalab.ifmo.ru

In this work we propose a novel method of resonant optical excitation of spin waves (magnons) in hybrid nanostructures via frequency comb. We consider a two-layer hybrid nanostructure consisting of an Au layer with a grating on the top and an yttrium iron garnet (YIG) thin film at the bottom (see Fig. 1a). Optically excited plasmons create the strong localized electromagnetic field at the Au-YIG interface. The plasmon evanescent fields induce time independent magnetic polarization via the transverse magneto-optical Kerr effect (TMOKE) [1]. Created magnetic polarization h_{ext} plays a role of excitation source of the spin waves in YIG film. But the main problem is the different frequency ranges of plasmons (optical range) and magnons (GHz range for YIG (see Fig. 1b)). We numerically show that by using the frequency comb as a source we can generate the magnetic polarization in resonance with the spin waves in YIG thus substantially increasing the magneto-optical response of the system. We hope that the results can be applied to development of the new optical control methods of spintronics systems.

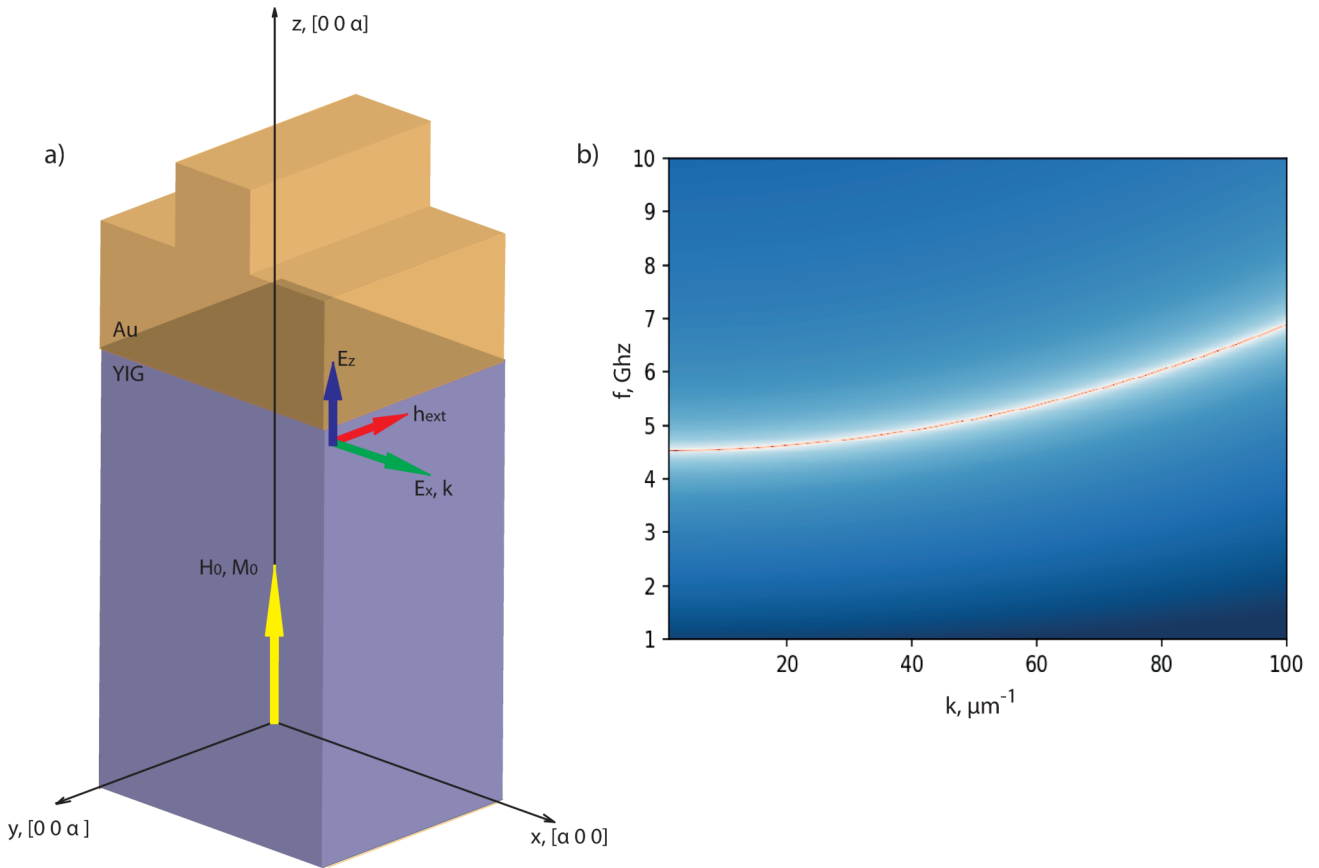


Fig. 1: a) Elementary cell of hybrid nanostructure. Arrows represent the corresponding values vectors. b) Dispersion diagram of magnons inside the YIG thin film.

References

- [1] V. I. Belotelov, A. K. Zvezdin, Inverse transverse magneto-optical Kerr effect, *Physics Review B*, **86**, 155133 (2012).

Quantum rings in the regime of strong light-matter coupling. Topological insulators

Kozin V.K.

ITMO University; University of Iceland
e-mail: kozin.valera@gmail.com

We demonstrate theoretically that a strong high-frequency circularly polarized electromagnetic field can turn a two-dimensional periodic array of interconnected quantum rings into a topological insulator. The elaborated approach is applicable to calculate and analyze the electron energy spectrum of the array, the energy spectrum of the edge states, and the corresponding electronic densities. As a result, the present theory paves the way to optical control of the topological phases in ring-based mesoscopic structures.

We developed the theory of electronic properties of semiconductor quantum rings with the Rashba spin-orbit interaction irradiated by an off-resonant high-frequency electromagnetic field (dressing field). Within the Floquet theory of periodically driven quantum systems, it is demonstrated that the dressing field drastically modifies all electronic characteristics of the rings, including spin-orbit coupling, effective electron mass and optical response. Particularly, the present effect paves the way to controlling the spin polarization of electrons with light in prospective ring-shaped spintronic devices.

References

- [1] V. K. Kozin, I. V. Iorsh, O. V. Kibis, I. A. Shelykh, Periodic array of quantum rings strongly coupled to circularly polarized light as a topological insulator, *Phys. Rev. B*, **97**, 035416 (2018).
- [2] V. K. Kozin, I. V. Iorsh, O. V. Kibis, I. A. Shelykh, Quantum ring with the Rashba spin-orbit interaction in the regime of strong light-matter coupling, *arXiv:1801.10250* [cond-mat.mes-hall].

Wire metasurface eigenmode impact on receive sensitivity enhancement of 1.5 T MRI machine

Kretov E.I., Shchelokova A.V., Slobozhanyuk A.P.

ITMO University, Saint Petersburg 197101, Russia

e-mail: egor.kretov@metalab.ifmo.ru

The quality of magnetic resonance imaging (MRI) is directly determined by receive sensitivity of a system [1]. In recent research [2], it was proposed a new conceptual idea to use wire metasurfaces for improving the sensitivity of a 1.5 T MRI scanner. Such metasurface can effectively spatially redistribute and enhance the electromagnetic field generated by a body coil. In this work, we performed an experimental investigation of wire metasurface eigenmode impact on receive sensitivity enhancement. The metasurface is formed as an array of parallel non-magnetic metallic wires, placed inside high permittivity media (Fig. 1a) [3]. Such design supports a set of eigenstates, which occur due to the splitting of the original resonance frequency dictated by the strong coupling between resonance wires located at a distance much smaller than the wavelength. For MRI purposes the first eigenmode is most useful since it has the highest penetration depth and for this eigenmode, the magnetic field is localized in the central region of the metasurface, while the electric field is concentrated near the edges of the wires (Fig. 1b). By changing a position of a small test sample on the metasurface, we check the efficiency of the receive sensitivity enhancement. Furthermore, we demonstrate that the signal increasing depends on the dimensions of the investigated object. Thus, we evaluate the optimal conditions to achieve the highest value of the received signal for this type of metasurface placed inside 1.5 T scanner.

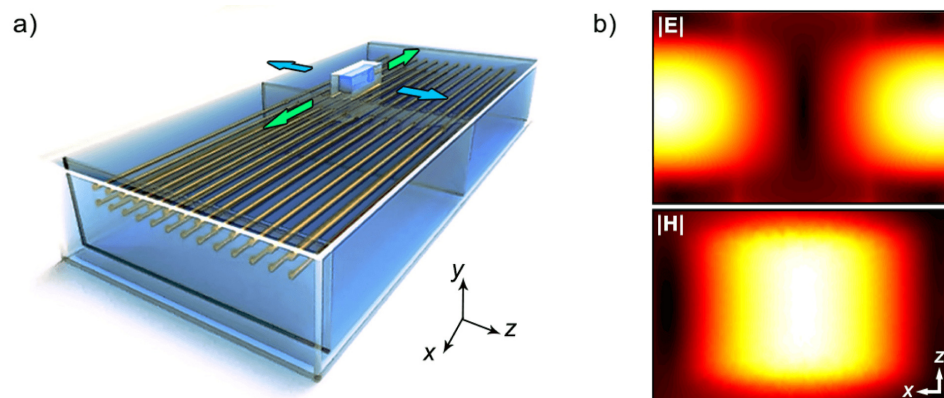


Fig. 1: (a) Schematic view of the metasurface design together with a small test object placed on the top of the structure. (b) Electric (top panel) and magnetic (bottom panel) fields distributions above the metasurface.

References

- [1] W. R. Hendee, Physics and applications of medical imaging, *Rev. Mod. Phys.*, **71**, S444 (1999).
- [2] A. P. Slobozhanyuk, A. N. Poddubny, et al., Enhancement of magnetic resonance imaging, *Adv. Mater.*, **28**, 1832–1838 (2016).
- [3] E. I. Kretov, A. V. Shchelokova, A. P. Slobozhanyuk, Impact of wire metasurface eigenmode on the sensitivity enhancement of MRI system, *Appl. Phys. Lett.*, **112**, 033501 (2018).

Polaritons in photonic structures with (In)GaAs and transition metal dichalcogenides as an active media

Dmitriy Krizhanovskii

Department of Physics and Astronomy, University of Sheffield, Sheffield S3 7RH, United Kingdom
e-mail: d.krizhanovskii@sheffield.ac.uk

When light propagates through an optically active semiconductor material hybridization of the optical and electronic excitations (photons and excitons) may occur. This leads to the formation of novel quasi-particles, so-called polaritons. Two photons colliding in free space do not interact: light beams just pass through each other with no effect on their propagation paths. By contrast the exciton component in the polariton wavefunction leads to giant repulsive interactions between the two colliding quasi-particles, which enable control of light by light at ultrafast speeds. This is potentially useful for applications in all-optical signal processing. In my talk I will present two polariton platforms based on optically active materials such as GaAs and heterostructures of transition metal dichalcogenides (TMDC) (MoSe₂, WSe₂). In polaritonic systems based on GaAs the quantum fluid effects (ultra-low-power polariton bright and dark solitons, vortices and condensation) will be briefly reviewed and the strength of polariton-polariton interactions will be discussed. While excitons and exciton-polaritons in GaAs usually exists at T up to 50–70 K the very large exciton binding energy and oscillator strength in atomically thin TMDCs allows very narrow polariton resonances to form in microresonators even with a single embedded TMDC monolayer and at 300 K. Besides TMDC monolayers being extremely thin potentially can be integrated into photonic circuits based on a variety of semiconductor and dielectric materials such as SiO₂, Si₃N₄, Ta₂O₅ and others, which makes it extremely favorable for the development of active nanophotonic components of various geometries. The other distinctive properties of TMDC monolayers are the very strong electron-electron exchange interactions and the electron and exciton polarisation in different valleys in k-space. In my talk, I will discuss how valley polarised and valley coherent exciton-polaritons are formed in this system and what mechanisms lead to the enhancement of linear or circular polariton polarization degree. Finally, the recent results on the optical nonlinearity in TMDC polariton platform will be presented and compared to that in GaAs-based system.

Photonic analogues of the Haldane and Kane–Mele models

Sylvain Lannebère¹, **Mário G. Silveirinha**^{1,2}

¹Department of Electrical Engineering, University of Coimbra and Instituto de Telecomunicações, 3030-290 Coimbra, Portugal

²University of Lisbon – Instituto Superior Técnico, Department of Electrical Engineering, 1049-001 Lisboa, Portugal

e-mail: sylvain.lannebere@co.it.pt, mario.silveirinha@co.it.pt

The Haldane model [1] played a fundamental role in the development of topological concepts in electronics. This model describes the electronic properties of a graphene-type material under the influence of a periodic magnetic field with zero-spatial average. Furthermore, the Haldane model is effectively the backbone of the theory of topological insulators: the Kane–Mele model [2] consists of two copies of the Haldane model with opposite magnetic field. However, despite the numerous connections between topological electronics and photonics developed in recent years [3, 4], so far there is no precise electromagnetic counterpart of these models, mainly due to the difficulties to mimic an effective magnetic field for photons.

Here building on our previous works [5, 6] and using an analogy between the two dimensional Schrödinger and Maxwell equations, we propose an implementation of the Haldane model in a photonic crystal with honeycomb symmetry made of dielectric cylinders embedded in a metallic background and a spatially variable pseudo-Tellegen response [7] that emulates a periodic effec-

tive magnetic field for photons [8]. The non-trivial electromagnetic topological properties of such a platform and in particular the presence of topologically protected unidirectional edge states at the interface with a trivial photonic insulator are demonstrated with numerical simulations.

In addition, it is shown that by applying a duality transformation [9] to the photonic Haldane model one obtains a precise analogue of the Kane–Mele model in photonics. Remarkably, the Kane–Mele model can be implemented using matched anisotropic dielectrics with identical permittivity and permeability, without requiring any form of bianisotropic couplings. The Kane–Mele model consists of two copies of the Haldane model, with each copy associated with a specific wave polarization. These findings evidence the possibility to observe bi-directional topologically protected edges-states in a fully reciprocal all-dielectric and non-uniform anisotropic metamaterial.

References

- [1] F. D. M. Haldane, Model for a quantum hall effect without landau levels: condensed-matter realization of the “parity anomaly”, *Phys. Rev. Lett.*, **61**, 2015–2018 (1988).
- [2] C. L. Kane, E. J. Mele, Quantum spin hall effect in graphene, *Phys. Rev. Lett.*, **95**, 226801 (2005).
- [3] A. B. Khanikaev, S. H. Mousavi, W-K. Tse, M. Kargarian, A. H. MacDonald, G. Shvets, Photonic topological insulators, *Nat. Mat.*, **12**, 233–239 (2013).
- [4] A. Slobozhanyuk, S. H. Mousavi, X. Ni, D. Smirnova, Y. S. Kivshar, A. B. Khanikaev, Three-dimensional all-dielectric photonic topological insulator, *Nat. Photonics*, **11**, 130–136 (2017).
- [5] S. Lannebère, M. G. Silveirinha, Effective Hamiltonian for electron waves in artificial graphene: A first-principles derivation, *Phys. Rev. B*, **91**, 045416 (2015).
- [6] S. Lannebère, M. G. Silveirinha, Link between the photonic and electronic topological phases in artificial graphene, *arXiv:1712.06126* (2017).
- [7] A. Serdyukov, I. Semchenko, S. Tretyakov, A. Sihvola, *Electromagnetics of Bi-anisotropic Materials: Theory and Applications*, Gordon & Breach Science Publishers, Singapore, 2001.
- [8] F. Liu, J. Li, Gauge field optics with anisotropic media, *Phys. Rev. Lett.*, **114**, 103902 (2015).
- [9] M. G. Silveirinha, PTD symmetry protected scattering anomaly in optics, *Phys. Rev. B*, **95**, 035153 (2017).

Sorting resonances and non-resonant enhancements: a kaleidoscope of recent highlights

Lapine M.

University of Technology Sydney, NSW, Australia
e-mail: mikhail.lapine@gmail.com

I will discuss several topics of metamaterial-related design, which may have a substantial theoretical and practical importance, however so far have been underestimated in our community [1].

One example is not even related to metamaterials directly, however is inspired by the growing importance of all-dielectric metamaterials, which prompts for dielectric nanoparticles. Even though a few research groups are capable of producing silicon nanoparticles with well-controlled size, current mass-production yields a great dispersion of sizes, so the output must be sorted. We have proposed [2] an all-optical way to sort dielectric nanoparticles according to their resonances, with a method to produce an angular spectrum of sizes with an easy distinction between sizes differing by 10%.

Another example is related to opto-acoustic metamaterials, assembled as a non-resonant composite medium, such as an array of spheres embedded in a different matrix. Such composites feature artificial electrostriction that can be greater than natural coefficients of the components, and are suitable to enhance stimulated Brillouin scattering (SBS) [3]. In particular, we have designed inverse opal structures of air and silicon [4], which is suitable for CMOS-compatible SBS processing.

Yet another example is the great potential of artificial diamagnetism, achieved with a simple and easily scalable array of non-resonant rings. Diamagnetic response of these structures, with the magnitudes of magnetic permeability below 0.1, is much stronger than natural diamagnetism. The key contribution to this result is mutual interaction and strong coupling in a dense array with appropriate symmetry [5]. Further advantage of this design is structural reconfigurability, permitting to dynamically tune permeability by several times.

Finally, I will provide an update on the strong effect of metamaterial boundaries and shape of finite metamaterial samples on their observable properties, as opposed to effective medium predictions. The eventual convergence towards effective medium approximation depends on shape and boundary structure, and is quite slow [6], which imposes direct consequences onto realistic designs.

I greatly acknowledge the contribution of A. P. Slobozhanyuk, M. A. Gorkach, D. A. Shilkin, M. R. Shcherbakov, M. J. A. Smith, C. Wolff, B. T. Kuhlmeier, C. Martijn de Sterke, L. Jelinek, R. Marques, P. A. Belov, A. A. Fedyanin, Y. S. Kivshar, R. C. McPhedran, and C. G. Poulton to various aspects of the reported research.

References

- [1] M. Lapine, New degrees of freedom in nonlinear metamaterials, *Phys. Stat. Sol. B*, **254**, 1600462 (2017).
- [2] D. A. Shilkin, E. V. Lyubin, M. R. Shcherbakov, M. Lapine, A. A. Fedyanin, Directional optical sorting of silicon nanoparticles, *ACS Photonics*, **4**, 2312–2319 (2017).
- [3] M. J. A. Smith, C. M. de Sterke, C. Wolff, M. Lapine, C. G. Poulton, Enhanced acousto-optic properties in layered media, *Phys. Rev. B*, **96**, 064114 (2017).
- [4] M. J. A. Smith, C. Wolff, C. M. de Sterke, M. Lapine, B. T. Kuhlmeier, C. G. Poulton, Stimulated Brillouin scattering enhancement in silicon inverse opal waveguides, *Opt. Express*, **24**, 25148–25153 (2016).
- [5] M. Lapine, A. K. Krylova, P. A. Belov, C. G. Poulton, R. C. McPhedran, Yu. S. Kivshar, Broadband diamagnetism in anisotropic metamaterials, *Phys. Rev. B*, **87**, 024408 (2013).
- [6] M. Lapine, R. C. McPhedran, C. G. Poulton, Slow convergence to effective medium in finite discrete metamaterials, *Phys. Rev. B*, **93**, 235156 (2016).

Numerical design of Au/Si core-shell nanoparticles

Larin A.O., Sun Y., Savelev R.S., Zuev D.A.

ITMO University, St. Petersburg 197101, Russia

e-mail: artem.larin@metalab.ifmo.ru

Combination of metal and dielectric materials in a single resonant optical nanostructure allows to achieve such optical properties as unidirectional scattering [1], efficient third harmonic generation [2], etc. These properties appear due to spectral matching of resonances that stem from metallic and dielectric constituent parts. This, in turn, demands a proper engineering of the nanostructure. Among all metal-dielectric nanostructures, core-shell nanoparticles are one of the most perspective for biosensing and lasing [3].

Here, we present the results of analytical and numerical simulations of metal-dielectric core-shell nanoparticles with gold core and silicon shell. We have considered particles with spherical and cylindrical shapes and have found optimal geometrical parameters in terms of spectral overlapping of the electric and magnetic dipole resonances. While spherical shape of the particle allows for analytical modeling and fast computation of its properties, the possible shape of the particles that can be fabricated in experiments are much closer to cylindrical shape.

Scattering by spherical core-shell particles was modeled analytically by employing the Mie theory. Data on the material properties were taken from the Refs. [4, 5]. The outer shell radius had a fixed value 150 nm, and the core radius varied in the range 10–100 nm. The simulation revealed

that electric dipole resonance that originates from the presence of the plasmonic core and magnetic dipole resonance that originates due to presence of the shell with high refractive index are spectrally matched when the core radius is 31 nm. The values of radii obtained for a sphere were then used as an approximation in the modeling of a cylindrical nanoparticle. Numerical simulations were performed in CST Microwave studio. The obtained parameters for cylindrical core-shell Au/Si nanoparticle makes possible spectral overlapping of dipole resonances at 1050 nm. Near this wavelength unidirectional scattering can be achieved. As a result we received the optimal geometrical parameters that can be further utilized for the experimental realization of the Au/Si core-shell nanoparticles.

References

- [1] H. Wang, et al., Janus magneto-electric nanosphere dimers exhibiting unidirectional visible light scattering and strong electromagnetic field enhancement, *ACS Nano*, **9**(1), 436–448 (2015).
- [2] S. Toshihiko, et al., Efficient third harmonic generation from metal–dielectric hybrid nanoantennas, *Nano letters*, **17**(4), 2647–2651 (2017).
- [3] W. Liu, et al., Broadband unidirectional scattering by magneto-electric core–shell nanoparticles, *ACS Nano*, **6**(6), 5489–5497 (2012).
- [4] P. B. Johnson, R. W. Christy, Optical constants of the noble metals, *Phys. Rev. B*, **6**, 4370–4379 (1972).
- [5] A. D. Rakićand, et al., Optical properties of metallic films for vertical-cavity optoelectronic devices, *Appl. Opt.*, **37**, 5271–5283 (1998).

Lamellas metamaterials: fabrication, characterization and applications

Lavrinenko A.V., Shkondin E., Takayama O., Repän T., Panah M.E.A.

Department of Photonics Engineering, Technical University of Denmark, Oersteds Plads, Bld. 343, DK-2800 Kongens Lyngby, Denmark

e-mail: alav@fotonik.dtu.dk

We report on our advances in fabrication of optical metamaterials with vertically oriented lamellas. Fabricating lamellas metamaterials we elaborated two material platforms. We apply the atomic layer deposition (ALD) technique to arrange vertical alignment of layers of heavily doped ZnO or TiN, which enables us to produce structured metamaterials operating either at certain intervals in the visible or in the near- and mid-infrared ranges. Applications of such laminae materials are illustrated with examples on surface waves' propagation and sensing.

The TiN-based lamellas structures were realized by the combination of ALD with advanced deep reactive ion etching [1]. The fabrication procedure is based on ALD deposition of TiN films on sacrificial Si templates with sub-sequential removal of Si. TiN is deposited at 500°C on a silicon trench template with the pitch of 400 nm and height of around 2.7 μm. Silicon between vertical TiN layers is selectively etched to fabricate the high aspect ratio TiN lamellas. Permittivity of TiN films with various thicknesses of 18–105 nm is characterized by an ellipsometer. Such grating structures can exhibit a sharp spectral increase in reflection, which is referred to as the Rayleigh–Woods anomaly [1]. The associated spectral position of the reflection peaks shifts depending on the changes in refractive indices of the surrounding media. We characterized the shifts for different liquids, such as distilled water, ethanol, and isopropanol. The bulk refractive index sensitivity of our sensing unit is evaluated to be around 430 nm/RIU.

Aluminum-doped zinc oxide (AZO) metamaterials are composed of multiple high aspect ratio (1:6.7) sub-wavelength AZO lamellas on a Si substrate. AZO exhibits a plasmonic response, possessing a negative real part of the permittivity in the near- and mid-IR regions. Periodically positioned AZO lamellas secure hyperbolic dispersion of the whole structure in the mid-infrared range supporting both surface waves and bulk plasmon waves in the broad wavelength range in mid-infrared [2]. The lamellas shape provides 14.5 times more surface area for residing of analyte molecules than the

flat surface. The whole structure is fabricated by the combination of deep UV lithography, dry etching, and ALD technique for AZO deposition, resulting in the uniform formation of deep trenches on a large scale area of $2 \times 2 \text{ cm}^2$. To demonstrate the sensing potential of the lamellas metamaterials, we coat all lamellas with a 5 nm thick SiO_2 layer by ALD, emulating the presence of an analyte SiO_2 layer exhibits strong phonon absorption around 8 μm wavelength. We measured free-space reflection of the samples with and without the 5 nm SiO_2 layer in the mid-IR wavelength range of 6.25–10 μm ($1600\text{--}1000 \text{ cm}^{-1}$). The reflection difference yields over 9% [3]. The enhanced absorption is achieved by two factors: interaction of bulk plasmon modes propagating in the lamellas with the analyte silica layer and profoundly extended surface area of the deeply profiled structure with the fixed footprint.

References

- [1] E. Shkondin, T. Repän, T. Takayama, A. V. Lavrinenko, High aspect ratio titanium nitride trench structures as plasmonic biosensor, *Opt. Mater. Express*, **7**, 4171–4181 (2017).
- [2] O. Takayama, E. Shkondin, A. Bogdanov, M. E. A. Panah, K. Golenitskii, P. Dmitriev, T. Repän, R. Malureanu, P. Belov, F. Jensen, A. V. Lavrinenko, Midinfrared surface waves on a high aspect ratio nanotrench platform, *ACS Photonics*, **4**, 2899–2907 (2017).
- [3] E. Shkondin, T. Repän, M. E. Aryaee Panah, A. V. Lavrinenko, T. Takayama, High aspect ratio plasmonic nanotrench structures with large active surface area for label-free midinfrared molecular absorption sensing, *ACS Appl. Nano. Mater.*, accepted (2018).

Strong coupling between silicon spherical nanoparticle and monolayer WS_2

Lepeshov S.¹, Krasnok A.^{1,2}, Kotov O.³, Alù A.²

¹ITMO University, St. Petersburg 197101, Russia

²The University of Texas at Austin, TX 78712, USA

³N. L. Dukhov Research Institute of Automatics, Moscow 127055, Russia

e-mail: s.lepeshov@gmail.com

Transition metal dichalcogenides (TMDCs) are an emerging class of two-dimensional semiconductors that enable attractive optoelectronic applications in the visible range, such as photodetection and light harvesting, phototransistors and modulation, light-emitting diodes and lasers [1]. In the atomic monolayer limit these materials are of particular interest because their bandgap becomes direct enabling enhanced interaction of the dipole transition with light. However, for practical applications it is necessary to increase the strength of coupling between elementary excitations of TMDC, excitons, and light. For this purpose, a variety of optical structures and devices has been utilized. Typical example of such structures providing enhanced photon-exciton interactions at the nanoscale are plasmonic nanoantennas. These nanoscale objects made of noble metals (gold, silver) coupled to monolayer TMDC enable the strong coupling regime, pronounced Fano resonance and plasmon-exciton resonant energy transfer. But typical plasmonic materials, gold and silver, have finite conductivities at optical frequencies leading to the inherent dissipation of electromagnetic energy. For many applications, heat generation at nanostructure is detrimental for their behaviour, which can be modified dramatically with temperature. Recently developed all-dielectric nanoantennas [2] made of high-index materials (Si, GaP, GaAs) with insignificant dissipation losses in the visible range can be more effective alternatives to plasmonic nanoantennas in the TMDC-nanoantenna composites. Here, we present our recent studies of resonance coupling in a single Si nanoparticle – monolayer TMDC (WS_2) nanostructures. We theoretically predict the strong coupling regime in Si nanoparticle covered by WS_2 monolayer at magnetic dipole (MD) Mie resonance. We show that resonance coupling can be enhanced by changing of surrounding dielectric material from air to water. Particularly, our theoretical studies of scattering cross section of this system based on Mie theory and coupled mode theory have demonstrated a Rabi splitting in water (see Fig. 1) with Rabi energy $\hbar\Omega = 208 \text{ meV}$ at

the intersection of excitonic resonance of WS₂ and MD resonance of Si nanoparticle with radius of 75 nm.

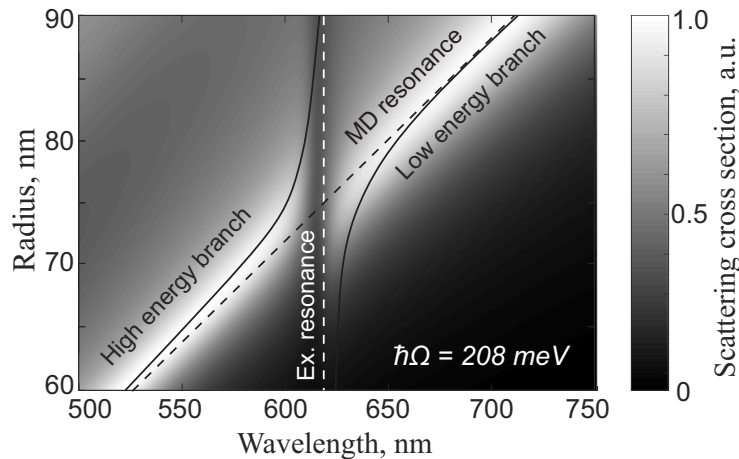


Fig. 1: Scattering cross section of Si-WS₂ core-shell system in water as a function of wavelength and SiNP radius.

References

- [1] Q. H. Wang, K. Kalantar-Zadeh, A. Kis, J. N. Coleman, M. S. Strano, Electronics and optoelectronics of two-dimensional transition metal dichalcogenides, *Nature nanotechnology*, **7**, 699 (2012).
- [2] A. E. Krasnok, A. E. Miroshnichenko, P. A. Belov, Y. S. Kivshar, All-dielectric optical nanoantennas, *Optics Express*, **20**, 20599–20604 (2012).

Topologically-protected transport in next-nearest-neighbour coupled ring resonator lattices

D. Leykam

Center for Theoretical Physics of Complex Systems, Institute for Basic Science, Daejeon, Korea
e-mail: dleykam@ibs.re.kr

S. Mittal, M. Hafezi

Joint Quantum Institute, NIST/University of Maryland, USA;
Department of Electrical and Computer Engineering and IREAP, University of Maryland, USA

Y.D. Chong

School of Physical and Mathematical Sciences, Nanyang Technological University, Singapore;
Centre for Disruptive Photonic Technologies, Nanyang Technological University, Singapore

Lattices of coupled microring resonators allow the photonic emulation of various topological band structure effects at optical frequencies [1]. Time-reversal symmetry is effectively broken by the excitation of either clockwise or anticlockwise circulating resonator modes. Previously this broken symmetry was used to implement an effective magnetic field for photons and observe topologically-protected quantum Hall-like edge states of light [2]. For many applications on-demand reconfiguration of the topological edge states is desirable, but this is difficult to achieve with existing approaches. Practical designs for reconfigurable topological phases have so far been limited to microwave metamaterials [3].

We present a simple design for reconfigurable topological edge states based on lattices of coupled optical ring resonators [5]. Our design is based on a lattice of resonant “site rings” coupled by off-resonant “link rings,” with the links implementing both nearest- and next-nearest neighbor couplings. The resulting tight binding model describing the limit of weakly coupled resonators resembles the Haldane model, and in particular no external modulation or effective magnetic field is required to obtain topological edge states. Consequently, topological phase transitions between trivial and Chern

insulator phases may be easily induced by thermal, electro-optic, or nonlinear effects, allowing the switching of the topological edge states guided along domain walls. Our model thus provides a promising route to achieving reconfigurable topological edge modes in optical devices, as well as for exploring the effect of optical nonlinearities on topological edge states.

References

- [1] L. Lu, J. D. Joannopoulos, M. Soljačić, Topological photonics, *Nature Photonics*, **8**, 821 (2014).
- [2] M. Hafezi, S. Mittal, J. Fan, A. Migdall, J. M. Taylor, Imaging topological edge states in silicon photonics, *Nature Photonics*, **7**, 1001 (2013).
- [3] X. Cheng, C. Jouvaud, X. Ni, S. H. Mousavi, A. Z. Genack, A. B. Khanikaev, Robust reconfigurable electromagnetic pathways within a photonic topological insulator, *Nature Materials*, **15**, 542 (2016).
- [4] M. Goryachev, M. E. Tobar, Reconfigurable microwave photonic topological insulator, *Phys. Rev. App.*, **6**, 064006 (2016).
- [5] D. Leykam, S. Mittal, M. Hafezi, Y. D. Chong, Reconfigurable topological phases in next-nearest-neighbor coupled resonator lattices, *arXiv:1802.02253* (2018).

Dielectric Yagi–Uda nanoantennas for unidirectional excitation of plasmons

Li, S.V.

ITMO University, St. Petersburg 197101, Russia

e-mail: s.li@metalab.ifmo.ru

Krasnok, A.E.

The University of Texas at Austin, Texas 78712, USA

e-mail: krasnokfiz@mail.ru

In the last several years high-index dielectric nanoparticles and nanostructures [1] proved to be a promising platform for various nanophotonic applications, in particular for modern light science, providing many fascinating applications, including high-efficient nanoantennas and metamaterials, enhanced nonlinear optical response, nonradiative sources, sensing, and all-optical data processing. High-index dielectric nanostructures are of a special interest for nonlinear nanophotonics, where they demonstrate an inherent magnetic resonance-enhanced frequency conversion processes, and special types of optical nonlinearity, such as electron-hole plasma photoexcitation [2], which are not inherent to plasmonic nanostructures.

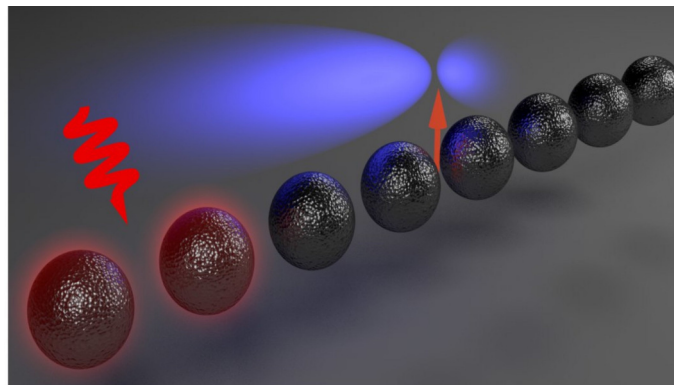


Fig. 1: General view of the considered nanoantenna and the dipole source (red arrow).

Here, we propose a novel geometry for highly tunable all-dielectric nanoantennas, consisting of a chain of silicon nanoparticles excited by an electric dipole source, which allows tuning their radiation properties via electron-hole plasma photoexcitation. We show that the slowly guided

modes determining the Van Hove singularity of the nanoantenna are very sensitive to the nanoparticle permittivity, opening up the ability to utilize this effect for efficient all-optical modulation. We show that by pumping several boundary nanoparticles with relatively low intensities may cause dramatic variations in the nanoantenna radiation power patterns and Purcell factor. We also demonstrate that ultrafast pumping of the designed nanoantenna allows unidirectional launching of surface plasmon-polaritons, with interesting implications for modern nonlinear nanophotonics.

References

[1] A. E. Krasnok, A. E. Miroshnichenko, P. A. Belov, Yu. S. Kivshar, All-dielectric optical nanoantennas, *Opt. Express*, **20**, 20599–20604 (2012).
 [2] S. Makarov, S. Kudryashov, I. Mukhin, A. Mozharov, V. Milichko, A. Krasnok, P. Belov, Tuning of magnetic optical response in a dielectric nanoparticle by ultrafast photoexcitation of dense electron-hole plasma, *Nano Letters*, **15**(9), 6187–6192 (2015).

Exceptional points in energy spectrum of nonlinear cavity arrays

Lyubarov M.D., Poddubny A.N.

ITMO University, 199034 St. Petersburg, Russia
 e-mail: markljubarov@gmail.com

Topological photonics has already become a universal roadmap to future disorder-immune nanooptics. Active, non-Hermitian [1] and quantum structures [2] have recently attracted special interest since they promise applications for compact photon sources integrated in topological optical chips.

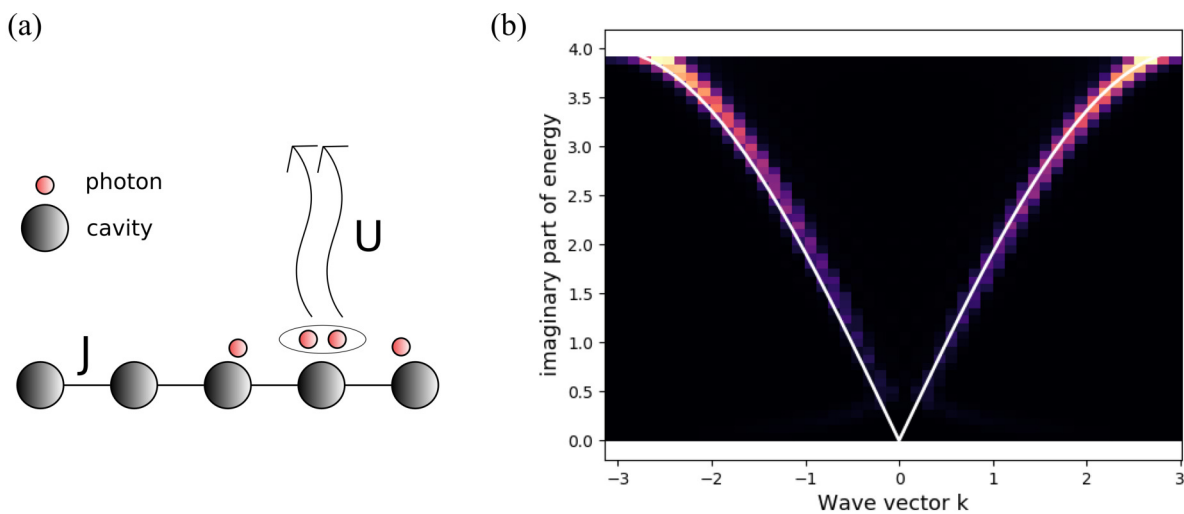


Fig. 1: (a) Scheme of the array of coupled resonators with the tunneling parameter J and nonlinear two-photon decay rate U . (b) Imaginary energy dispersion for bound photon pairs. Solid white curve shows the analytical result $E = 2\sqrt{4J^2 \cos^2 \frac{k}{2} - U^2}$, color map has been obtained by Fourier analysis of eigenstates in the finite array with $N = 30$ cavities and $U = 2J$.

Here, we study the propagation of photon pairs in the array of coupled cavities with nonlinear losses, see Fig. 1(a). We introduce the non-Hermitian Bose-Hubbard model, described by the Hamiltonian

$$H = \hbar\omega_0 \sum_{j=1}^N a_j^\dagger a_j + iU \sum_{j=1}^N a_j^\dagger a_j (a_j^\dagger a_j - 1) + J \sum_{j=1}^{N-1} (a_j^\dagger a_{j+1} + a_{j+1}^\dagger a_j),$$

where a_j are the photon annihilation operators, J is the tunneling parameter and U is the nonlinear loss parameter. The model hosts the photon pair states where the two photons are bound to each

other [3]. In stark contrast to the Hermitian case, the energy dispersion law is nonanalytical and features exceptional points, see Fig. 1(b). Our results in the quantum regime can be also directly mapped to the classical propagation of two photon beams at different frequencies ω_1 and ω_2 in coupled waveguide arrays where the nonlinear loss is due to the two-photon absorption. The generalizations of the problem to the dimerized cavity arrays will be discussed as well.

We believe that our results provide useful insights in the fundamental physics of non-Hermitian topological structures.

References

- [1] S. Weimann, *et al.*, *Nature Materials*, **16**, 433–438 (2017).
- [2] S. Barik, *et al.*, *Science*, **359**, 666–668 (2018).
- [3] K. Winkler, *et al.*, *Nature*, **441**, 853–856 (2006).

Dispersive wave emission from dark solitons and their collision in optical fibers

T. Marest¹, C. Mas Arabi¹, M. Conforti¹, A. Mussot¹, **A. Kudlinski**¹, C. Milian², D.V. Skryabin^{2,3}

¹Univ. Lille, CNRS, UMR 8523 – PhLAM – Physique des Lasers Atomes et Molécules, F-59000 Lille, France

²Department of Physics, University of Bath, Bath BA2 7AY, United Kingdom

³ITMO University, St. Petersburg 197101, Russian Federation

e-mail: alexandre.kudlinski@univ-lille.fr

We report the experimental observation of dispersive wave emission from gray solitons in an optical fiber. We also observed the nonlinear wave mixing occurring during the collision of a dark soliton and a linear wave.

Dark solitons are a class of solution of the defocusing nonlinear Schrödinger equation (NLSE) [1]. In optical fibers, this corresponds to the normal dispersion region. They exhibit an intensity dip (associated with a phase jump) over a uniform background. Dark solitons having a zero intensity at their core and an abrupt π phase jump are called black solitons or fundamental dark solitons. When the minimum intensity does not drop to zero and the phase change is smooth and smaller than π , they are termed gray solitons. The amplitude of dark solitons take the form:

$$A(t) = \cos(\phi) \tanh\left(\frac{t}{T_0} \cos(\phi)\right) - i \sin(\phi),$$

where ϕ is the grayness parameter ($\phi = 0$ corresponds to the black soliton) and T_0 is the duration of the dark dip. In this work, we observe experimentally for the first time the process of dispersive wave emission from dark solitons, in accordance with old theoretical predictions [2, 3], and we study the impact of dark soliton grayness on the efficiency of dispersive wave emission. Finally, we observe the nonlinear wave mixing occurring during the collision between a dark soliton and a dispersive wave.

We generate the odd dark pulses required to excite dark solitons by using two commercially available waveshapers. Short pulses from an optical parametric oscillator (220 fs, 1550 nm) are sent to a first waveshaper in which only the amplitude is shaped. At this stage, the grayness of the dark pulses can be controlled accurately. Then, the generated dark pulses are amplified and sent to a second waveshaper where the antisymmetric phase profile is applied. The resulting pulses are shaped both in amplitude and phase and have therefore the required properties to excite a dark solitons in the fiber (see example of cross-correlation and spectrum measurements of the shaped pulses at the fiber input in Fig. 1a and 1b, respectively). These pulses are then launched in a 3.15 km long dispersion shifted fiber (DSF), in the low normal dispersion region. Figure 1c shows the measurement of the output spectrum for various values of the grayness parameter ϕ . For ϕ values between $-\pi/6$ and $\pi/20$, a dispersive wave is emitted across the zero-dispersion wavelength (ZDW) and follows the

theoretical phase-matching curve (black solid line), while for ϕ values outside this range, none is observed. In Fig. 1d, we plot the energy of dispersive wave as a function of grayness parameter. The theoretical curve (red line) is obtained using an analytical estimation of the dispersive wave energy from e.g. [4].

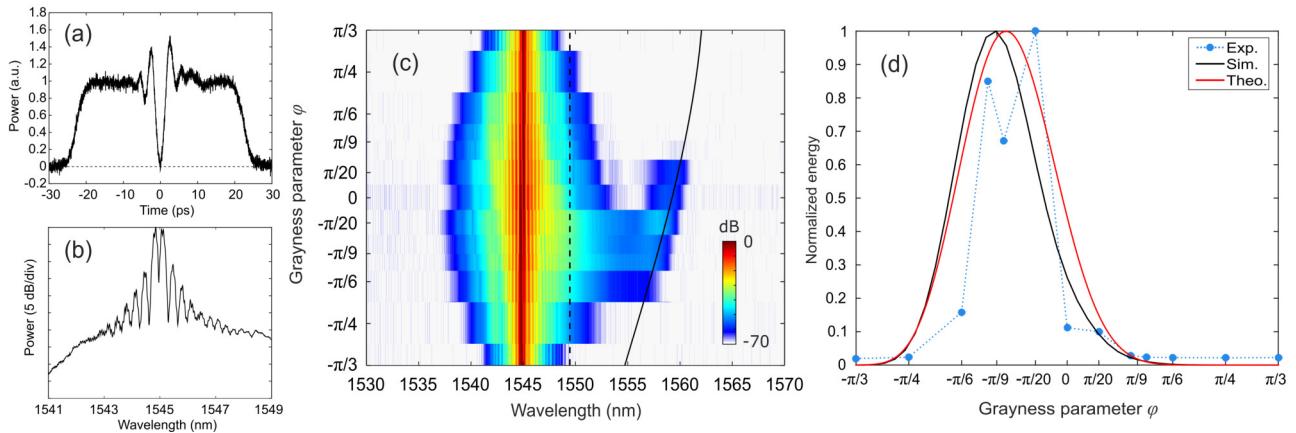


Fig. 1: (a)-(b) Example of temporal and spectral measurement of the input odd dark pulse. (c) Measured spectra at the fiber output as a function of grayness parameter (black solid line: phase-matching relation, black dashed line: ZDW). (d) Dispersive wave energy as a function of grayness parameter (black line: generalized NLSE simulations, red line: theory adapted from [4], blue markers: measurements).

The black line is obtained from numerical simulations of the generalized NLSE and markers correspond to measurements, in good agreement. For large $|\phi|$ values, the dark soliton spectrum is narrow, so that the spectral overlap with anomalous dispersion region is low, which explains the decrease in dispersive wave emission efficiency (similarly to the bright soliton case [5]). Additionally, for large positive ϕ values, the theoretical phase-matching wavelength goes away from the ZDW, which further reduces the dispersive wave emission efficiency. In a second set of experiments, we study the collision of a dispersive wave with a dark soliton. The experimental setup is mainly the same as in the previous experiment, but instead of being generated from the dark soliton in the fiber, here the dispersive wave is shaped directly in the input short pulse spectrum. The first waveshaper is used to shape the dark pulse and the dispersive wave pulse (called the probe here) at a different wavelength, and the second waveshaper is used to adjust the odd-symmetry phase profile of the dark pulse and the delay of the probe pulse.

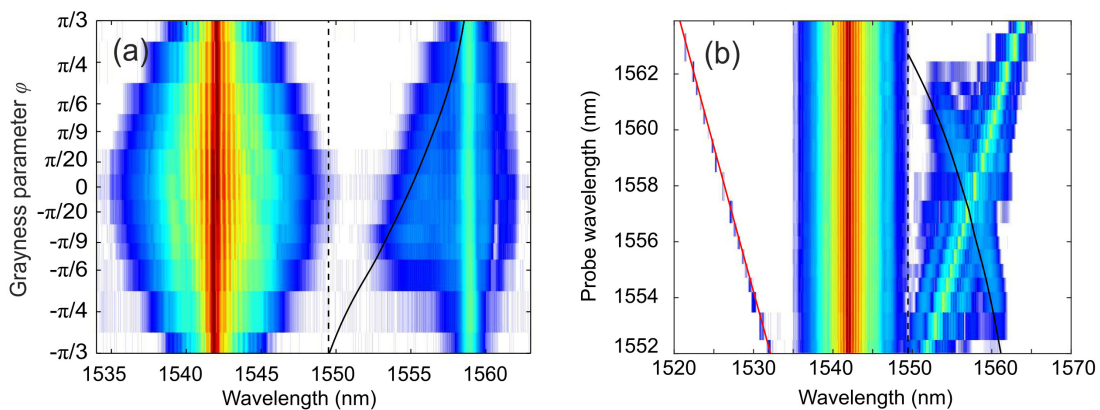


Fig. 2: Experimental observation of the nonlinear wave mixing occurring during the collision between a dark soliton and a dispersive wave. (a)-(b) Measurement of the output spectrum as a function of (a) dark soliton grayness for a fixed probe wavelength of 1559 nm and (b) probe wavelength for a fixed soliton grayness $\phi = 0$ (black soliton). Dashed line: ZDW, black solid line: theoretical solution of FWM between the dark soliton and the probe, red solid line: theoretical wavelength of FWM between the dark soliton background and the probe.

Figure 2a shows the measurement of the output spectrum for various values of the grayness parameter. The dark soliton is centered around 1542 nm and the probe wave is located at 1559 nm. For ϕ values higher than $-\pi/6$, a radiation resulting from the four wave mixing (FWM) between the probe and the dark soliton is observed [6]. It closely follows the FWM phase-matching relation (black solid line) that we have obtained by adapting the well-known theory for bright solitons [7]. In Fig. 2b, we show the measured spectra obtained by varying the probe wavelength, for a black soliton (i.e. with $\phi = 0$). Again, a new spectral component resulting from the FWM occurring at the collision between the dark soliton and the probe wave is observed, in excellent agreement with the theoretical curve (black solid line). In this case, we also observe a new radiation at short wavelength, that we can identify as the FWM between the probe wave and the quasi-cw background over which the dark soliton is located (red solid line). Numerical simulations of the generalized NLSE (not shown here) are in excellent agreement with the experiments of Fig. 2a and b. Additionally, we can derive analytically the conversion efficiency of the FWM process, again by adapting the bright soliton theory from e.g. [8], and we can simulate it using the generalized NLSE. The results (not shown here) are in excellent agreement with the experiments of Figs. 2a and b. A detailed analysis of these results will be presented at the conference. To summarize, we have observed a grayness-dependent emission of dispersive waves from dark solitons in an optical fiber. We have also observed a grayness-dependent generation of new radiations resulting from the four-wave mixing process occurring during the collision of dark solitons and linear waves.

References

- [1] Y. S. Kivshar, B. Luther-Davies, Dark optical solitons: physics and applications, *Phys. Rep.*, **298**, 81–197 (1998).
- [2] V. I. Karpman, Stationary and radiating dark solitons of the third order nonlinear Schrödinger equation, *Phys. Lett. A*, **181**, 211–215 (1993).
- [3] V. V. Afanasjev, Y. S. Kivshar, C. R. Menyuk, Effect of third-order dispersion on dark solitons, *Opt. Lett.*, **21**, 1975–1977 (1996).
- [4] C. Milian, D. V. Skryabin, A. Ferrando, Continuum generation by dark solitons, *Opt. Lett.*, **34**, 2096–2098 (2009).
- [5] N. Akhmediev, M. Karlsson, Cherenkov radiation emitted by solitons in optical fibers, *Phys. Rev. A*, **51**, 2602–2607 (1995).
- [6] I. Oreshnikov, R. Driben, A. V. Yulin, Weak and strong interactions between dark solitons and dispersive waves, *Opt. Lett.*, **40**, 4871–4874 (2015).
- [7] A. V. Yulin, D. V. Skryabin, P. S. J. Russell, Four-wave mixing of linear waves and solitons in fibers with higher-order dispersion, *Opt. Lett.*, **29**, 2411–2413 (2004).
- [8] A. Choudhary, F. König, Efficient frequency shifting of dispersive waves at solitons, *Opt. Express*, **20**, 5538–5546 (2012).

All-dielectric metamaterials with Mie-driven resonant electric response

Ekaterina E. Maslova¹, Mikhail V. Rybin^{1,2}

¹Department of Physics and Engineering, ITMO University, St. Petersburg 197101, Russia

²Ioffe Institute, St. Petersburg 194021, Russia

e-mail: ripchinskaya@gmail.com

Metamaterials (MM) are artificial composite media, which properties are determined by resonances supported by their structural elements. In contrast to photonic crystals, MM allow a homogenization procedure, which yields the effective parameters (refractive index, dielectric permittivity and magnetic permeability) varied in a wide range of values. A special design of MM offers media with effective parameters being negative, high positive and near-zero as well. MM enable left-handed

media, which is caused by simultaneously negative values of dielectric permittivity and magnetic permeability. Nowadays MM attract a lot of attention because of amazing applications for creating invisibility cloaks, flat superlenses and many others, which become possible due to engineered effective dielectric permittivity and magnetic permeability. Unusual effective parameters can be obtained using metallic elements, but such MM have significant losses in the visible range. Recently, negative values of the effective magnetic permeability were shown to be possible in structures with transparent high dielectric index elements sustaining Mie resonances [1]. These dielectric MM (DMM) make it possible to achieve a resonant magnetic response in a structure made of dielectric materials. However, to the best of our knowledge, DMM with a resonant effective dielectric permittivity has yet been reported.

Here we present for the first time dielectric structures with the resonant singularities in effective dielectric permittivity due to the electric Mie resonances for the TM polarization. We consider periodic structures of dielectric homogeneous rods arranged in square and hexagonal lattices. The variable parameters of the photonic structures are the dielectric permittivity of the rods and its radius to the lattice constant ratio that is related to the filling factor. Following the paper [2] we build phase diagrams “photonic crystal – metamaterial” and analyze them. We find the parameters of the structure, which allows the metamaterials phase. The phase diagrams show that the phase transitions for the TM polarization occur in narrow ranges of the parameters. The reason is in a stronger coupling between the electric Mie modes localized in neighbor cylinders respective to the weaker coupling between their magnetic counterparts. Thus, DMM for the TM-polarized wave possess a low rod density, which makes them attractive for applications exploiting light-matter interaction.

To verify the existence of metamaterial phase we consider a prism made of DMM with a near-zero effective dielectric index. The prism is formed by a structure with a square lattice. We reveal that the electromagnetic field at the specific MM frequency is homogeneous over the entire volume of the structure. The observed effect is not affected by the crystal axes orientation relative to the prism boundaries. Therefore, this result confirms the transition of the structure to the MM regime with zero effective dielectric index.

References

- [1] A. I. Kuznetsov, et al., Optically resonant dielectric nanostructures, *Science*, **354**, aag2472 (2016).
- [2] M. V. Rybin, et al., Phase diagram for the transition from photonic crystals to dielectric metamaterials, *Nature Commun.*, **6**, 10102 (2015).

Modeling of metamaterial superabsorbers in two dimensions

Medvedev Iu., Ferreira H., Maslovski S.

Instituto de Telecomunicações, DEEC FCTUC Polo-2, 3030-290 Coimbra, Portugal

e-mail: stas@co.it.pt

As is known from earlier studies, the scattering and absorption cross sections of resonant bodies can be much greater than those of non-resonant objects with the same geometric dimensions [1]. The idea of optimal resonant absorption is used, e.g. when designing compact receiving antennas, where a conjugate matched load compensates the excess reactance of the antenna and tunes it in resonance with the incident field, providing for the maximum of the received power. By using this physical principle for every possible incident spherical harmonic it can be shown that there is no upper limit on the effective absorption cross section of a finite-size resonant object [1]. In this work we aim at modeling such superabsorption effect in a setup with two dimensions due to difficulties in practical demonstration of this effect in three dimensions. The superabsorption effect is modeled by a wormhole structure composed of two separate meshes of transmission line (TL) based unit cells [Fig. 1(a)]: the unloaded double positive (DPS) mesh and the loaded double negative (DNG) mesh placed one atop another and electrically connected at the circumference of the wormhole. Theoretical

analysis of such a structure has been done based on the developed analytical models of unit cells of each type. Dispersion relations for DPS and DNG cells and the Bloch wave impedances have been obtained [Fig. 1(b,c)]. For the superabsorption effect to appear the absorber must be conjugate impedance matched to the surrounding space, which means that the DPS and DNG cells in the top and bottom halves of the structure have to satisfy this condition [2].

The considered single cells, a linear array of DPS-DNG-DPS cells and the complete wormhole structure have been also simulated in the CST Microwave Studio. Characteristic dispersion curves and Bloch wave impedances for both types of cells obtained with CST Microwave Studio agree well with the results of the analytical model. Simulation also confirm propagation of the backward waves in the DNG region and prove that both regions are conjugate impedance matched. Wormhole simulation results obtained so far show the presence of the superabsorption effect, and indicate that metamaterial object performs better than a simple black body type absorber.

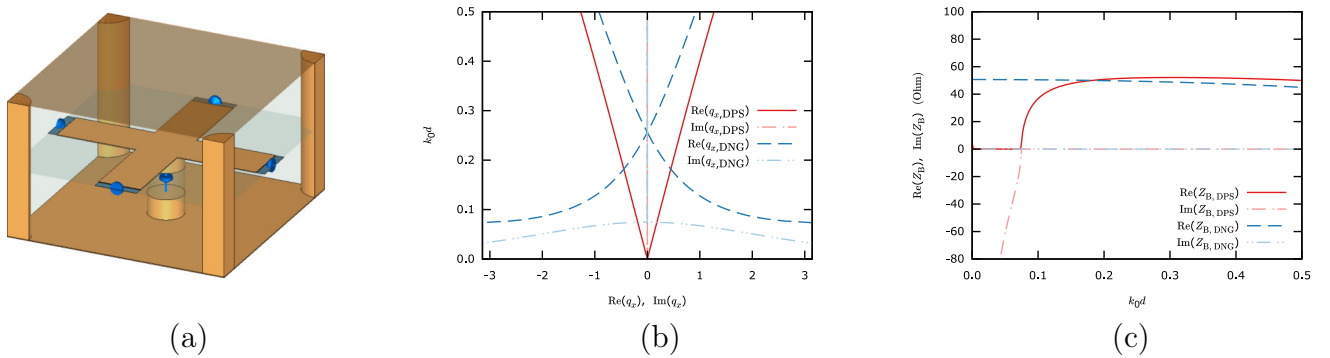


Fig. 1: CST model of DNG cell (a), dispersion characteristics (b), and Bloch wave impedances(c) of DPS and DNG cells.

References

- [1] S. Maslovski, C. Simovski, S. Tretyakov, Overcoming black body radiation limit in free space: metamaterial superemitter, *New J. Phys.*, **18**, 013034 (2016).
- [2] S. I. Maslovski, C. R. Simovski, S. A. Tretyakov, Conjugate-impedance matched metamaterials for super-Planckian radiative heat transfer, *Proc. SPIE 9883, Metamaterials X*, 988300 (2016).

Development of hyperbolic metamaterials for the control of biological molecules fluorescence

Mikheeva E.^{1,2}, Lumeau J.¹, Enoch S.¹, Wenger J.¹, Moreau A.¹, Lemarchand F.¹, Voznuk I.², Abdeddaim R.¹

¹Aix Marseille Univ, CNRS, Centrale Marseille, Institut Fresnel, F-13013 Marseille, France

²Multiwave Innovation SAS, 2 Marc Donadille, 13453 Marseille, France

e-mail: elena.mikheeva@fresnel.fr

Metamaterials are artificial structures consisting of periodic sub-wavelength elements, they produce a particular electromagnetic response which often cannot be obtained from conventional media. One class of metamaterials called hyperbolic metamaterials (HMM) is widely studied nowadays due to their various applications such as sub-wavelength imaging and local density of states engineering [1]. In this work, HMM consisting of alternating gold, copper, and niobium pentoxide layers was designed and fabricated with plasma assisted electron beam deposition technique. Afterward, the produced material was structured using focused ion beam milling and its influence on the Alexa Fluor 647 biomolecules spontaneous emission was studied experimentally with fluorescent correlation spectroscopy and time-correlated single photon counting techniques. Combining these techniques allows us apart from the molecules lifetime reduction observed for HMM before [2], to measure also the brightness enhancement per molecule which depends only on the radiative decay mechanism. The

same measurements were previously done for the structured gold films [3] which let us compare the results. HMM has shown significant emission enhancement compatible with the one produced by a single gold aperture which is known for its good plasmonic properties.

References

- [1] C. L. Cortes, W. Newman, S. Molesky, Z. Jacob, Quantum nanophotonics using hyperbolic metamaterials, *Journal of Optics*, **14**(6), 063001 (2012).
- [2] K. H. Krishna, K. V. Sreekanth, G. Strangi, Dye-embedded and nanopatterned hyperbolic metamaterials for spontaneous emission rate enhancement, *Journal of the Optical Society of America B*, **33**(6), 1038 (2016).
- [3] J. Wenger, D. Gerard, J. Dintinger, O. Mahboub, N. Bonod, E. Popov, T. W. Ebbesen, H. Rigneault, Emission and excitation contributions to enhanced single molecule fluorescence by gold nanometric apertures, *Optics Express*, **16**(5), 3008–3020 (2008).

Nonradiating excitations with dielectric nanoparticles

Andrey Miroshnichenko

School of Engineering and Information Technology, UNSW Canberra, Campbell, 2600, ACT, Australia

e-mail: andrey.miroshnichenko@unsw.edu.au

The possibility of the existence of non-radiating sources has attracted the attention of physicists for many years in different branches of science, starting from the beginning of quantum mechanics. One of the intriguing examples is the so-called anapole moment proposed by Zel'dovich in connection with the radiationless properties of a toroid solenoid. Furthermore, such electromagnetic configurations were recently suggested to classically describe the nature of dark matter. Recently, we demonstrated that one of the simplest systems allowing for direct observation of anapole mode in the visible is high-refractive index sub-wavelength nanoparticles. They provide new ways for excitation and investigation of the electro-magnetic properties of such topologically nontrivial excitations.

Purcell effect in a disordered photonic crystals

Morozov K.M.^{1,2}, Gubaydullin A.R.^{1,2}, Ivanov K.A.², Pozina G.P.³, Kaliteevski M.A.^{1,2,4}

¹St. Petersburg National Research Academic University, St. Petersburg, 194021 Russia

²ITMO University, St. Petersburg, 197101 Russia

³Department of Physics, Chemistry and Biology, Linköping University, 58183, Linköping, Sweden

⁴Toffe Institute, Russian Academy of Sciences, St. Petersburg, 194021 Russia

e-mail: morzconst@gmail.com, m.kaliteevski@mail.ru

Interplay between the Bragg interference and random scattering of light in photonic structures with disorder gives rise to a wide range of fascinating optical phenomena, such as Anderson localization of light [1]. We demonstrate that presence of disorder in photonic crystals could lead to modification of spontaneous emission rate in the photonic band gap (PBG) frequency region [2]. There are two different regimes of the Purcell effect as function of amount disorder: an enhancement of spontaneous emission at the edge of PBG in case of moderate disorder, and the spontaneous emission rate enhancing within PBG due to appearance of high quality factor states for the large level of disorder. Was demonstrated that for the PBG edges, mean value of Purcell coefficient is falling with the increase of disorder, and its standard deviation demonstrates a non-monotonic behaviour characterized by a maximum, but for the PBG centre, both the standard deviation and the mean value of the Purcell coefficient demonstrate a monotonic growth with disorder.

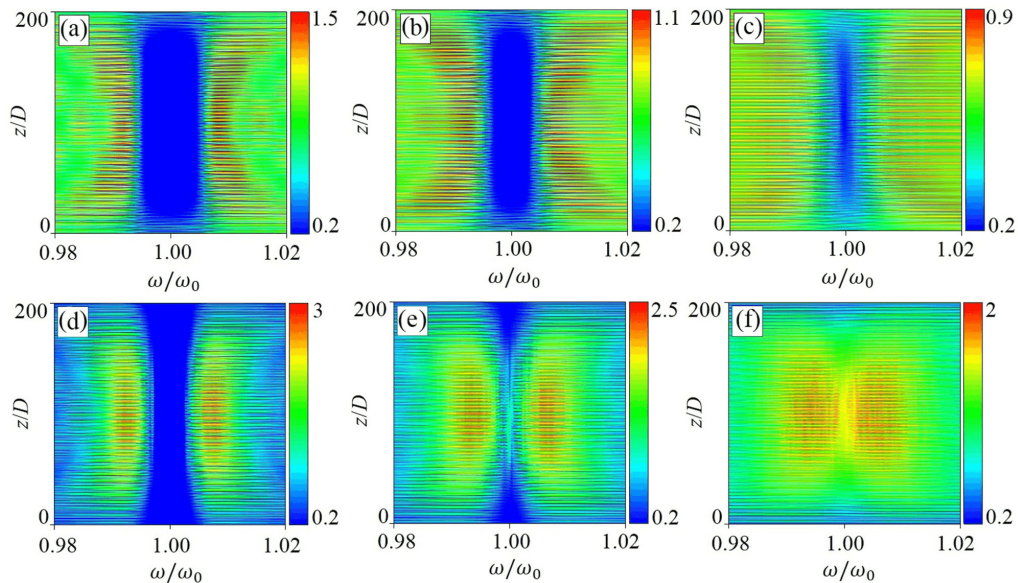


Figure shows dependence of the modal Purcell factor on the frequency and position of the emitter placed inside a disordered structure (200 pairs of layers A and B with the same thickness $D/2$; the center of the PBG is at ω_0 ; relative width of the PBG $\Delta\omega/\omega_0 \approx 0.016$) averaged over an ensemble of 10^4 structures with $\delta = 0.07$ (a) 0.1 (b) and 0.15 (c). And dependence of the standard deviation σ (d, e, f) corresponding of the modal Purcell factor, on the frequency and the emitter position. The value of a disorder parameter is (a,d) $\delta = 0.07$; (b,e) 0.1; (c,f) 0.15.

References

- [1] M. F. Limonov, R. M. De La Rue, *Optical Properties of Photonic Structures: Interplay of Order and Disorder*, CRC Press, 2016.
- [2] K. M. Morozov, et al., Different regimes of Purcell effect in disordered photonic crystals, *Phys. Rev. B*, (2018), submitted.

Full characterisation in phase and amplitude of the Fermi–Pasta–Ulam recurrence process in optical fibers

Arnaud Mussot, Pascal Szriftgiser, Corentin Naveau, Matteo Conforti, Alexandre Kudlinski, François Copie

Univ. Lille, CNRS, UMR 8523-PhLAM – Physique des Lasers Atomes et Molécules, F-59000 Lille, France

e-mail: arnaud.mussot@univ-lille1.fr

Stefano Trillo

Department of Engineering, University of Ferrara, Via Saragat 1, 44122 Ferrara, Italy

Fermi–Pasta–Ulam (FPU) recurrence process is a universal phenomenon that describes the natural return cycle of a nonlinear system into its initial state after experiencing a complex nonlinear coupling dynamics. In optical fibers it has been observed with reference to the nonlinear stage of modulation instability (MI) [1, 2], which also plays a key role in supercontinuum and rogue wave formation. However, the nonlinear MI is characterized by a broken symmetry [3, 4], which entails that, in a suitable phase-space, two qualitatively different types of evolutions can be followed by evolving from the modulated pump to a comb of sideband pairs and back to the pump. To date, the observation of such a broken symmetry has been elusive because of the intrinsic challenge of measuring the longitudinal evolution of the relative phase of the comb lines.

In this work, we report the first complete experimental observation of the broken symmetry of FPU recurrence associated with MI in optical fibers by means of a heterodyne optical time domain reflectometer (HOTDR). The HOTDR allows for recording the two qualitatively different phase

portraits of FPU recurrence, contrasted in Fig. 1(a,b,c) and (d,e,f), respectively, and accessible by changing the input modulation phase. Fig. 1(a) displays the longitudinal evolution of the normalized pump and sideband powers, and Fig. 1(b) their relative phase, when a pure amplitude modulation is injected at the fiber input (in-phase input, $\phi = 0$). First, two whole cycles of recurrence have been experimentally observed which is unprecedented in optical fiber systems. Second, the projection onto the phase-plane in Fig. 1(c) clearly shows that the relative phase remains confined in the right semi-plane ($-\pi/2 < \phi < \pi/2$), meaning that maximum compression points are in phase in the time domain (see inset calculated from numerical simulations). Conversely, by changing the input phase to $\phi = \pi/2$ (pure frequency modulation) a completely different scenario occurs (Fig. 1(d,e,f)). In this case, the two successive recurrences alternate in the right and left semi-planes, corresponding to a π phase shift between maximum recompression points in the time domain (see inset in (f) from numerics). The two phase portraits in Fig. 1(c) and (f) clearly correspond to the equivalent motion of a particle exploring either one of the wells or both wells of a double-well potential, which is the accessible signature of the broken symmetry associated with the nonlinear MI ruled by the nonlinear Schrödinger equation. The HOTDR reveals these two evolutions in the same system, simply by changing the input modulation phase. This is a key feature related to the conservative nature of the dynamics which is preserved in our system due to Raman-compensation of the fiber losses. In this sense, our results differ from the observation of shifted recurrence of MI observed recently in a deep water tank, which is induced by the unavoidable losses [5]. In summary, our original experimental technique permitted to reveal a novel regime of the nonlinear stage of MI where different types of recurrence turn out to coexist, being controllable via the input.

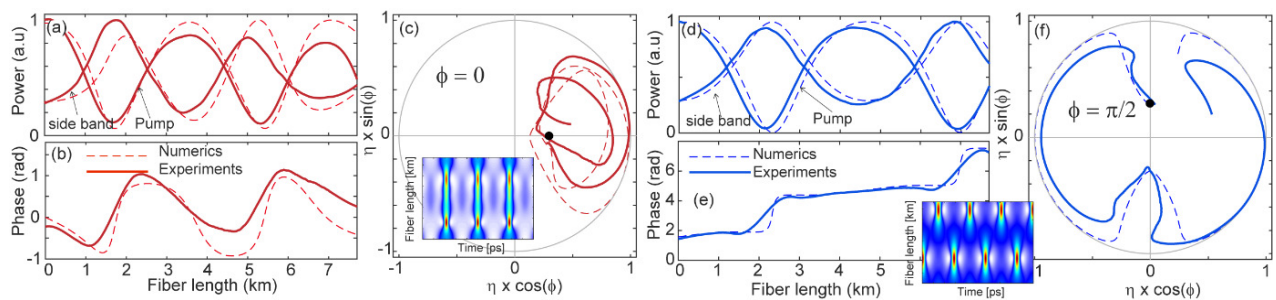


Fig. 1: Evolution with fiber length (a) of the normalized power of the pump and of the sideband, (b) of the pump-signal relative phase (ϕ) (c) Phase portrait of the sideband corresponding to (a) and (b). (a) to (c) AM case ($\phi = 0$, red lines) and (d) to (f) FM case ($\phi = \pi/2$, blue lines). Dashed lines represent numerical simulations and solid lines experimental results. Insets: temporal evolution of the intensity from simulations. Parameters: $\beta_2 = -19 \times 10^{-27} \text{ s}^2/\text{m}$, $\gamma = 1.3 \text{ W/km}$, pump power 450 mW, sideband power 63.6 mW, sideband detuning 35 GHz, $P = 1555 \text{ nm}$, fiber length 7.7 km. Linear losses are compensated by means of distributed Raman amplification. Powers are normalized to maximum values. $\eta(z)$ is the normalized sideband power, $\phi(z)$ is the relative phase between one of the sideband and the pump.

References

- [1] G. Van Simaey, P. Emplit, M. Haelterman, Experimental demonstration of the Fermi–Pasta–Ulam recurrence in a modulationally unstable optical wave, *Phys. Rev. Lett.*, **87**, 033902 (2001).
- [2] N. N. Akhmediev, Nonlinear physics: Déjà vu in optics, *Nature*, **413**, 267–268 (2001).
- [3] N. N. Akhmediev, V. I. Korneev, Modulation instability and periodic solutions of the nonlinear Schrödinger equation, *Teor. Mat. Fiz.*, **69**, 189–194 (1986).
- [4] S. Trillo, S. Wabnitz, Dynamics of the nonlinear modulational instability in optical fibers, *Opt. Lett.*, **16**, 986–988 (1991).
- [5] O. Kimmoun, H. C. Hsu, H. Branger, M. S. Li, Y. Y. Chen, C. Kharif, M. Onorato, E. J. R. Kelleher, B. Kibler, N. Akhmediev, A. Chabchoub, Modulation instability and phase-shifted Fermi–Pasta–Ulam recurrence, *Sci. Rep.*, **6**, 28516 (2016).

Study of high-index dielectric nanoparticles by means of virtual surface currents method

Neerad Nandan¹, Mikhail V. Rybin^{1,2}

¹Department of Physics and Engineering, ITMO University, Saint Petersburg, 197101, Russia

²Ioffe Institute, Saint Petersburg 194021, Russia

e-mail: nrdnandan@metalab.ifmo.ru, m.rybin@metalab.ifmo.ru

In previous decades, metallic nanoparticles with plasmon resonances played important role in nanophotonics. Recently, a submicron high-index dielectric particles attract a lot of attention [1]. Unlike metals, dielectric nanostructures do not exhibit high losses in infrared and visible spectrum and support both electric and magnetic resonances. Due to such properties, these structures can find application in lowthreshold nanolasers, biosensors, parametric amplifiers, and nanophotonics quantum circuits and others. Thus, it is important to develop a convenient tool to analyze optical properties of dielectric nanoparticles.

We can use multipole expansion technique for spherical nanoparticles because their surfaces do not mix multipoles with different moments. It allows rigorous analytical Mie solutions to the problem. However for the nanoparticle with complex shape we have to use numerical approaches such as FDTD, FDM and other methods or just use commercial software like COMSOL, CST etc. Also one can perform a procedure of dehomogenization media into electric dipole and solve the coupled dipole problem [2]. All these methods divide the volume of complex nanoparticle into a dense mesh and solve a mathematical problem with the cubic dependence of the computational cost on the particle size to wavelength ratio.

In this work we apply a surface current technique to study scattering on small nanoparticles. It allows us to reduce the computational cost to the quadratic dependence because mesh is applied to the surface only rather than the particle volume. The problem is divided into two parts: the first for the external fields being the sum of the incident wave and the scattered field generated by the surface currents; the second for the internal field generated by the surface currents. We assume that there are zero internal fields for the first problem and zero external fields for the second one. Also we assume that external and internal fields are generated by the currents of opposite sign. Therefore, for the entire problem surface currents cancel each other.

The main challenge of this approach is to define currents radiating selectively into the external direction from the surface or into the internal direction. The current in the elemental area is described as electric dipole that emits the wave in both inside and outside direction. To solve this problem we consider a Huygens source being a pair of electric and magnetic dipoles that radiates either in forward or backward direction selectively. Hence we have to take into account both magnetic and electric currents. The magnetic currents do not exist in nature however we can use them since they vanish in the entire problem being virtual.

We develop the method of virtual electric and magnetic currents by considering Maxwell's equation in a symmetric form that contains both electric and magnetic currents and charges. We verify our method by comparison with the rigorous analytical Mie solution for spherical silicon nanoparticles, and then we perform calculation for the non-spherical nanoparticles, which is important for many applications.

References

- [1] A. I. Kuznetsov, A. E. Miroshnichenko, et al., Optically resonant dielectric nanostructures, *Science*, **354**(6314), aag2472 (2016).
- [2] A. B. Evlyukhin, C. Reinhardt, B. N. Chichkov, Multipole light scattering by nonspherical nanoparticles in the discrete dipole approximation, *Phys. Rev. B*, **84**(23), 235429 (2011).

Control of second order correlation function of plasmonic resonator by NV-center

N.E. Nefedkin^{1,2,3}, E.S. Andrianov^{1,2}, A.A. Pukhov^{1,2,3}, A.P. Vinogradov^{1,2,3}, A.A. Lisiansky⁴

¹All-Russia Research Institute of Automatics, 22 Sushchevskaya, Moscow 127055, Russia

²Moscow Institute of Physics and Technology, 9 Institutskiy per., 141700 Dolgoprudny, Moscow reg., Russia

³Institute for Theoretical and Applied Electromagnetics RAS, 13 Izhorskaya, Moscow 125412, Russia

⁴Department of Physics, Queens College of the City University of New York, Queens, NY 11367, USA
e-mail: andrianov.es@mipt.ru

Currently, a substantial progress has been achieved in creating nano-sized sources of coherent radiation [1]. Radiation sources for quantum information transmission lines in addition to high temporal coherency must also have a desirable correlation function of the second order. Usually, single-photon radiation sources are required. To increase the speed of single-photon sources, single molecules and NV centers interacting with plasmonic structures are used [2]. However, in such systems, due to the Purcell effect [3], the correlation function of the second order of radiation is modified. Therefore, it is needed to create radiation sources with the required correlation function of the second order that can be tuned by changing the topology of the plasmonic resonator [2]. In this work we consider the second order correlation function of electromagnetic field irradiated by plasmonic resonator which is excited by NV center and show that it is strongly depend both on Rabi constant of interaction and temperature of surrounding medium. In the case of high temperature, at low pumping rates of NV center, the second order correlation function equals two as it takes place for black-body radiation. However, in the opposite case, when Rabi constant is much larger then temperature, the second order correlation function equals zero as it takes place for single two-level emitter. We show that the reason of such behavior is non-linear dependence of Rabi-splitting on the occupation number of plasmonic mode. At high pumping rates in both cases the second order correlation function tends to unity as in laser above threshold.

References

- [1] I. Aharonovich, D. Englund, M. Toth, Solid-state single-photon emitters, *Nature Photonics*, **10**, 631–641 (2016).
- [2] R. Saez-Blazquez, J. Feist, A. I. Frenandez-Dominguez, F. J. Garcia-Vidal, Enhancing photon correlations through plasmonic strong coupling, *Optica*, **4**, 1363 (2016).
- [3] E. M. Purcell, Spontaneous emission probabilities at radio frequencies, *Phys. Rev.*, **69**, 674 (1946).

Optical orientation of excitons in nanocrystals of inorganic perovskites

Nestoklon M.O.¹, Goupalov S.V.^{1,2}, Dzhioev R.I.¹, Ken O.S.¹, Korenev V.L.¹, Kusrayev Yu.G.¹, Sapega V.F.¹, de Weerd C.³, Gomez L.³, Gregorkiewicz T.³, Lin Junhao⁴, Suenaga Kazutomo⁴, Fujiwara Yasufumi⁵, Matyushkin L.B.⁶, Yassievich I.N.¹

¹Ioffe Institute, 194021 St. Petersburg, Russia

²Department of Physics, Jackson State University, Jackson MS 39217, USA

³Van der Waals-Zeeman Institute, University of Amsterdam, The Netherlands

⁴AIST, AIST Central 5, Tsukuba 305-8565, Japan

⁵Osaka University, 2-1 Yamadaoka, Suita, Osaka 565-0871, Japan

⁶St. Petersburg Electrotechnical University LETI, 197376 St. Petersburg, Russia

e-mail: nestoklon@coherent.ioffe.ru

The optoelectronic properties of halide perovskite thin films are comparable to those of direct-gap semiconductors, which makes them promising for generating and detecting spin. We use the polar-

ization spectroscopy of excitons in a 2D layer of CsPbI₃ perovskite nanocrystals (NCs) and measure the anisotropic exchange splitting of exciton levels. Perovskite NCs were synthesized following the method of Protesescu et al. [1] and the synthesized colloidal solution was deposited on a quartz glass substrate. Scanning transmission electron microscopy images show that the NCs have the shape of the cuboid with edge size close to 10 nm and the average aspect ratio about 10%. Then we study the samples using the standard technique following the work by Dzhioev et al [2]. An appearance of the circularly polarized excitonic photoluminescence (PL) under the circularly polarized excitation is known as the optical orientation of excitons, while the linear polarization of the excitonic PL under the linearly polarized excitation is known as the optical alignment of excitons. The suppression of the optical orientation at zero magnetic field, together with the strong optical alignment of excitons indicates that the PL is dominated by the neutral excitons and the bright exciton state is split at zero field into linearly polarized components. The results of the measurements may be fitted assuming that the exchange splitting of excitons is dominated by the long-range exchange caused by the NC shape with the Gaussian distribution. From the best fit (see Fig. 1) we extract the dispersion of the long-range exchange splitting (or, namely, the ensemble-averaged splitting between linearly polarized components of the bright exciton state) $\sigma_\delta = 120 \mu\text{eV}$ [3]. Our theoretical estimate gives about half of this value. We note, however, that both the anisotropic shape of NCs and the possible low-symmetry phase of the underlying crystal structure may cause the anisotropic fine-structure splitting. Optical spectroscopy alone cannot be used to rule out either of these possibilities.

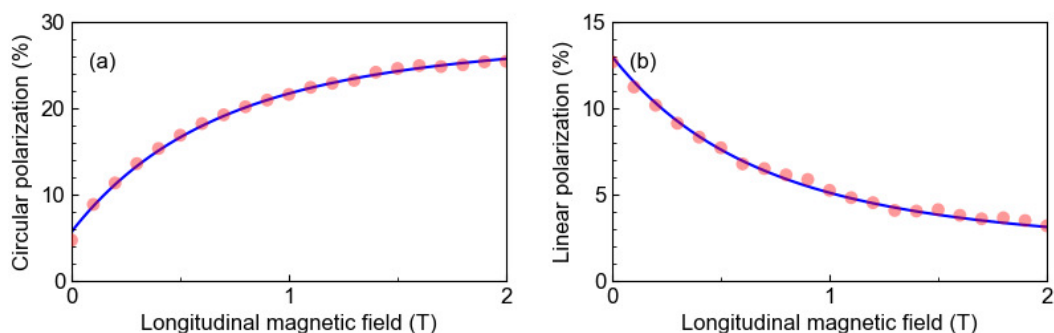


Fig. 1: Polarization spectroscopy of the PL of the sample at $\lambda_{\text{ex}} = 705 \text{ nm}$, $W = 0.6 \text{ W/cm}^2$, $T = 2 \text{ K}$. Curve a: optical orientation $\rho_c^{\sigma^+}(B_F)$; Curve b: optical alignment $\rho_L^\ell(B_F)$. Dots show the experimental data and the lines show the analytical fit.

References

- [1] L. Protesescu, S. Yakunin, *et al.*, *Nano Lett.*, **15**, 3692 (2015).
- [2] R. I. Dzhioev, B. P. Zakharchenya, *et al.*, *JETP Lett.*, **65**, 804 (1997).
- [3] M. O. Nestoklon, S. V. Goupalov, *et al.*, *arXiv:1802.00726* (2018).

Metacage for controllable field distribution in MRI

A. Nikulin, A. Ourir, J. de Rosny

Institut Langevin, CNRS, ESPCI, PSL, 75005 Paris, France

e-mail: a.ourir@espci.fr

MRI is a unique non-ionizing apparatus to survey the anatomy of the body. It becomes unavoidable for many medical applications. Radio frequency (RF) coils are one of the key devices in MRI. They are used to synchronize spins of some nuclei that are precessing at the Larmor frequency under the effect of the strong static magnetic field. They are also used in Rx mode to probe the spin relaxation. Quality of the images strongly depends on the properties of RF coils. At 1.5 T, one of the reference coil to create a homogeneous RF field in a large volume (e.g., brain) is the birdcage [1]. However at 7 T, because wavelength is shorter, the field becomes heterogeneous [1]. To overcome this limitation,

we propose to use a metamaterial to shape the magnetic field. This metacage is directly inspired from the metamaterial interpretation of a birdcage.

Indeed, a birdcage coil can be represented as a classical transmission line that form an annular ring. It is typically composed of 8 up to 32 unit cells. Each of these lasts is made of a resistance (R), an inductance (L) and a capacitance (C). At its fundamental mode (Fig. 1(a)), the phase shift of each unit cell is given by the number of legs N , i.e., $2\pi/N$ [2].

We propose to revisit the birdcage in terms of transmission matrix. The estimation of the eigenmodes and eigenvalues of each unit cell leads to the concept of metacage where the phase shift of each cell can be tuned independently while keeping the transmission line impedance fixed. An analogy with the phase conjugation provides the optimal phase shift distribution to focus the magnetic field in a given region of interest (Fig. 1(b,c)).

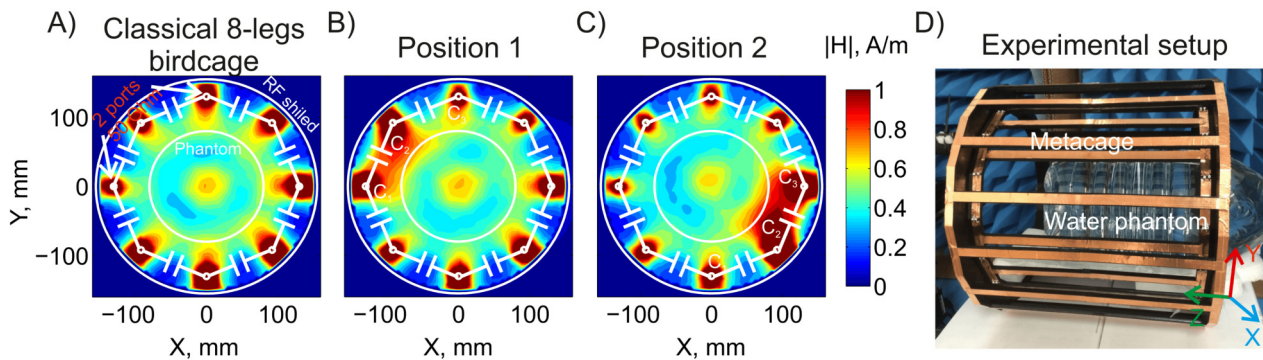


Fig. 1: Distribution of magnetic field magnitude: A — classical 8-legs birdcage coil; B — corresponds to position 1 of other combination L and C ; C — corresponds to position 2; D — photo of experimental setup.

To validate this idea, we have developed a prototype of such a metacage made of 8 unit cells (Fig. 1(d)). It is excited with two 50-Ohm ports connected to two unit cells. We demonstrated numerically with a full wave simulation and experimentally that the magnetic field can be controlled with this approach. This birdcage is well impedance matched ($|S_{11,22}| < -10$ dB) at the desired Larmor frequency (300.1 MHz) of hydrogen 1H at 7 T. Besides, a high level decoupling ($|S_{12}| < -10$ dB) between the 2 ports is reached.

This project has received funding from the European Union’s Horizon 2020 research and innovation program under grant agreement No. 736937.

References

[1] J. T. Vaughan, J. R. Griffiths, *RF Coils for MRI*, John Wiley and Sons Ltd, 2012.
 [2] C. E. Hayes, W. A. Edelstein, J. F. Schenck, O. M. Mueller, M. Eash, An efficient, highly homogeneous radiofrequency coil for whole-body NMR imaging at 1.5 T, *Journal of Magnetic Resonance*, **63**, 622–628 (1985).

Double-tuned birdcage-like coil based on metasurfaces

A. Nikulin¹, A. Ourir¹, J. de Rosny¹, G. Lerosey¹, B. Larrat², F. Kober³, R. Abdeddaim⁴, S. Glybovski⁵

¹Institut Langevin, CNRS, ESPCI, PSL, Paris 75005, France

²DRF/I2BM/Neurospin/UNIRS, 91191 Gif-sur-Yvette Cedex, France

³Aix-Marseille University, CNRS, CRMBM, UMR 7339, Marseille, France

⁴Aix Marseille University, CNRS, Centrale Marseille, Institut Fresnel, 13013 Marseille, France

⁵ITMO University, St. Petersburg 197101, Russia e-mail: anton.nikulin@espci.fr

In this work, we propose an original dual band volume coil for two nuclei preclinical MRI application. It has been shown previously that coupling of loop feed with hybridized coupled resonators

can improve the Radio frequency (RF) field homogeneity and signal-to-noise ratio (SNR) in the case of single nuclei application [1]. Such structure has been proposed later for the realization of a surface coil that operates at two independent frequencies providing independent tuning and matching [2]. In this paper, we propose a volume receive/transmit MRI antenna based on two independent metasurfaces that can be used simultaneously for fluorine and hydrogen $^{19}\text{F}/^1\text{H}$ imaging at 7 Tesla small animal. The proposed two-band coil can be tuned independently for the desired resonant frequencies by adjusting the length of the two sets of wires. This approach of tuning avoids the use of additional electronic circuits losses. Our design avoids fundamental limitations related to the efficiency of classical two-band birdcages working as combination of low-pass and high-pass birdcages for high field MRI applications [3]. Such two-band birdcages work well only in the application with low- γ and high- γ nuclei, for instance $^{31}\text{P}/^1\text{H}$, i.e. for low and high Larmor-frequency nuclei simultaneously [3].

The proposed double-tuned coil is based on the merging of two metasurfaces. Each metasurface made of non-magnetic metallic rods and capacitors. The capacitors are etched on the low loss dielectric substrate. The geometry is chosen in order that modes of the two metasurfaces should be resonant at the almost desired frequencies (282.6/300.1 MHz). The coarse tuning of the resonant frequencies is achieved by changing the length of wires. But it is still necessary to use a matching circuit that is required to achieve the exact frequencies and the good matching level ($|S_{11}| < -10$ dB). We have numerically and experimentally validated the concept of the proposed double-tuned coil based on metasurfaces for ($^{19}\text{F}/^1\text{H}$) MRI at 7 Tesla.

This project has received funding from the European Union's Horizon 2020 research and innovation program under grant agreement No. 736937.

References

- [1] C. Jouvaud, R. Abdeddaim, B. Larrat, J. de Rosny, Volume coil based on hybridized resonators for magnetic resonance imaging, *Applied Physics Letters*, **108**, 023503 (2016).
- [2] A. Hurshkainen, A. Nikulin, S. Glybovski, R. Abdeddaim, C. Vilmen, S. Enoch, I. Melchakova, P. Belov, D. Bendahan, A metamaterial-inspired MR antenna independently tunable at two frequencies, *Metamaterials, 11th International Conference*, 115–117 (2017).
- [3] J. T. Vaughan, J. R. Griffiths, *RF Coils for MRI*, John Wiley and Sons Ltd, 2012.

Parity-Time-Symmetric Optics, extraordinary momentum and spin in evanescent waves, and the quantum spin Hall effect of light

Franco Nori

RIKEN, Saitama, Japan; The University of Michigan, Ann Arbor, USA
e-mail: fnori@riken.jp

This talk provides a brief and pedagogical overview to parity-time-symmetric optics, extraordinary momentum and spin in evanescent waves, and the quantum spin Hall effect of light.

1. *Parity-Time-Symmetric Optics*. Optical systems combining balanced loss and gain provide a unique platform to implement classical analogues of quantum systems described by non-Hermitian parity-time (PT)-symmetric Hamiltonians [1–7]. Such systems can be used to create synthetic materials with properties that cannot be attained in materials having only loss or only gain. We report PT-symmetry breaking in coupled optical resonators. We observed non-reciprocity in the PT-symmetry-breaking phase due to strong field localization, which significantly enhances nonlinearity. In the linear regime, light transmission is reciprocal regardless of whether the symmetry is broken or unbroken. We show that in one direction there is a complete absence of resonance peaks whereas in the other direction the transmission is resonantly enhanced, which is associated with the use of resonant structures. Our results could lead to a new generation of synthetic optical systems enabling on-chip manipulation and control of light propagation.

2. *The quantum spin Hall effect of light: photonic analog of 3D topological insulators.* Maxwell's equations, formulated 150 years ago, ultimately describe properties of light, from classical electromagnetism to quantum and relativistic aspects. The latter ones result in remarkable geometric and topological phenomena related to the spin-1 massless nature of photons. By analyzing fundamental spin properties of Maxwell waves, we show [8] that free-space light exhibits an intrinsic quantum spin Hall effect — surface modes with strong spin-momentum locking. These modes are evanescent waves that form, for example, surface plasmon-polaritons at vacuum-metal interfaces. Our findings illuminate the unusual transverse spin in evanescent waves and explain recent experiments that have demonstrated the transverse spin-direction locking in the excitation of surface optical modes. This deepens our understanding of Maxwell's theory, reveals analogies with topological insulators for electrons, and offers applications for robust spin-directional optical interfaces. Related work can be found in [9–18].

References

- [1] B. Peng, et al., Parity-time-symmetric whispering-gallery microcavities, *Nature Physics*, **10**, 394–398 (2014).
- [2] B. Peng, et al., Loss-induced suppression and revival of lasing, *Science*, **346**, 328 (2014).
- [3] B. Peng, et al., What is and what is not electromagnetically induced transparency in whispering-gallery microcavities, *Nature Communications*, **5**, 5082 (2014).
- [4] H. Jing, Ş. K. Özdemir, X. Y. Lu, J. Zhang, L. Yang, F. Nori, PT-Symmetric Phonon Laser, *Phys. Rev. Lett.*, **113**, 053604 (2014).
- [5] F. Monifi, et al., Optomechanically induced stochastic resonance and chaos transfer between optical fields, *Nature Photonics*, **10**, 399–405 (2016).
- [6] Z. P. Liu, et al., Metrology with PT-symmetric cavities: enhanced sensitivity near the PT-phase transition, *Phys. Rev. Lett.*, **117**, 110802 (2016).
- [7] D. Leykam, K. Y. Bliokh, C. Huang, Y. D. Chong, F. Nori, Edge modes, degeneracies, and topological numbers in non-Hermitian systems, *Phys. Rev. Lett.*, **118**, 040401 (2017).
- [8] K. Y. Bliokh, D. Smirnova, F. Nori, Quantum spin Hall effect of light, *Science*, **348**, 1448–1451 (2015); Highlighted in a Perspectives [*Science*, **348**, 1432 (2015)].
- [9] K. Y. Bliokh, F. Nori, Transverse spin of a surface polariton, *Phys. Rev. A*, **85**, 061801 (2012).
- [10] K. Y. Bliokh, A. Y. Bekshaev, F. Nori, Dual electromagnetism: helicity, spin, momentum, and angular momentum, *New J. Phys.*, **15**, 033026 (2013).
- [11] K. Y. Bliokh, J. Dressel, F. Nori, Conservation of the spin and orbital angular momenta in electromagnetism, *New J. Phys.*, **16**, 093037 (2014).
- [12] J. Dressel, K. Y. Bliokh, F. Nori, Space-time algebra as a powerful tool for electromagnetism, *Physics Reports*, **589**, 1–71 (2015).
- [13] K. Y. Bliokh, Y. S. Kivshar, F. Nori, Magnetoelectric effects in local light-matter interactions, *Phys. Rev. Lett.*, **113**, 033601 (2014).
- [14] K. Y. Bliokh, A. Y. Bekshaev, F. Nori, Extraordinary momentum and spin in evanescent waves, *Nature Communications*, **5**, 3300 (2014).
- [15] A. Y. Bekshaev, K. Y. Bliokh, F. Nori, Transverse spin and momentum in two-wave interference, *Phys. Rev. X*, **5**, 011039 (2015).
- [16] K. Y. Bliokh, F. Nori, Transverse and longitudinal angular momenta of light, *Physics Reports*, **592**(26), 1–38 (2015).
- [17] K. Y. Bliokh, F. J. Rodriguez-Fortuno, F. Nori, A. V. Zayats, Spin-orbit interactions of light, *Nature Photonics*, **9**, 796–808 (2016).
- [18] M. Antognozzi, et al., Direct measurements of the extraordinary optical momentum and transverse spin-dependent force using a nano-cantilever, *Nature Physics*, **12**, 731–735 (2016).

Optical coupling between dielectric Mie-resonant nanodisks and waveguides probed by third harmonic generation microscopy

Okhlopkov K.I.¹, Ezhov A.A.¹, Shafirin P.A.¹, Orlikovsky N.A.², Shcherbakov M.R.^{1,3}, Fedyanin A.A.¹

¹Faculty of Physics, Lomonosov Moscow State University, 19991 Moscow, Russia

²Bauman Moscow State Technical University, 105005 Moscow, Russia

³School of Applied and Engineering Physics, Cornell University, Ithaca, 14853 NY, USA

e-mail: okhlopkov@nanolab.phys.msu.ru, alexander-ezhov@yandex.ru,

shafirin@nanolab.phys.msu.ru, orlikovskiy-na@bmstu.ru,

shcherbakov@nanolab.phys.msu.ru, fedyanin@nanolab.phys.msu.ru

Subwavelength dielectric and semiconductor nanostructures made of high-refractive-index materials possess strong Mie-type resonances at the visible and near-infrared spectral ranges [1]. Under resonant conditions, electromagnetic fields are tightly confined inside these structures. This leads to the enhancement of nonlinear effects by several orders of magnitude compared with those in bulk materials [2].

Although the optical properties of Mie-resonant nanoparticles combined into oligomers with different numbers of particles have been extensively studied [3], the investigation of optical coupling between a single subwavelength dielectric nanoparticle and the core element of integrated nanophotonics — a silicon waveguide — has been lacking so far. In this contribution, we demonstrate optical coupling between single silicon nanoparticles and dielectric waveguides using third harmonic generation (THG) microscopy.

The proposed “silicon nanodisk – waveguide” pairs were fabricated out of a silicon-on-insulator (SOI) wafer with a thickness of the top silicon layer of 280 nm. The chosen diameters of the nanodisks are 380, 430 and 480 nm, the distances between the nanodisks and the waveguides are 105, 185 and 320 nm, the width of the waveguides is 435 nm. For third harmonic generation microscopy, we used a laser scanning confocal microscope complemented by a femtosecond Er³⁺ fiber laser with a pulse duration of 120 fs, a pulse repetition rate of 70 MHz, a central wavelength of 1545 nm, and a width of the spectrum of 40 nm. The proposed system was investigated under two polarisations of the incident light — when the electric field is orthogonal and parallel to the waveguide. It has been found that the nanodisks with a diameter of 480 nm resonantly enhance the THG due to the excitation of the magnetic dipole resonance at a wavelength of 1545 nm. The maximum enhancement of 26 is achieved when the nanodisk is located at a distance of 185 nm from the waveguide. If the gap between the nanodisk and the waveguide is changed from 185 nm to 105 nm, the THG enhancement is drastically decreased by a factor of 4.5. Using linear and nonlinear finite-difference time-domain simulations, it has been shown that the dependence of the THG signal on the gap size arises from the modification of local fields and radiative losses of the system. We have also shown that the magnetic dipole resonance is shifted by up to 15 nm, when the gap size is varied. This is a clear evidence of the optical coupling between the nanodisk and the waveguide and this study is a new important step toward application of all-dielectric nanoparticles for photonic chips.

References

- [1] A. I. Kuznetsov, A. E. Miroshnichenko, Y. H. Fu, J. Zhang, B. S. Luk'yanchuk, *Magnetic light*, *Sci. Rep.*, **2**, 492 (2012).
- [2] M. R. Shcherbakov, D. N. Neshev, B. Hopkins, A. S. Shorokhov, I. Staude, E. V. Melik-Gaykazyan, M. Decker, A. A. Ezhov, A. E. Miroshnichenko, I. Brener, A. A. Fedyanin, Y. S. Kivshar, *Enhanced third-harmonic generation in silicon nanoparticles driven by magnetic response*, *Nano Lett.*, **14**, 6488–6492 (2014).
- [3] A. E. Miroshnichenko, Y. S. Kivshar, *Fano resonances in all-dielectric oligomers*, *Nano Lett.*, **12**, 6459–6463 (2012).

All-dielectric metasurfaces for unconventional scattering

Willie J. Padilla, Andrew Cardin, Kebin Fan

Department of Electrical and Computer Engineering, Duke University, USA

e-mail: willie.padilla@duke.edu

Metamaterials formed from a single functional layer — termed metasurfaces — have been shown using metal-insulator-metal, metal-insulator, and all-dielectric materials. Here we experimentally demonstrate all-dielectric metasurfaces which realize high variable transmission with a large phase. Further we shown the ability of all-dielectric metasurfaces to achieve high absorption within the same structure, with only a moderate change in material loss.

Arrays of dielectric cylinders support two fundamental dipole active eigenmodes, which can be manipulated to elicit a variety of electromagnetic responses in all-dielectric metamaterials [1]. Dissipation is a key parameter that determines the functionality. We show that through altering the material loss, DMSs may exhibit high transmission large phase advance characteristics of importance for construction of Huygens' metasurfaces. Further, with a small amount of loss added, the DMS may operate as a high absorber of electromagnetic radiation [2]. We show the broad versatility of the all-dielectric metasurface systems using semiconductor as the base material, and demonstrate that strongly different properties may be obtained dynamically through photodoping.

Figure 1 shows an optical microscope image of an array of cylindrical resonators. The geometry has been tuned to achieve both an electric and magnetic dipole like mode at terahertz (THz) frequencies [2]. The right panel of Fig. 1 shows the simulated transmission as a function of frequency for a number of different silicon doping densities, ranging from zero doping (blue curve) to $n = 1.6 \times 10^{15} \text{ cm}^{-3}$ (red curve). We will present experimental verification of simulated results shown in Fig. 1, and show that similar results can be obtained dynamically through photodoping. The physics underlying the DMSs is shown to be well described by temporal coupled mode theory.

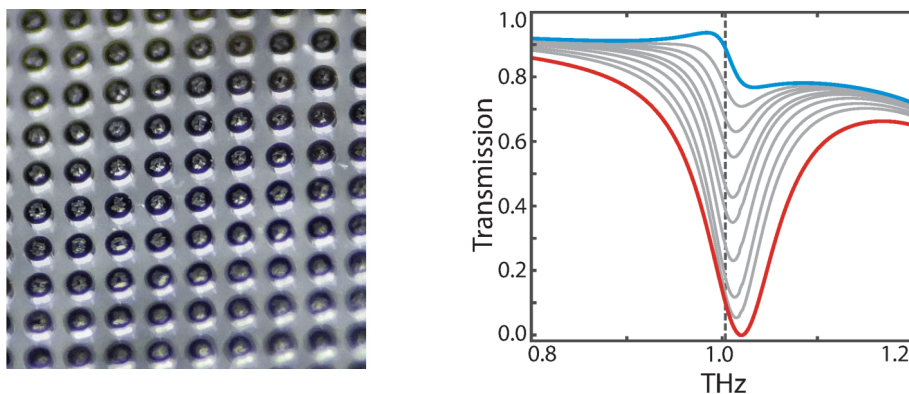


Fig. 1: Left panel shows a microscope image of a square array of cylindrical resonators fashioned from silicon. Right panel shows the simulated transmission as a function of frequency for a number of different silicon doping densities, ranging from zero doping (blue curve) to $n = 1.6 \times 10^{15} \text{ cm}^{-3}$ (red curve).

Acknowledgements. This work was funded by a grant from the Department of Energy (DOE) DE-SC0014372.

References

- [1] X. Ming, X. Liu, L. Sun, W. J. Padilla, Degenerate critical coupling in all-dielectric metasurface absorbers, *Optics Express*, **25**, 24658–24669 (2017).
- [2] X. Liu, K. Fan, I. V. Shadrivov, W. J. Padilla, Experimental realization of a terahertz all-dielectric metasurface absorber, *Optics Express*, **25**, 191–201 (2017).

Reversible light-by-light control through a giant ac Stark effect in a strongly coupled light-matter system

Dmitry Panna¹, Nadav Landau¹, Leonid Rybak¹, Shai Tsesses¹, Guy Adler¹, Sebastian Brodbeck², Christian Schneider², Sven Hofling², Alex Hayat¹

¹Department of Electrical Engineering, Technion, Haifa 32000, Israel

²Technische Physik, Universität Würzburg, Am Hubland, D-97074 Würzburg, Germany

e-mail: alex.hayat@ee.technion.ac.il

Changing photon energy by photons enables a wide range of nonlinear and quantum-optical studies. However, this energy conversion is based on low-efficiency multiphoton transitions in weak light-matter coupling. Once the photon energy has been changed the reverse process, in which photon gives the obtained energy back to the system, required for true photon-by-photon control, is extremely unlikely. Strong light-matter coupling imparts light properties to matter for high-temperature quantum condensation and matter properties to light for photon-photon interaction. Reversible control of matter energy levels by light is widely used through a noninvasive ac Stark effect. Nevertheless, in strongly coupled light-matter systems, the recently observed small ac Stark shift was indistinguishable from the shift of the uncoupled matter energy level. We demonstrate reversible control of photon energy by photon via a giant ac Stark in a specially designed strongly-coupled microcavity. The observed shift, larger than Rabi energy, sheds new light on photon-photon interaction and paves the way for all-optical quantum technologies.

Self-assembling of ordered domains of silver nanoparticles into the mordenite channel system

V. Petranovskii¹, Y. Kotolevich¹, S. Miridonov², P. Sánchez-Lopez¹, F. Chávez-Rivas³, R. Machorro¹, S. Fuentes¹

¹Universidad Nacional Autónoma de México, Centro de Nanociencias y Nanotecnología, Apdo. Postal 14, C.P. 22800, Ensenada, B. C., México

²Departamento de Óptica, Centro de Investigación Científica y de Educación Superior de Ensenada. C.P. 22860, Ensenada, B. C., México

³Departamento de Física, ESFM-Instituto Politécnico Nacional, México D.F., 07738, México

e-mail: vitalii@cnyunam.mx

In this work, zeolite of the mordenite type with a molar ratio ($\text{SiO}_2/\text{Al}_2\text{O}_3$) of 13 was selected to prepare monometallic (Ag or Fe) and bimetallic (Fe/Ag) systems. Ag and Fe ions were introduced by the ion exchange method from aqueous solutions of AgNO_3 and FeSO_4 at a concentration of 0.03 N. The materials were characterized by XRD for the evaluation of phase crystallinity, the chemical composition of the samples was determined by the EDS and ICP technique, the type of metal species was identified by UV Vis spectroscopy, the surface area was calculated by the BET method and the morphology was studied on TEM micrographs. Diffraction patterns shows the changes such as decrease intensity of some mordenite peaks and the addition of others corresponding to metallic silver. The UV-Vis showed that the monometallic (Ag or Fe) and bimetallic (Fe/Ag) systems have an absorption below 230 nm, corresponding to the electronic transition of the isolated ion Ag^+ , and the presence of a band 278 nm which can be attributed to the charge transfer of Fe^{3+} or Fe^{2+} oxides. The TEM micrographs revealed that the presence of Fe in the Ag/MOR system does not allow for extensive Ag agglomeration; while the ordered domains of silver nanoparticles of the same size were observed. This phenomenon confirms the inherent property of zeolite in the directing and assembling the superstructures.

Emission enhancement in dielectric nanocomposites

Alexander Yu. Petrov^{1,2}, Dirk Jalas¹, K. Marvin Schulz¹, Manfred Eich³

¹Institute of Optical and Electronic Materials, Hamburg University of Technology (TUHH), Eißendorfer Straße 38, 21073 Hamburg, Germany

²ITMO University, 49 Kronvervskii Ave., 197101, St. Petersburg, Russia

³Institute of Materials Research, Helmholtz-Zentrum Geesthacht, Max-Planck-Strasse 1, Geesthacht, D-21502, Germany

e-mail: a.petrov@tuhh.de

Metal-dielectric hyperbolic metamaterials can show a significant emission enhancement due to a large local density of states [1]. At the same time, extraction of radiation emitted into a hyperbolic met-amaterial is limited by absorption in the metal and light trapping in the hyperbolic medium due to emission into high-k-vector modes. Alternatively, dielectric metamaterials are discussed [2]. Here we investigate the Purcell enhancement for emitters in dielectric nano composites, where the active material compound is incorporated inside a high-index dielectric host medium [3]. We show, by means of numerical simulations supported by an analytic model, that the radiative decay in such dielectric nanocomposites is greatly affected by the shape and arrangement of its constituents. We find that for the same filling fractions of constituting materials, the radiative decay rate can differ by orders of magnitude. E.g. for the case of diluted luminescent nanoparticles with refractive index of 1.43 inside a host with refractive index of 3.5, we show broadband Purcell factors of up to 40, which is of the same order as what can be achieved by narrowband resonant effects with deliberately patterned high Q dielectric resonators. Further, we investigate the spatial distribution of Purcell factors in active nanocomposites. We present a simple analytic model to calculate the average Purcell factor in arbitrary 3D composites based on the reciprocity theorem and a quasistatic approximation. It is shown that in dielectric nanocomposites the low-index active compound should occupy gaps between high index particles to achieve maximal Purcell enhancement. As shown in Fig. 1, even when structuring composites with 50/50% mixture of active compound and high index material a significant average Purcell enhancement in the order of 5 is observed (Fig. 1b) which is going beyond the pure increase of the average refractive index (Fig. 1a). The presented composites are optically isotropic.

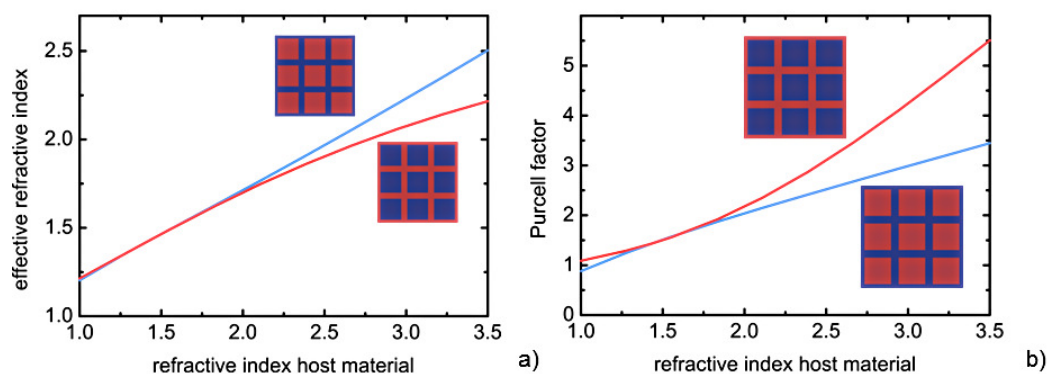


Fig. 1: (a) Effective refractive index of 3D composite structure employing both 50 vol% of the low-refractive index active compound ($n = 1.43$) and 50 vol% of host material versus refractive index of host material. The emitting material is shown in red, the host material in blue. (b) Purcell factor for the emitter in the low index active material vs refractive index of the host material. (blue line: active material is inside the cubes, red line: active material outside the cubes.)

References

- [1] A. N. Poddubny, P. A. Belov, Y. S. Kivshar, Spontaneous radiation of a finite-size dipole emitter in hyperbolic media, *Phys. Rev. A*, **84**, 23807 (2011).

- [2] S. Jahani, Z. Jacob, All-dielectric metamaterials, *Nature Nanotechnology*, **11**, 23 (2016).
- [3] D. Jalas, K. M. Schulz, A. Petrov, M. Eich, Emission enhancement in dielectric nanocomposites, in review at *Opt. Express*; *arXiv:1710.06833* [physics.optics].

Visualization of elliptic and hyperbolic dispersion regimes of guided optical modes in all-dielectric metasurface

Pidgayko D., Sinev I., Permyakov D., Samusev A., Sychev S., Bogdanov A., Lavrinenko A.
ITMO University, 49 Kronverksky Pr., St. Petersburg, 197101, Russia
e-mail: d.pidgayko@metalab.ifmo.ru

Rutckaia V., Schilling J.

ZIK SiLi-nano, Karl-Freiherr-von-Fritsch-Strasse 3 D - 06120 Halle (Saale), Germany

Metasurfaces are two-dimensional analogues of metamaterials, are capable of providing unprecedented control over light polarization, propagation direction, phase, amplitude, wave front, etc. The main advantage of metasurfaces over bulk metamaterials is compatibility with modern planar fabrication technologies, which facilitates their implementation in optoelectronics [1].

Hyperbolic metasurfaces attract special interest. Negative curvature of the isofrequency contours of modes in hyperbolic regime leads to manifestation of a number of interesting phenomena such as negative refraction, Purcell effect, channeling etc. Several possible realizations of hyperbolic metasurfaces have been proposed recently, e.g. subwavelength plasmonic grating [2], or 2D array of plasmonic elliptic nanoparticles [3, 4]. The main drawback of these systems is high absorption in plasmonic materials, which leads to limited propagation length of surface waves. The problem of high losses can be solved by using all-dielectric materials. However, until now hyperbolic dispersion regime for guided modes in all-dielectric structures has not been investigated. Moreover, methods of direct imaging of isofrequency contours for modes below the light cone have not been used.

In this work, we investigate all-dielectric anisotropic subwavelength grating based on silicon on insulator platform. The modes excited in this structure demonstrate both hyperbolic and elliptic behavior dispersion regimes in different wavelength ranges. We directly image the isofrequency contours for different wavelengths and polarization of the excitation using a back focal plane microscope with high NA objective combined with solid ZnSe immersion lens [5]. This unique setup allows to excite surface waves in the metasurface via frustrated total internal reflection mechanism. After obtaining the isofrequency contours in broad spectral range (700–1100 nm), we reconstruct the full dispersion surface $\omega(k_x, k_y)$. The reconstructed pattern unambiguously reveal both elliptic and hyperbolic dispersion regimes characterized by different curvatures of the isofrequency surface.

To conclude, we showed that the setup for back focal plane microscopy combined with solid immersion lens is a universal tool for the experimental characterization of dispersion of surface modes in metasurfaces. Using it, we demonstrated that all-dielectric anisotropic metasurface supports surface waves with both hyperbolic and elliptic dispersion regimes.

References

- [1] S. B. Glybovski, S. A. Tretyakov, P. A. Belov, Yu. S. Kivshar, C. R. Simovski, Metasurfaces: From microwaves to visible, *Physics Reports*, **634**, 1–72 (2016).
- [2] A. A. High, R. C. Devlin, A. Dibos, M. Polking, D. S. Wild, J. Percel, N. P. de Leon, M. D. Lukin, H. Park, Visible-frequency hyperbolic metasurface, *Nature*, **522**, 192–196 (2015).
- [3] O. Y. Yermakov, A. I. Ovcharenko, M. Song, A. A. Bogdanov, I. V. Iorsh, Yu. S. Kivshar, Hybrid waves localized at hyperbolic metasurfaces, *Physical Review B*, **91**, 235423 (2015).
- [4] A. Samusev, I. Mukhin, R. Malureanu, O. Takayama, D. V. Permyakov, I. S. Sinev, D. Baranov, O. Yermakov, I. V. Iorsh, A. A. Bogdanov, A. V. Lavrinenko, Polarization-resolved characterization of plasmon waves supported by an anisotropic metasurface, *Optics Express*, **25**(26), 32631–32639 (2017).

- [5] D. V. Permyakov, I. S. Sinev, S. K. Sychev, A. S. Gudovskikh, A. A. Bogdanov, A. V. Lavrinenko, A. K. Samusev, Visualization of isofrequency contours of strongly localized waveguide modes in planar dielectric structures, *JETP Letters*, **107**(1), 10–14 (2018).

Routing emission of plasmons by a magnetic field

Poddubny A.N.

Ioffe Institute, 194021 St. Petersburg, Russia

e-mail: poddubny@coherent.ioffe.ru

Magneto-optical phenomena such as the Faraday and Kerr effects play a decisive role for establishing control over polarization and intensity of optical fields propagating through a medium. Intensity effects where the direction of light emission depends on the orientation of the external magnetic field are of particular interest as they can be used for routing the light.

In this work we report on a new class of transverse emission phenomena for light sources located in the vicinity of a surface, where directionality is established perpendicularly to the externally applied magnetic field [1], see the Fig. 1. We demonstrate the routing of emission for excitons in a diluted-magnetic-semiconductor quantum well. The directionality is significantly enhanced in hybrid plasmonic semiconductor structures due to the generation of plasmonic spin fluxes at the metal-semiconductor interface. Indeed, subwavelength optical fields possess strong transverse spin locked to their propagation direction, enabling photonic and plasmonic spin Hall effects [2] and boosting the transverse emission directionality.

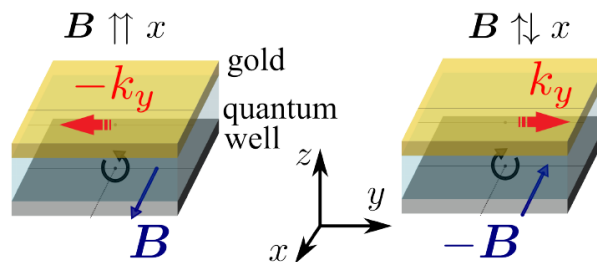


Fig. 1: Scheme of plasmon emission in a gold layer on top of a quantum well and their routing by a transverse magnetic field.

References

- [1] F. Spitzer, A. N. Poddubny, I. A. Akimov, V. F. Sapega, L. Klompmaker, L. E. Kreilkamp, L. V. Litvin, R. Jede, G. Karczewski, M. Wiater, T. Wojtowicz, D. R. Yakovlev, M. Bayer, *arXiv*: 1712.05703 (2017).
- [2] P. Lodahl, S. Mahmoodian, S. Stobbe, A. Rauschenbeutel, P. Schneeweiss, J. Volz, H. Pichler, P. Zoller, *Nature*, **541**, 473–480 (2017).

Bound state in the continuum supported by a low refractive index contrast waveguide in a woodpile structure

L.Yu. Pogorelskaya, A.A. Bogdanov, K.B. Samusev, A.D. Sinelnik

The International Research Centre for Nanophotonics and Metamaterials, ITMO University, St. Petersburg 197101, Russia

e-mail: lydia.pogorelskaya@metalab.ifmo.ru

In traditional resonators, for example, those that employ the whispering gallery mode effect, high refractive index contrast between the waveguide and the claddings material is essential to obtain high quality factor. We propose a resonator with Q-factor, which does not depend on refractive index

contrast because it is based on bound states in the continuum (BICs). These states remain localized due to destructive interference rather than total internal reflection. BICs are states with energies lying within the radiation modes continuum (above the light line in optical systems), in theory they have infinite quality factor. BICs were first described theoretically by von Neumann and Wigner in 1929 [1] for artificial quantum system; active research on BICs in optical systems is conducted actively in the last ten years both theoretically and experimentally. There are theoretical examples of a BIC-based waveguide with low refractive index on a high index thin membrane [2] and of BIC existing in fiber Bragg gratings with vanishing index contrast [3].

In our work we analyze BIC in the woodpile structure composed of waveguide layer with higher effective refractive index (~ 1.4) on top of several layers with lower effective index (~ 1.2) on SiO₂ substrate. If we consider such waveguide suspended in air, symmetry protected BIC is observed in Γ -point, the zeroth diffraction channel is forbidden due to destructive interference. However, higher order diffraction channels (that are not forbidden) may be opened in high index substrate, thus enabling leakage and destroying BIC [4]; we use layers with low effective refractive index to isolate waveguide from the substrate. The design of the structure was developed numerically using Fourier modal method (FMM). Samples were realized experimentally using 3D laser lithography (direct laser writing).

We demonstrate high-Q resonator based on BIC in a woodpile structure. This structure opens a path for realizing promising BIC states in polymer structures fabricated by such perspective and fast technique as direct laser writing.

This work was supported by the Russian Foundation for Basic Research (16-37-60064, 17-02-01234), the Ministry of Education and Science of the Russian Federation (3.1668.2017/4.6), the President of Russian Federation (MK-403.2018.2).

References

- [1] J. von Neumann, E. Wigner, Über merkwürdige diskrete Eigenwerte, *Phys. Z.*, **30**, 465–467 (1929).
- [2] C. L. Zou, Guiding light through optical bound states in the continuum for ultrahigh-Q microresonators, *Laser Photonics Rev.*, **9**(1), 114–119 (2015).
- [3] X. Gao, et al., Bound states in the continuum in low-contrast fiber Bragg gratings, *arXiv:1707.01247*, (2017).
- [4] Z. F. Sadrieva, et al., Transition from optical bound states in the continuum to leaky resonances: role of substrate and roughness, *ACS Photonics*, **4**(4), 723–727 (2017).

Inherently nonreciprocal: nonlinear nanomaterials

Poutrina E.^{1,2}, **Urbas A.M.**¹

¹Materials and Manufacturing Directorate, Air Force Research Laboratory, WPAFB, Ohio, USA

²UES, Inc., 4401 Dayto-Xenia Road, Dayton, OH 45432, USA

e-mail: epoutrina@ues.com

We show that nonlinear multipole interference allows a nonreciprocal directionality of nonlinear generation from a nanoelement, with the generation direction decoupled from the direction of the excitation beam. Alternatively, a tailored design of the effective nonlinear polarizabilities of a nanoelement can ensure directionally selective inhibition of a given nonlinear process. We attribute the presented phenomena to the existence of shared (electric or magnetic) ‘pathways’ when inducing the electric and magnetic Mie resonances via a nonlinear interaction. These shared pathways allow a simultaneous phase change of *all* (electric *and* magnetic) nonlinearly generated multipoles when switching the phase of *a single* (electric *or* magnetic) vector of the fundamental field [1, 2]. We discuss that, in the case of nonlinear response, an interference can occur not only between electric and magnetic multipolar modes, but also between various effective hyperpolarizability terms *within* each

of these modes. As a result, non-reciprocity just in terms of a change in the efficiency of nonlinear generation, when reversing any subset of the fundamental beams, is inherent to and expected in the nonlinear response of most nanoelements, even symmetric ones, and for most of the nonlinear processes. Both non-reciprocal directionality and inhibition of a nonlinear process require engineering of a) the relative strengths of nonlinear electric and magnetic multipolar modes of a nanoelement and b) the relative strengths of various terms within each of these modes. This balance of strengths and the resulting phenomena are not expected to occur in the nonlinear response of natural materials but, as we reveal, can be realistically achieved by designing the nonlinear multipolar response of nanostructures. We demonstrate the introduced concept both numerically and experimentally using plasmonic dimer geometries and patterned LiNbO₃ films. The proposed concept offers the flexibility of achieving all the explored phenomena via the response of sub-wavelength elements, which can then be used as building blocks in developing a nonlinear medium with similar, inherently incorporated, unique features. As a numerical example, we demonstrate a metasurface formed by a planar arrangement of such non-reciprocal optical antennas, acting as a one-way nonlinear mirror (Fig. 1).

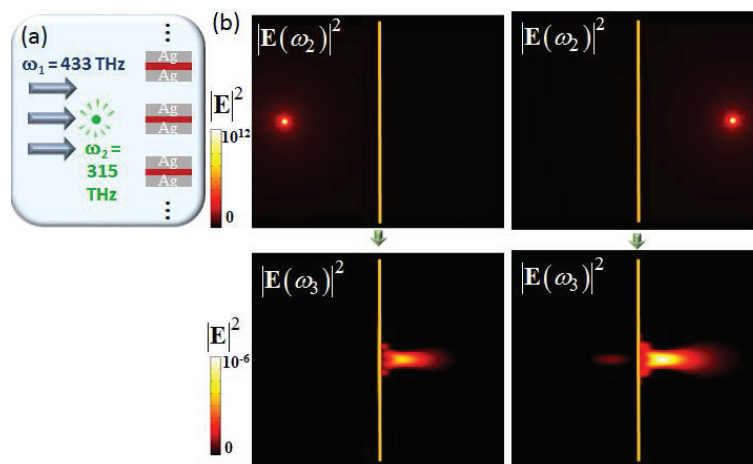


Fig. 1: Metasurface operating as a one-way nonlinear mirror. (a) Simulations geometry. (b) An image of the source at frequency ω_2 is nonlinearly generated at frequency $\omega_3 = \omega_1 - \omega_2$ on the same side of the metasurface (yellow line) independently of the source location.

References

- [1] E. Poutrina, A. M. Urbas, *Sci. Rep.*, **6**, 25113–6 (2016).
- [2] E. Poutrina, A. M. Urbas, *J. of Optics*, **16**, 114005–15 (2014).

Synthesis of high-quality CsPbBr₃ nanolasers at ambient conditions

Pushkarev A.P.¹, Korolev V.I.¹, Markina D.I.¹, Komissarenko F.E.¹, Sannikov D.A.², Zasedatelev A.V.², Lagoudakis P.G.², Zakhidov A.A.¹, Makarov S.V.¹

¹Department of Nanophotonics and Metamaterials, ITMO University, St. Petersburg, Russia

²Skolkovo Institute of Science and Technology, Moscow, Russia

e-mail: anatoly.pushkarev@metalab.ifmo.ru

Since the breakthrough reports dedicated to utilization of MAPbI₃ material for efficient photoconversion in solar cells, researchers working in the field of organic electronics and dielectric nanophotonics have been discovering new applications of lead halide perovskites. One of the recent cutting-edge applications is perovskite nanowires generating laser emission in the broad spectral range 420–800 nm [1, 2] that can be exploited for the development of photonic chips capable of super fast information processing. Although such nanowires have already demonstrated lasing with very low excitation threshold 0.22–40 $\mu\text{J cm}^{-2}$, high cavity quality factor ($Q = 1500\text{--}3600$) and short radiative decay ($\tau \approx 20$ ps), there are some problems with their fabrication and operation stability as

well as many questions regarding the mechanism of their functioning. The issue related to production of the nanowires stems from the methods of synthesis presented in the literature. To the best of our knowledge they can be grown as a dense nanoforest onto substrates covered by PEDOT:PSS thin film in alcohol solution or by means of metal halides thermal coevaporation in argon atmosphere. Further optical characterization and practical application of the individual nanolasers requires their separation and careful transfer to the auxiliary substrate. The reshaping caused to the nanowires (especially very long ones with lengths larger than 10 μm) during these procedures dramatically decreases their performance. Furthermore, the wet synthesis presented in previous works was conducted in N_2 -filled glove box for 12–24 h that makes it non-convenient for large scale fabrication.

Herein we report the rapid production of separated nanowires onto bare ITO-coated glass substrate at ambient conditions. CsPbBr_3 in DMSO was spin-casted onto the substrates and then treated with antisolvent vapor to give the wide dispersion of the whiskers with lengths from 5 to 50 μm and different aspect ratio (Fig. 1a). SEM images of the samples confirm the formation of well-shaped objects with orthorhombic facets (Fig. 1b). The measured under pulse laser excitation ($\lambda = 400 \text{ nm}$, $\tau = 100 \text{ fs}$) 11 μm nanowires showed laser generation with high $Q = 2200$ and relatively low excitation threshold (Fig. 1c,d).

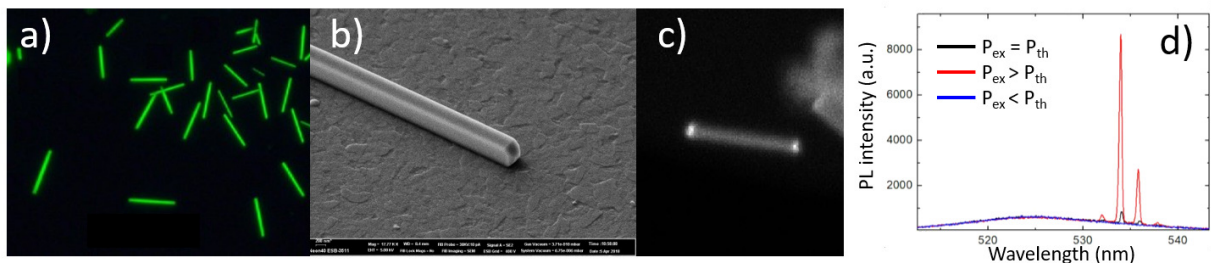


Fig. 1: Fluorescent image of nanowhiskers (a), SEM image (b), 11 μm nanolaser in action (c), PL spectra (d).

References

- [1] H. Zhu, et al., *Nature Mater.*, **14**, 636 (2015).
- [2] K. Park, et al., *J. Phys. Chem. Lett.*, **7** 3703 (2016).

Metamaterial based enhancements of RF-coils for ultra high-field magnetic resonance imaging

Andreas Rennings, Zhichao Chen, Benedikt Sievert, Jan Taro Svejda, Daniel Erni

General and Theoretical Electrical Engineering (ATE), Faculty of Engineering, University of Duisburg-Essen, 47048 Duisburg, Germany

e-mail: andre.rennings@uni-due.de

In this contribution we summarize our research in the field of metamaterial based enhancements of RF-coils for ultra high-field magnetic resonance imaging (UHF-MRI). Over the years, we proposed several metamaterial based RF-coils or antennas for UHF-MRI. The approaches can be divided into two general concepts, a first one, where the coil itself is a 1-D metamaterial structure, and a second one, where the RF-shield behind a conventional loop coil or dipole antenna is a 2-D metamaterial structure, also called metasurface. The first approach, where the coil itself is a periodic structure, namely a composite right/left-handed (CRLH) meta-line, is strongly related to the so-called dispersion engineering [1]. The additional degrees of freedom in the CRLH unit cell design can be utilized to obtain tailored current distributions that are required to excite the desired RF electromagnetic fields. The dispersion of a CRLH meta-line enables a resonance of zeroth order, which comes along with a spatially constant RF current exciting a longitudinally homogeneous B_1 -field [2]. Another

unique feature of the CRLH meta-line is its intrinsic dual-band property, meaning that there are two distinct frequencies with the same phase-shift over the unit cell, yielding the same current distribution along the RF coil element. We utilized this in a natural manner for dual-tuned RF coils applied for combined proton/X-nuclei (e.g. Sodium) imaging [3]. The second concept considers conventional coil elements (loops or electric dipoles) backed by an RF shield with tailored surface impedance. Instead of the usual metal plate we proposed a 2D-metamaterial based shield with high-impedance surface (HIS) mimicking a perfect magnetic conductor. Such a HIS shield causes in-phase image currents yielding an enhanced B1-field above the coil. We evaluated the HIS shield for loop [4] and dipole elements (cf. Fig. 1) and compared the performance to conventional metal shields.

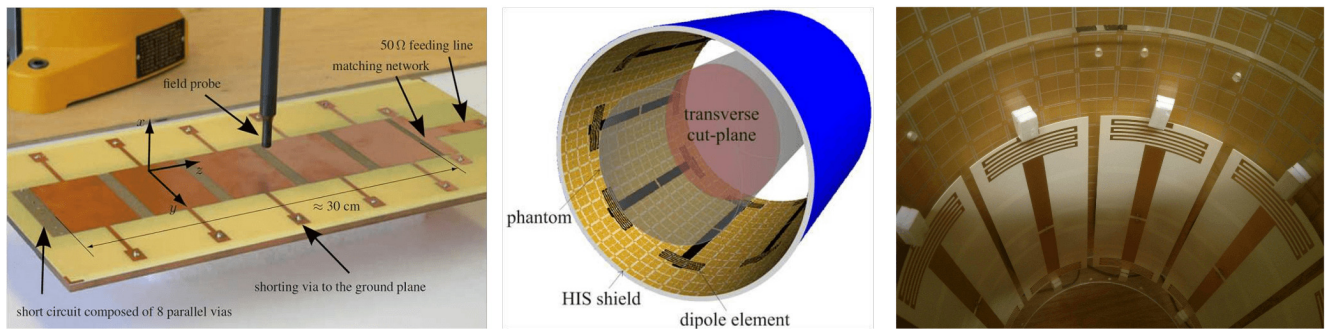


Fig. 1: First zeroth-order resonant RF-coil element (left) as a 1-D metamaterial [2] and dipole array with a high-impedance-surface RF-shield behind (right) as a 2-D metasurface.

References

- [1] C. Caloz, T. Itoh, *Electromagnetic Metamaterials: Transmission Line Theory and Microwave Applications*, Wiley and IEEE Press, Hoboken, NJ, 2006.
- [2] A. Rennings, et al., A CRLH metamaterial based RF coil element for magnetic resonance imaging at 7 Tesla, *EuCAP 2009*, March 23–27, Berlin, Germany, 3231–3234, 2009.
- [3] J. T. Svejda, D. Erni, A. Rennings, An intrinsically double tuned half-wavelength CRLH resonator for combined $^{23}\text{Na}/^1\text{H}$ MRI, *ESMRMB 2013*, October 3–5, Toulouse, France, 2013.
- [4] Z. Chen, K. Solbach, D. Erni, A. Rennings, Improving B1 efficiency and signal-to-noise ratio of surface coils by a high-impedance-surface RF shield for 7-T magnetic resonance imaging, *IEEE Trans. Microw. Theory Techn.*, **65**(3), 988–997 (2017).

Hybridized magnetic enhancer and metacage as new volume antenna for high field MRI

Julien de Rosny¹, Redha Abdeddaim², Camille Jouvaud¹, Benoît Larrat³, Anton Nikulin¹, Abdelwaheb Ourir¹

¹ ESPCI Paris, PSL Research University, CNRS, Institut Langevin, 75005 Paris, France

² Aix Marseille Univ, CNRS, Centrale Marseille, Institut Fresnel, Marseille, France

³ CEA, DRF, JOLIOT, NeuroSpin, UNIRS, Gif-sur-Yvette, France

e-mail: julienderosnyatespci@gmail.com

A few years ago, we introduced a new electromagnetic device based on hybridization of modes which considerably increases the uniformity and the penetration depth of the B₁ radio frequency (RF) generated by a classical loop coil used in an ultra-high field Magnetic Resonant Imaging (MRI) apparatus. This Hybridized Magnetic Enhancer (HME) takes advantage of 2 magnetic resonances from the 4 resonances resulting from the hybridization of the fundamental modes of four closed electrical dipoles. The properties of the HME are studied with full wave numerical simulations. The distribution of the RF magnetic field is experimentally confirmed on a 7-Tesla MRI with gelatin

phantoms. Finally, the HME is validated in-vivo by imaging the head of an anesthetized rodent. A global increase of the signal to noise has been measured with a local maximum equal to 200%. The link of HME with the well-known birdcage MRI antenna is highlighted. However this solution cannot compensate strong aberration that appears above 7 T for large volume when one wants to image the human brain, for instance. To overcome this limitation, we very recently introduced the concept of metacage. The aim of this volume magnetic antenna is to control the wave propagation along a metasurface in order to generate B+ field (circularly polarized magnetic field) as will. After modeling the metacage in terms of transmission line, its working principle is illustrated with a metacage mimicking a magnetic phase conjugate mirror in a simple configuration using a finite element simulation. A full-wave simulation of a much more realistic metacage confirms the relevance of this concept. Finally, a first experimental prototype has been realized. The preliminary experimental results are very encouraging. The metacage project has received funding from the European Unions Horizon 2020 Research and Innovation programme under Grant Agreement No. 736937.

Light induced collective dynamics and “Mock Gravity” interactions between plasmonic nanoparticles

Sáenz J.J.

Donostia International Physics Center (DIPC), Donostia-San Sebastián 20018, Spain
e-mail: juanjo.saenz@dipc.org

Appropriate combinations of laser beams can be used to trap and manipulate small particles with “optical tweezers” as well as to induce significant “optical binding” forces between particles. These forces are, in general, non-conservative (curl forces). Here we review a number of intriguing predictions regarding the dynamics of plasmonic nanoparticles under crossed laser fields [1–3]. In particular, we will focus on our recent results [3] concerning the self-organized collective behaviour of gold nanoparticles moving in aqueous solution under a nonconservative optical vortex lattice. As we will see, above a critical field intensity and concentration, the interplay between optical forces, thermal fluctuations and hydrodynamic pairing leads to a spontaneous transition towards synchronised motion exhibiting a rich assortment of collective dynamics.

Optical forces between small particles are usually strongly anisotropic depending on the interference landscape of the external fields. This is in contrast with the familiar isotropic van der Waals and, in general, Casimir–Lifshitz interactions between neutral bodies arising from random electromagnetic waves generated by equilibrium quantum and thermal fluctuations. We recently showed that artificially created random fluctuating laser fields can be used to induce and control isotropic dispersion forces between small colloidal particles [4]. Interestingly, when the light frequency of a quasi monochromatic isotropic random field is tuned to an absorption line (at the so-called Fröhlich resonance) the attractive force between two resonant plasmonic nanoparticles follows a “ $1/r^2$ ” gravity-like inverse square distance law [5]. Our results generalise Lorentz’s [6] (and Spitzer–Gamow’s “Mock Gravity” [7]) electromagnetic version of the remarkable Fatio–LeSage’s corpuscular theory of gravity.

References

- [1] S. Albaladejo, M.I. Marqués, F. Scheffold, J.J. Sáenz, Giant enhanced diffusion of gold nanoparticles in optical vortex fields, *Nano Letters*, **9**, 3527–3531 (2009).
- [2] J. Luis-Hita, J.J. Sáenz, M.I. Marqués, Arrested dimer’s diffusion by self-induced back-action optical forces, *ACS Photonics*, **3**, 1286–1293 (2016).
- [3] R. Delgado-Buscalioni, M. Meléndez, J. Luis-Hita, M.I. Marqués, J.J. Sáenz, Strong collective currents of gold nanoparticles in an optical vortex lattice, *arXiv:1709.04424* (2017).
- [4] G. Brügger, L.S. Froufe-Pérez, F. Scheffold, J.J. Sáenz, Controlling dispersion forces between small particles with artificially created random light fields, *Nature Communications*, **6**, 7460 (2015).

- [5] J. Luis-Hita, M. I. Marqués, R. Delgado-Buscalioni, N. de Sousa, L. S. Froufe-Pérez, F. Scheffold, J. J. Sáenz, Light induced “Mock Gravity” at the nanoscale, *arXiv:1802.05648* (2018).
- [6] H. A Lorentz, *Lectures on Theoretical Physics*, Macmillan and Co., Limited, London, 1927.
- [7] G. Gamow, On relativistic cosmogony, *Reviews of Modern Physics*, **21**, 367 (1949).

Tunable metasurface composed of periodic metal-dielectric resonators

Sarychev A.K., Afanasev K.N., Bykov I.V., Boginskaya I.A., Ivanov A.V., Lagarkov A.N., Merzlikin A.M., Ryzhikov I.A., Sedova M.V.

Institute for Theoretical and Applied Electrodynamics, RAS, Moscow 125412, Russia

e-mail: sarychev_andrey@yahoo.com

Evtushenko E.G., Kurochkin I.N.

Emanuel Institute of Biochemical Physics, RAS, Moscow 119334, Russia, and Faculty of Chemistry, Lomonosov Moscow State University, Moscow 119991, Russia

Mikheev V.V., Negrov D.V.

Moscow Institute of physics and technology, Dolgoprudny, Moscow Region, 141701, Russia

Anomalous optical response of the periodic metasurface made of silicon resonators is investigated. The resonators are manufactured in form of two-dimensional bars and covered by semicontinuous silver film (Fig. 1a). The calculations as well as real experiments demonstrate the Wood anomaly in visible and near IR spectral ranges. We believe that the anomaly is associated with excitation of the surface waves on the metasurface when the incident light diffracts on periodic bars. The multiple metal-dielectric resonances result in much enhanced local electromagnetic fields in-between metal particles placed on the surface of dielectric bars. The resonances can be tuned by varying angle of incidence, polarization, and geometry of the dielectric bars.

The meta-surface is formed on Si(100) substrate by using high-resolution e-beam lithography (Crestec CABL 9000C) and subsequent reactive ion etching of silicon (CORIAL 200I). In order to achieve suitable aspect ratio of trenches the etching was carried out through the positive e-beam resist ARP 6200.04 in SF₆/Ar atmosphere with high bias voltage. Since high bias voltage in dry etching process leads to high etching speed of resist, trenches depth is limited by ARP 6200.04 thickness and assumed to be 80 nm. The resist is preliminary exposed with the acceleration voltage of 50 kV and the exposure dose 160 $\mu\text{Q}/\text{cm}^2$. The resist is then developed in AR 600-546 developer (Fig. 1a). The top metallization comprising of 20 nm thick silver layer which is deposited by e-beam evaporation.

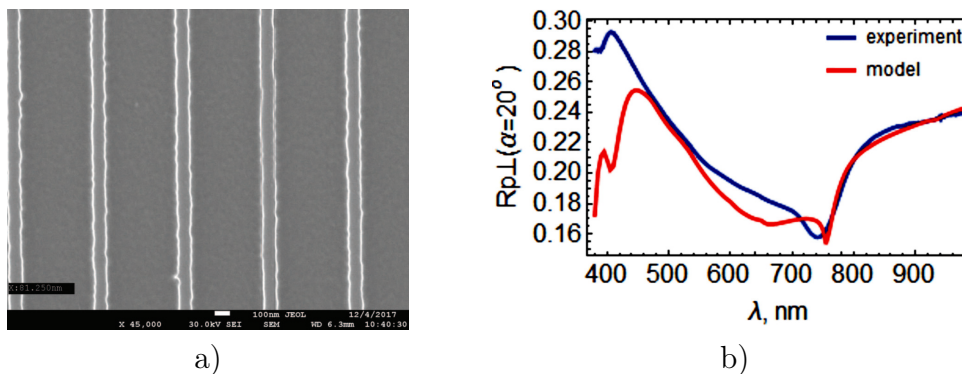


Fig. 1: (a) Scanning electron microscopy image of silicone microbar metasurface with period 560 nm, height of bars 80 nm; (b) Reflectance for -p polarization, angle of incidence 20°.

Full scale computer simulation calculations as well as real reflection experiments demonstrate the Wood anomalies as it is shown in (Fig. 1b). The reflectance sharply decreases at the resonance wavelength. The minimum in the reflectance corresponds to the maximum of the ohmic loss in the metasurface. Therefore, the minimum in the reluctance corresponds to the maximum of the surface

electric field. For a given angle of incidence the resonance wavelength corresponds to the appearance of the first diffraction order, namely $\lambda = L(1 + \sin \alpha)$, where L is the metasurface period. It is easy to tune the resonance frequency by changing just the angle of the incidence. Thus we can tune a sensor, based on the periodic metal-dielectric metasurface, for a characteristic wavelength of the analyte to be detected.

The work is supported by Russian Foundation for Basic Research (RFBR) (grant 17-08-01448) and Program of Presidium of Russian Academy of Sciences no. 56.

Topological photonics and topological insulator lasers

Moti Segev

Solid State Institute and Physics Department Technion – Israel Institute of Technology, Haifa 32000, Israel

e-mail: msegev@technion.ac.il

The past few years have witnessed the emergence of the new field of Topological Photonics. The first pioneering papers were intended to transfer the concepts of topological insulators from the electronic condensed matter systems to the electromagnetic and photonics settings. This meant transforming fermionic concepts into the bosonic nature of photons. But in the years that followed, many new ideas have emerged, some are universal — making immediate impact of fields beyond photonics, and some are unique to photonic systems. The natural progress in this field is now exemplified by the recent discovery of topological insulator lasers, an idea that started as a quantum simulator and developed all the way to a promising application.

Simultaneous forward-backward scattering suppression through nonresonant multipole excitation

Shamkhi H.K., Baryshnikova K.V., Shalin A.S.

Department of Nanophotonics and Metamaterial, ITMO University, St. Petersburg 197101, Russia

e-mail: h.shamkhi@optomech.ifmo.ru, k.baryshnikova@optomech.ifmo.ru

In the appearance of both electric and magnetic features, the scattering characteristics of a small particle present marked differences concerning pure electric or magnetic responses. Even in the simplest case of small or dipolar scatterers, exceptional scattering effects of magnetodielectric particles were theoretically established by Kerker et al [1]. Assuming linearly polarized light exciting dielectric sphere, the generalized Kerker's condition for backward radiation suppression can be described by [2, 3]

$$\sum_{n=1}^{\infty} \frac{2n+1}{3} [(-1)^n a_n + (-1)^{n+1} b_n] = 0, \quad (1)$$

where a_n and b_n are Mie coefficients and index n stand for the multipole order, although the forward radiation intensity cannot be exactly zero according to the optical theory, it presents a minimum at [3]

$$\sum_{n=1}^{\infty} \frac{2n+1}{3} [(-1)^n a_n + (-1)^{n+1} b_n] = - \sum_{n=1}^{\infty} \frac{2n+1}{3} [(-1)^n a_n + (-1)^{n+1} b_n]^*. \quad (2)$$

The occurrence of both previous conditions at a specific frequency leads to destructive interference in both forward and backward directions and redistribute of the scattered power into side directions (see Fig. 1). The result is maybe useful for predicting of the perfect absorbance in meta-surfaces.

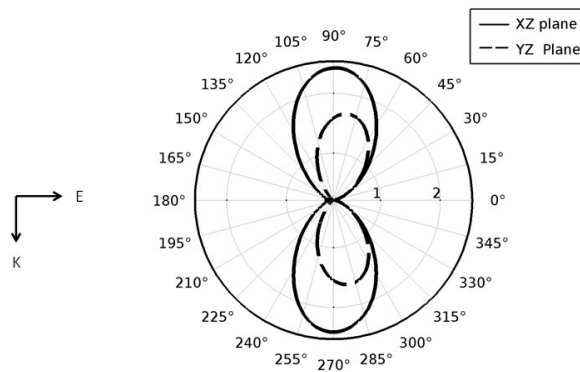


Fig. 1: Scattering diagrams for the 7.5 mm ceramic sphere with permittivity 16 in vacuum at frequency 7.7 GHz.

References

- [1] M. Kerker, D. Wang, C. L. Giles, Electromagnetic scattering by magnetic spheres, *J. Opt. Soc. Am.*, **73**, 765–767 (1983).
- [2] C. F. Bohren, D. R. Huffman, *Absorption and Scattering of Light by a Small Particle*, John Wiley and Sons, 1998.
- [3] G. Raquel, et al., Electric and magnetic dipolar response of germanium nanospheres: interference effects, scattering anisotropy, and optical forces, *J. of Nanophotonics*, **5**, 053512 (2011).

Quantum optics with LiNbO₃ integrated waveguide circuits: Generation and manipulation of two-photon interference and progress towards the integration of superconducting detectors

Sharapova, P.R., Reichelt, M., Nikitin, A., Meier, T.

Theoretical Physics and CeOPP, University of Paderborn, D-33098 Paderborn, Germany
e-mail: torsten.meier@uni-paderborn.de

Luo, K.H., Herrmann, H., Höpker, J.P., Krapick, S., Bartley, T.J., Silberhorn, C.

Experimental Physics and CeOPP, University of Paderborn, D-33098 Paderborn, Germany

Lita, A., Verma, V., Gerrits, T., Nam, S.W., Mirin, R.

National Institute of Standards and Technology, 325 Broadway, Boulder, Colorado, USA

Quantum optical effects can be applied to overcome classical performance limitations in several fields such as communication security, metrology, and computation. The practical implementation and thus the exploitation of basic physical quantum effects in devices requires the development of reliable and stable miniaturized components. Here, we present and discuss perspectives on current developments on advanced quantum optical circuits which are monolithically integrated in the lithium niobate platform [1].

A set of basic components comprising photon pair sources based on parametric down conversion (PDC), passive routing elements as well as active electro-optically controllable switches and polarization converters form the basis for a broad range of diverse quantum optical waveguide circuits [1]. The state-of-the-art of these components and models that properly describe their performance are reviewed [1]. As an example we analyze a circuit providing on-chip two-photon interference and demonstrate that entangled states are able to significantly extend the functionality of Hong–Ou–Mandel (HOM) interferometers [2].

The rather poor efficiency of conventional single photon detectors, in particular at telecom wavelengths, is often significantly detrimental to the observation of quantum optical effects in experiments. Superconducting detectors are well-established tool that combine high efficiency with a fast response

and low noise. We report on simulations and measurements of the absorption of superconducting thin films mounted on LiNbO₃-based waveguides and discuss the perspectives of integrating superconducting detectors on this platform [3].

References

- [1] P. R. Sharapova, K. H. Luo, H. Herrmann, M. Reichelt, T. Meier, C. Silberhorn, *New Journal of Physics*, **19**, 123009 (2017).
- [2] P. R. Sharapova, K. H. Luo, H. Herrmann, M. Reichelt, C. Silberhorn, T. Meier, *Phys. Rev. A*, **96**, 043857 (2017).
- [3] J. P. Höpker, M. Bartnick, E. Meyer-Scott, F. Thiele, S. Krapick, N. Montaut, M. Santandrea, H. Herrmann, S. Lengeling, R. Ricken, V. Quiring, T. Meier, A. Lita, V. Verma, T. Gerrits, S. Woo Nam, C. Silberhorn, T. J. Bartley, *Proc. SPIE*, **10358**, Quantum Photonic Devices, 1035809 (2017).

Modified excited states dynamics in the localized plasmon — molecular exciton hybrids

Timur Shegai

Chalmers University of Technology, Department of Physics, Gothenburg, Sweden

e-mail: timurs@chalmers.se

Strong light-matter interactions in microcavities have been long known to provide means to alter optical and nonlinear properties of the coupled system. As a result of this interaction, one typically observes the emergence of new polaritonic eigenstates of the coupled system. These states are of hybrid nature and possess both light and matter characteristics, which is reflected in vacuum Rabi splitting, observed in the absorption or transmission spectra. Because of the hybrid nature of these states, the excited state temporal dynamics can be significantly altered in comparison to the uncoupled system dynamics. This, in turn, can have profound effects on the emission and photochemical processes.

Here, we show that individual plasmonic nanoantennas can strongly couple to molecular J-aggregates, resulting in splitting up to 400 meV, i.e. $\approx 20\%$ of the resonance energy. Moreover, we observe mode splitting not only in elastic scattering but also in photoluminescence of individual hybrid nanosystems, which manifests a direct proof of strong coupling in plasmon-exciton nanoparticles. This situation is drastically different from the photoluminescence of uncoupled molecules, which signals the involvement of polaritonic states into the relaxation pathways of the hybrid system. We also discuss how the involvement of these pathways can modify other relevant excited state dynamics, including photochemical processes.

Microwave transparency of a superconducting quantum metamaterial

K.V. Shulga^{1,2}, M.V. Fistul^{1,2,3}, I. Besedin¹, A.V. Ustinov^{1,2,4}

¹National University of Science and Technology MISIS, 119049 Moscow, Russia

²Russian Quantum Center, 143025 Moscow region, Russia

³Theoretische Physik III, Ruhr-Universität Bochum, D-44801 Bochum, Germany

⁴Physikalisches Institut, Karlsruhe Institute of Technology, D-76131, Karlsruhe, Germany

e-mail: ustinov@kit.edu

Quantum mechanics is expected to govern the electromagnetic properties of a quantum metamaterial, an artificially fabricated medium composed of many quantum objects acting as artificial atoms. Propagation of electromagnetic waves through such a medium is accompanied by excitations

of intrinsic quantum transitions within individual meta-atoms and modes corresponding to the interactions between them. I will discuss an experiment [1] in which an array of double-loop type superconducting flux qubits is embedded into a microwave transmission line. We observed that in a broad frequency range the transmission coefficient through the metamaterial periodically depends on externally applied magnetic field. Field-controlled switching of the ground state of the meta-atoms induces a large suppression of the transmission. Moreover, the excitation of meta-atoms in the array leads to a large resonant enhancement of the transmission. We anticipate possible applications of the observed frequency-tunable transparency in superconducting quantum networks.

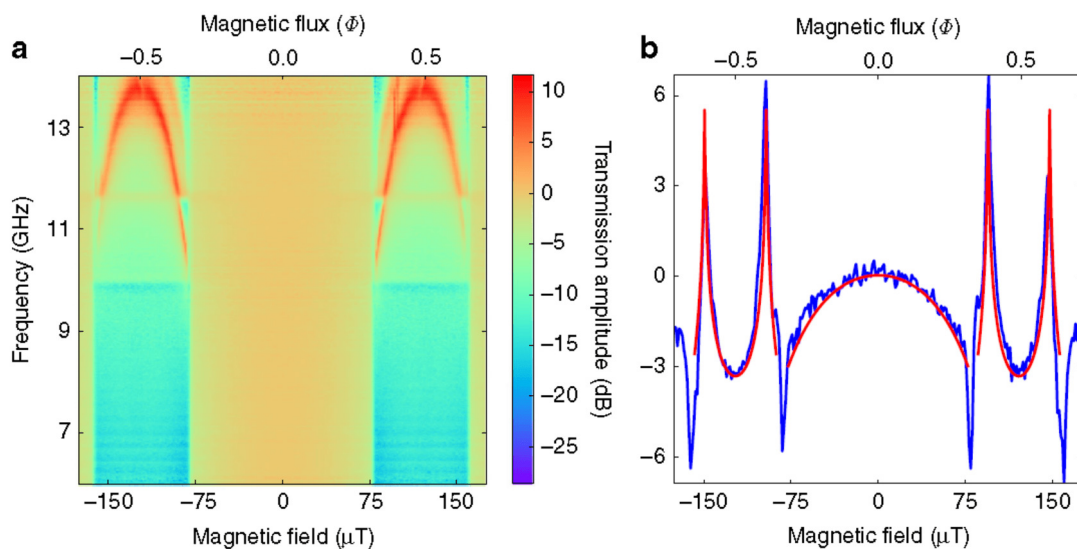


Fig. 1: Transmission of microwaves through the quantum metamaterial in different regimes. (a) The measured dependence of the amplitude of transmission coefficient (normalized to the value at zero field) on applied magnetic field and frequency. (b) A cross-cut of (a) at the fixed frequency of 13 GHz. The sharp peaks correspond to coherent tunneling between quantum states in the qubits. Red curve is a fit to theory.

References

- [1] K. V. Shulga, E. Ilichev, M. V. Fistul, I. S. Besedin, S. Butz, O. V. Astafiev, U. Huebner, A. V. Ustinov, *Nature Communications*, **9**, 150 (2018).

Active nanophotonics: from graphene-integrated plasmonic metasurfaces and metagates to photon-accelerating semiconductor nanostructures

Gennady Shvets

School of Applied and Engineering Physics, Cornell University, Ithaca, New York 14853, USA
e-mail: gs656@cornell.edu

Plasmonic metasurfaces enhance light-matter interaction by focusing light into extremely sub-wavelength dimensions. These carefully designed structures have been used in extremely thin optical component which can mold the wavefront, with exciting applications in optical lenses, beam steering, and biosensing applications. Adding dynamic tunability to these devices opens up the possibility for new application in single pixel detection and 3D imaging as well as optical modulators and switches. In this talk, I will concentrate on the experiments and modeling of plasmonic and semiconductor metasurfaces that rely on free carriers for controlling their optical responses. The possibilities for light control using free carriers are particularly tantalizing in the infrared part of the spectrum. I will discuss two types of such active nanophotonic structures. The first type is plasmonic metasurfaces integrated with graphene. I will describe our recent experimental results demonstrating rapid

amplitude and phase modulation of mid-infrared light, as well as our new theoretical proposals for developing reconfigurable topological devices that can route light around sharp turns and interfaces. The second type of active nanophotonic structures are the Photon-Accelerating Semiconductor Infrared Metasurfaces (PASIM) that can be used to control light propagation through self-consistent generation of electron-hole pairs. First-principles particle-in-cell simulations reveal that such metasurfaces can trap and frequency-shift light via the process of photon acceleration. Computational challenges to modeling active metasurfaces will be discussed, and new experimental results will be presented.

Light-trapping in organic solar cells by silver nanoantennas

Simovski C.R.^{1,2}, Voroshilov P.M.^{1,2}, Papadimitratos A.³, Zakhidov A.A.^{3,4}

¹Aalto University, School of Electrical Engineering, FI00076, Finland

²ITMO University, Kronverkski 47, St. Petersburg, Russia

³University of Texas at Dallas, Richardson 75080, USA

⁴National University of Science and Technology MISiS, Moscow 119049, Russia

e-mail: konstantin.simovski@aalto.fi

In this work, we study report an experimental study of the enhancement of overall power conversion efficiency and other operational parameters of a typical organic solar cell (OSC) based on fullerenes. Such OSCs have a subwavelength small thickness of the photovoltaic layer. The enhancement of the useful ((photovoltaic) absorption was predicted in our earlier works for similar, but not exactly same, structures. This enhancement is granted by an originally proposed light trapping structure (LTS) that represents a planar array (metasurface) of silver nanoantennas. Our metasurface supports collective modes, that are leaky and, therefore, can be excited by a plane wave in a substantial part of the solar frequency spectrum. It was shown that the excitation of these modes theoretically provides the subwavelength light enhancement (hot spots) in whatever substrate with optical losses. However, for practical applications the most suitable solar cell to be enhanced by our metasurface is namely a fullerene-based OSC. It is important that hot spots of the light-trapping modes are excited fully outside the metal elements that implies low parasitic losses.

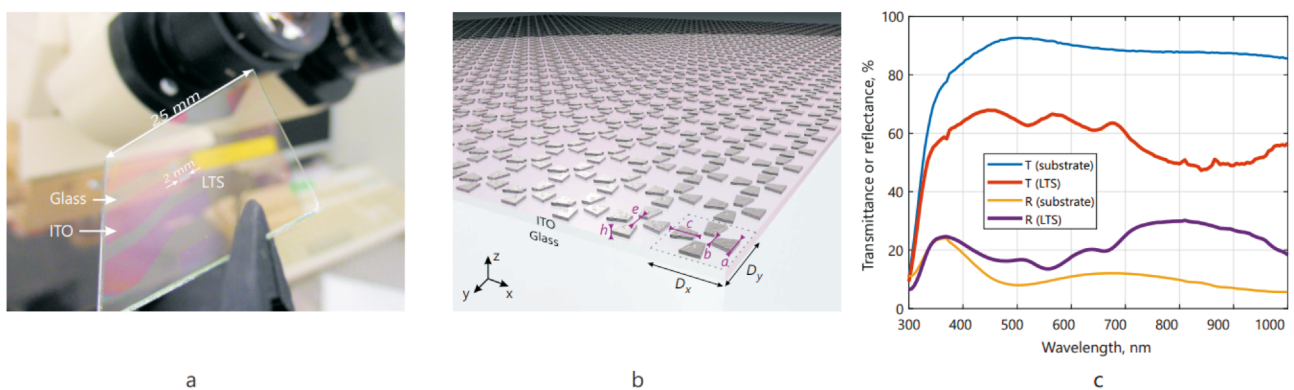


Fig. 1: (a) Photo of the sample with our LTS. (b) Scheme of the metasurface geometry. The geometrical parameters are as follows: $D_x = D_y = 1000$ nm, $a = 300$ nm, $b = 150$ nm, $c = 300$ nm, $e = 250$ nm, $h = 35$ or 50 nm (two different samples). (c) Transmission and reflection spectra measured for 50-nm thick LTS on a bilayer ITO/glass and for a bare bilayer.

In Fig. 1(a) we show the picture of our experimental sample, in Fig. 1(b) — the scheme of our metasurface, and in Fig. 1(c) — the plot of the plane-wave transmission and reflection coefficients. It shows how the absorption in the transparent electrode grows in presence of the metasurface. Here we have studied our metasurface located on top of a 150-nm thick indium-tin oxide (ITO) layer on a glass substrate. We found that in the range of the visible light (in the present geometry it is that of our light-trapping modes) the integral increase of the absorption in ITO is close to 20%. Although the

Ag nanoantennas occupy 40% of the photoactive OSC area, the integral reflection loss in this range is only 19%. Both these results fully agree with numerical simulations. The increased absorption in ITO is a parasitic effect but it leaves the room for the increase of the useful absorption, when the glass substrate is replaced by our solar cell (in which this ITO layer becomes a front electrode).

We have fabricated a sufficient set of samples of OSCs. Some were covered by a standard anti-reflecting coating, some comprised our LTS. The last one increases the total absorption in the visible range nearly twice. This result fits numerical simulations, which also predict 50% for the gain in the useful absorption and 20% for the increase of the photocurrent. Measurements have shown the mean (over all working samples) increase of the photocurrent 8% granted by our LTS compared to the conventional design. We have found and implemented a specific design for which the fill factor is also affected positively. For this design we have obtained a small damage for the open-circuit voltage and the mean power conversion efficiency improvement equals to 18%. This gain is higher than that reported in the literature as the gain due to previously known plasmonic LTSs developed for such solar cells [1].

This study finalizes the doctoral research by Pavel Voroshilov of the light-trapping capacities of nanoantennas supporting the advantageous light-trapping modes [2–5]. It also opens the door for implementing the OSCs incorporated into window glass whose theory was developed in [2]. In [2] the geometric parameters of the metasurface corresponded to the light-trapping in the near-infrared part of the solar light, whereas the whole structure was transparent in the visible range. Therefore, one could harvest some electric power from the window without the damage for the illumination. Though, in the present work the structure was impervious for the visible light, the sufficient agreement between the simulations and the experiment shows that our theory is really adequate. Our metasurface enhances the useful absorption without a noticeable damage for other operation characteristics. Therefore, we believe that it will work similarly (in the theory — better) in its infrared implementation.

References

- [1] S. Ahn, D. Rourke, W. Park, Plasmonic nanostructures for organic photovoltaic devices, *Journal of Optics*, **18**, 033001(1–10) (2016).
- [2] P. M. Voroshilov, C. R. Simovski, P. A. Belov, Nanoantennas for enhanced light trapping in transparent organic solar cells, *Journal of Modern Optics*, **61**, 1743–1748 (2014).
- [3] P. M. Voroshilov, C. R. Simovski, Leaky domino-modes in regular arrays of substantially thick metal nanostrips, *Photonics and Nanostructures Fundamentals and Applications*, **20**, 18–30 (2016).
- [4] I. S. Sinev, P. M. Voroshilov, I. S. Mukhin, A. I. Denisyuk, M. E. Guzhva, A. K. Samusev, P. A. Belov, C. R. Simovski, Demonstration of unusual nanoantenna array modes through direct reconstruction of the near-field signal, *Nanoscale*, **7**, 765–770 (2015).
- [5] C. Simovski, D. Morits, P. Voroshilov, M. Guzhva, P. Belov, Y. Kivshar, Enhanced efficiency of light-trapping nanoantenna arrays for thin-film solar cells, *Optics Express*, **21**, A714–A725 (2013).

Glassy metasurfaces: structural and optical studies

A.D. Sinelnik¹, M.V. Rybin^{1,2}, S.Y. Lukashenko¹, K.B. Samusev^{1,2}, M.F. Limonov^{1,2}

¹Department of Physics and Engineering, ITMO University, St. Petersburg 197101, Russia

²Ioffe Institute, St. Petersburg 194021, Russia

e-mail: m.limonov@mail.ioffe.ru

The aim of this work was the synthesis, structural and diffraction studies of ordered and disordered woodpile photonic structures including woodpile-type glassy metasurfaces. The structures were fabricated by the two-photon polymerization method. The correspondence of the resulting

materials to the designed structures was confirmed by scanning electron microscopy. By specially choosing the lattice parameters and laser wavelength, we visualized the optical diffraction patterns on a flat screen positioned behind the sample. A detailed interpretation of the complex diffraction patterns was enabled by analysis of the structural factor in the Born approximation.

We fabricated the disordered structures as follows. Each individual rod in the xy woodpile layer was turned about its center (along x - or y -axis) by random angle with respect to the ordered state. We observed a wide range of optical phenomena from Laue diffraction and laser speckle to a great variety of intermediate light scattering regimes (Fig. 1). We found that the zero-order and first-order Laue diffraction show different behavior as a function of the disorder parameter. The zero-order diffraction is not significantly modified for small and intermediate disorder, but the first-order diffraction can be affected strongly even for small disorder.

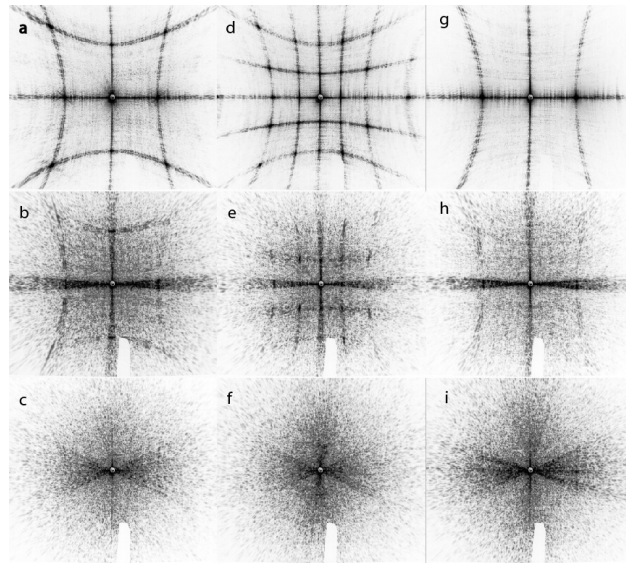


Fig. 1: Diffraction pattern evolution for samples with lattice parameters $a_x = a_y = 1 \mu\text{m}$ (a), $\tilde{a}_x = \tilde{a}_y = 1 \mu\text{m}$ (b, c), $a_x = a_y = 2 \mu\text{m}$ (d), $\tilde{a}_x = \tilde{a}_y = 2 \mu\text{m}$ (e, f), $a_x = 1 \mu\text{m}$, $a_y = 0.5 \mu\text{m}$ (g), $\tilde{a}_x = 1 \mu\text{m}$, $\tilde{a}_y = 0.5 \mu\text{m}$ (h, i). Disorder parameter $p = 0$ (a, d, g), $p = 0.1$ (b, e, h), $p = 0.5$ (c, f, i).

Unexpected interplay between order and disorder was observed from anisotropic glassy samples when orientational disorder was introduced only in one direction of square woodpile structure. With increasing of the disorder, the first-order diffraction patterns from ordered set of rods becomes randomized and finally hardly observed while first-order patterns from disordered set of rods continue to be bright and sharp, despite the fact that one might expect reversed situation with disordered diffraction patterns arising from disordered set of rods. To explain this effect, we demonstrate theoretically and experimentally that the light scatters only from intersection points of different rods. This conclusion can be considered as general features of light scattering in dielectric photonic structures and lead to new understanding about light propagation in random photonic structures.

Extreme states and statistics in the gas of solitons

Slunyaev A.V., Pelinovsky E.N., Shurgalina E.G.

Institute of Applied Physics, Nizhny Novgorod, 46 Ulyanova Street & N. Novgorod State Technical University n. a. R. E. Alekseev, Nizhny Novgorod, 24 Minina Street
e-mail: slunyaev@appl.sci-nnov.ru

The soliton gas may be understood as a particular limiting case of strongly nonlinear waves in integrable (or near integrable) system, where most of the field is represented with solitons (or envelope solitons or breathers, etc.) which can interact elastically with other waves (or with tiny manifestations of inelasticity). There is a number of practically important situations in the modern

physics when the properties of the soliton gas play the role (see references in the cited papers). Probably the brightest example is optical solitons in the data transmission fibers; solitary waves on the sea surface and in the stratified sea are the other applications, which are closest to the authors' interests.

In contrast to the kinetic theory for solitons in integrable systems developed by V. E. Zakharov and G. A. El & A. M. Kamchatnov (which describe the transport of eigenvalues of the associated scattering problem), we make focus on the statistical properties of the field, which essentially depend on the wave phases. The study is based on two main approaches: (i) consideration of pairwise or multiple soliton interactions as the elementary acts of the soliton turbulence, and (ii) direct numerical simulation of the soliton ensembles.

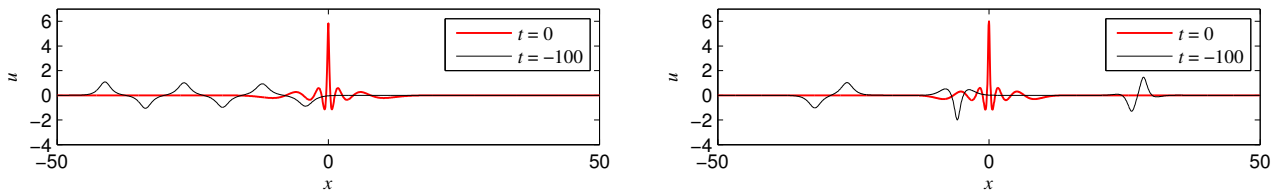


Fig. 1: Focusing of 6 solitons (left) and 3 breathers (right), the modified KdV framework.

In particular, optimal conditions on the soliton focusing are determined based on the exact solutions of a few integrable equations (Korteweg – de Vries equation, modified Korteweg – de Vries equation, Gardner equation, focusing nonlinear Schrödinger equation). Examples of the optimal focusing are given in the provided figure (trains well before and at the moment of focusing).

The nonlinear properties of the governing equations play the fundamental role in whether the nonlinear dynamics is characterized by higher probability of extreme waves or not.

The review on the recent (e.g. [1–3]) and on-going research will be given in the talk.

Support from RFBR Grant No. 18-02-00042 is acknowledged.

References

- [1] E. N. Pelinovsky, E. G. Shurgalina, A. V. Sergeeva, T. G. Talipova, G. El, R. H. J. Grimshaw, Two-soliton interaction as an elementary act of soliton turbulence in integrable systems, *Phys. Lett. A*, **377**, 272–275 (2013).
- [2] E. G. Shurgalina, E. N. Pelinovsky, Nonlinear dynamics of solitonic gas: Modified Korteweg – de Vries equation framework, *Phys. Lett. A*, **380**, 2049–2053 (2016).
- [3] A. V. Slunyaev, E. N. Pelinovsky, The role of multiple soliton interactions in generation of rogue waves: the mKdV framework, *Phys. Rev. Lett.*, **117**, 214501 (2016).

Metamaterial inspired structures for enchantment performance of RF-coils for MRI

Solomakha G.A., Glybovski S.B.

Department of Nanophotonics and Metamaterials, ITMO University, 197101 Saint Petersburg, Russia
e-mail: g.solomakha@metalab.ifmo.ru

Magnetic resonance imaging (MRI) and magnetic resonance spectroscopy (MRS) has become one of the main methods of non-invasive investigation of properties biological objects including human body tissues. The radiofrequency (RF) coils among of the most important components of MRI and MRS systems. Their main functions are excitation of spins in the studies subject located in a permanent magnetic field (B_0) and reception of their response signals. When an RF signal is applied to the input port of the coil and the coil placed creates RF-fields (commonly called B_1), orthogonal to the direction of the permanent magnetic field B_0 , exciting the spin at their nuclear magnetic resonance frequency (Larmor frequency). In this case, excitation of spins results in a change in their orientation.

Design of RF-coils, that acts as near-field resonators or as antennas depending on the operational permanent field, are very challenging problem because of the presence of a high-permittivity and lossy human body, strict limitation on deposited RF power in body tissues in in transmit regime and maximum SNR in receive regime.

According to the definition by METAMORPOSE-VI [1], a metamaterial is an arrangement of artificial structural elements, designed to achieve advantageous and unusual electromagnetic properties, including enchantment of magnetic and electric fields. Recently, the field control with passive two-dimensional periodic structures has been extended to densely packed arrays of electrically small inclusions still having engineered electromagnetic response. These structures have been called “metasurfaces”, which are 2D analogues of metamaterials [2]. These unique electromagnetic properties, used in RF-coils engineering, could be very useful in to enhance performance of MRI.

In this work we review and discuss major works on applications of metamaterials, metasurfaces and metamaterial-inspired structures in high-field and ultra high-field MRI.

References

- [1] The Virtual Institute for Artificial Electromagnetic Materials and Metamaterials, <http://www.metamorphose-vi.org/index.php/metamaterials>, 2017.
- [2] S.B. Glybovski, et al., Metasurfaces: From microwaves to visible, *Physics Reports*, **634**, 1–72 (2016).

Interaction-induced two-photon topological states

Stepanenko A.A.^{1,2}, Gorlach M.A.¹

¹ITMO University, Saint Petersburg, 197101, Russia

²St. Petersburg National Research Academic University of the Russian Academy of Sciences, Saint Petersburg, 194021, Russia

e-mail: stepanenkoery@yandex.ru, m.gorlach@metalab.ifmo.ru

Su–Schrieffer–Heeger model (SSH) is the canonical example of one-dimensional topological system, which is implemented to date in a variety of systems from mechanical to the optical ones. While the behavior of the linear SSH model is well understood, the quest for dynamically reconfigurable topological pathways calls for deeper understanding of its nonlinear generalizations. Recently, the emergence of the self-induced topological states has been examined in the context of classical Kerr-type nonlinearity [1]. However, the formation of the interaction-induced few-body topological states in strongly correlated quantum regime still remains largely unexplored featuring such intriguing physics as formation of repulsively bound boson pairs (doublons) [2].

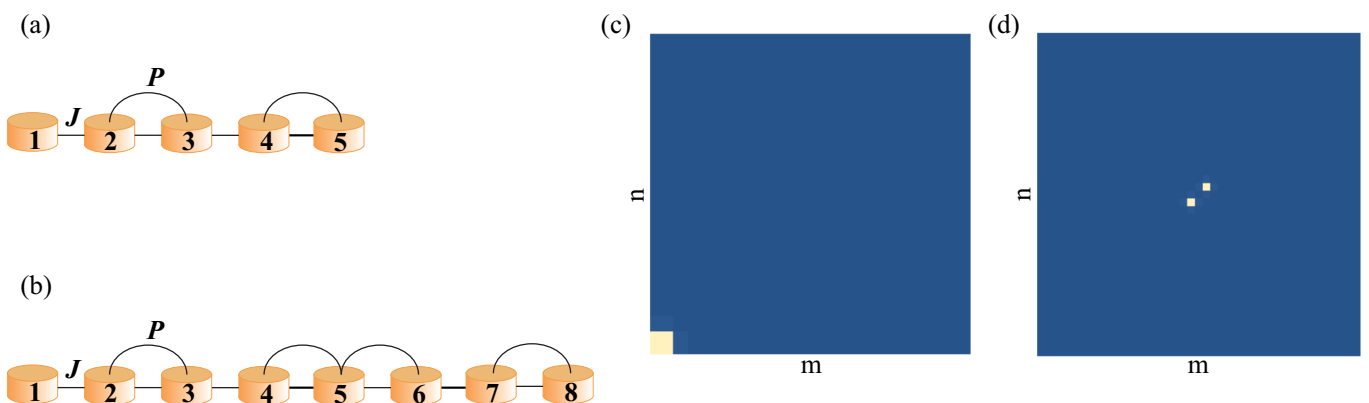


Fig. 1: Schematics of the system under study and doublon topological states. (a,c) Doublon edge state at the open boundary of the array. (b,d) Doublon interface state at the domain wall. $U = 5J$. $P = 5J$.

In this work, we make a conceptual step forward extending the standard Bose–Hubbard model by direct two-particle tunneling process which is indeed present in cold atom systems [3]. The Hamiltonian of the system under study [Fig. 1(a,b)] for the fixed photon polarization reads:

$$\hat{H} = \omega_0 \sum_m \hat{n}_m + U \sum_m \hat{n}_m(\hat{n}_m - 1) - J \sum_m (\hat{a}_m^\dagger \hat{a}_{m+1} + \hat{a}_{m+1}^\dagger \hat{a}_m) + \frac{P}{2} \sum_m (\hat{a}_{2m}^\dagger \hat{a}_{2m}^\dagger \hat{a}_{2m+1} \hat{a}_{2m+1} + \text{H.c.}),$$

where \hat{a}_m^\dagger and \hat{a}_m are the photon creation and annihilation operators for the m -th cavity with eigenfrequency ω_0 ($\hbar = 1$), $\hat{n}_m = \hat{a}_m^\dagger \hat{a}_m$, J and P are the tunneling amplitudes for the single photon and for the photon pair, respectively, U is the effective photon-photon interaction strength.

While such model is topologically trivial at the single particle level, we demonstrate that in the two-boson regime the system exhibits SSH-type behavior forming the topological states in edge and domain wall configurations [Fig. 1(c,d)].

References

- [1] Y. Hadad, A. B. Khanikaev, A. Alu, *Physical Review B*, **93**, 155112 (2016).
- [2] K. Winkler, G. Thalhammer, F. Lang, R. Grimm, J. Hecker Denschlag, A. J. Daley, A. Kantian, H. P. Büchler, P. Zoller. *Nature*, **441**, 853–856 (2006).
- [3] O. Dutta, M. Gajda, P. Hauke, M. Lewenstein, D.-S. Lühmann, B. A. Malomed, T. Sowiński, J. Zakrzewski. *Reports on Progress in Physics*, **78**, 066001 (2015).

Quantum photonics with dielectric metasurfaces

Sukhorukov A.A.

Nonlinear Physics Centre, Research School of Physics and Engineering, Australian National University, Canberra, ACT 2601, Australia
e-mail: andrey.sukhorukov@anu.edu.au

We overview the latest theoretical and experimental results, revealing new opportunities for transformation and measurement of quantum multi-photon states with all-dielectric metasurfaces. Specifically, we present a tailored design and experimental demonstration of metasurfaces for the reconstruction of the full multi-photon quantum state, including phase, coherence, and multi-particle entanglement [1]. We realize an all-dielectric metasurface which spatially splits a tomographically full set of components of multi-photon polarization states, such that a simple averaging measurement of correlations with polarization-insensitive on-off detectors enables accurate reconstruction of multi-photon density matrices.

We also introduce a new conceptual approach for implementing arbitrary complex birefringence with all-dielectric metasurfaces. We formulate a practical design principle of complex birefringent metasurface unit cell composed of two types of nanopillars. It is provably optimal by achieving any desirable polarisation transformation with the minimum required amount of loss, while enabling fundamentally new possibilities for polarisation control which cannot be achieved with lossless birefringent media. In particular, we optimized and fabricated metasurface structures for implementing polarisation beam-splitters with an arbitrary phase between the output polarisations, which can lead to the anti-coalescence of entangled photon pairs in the Hong–Ou–Mandel interference, rather than the bunching behavior observed in a conventional regime.

The fundamental conceptual and practical advances in realization of multi-photon quantum interference, taking place at sub-wavelength scale within its short interaction with the metasurface, pave the road to novel types of ultra-thin metadevices for the manipulation and measurement of multi-photon quantum entangled photon states.

Acknowledgements. This presentation is based on results of collaborations driven by researchers who co-authored Refs. [1, 2].

References

- [1] K. Wang, S.S. Kruk, L. Xu, M. Parry, H. P. Chung, A. S. Solntsev, J. Titchener, I. Kravchenko, Y. H. Chen, Y. S. Kivshar, D. N. Neshev, A. A. Sukhorukov, Quantum polarization tomography with all-dielectric metasurfaces, In *CLEO/Europe-EQEC*, Optical Society of America, EH-7.3 (2017).
- [2] S. Lung, K. Wang, A. A. Sukhorukov, Complex birefringence with dielectric metasurfaces for non-conventional polarisation control, In *Conference on Lasers and Electro-Optics*, Optical Society of America, JW2A.99 (2018).

Tunable resonant coupling of excitonic states with Mie modes in halide perovskite nanoparticles

Tiguntseva E.Y.¹, Pushkarev A.P.¹, Makarov S.V.¹, Zakhidov A.A.², Kivshar Yu.S.³

¹ITMO University, Kronverskiy pr. 49, St. Petersburg 197101, Russia

²University of Texas at Dallas, Richardson, TX, USA

³Australian National University, Canberra ACT 2601, Australia

e-mail: e.tiguntseva@metalab.ifmo.ru, s.makarov@metalab.ifmo.ru,
zakhidov@utdallas.edu, ysk@internode.on.net

The ability to couple exciton resonance with light in halide perovskites nanostructures efficiently at room temperature is enormously important for modern laser technologies, photodetectors, and solar cells. Here, we review first observations of broadly tunable coupling of exciton with the Mie resonances in halide perovskite nanoparticles of a quasi-spherical shape. The nanoparticles were fabricated by femtosecond laser ablation [1]. The coupling behavior is observed in the dark field spectra from single nanoparticles, as well as in extinction spectra of random arrays of perovskite nanoparticles. In the latter case, chemical tunability of the exciton resonance allows one to shift the spectral position of the Fano resonance across 100 nm in the visible range. Our finding offers additional degree of control for optical properties of the perovskite nanostructures used in modern optoelectronic devices. Moreover, novel method of chemical tuning of the resonant properties of perovskite nanoparticles paves the way to control of emission properties of the integrated light-emitting nanoantennas.

References

- [1] E. Y. Tiguntseva, et al., Light-emitting halide perovskite nanoantennas, *Nano Letters*, **18**, 1185–1190 (2018).

Halide perovskite nanoparticles with enhanced photoluminescence

Tiguntseva E.Y.¹, Zakhidov A.A.^{1,2}, Kivshar Yu.S.^{1,3}, Makarov S.V.¹

¹ITMO University, St. Petersburg 197101, Russia

²University of Texas at Dallas, Richardson, Texas 75080, United States

³Australian National University, Canberra ACT, Australia

e-mail: e.tiguntseva@metalab.ifmo.ru

Hybrid perovskites of the MAPbX family represent a class of dielectric materials with excitonic states at room temperature, refractive indices ($n = 2-3$) high enough for the efficient excitation of Mie resonances, low losses at the exciton wavelength, chemically tunable band gap over the entire visible range (400–800 nm) [1], high defect tolerance [2], and high quantum yield (more than 30% [3]) of photoluminescence (PL) [4]. These properties make them perfect candidates for effective nanoscale light sources. In this work, we fabricate by laser printing method [5] perovskite nanoparticles (NPs) supporting electric and magnetic dipolar and multipolar Mie resonances.

The study of white-light scattering from the perovskite NPs with different diameters reveals their resonant behavior in visible and infrared ranges. NP with diameter 415 nm exhibits a pronounced maximum around the spectral position of the exciton line ($\lambda \approx 770$ nm) (Fig. 1a). According to our analytical calculations based on the mode decomposition with the Mie theory, the experimentally obtained spectrum can be theoretically described by several Mie resonant modes in 440 nm spherical perovskite NP (Fig. 1a). Moreover, when the spectral position of the exciton line coincides with the position of the MQ resonance, the PL signal normalized to the emitting material volume becomes five times stronger than that for slightly smaller NPs and two times stronger in comparison with 0.5 μm perovskite film (Fig. 1b).

We have proposed a novel type of light-emitting nanoantennas made of hybrid perovskites, which demonstrate enhanced PL. Our results pave the way towards new optoelectronics applications of nanophotonics based on halide perovskite materials.

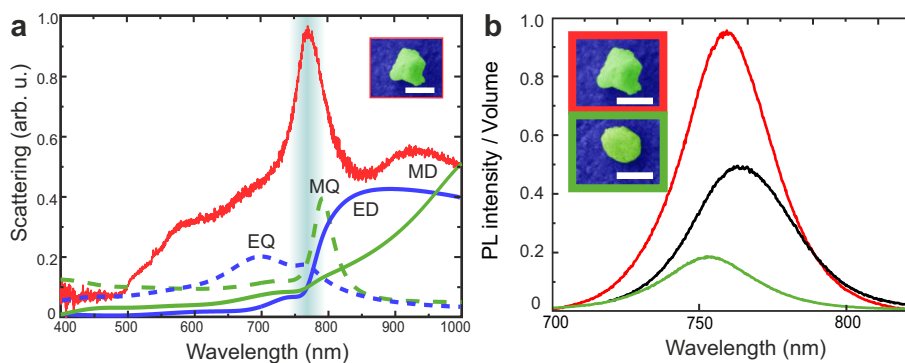


Fig. 1: (a) Red curve corresponds to experimental DF scattering spectrum for single perovskite NP with diameter 415 nm. Green and blue lines stand for analytical mode decomposition for single spherical perovskite NP of 440 nm in homogeneous air media. (b) PL spectra of NPs (marked by the corresponding colors of the frames of SEM image) and for 0.5 μm perovskite film. Scale bar in the SEM image is 400 nm.

References

- [1] C. M. Sutter-Fella, et al., *Nano Letters*, **16**, 800–806 (2015).
- [2] W.-J. Yin, et al., *Applied Physics Letters*, **104**, 063903 (2014).
- [3] S. Koch, et al., *CS Energy Lett.*, **1**, 438–444 (2016).
- [4] E. Y. Tiguntseva, et al., *Nano Letters*, **1**, (2018).
- [5] P. A. Dmitriev, et al., *Nanoscale*, **8.9**, 5043–5048 (2016).

Chiral photonic crystal slabs and metasurfaces for emitters of circularly polarized light

Tikhodeev S.G.

Department of Physics, Lomonosov MSU, Leninskie Gory, 1, Moscow, 119991, Russia;
Prokhorov General Physics Institute, RAS, Vavilova Street 38, Moscow 119991, Russia
e-mail: tikh@gpi.ru

Embedding semiconductor light emitting nanostructures such as quantum dots or quantum wells into chiral metasurfaces or photonic crystal slabs allows to create compact sources of circularly polarized light including lasers [1–5]. They need neither static magnetic field nor thick quarter-wavelength plates.

For example, a circularly polarized photoluminescence of achiral InAs quantum dots from a GaAs/AlGaAs waveguiding structure with chiral photonic slab was demonstrated, with a degree of circular polarization exceeding 95% [4]. A close to circularly polarized lasing was achieved [5] at room temperature and under optical pump from an AlAs/AlGaAs Bragg microcavity with GaAs quantum

wells in the active region and chiral etched upper distributed Bragg refractor. Recently a close to circular lasing of this structure was also demonstrated in the strong coupling exciton-polariton regime at low temperature.

In my talk I will discuss the physical mechanisms allowing to control the polarization state of light emission from photonic structures with chiral photonic crystals and metasurfaces.

References

- [1] K. Konishi, et al., *Phys. Rev. Lett.*, **106**, 057402 (2011).
- [2] A. A. Maksimov, et al., *Phys. Rev. B*, **89**, 045316 (2014).
- [3] S. V. Lobanov, et al., *Optics Lett.*, **40**, 1528 (2015).
- [4] S. V. Lobanov, et al., *Phys. Rev. B*, **92**, 205309 (2015).
- [5] A. A. Demenev, et al., *Appl. Phys. Lett.*, **109**, 171106 (2016).

Chiral optical Tamm states: method of images

Timofeev I.V.^{1,2}, Pankin P.S.^{1,2}, Vetrov S.Ya.^{1,2}, Arkhipkin V.G.^{1,2}, Lee W.³, Zyryanov V.Ya.¹

¹Kirensky Institute of Physics, Federal research center – Krasnoyarsk scientific center SB RAS, Krasnoyarsk 660036, Russia

²Siberian Federal University, Krasnoyarsk 660041, Russia

³College of Photonics, National Chiao Tung University, Guiren Dist., Tainan 71150, Taiwan

e-mail: tiv@iph.krasn.ru, p.s.pankin@mail.ru, s.vetrov@inbox.ru, avg@iph.krasn.ru, wlee@nctu.edu.tw, zyr@iph.krasn.ru

Method of images [1] is capable of simplifying the problem geometry by symmetry. The method can be generalized from electrostatics to optical frequency, from Laplace's to Helmholtz's equation. For example, it reveals obvious analogy between optical Tamm states [2] and photonic crystal odd and even defect modes splitted through the mirror symmetry plane. In this study the method of images is applied to cholesteric liquid crystal. Cholesteric birefringence is due to a preferred orientation of molecules. This orientation is constant in the interface-parallel cross-sections, and it uniformly rotates with increasing distance from the interface. Its cyclic nature produces translational order and photonic band-gap. Near the interface, a chiral optical Tamm state is described [3]. But it is impossible for conventional metallic mirror at normal light incidence (Fig. 1, left). And a mirror is necessary with the effect of a half-wave phase plate to maintain polarization matching with proper chirality. Technically this mirror is achieved by some metasurfaces or anisotropic slabs. This mirror projects the half-space to another half-space with the same handedness (Fig. 1, right). Thus, the method of images reveals a new connection of chiral optical Tamm state to cholesteric liquid crystal twist-defect mode with its wavelength-tunable laser applications.

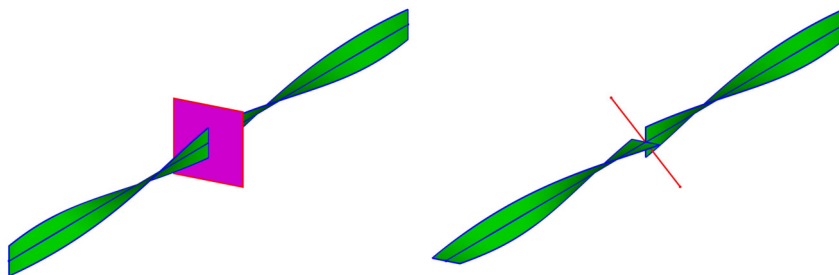


Fig. 1: Cholesteric liquid crystal, represented by green strips, twisted according to preferred molecular orientation helix. [left] The half-space is bounded by an ideal metallic mirror (magenta square). The enlarged region is constructed by reflection from the mirror plane. At normal light excitation the problem has neither surface mode nor defect mode solutions. [right] A polarization-preserving anisotropic mirror constructs the enlarged region by rotation about the mirror optical axis (red line). At normal light excitation this scheme supports both surface mode and twist-defect mode.

References

- [1] L. D. Landau, *Electrodynamics of Continuous Media*, Pergamon Press, Oxford, 1960.
- [2] M. A. Kaliteevski, I. Iorsh, S. Brand, R. A. Abram, J. M. Chamberlain, A. V. Kavokin, I. A. Shelykh, Tamm plasmon-polaritons: Possible electromagnetic states at the interface of a metal and a dielectric Bragg mirror, *Phys. Rev. B*, **76**, 165415 (2007).
- [3] I. V. Timofeev, P. S. Pankin, S. Y. Vetrov, V. G. Arkhipkin, W. Lee, V. Y. Zyryanov, Chiral optical Tamm states: temporal coupled-mode theory, *Crystals*, **7**, 113 (2017).

Short pulse propagation in PT-symmetric photonic crystals with material dispersion

Tsvetkov D.M., Bushuev V.A., Mantsyzov B.I.

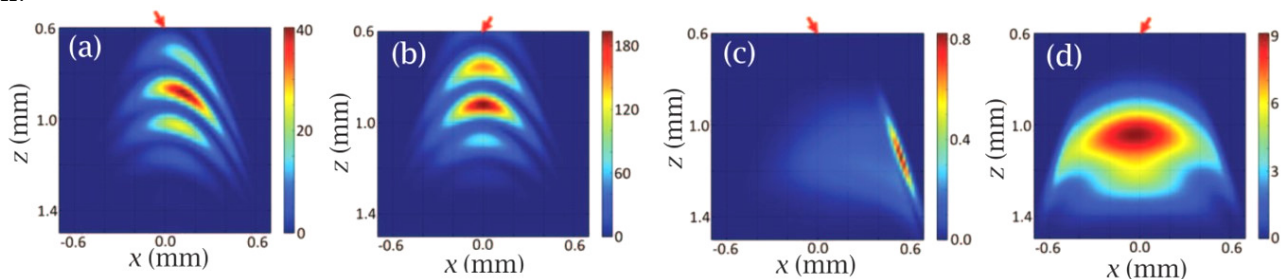
Department of Physics, M. V. Lomonosov Moscow State University, Moscow, Russia
e-mail: bmantsyzov@gmail.com

Konotop V.V.

Faculdade de Ciencias and Departamento de Física, Universidade de Lisboa, Lisboa, Portugal

The concept of parity-time (PT) symmetry in the non-Hermitian optics requires delicate balance between real and imaginary parts of the dielectric permittivity [1, 2]. The last requirement for the distribution of absorption and gain, described by the imaginary part of the dielectric permittivity, strictly speaking, is written for a given frequency of light and as such, is applicable only for this specific frequency. This point has fundamental importance in optical applications, in view of the causality principle. Mathematically, this is expressed through the Kramers–Kronnig relations, which can be satisfied only for isolated frequencies [3]. Therefore, the major development of the PT-symmetric optics is achieved, so far, within the paraxial approximation proposed, rather than with optical pulses, as initially suggested in Refs. [1, 2].

The main goal of the present work is to show that imperfectness of atomic resonances may allow for sustaining of PT symmetry in strongly dispersive media. Thus, such media with inhomogeneously broadened spectrum line are suitable for exploring short pulse dynamics in PT-symmetric environment. Using spectral method we solve the boundary diffraction problem of picoseconds pulse propagation in PT-symmetric photonic crystals (PC) under the condition of dynamical Bragg diffraction.



In the figure we demonstrate the restoration of effect of unidirectional diffraction for a pulse in PC in the Laue geometry of the Bragg diffraction in the exceptional point and at exact Bragg angle of incidence. The figure shows the snapshots of the intensity distributions of the pulse for the case of weak [(a), (b)] and sufficiently large [(c), (d)] inhomogeneous broadening. The PT symmetry is not verified for the pulse spectrum in the former case, and the shapes of the pulses with positive and negative angles of incidence weakly differ from each other showing the similarity of the distribution [(a), (b)]. Strong asymmetry, which is characteristic for the case of PT symmetry, is observed at large inhomogeneous broadening [(c), (d)]. For any pulse characterized by the spectral width smaller than the inhomogeneous line broadening, such a medium is close to PT-symmetric. As illustration of how PT symmetry can affect pulse propagation we describe unidirectional diffraction by a PC in Laue and Bragg geometries. As soon as the spectral characteristics are involved, the approach paves the way for a frequency control on the pulse dynamics in the PT-symmetric media.

References

- [1] A. Ruschhaupt, F. Delgado, J. G. Muga, *J. Phys. A*, **38**, L171 (2005).
- [2] R. El-Ganainy, K. G. Makris, D. N. Christodoulides, et al., *Opt. Lett.*, **32**, 2632 (2007).
- [3] A. A. Zyablovsky, A. P. Vinogradov, A. V. Dorofeenko, et al., *Phys. Rev. A*, **89**, 033808 (2014).

CdSe nanoplatelets as a new generation of ultrafast ionizing radiation detectors

R.M. Turtos, S. Gundacker, E. Auffray, P. Lecoq

CERN, 1211 Genève 23, Switzerland

e-mail: rosana.martinez.turtos@cern.ch

B. Mahler, C. Dujardin

ILM, Université Claude Bernard Lyon1 – CNRS, Bât Kastler, 10 rue Ada Byron, Lyon, France

e-mail: benoit.mahler@univ-lyon1.fr

In the field of fast timing research, direct band-gap semiconductors synthesized as colloidal nanocrystals have proven to be a promising source of prompt photon emission under high energetic ionizing radiation [1]. State-of-the-art inorganic single crystals commonly used in high-energy-physics (HEP) experiments and/or time-of-flight positron emission tomography are able to produce scintillating light at a rate of around 1 photon/MeV per picosecond. This rate strongly determines and limits the time resolution reached in radiation detector systems used nowadays. Lowering the accuracy at which we measure timing in scintillator-based calorimeters would highly impact particle tracking algorithms and image reconstruction techniques, both in HEP and medical imaging.

In this contribution we present light emission properties of CdSe nanoplatelets (NPLs) with and without a CdS crown using a pulsed X-rays tube with energies up to 30 keV and an impulse response function of 330 ps FWHM. We found that in agreement with electron excitation, the CdSe radio-luminescence appears to be at least 10 nm red-shifted from the main excitonic emission showing a fast decay component of $\mathcal{O}(100)$ ps for around 50% of the photons emitted. This red-shifted fast emission is also able to induce a small Stokes shift (~ 84 meV), radically changing the self-absorption characteristics of direct band-gap semiconductors, allowing for an incremental build-up of NPLs thick films on the order of tenths of μm (Figure 1). Furthermore, light output measurements of drop-casted CdSe/CdS core-crown NPLs films using $\text{Lu}_{2-x}\text{Y}_x\text{SiO}_5$ as a substrate, point towards a time-photon density on the order of 10 ph/MeV per picosecond. We show that the combination of state-of-the-art scintillators with high stopping power and the ultrafast photon emission of CdSe nanoplatelets opens the way to new radiation detector concepts with unprecedented timing performance.

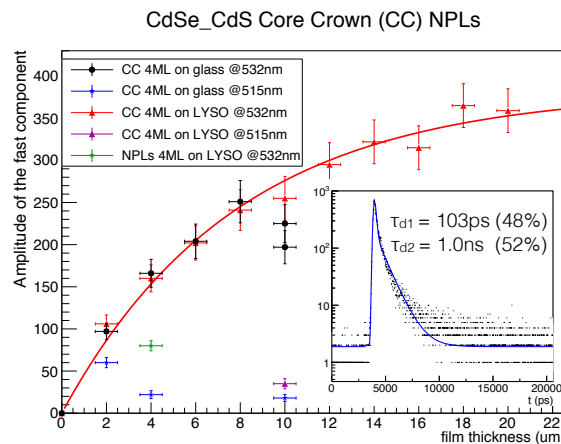


Fig. 1: Light output of CdSe NPLs films drop-casted on LYSO tiles of $3 \times 3 \times 0.2 \mu\text{m}^3$ for the excitonic (@515 nm) and multiexcitonic (@532 nm) emission. The NPLs time profile @532 nm is shown as inset.

Acknowledgments. This work was carried out in the frame of Crystal Clear collaboration and supported by the COST Action TD1401 (FAST) and ERC Advanced Grant no. 338953 (TICAL, P.I. Paul Lecoq).

References

- [1] R. M. Turtos, et al., Ultrafast emission from colloidal nanocrystals under pulsed X-ray excitation, *JINST*, **11**(10), P10015 (2016).

Sensing strategies for dielectric characterization and solute concentration measurement in liquids based on metamaterials-inspired resonators in microstrip technology

P. Velez, J. Mata-Contreras, F. Martin

GEMMA/CIMITEC, Departament d'Enginyeria Electronica, Universitat Autònoma de Barcelona, 08193 Bellaterra, Spain

e-mail: paris.velez@uab.cat, FranciscoJavier.Mata@uab.cat, ferran.martin@uab.cat

K. Grenier, D. Dubuc

MH2F, LAAS-CNRS, 7th, Avenue du Colonel Roche BP 54200 31031 Toulouse, Cedex 4, France

e-mail: grenier@laas.fr, dubuc@laas.fr

In recent years, metamaterial-inspired resonators, such as split ring resonators (SRR) and complementary split ring resonators (CSRR), have been used for sensing purposes in the microwave range [1–3]. Usually, these sensors are designed in planar technology by coupling the resonators to a host line. The sensing effect is based on the change of the electromagnetic properties of the resonators due to the presence of a material under test (MUT) close to them. In this work, some examples of microwave sensors for dielectric characterization and determination of solute concentration in deionized (DI) water are reported. Typically, in these microwave sensors the sensing principle is based on the change in the resonant frequency, phase shift and/or quality factor of the resonant particles due to the material to be sensed. For example, the complex dielectric constant of some MUT can be extracted by the frequency position and the magnitude of transmission/reflection coefficient in a transmission line loaded with resonators. This kind of sensing strategy is susceptible to environmental changes (temperature, humidity, etc.). To avoid this limitation, differential sensors, or sensors where the output variable is invariant to ambient conditions, become a good solution.

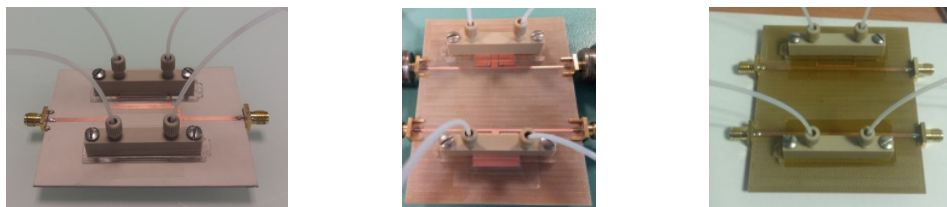


Fig. 1: Microwave sensors based on splitter/combiner configuration (a), uncoupled OCSRR-loaded transmission lines (b) and uncoupled SRR-loaded transmission lines (c).

As a first example, the authors reported a splitter/combiner configuration implemented in microstrip technology loaded with symmetric resonators (SRR) (Fig. 1a) for dielectric characterization of DI water/ethanol mixtures. One of the main problems of permittivity sensors implemented by means of resonator loaded lines is their limited capability to detect small changes between the reference material and MUT. In this work the authors reported a new strategy to design a high sensitivity microwave sensor based on uncoupled microstrip transmission lines loaded symmetrically with symmetric resonators (SRRs and OCSRRs) (Fig. 1b and Fig. 1c). The principle of sensing is based on the cross-mode transmission coefficient (S_{21}^{DC}) which is related to the level of asymmetries produced

by the MUT. These sensors are applied in this work to the measurement of the complex dielectric constant of liquids and to the determination of solution concentration in DI water.

References

- [1] A. Ebrahimi, W. Withayachumnankul, S. Al-Sarawi, D. Abbott, High-sensitivity metamaterial-inspired sensor for microfluidic dielectric characterization, *IEEE Sensors J.*, **14**(5), 1345–1351 (2014).
- [2] A. Abduljabar, D. Rowe, A. Porch, D. Barrow, Novel microwave microfluidic sensor using a microstrip split-ring resonator, *IEEE Trans. Microw. Theory Techn.*, **62**(3), 679–688 (2014).
- [3] M.S. Boybay, O.M. Ramahi, Material characterization using complementary split-ring resonators, *IEEE Trans. Instrum. Meas.*, **61**(11), 3039–3046 (2012).

Ultra-high field MRI radiofrequency excitation inhomogeneities mitigation in the head: optimization of dielectric pad mixture and locations

Alexandre Vignaud¹, Zo Raolison¹, Marc Dubois², Lisa Leroi¹, Ana L. Neves², Franck Mauconduit¹, Stefan Enoch², Nicolas Malléjac³, Pierre Sabouroux², Anne-Lise Adenot-Engelvin³, Redha Abdeddaim²

¹CEA, DRF/JOLIOT/Neurospin & University Paris-Saclay, Gif-sur-Yvette, France

²Aix Marseille Univ, CNRS, Centrale Marseille, Institut Fresnel, Marseille, France

³CEA–DAM Le Ripault, Monts, France

e-mail: alexandre.vignaud@cea.fr

Synopsis: With higher signal and contrast to noise ratio, UHF MRI (≥ 7 Tesla) images provide unprecedented potential for clinical and neuroscientific research. However, several limitations have been reported, hindering clinical application of these devices. At such field strengths, one of the main issues is the heterogeneous excitation of the nuclear spins. Typically, it leads to shadows or contrast losses across the human brain images, making the impacted regions sometimes barely exploitable.

A simple and cost efficient approach to address these inhomogeneities is the use of relative High-Dielectric Constant (HDC) materials in radiofrequency (RF) coils [1]. Their high displacement current alters the global RF distribution in the transmit coil and generates a secondary localized RF field used to tune the B_1^+ field. The current most effective HDCs found in the literature are small rectangular pads filled with BaTiO₃ water mixtures. Unfortunately, major drawbacks prevents their use in high field clinical routine: performance drops over time and manufacturing made difficult by the ecotoxicity of this perovskite power. In addition, to date, to the knowledge of the authors, there is no study inferring the number, location, size, geometry and permittivity of the pads in order to increase substantially the RF field simultaneously in both temporal lobes and cerebellum, which are the most altered areas in the brain at those fields [2].

In this work, we synthesize recent findings on BaTiO₃ preparation to enhance its properties [3] and concerning a serious alternative based on Silicon Carbide (SiC) [4]. Finally, we demonstrate through simulations that the most intuitive approach consisting in setting pads in front of each weak regions does not lead to the most efficient outcome [5].

Acknowledgements: This work has been supported by the Programme Transversal du CEA, FET-OPEN M-CUBE Project and France Life Imaging (FLI).

References

- [1] A. Webb, et al., *Concepts Magnetic Resonance*, **38**, 148–184 (2011).
- [2] O'Reilly, et al., *Journal of Magnetic Resonance*, **270**, 108–114 (2016).

- [3] A. L. Neves, et al., *Magn. Reson. Med.*, doi: 10.1002/mrm.26771 (2017).
- [4] A. L. Neves, et al., *Proceeding of the International Society of Magnetic Resonance in Medicine 2018*, Paris; poster no. 8137.
- [5] A. L. Neves, et al., *Proceeding of the International Society of Magnetic Resonance in Medicine 2018*, Paris; poster no. 7971.

Time-delay modeling of short pulse generation in lasers

Vladimirov A.G.^{1,2}, Pimenov A.¹

¹Weierstrass Institute, Mohrenstr. 39, 10117 Berlin, Germany

²N. I. Lobachevsky State University of Nizhny Novgorod, pr. Gagarina 23, Nizhny Novgorod, Russia

e-mail: vladimir@wias-berlin.de, pimenov@wias-berlin.de

An approach to the modelling of nonlinear dynamics in multimode lasers using delay differential equations (DDEs) is discussed. DDE models of different multimode laser devices: passively mode-locked semiconductor lasers generating short optical pulses [1, 2], frequency swept lasers used in optical coherence tomography, and broad area external cavity lasers capable of generating 3D localized structures of light (so-called light bullets) are developed and studied numerically and analytically. We present the results of numerical simulations of different dynamical states in these lasers and apply asymptotic approaches to the stability analysis of stationary and periodic operation regimes in the large delay time limit. In particular, distributed and nonlocal delay models for modelling the effects of dispersion [3] and transverse diffraction [4] on the laser dynamics are discussed.

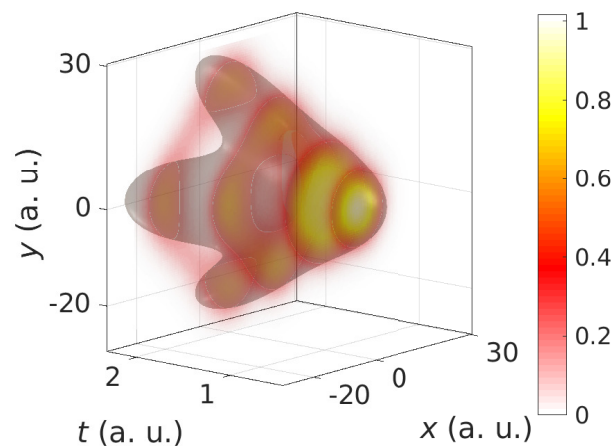


Fig. 1: Spatiotemporal profile of the intensity of light bullet in a broad area semiconductor mode-locked laser [4].

References

- [1] A. G. Vladimirov, D. V. Turaev, Model for passive mode-locking in semiconductor lasers, *Phys. Rev. A*, **72**, 033808 (2005).
- [2] D. Puzyrev, A. G. Vladimirov, A. Pimenov, S. V. Gurevich, S. Yanchuk, Bound pulse trains in arrays of coupled spatially extended dynamical systems, *Phys. Rev. Lett.*, **119**, 163901 (2017).
- [3] A. Pimenov, S. Slepneva, G. Huyet, A. G. Vladimirov, Dispersive time-delay dynamical systems, *Phys. Rev. Lett.*, **119**, 163901 (2017).
- [4] A. Pimenov, J. Javaloyes, S. V. Gurevich, A. G. Vladimirov, Light bullets in a time-delay model of a wide-aperture mode-locked semiconductor laser, *Philosophical Transactions of the Royal Society A*, accepted (2018).

Second-harmonic generation in Mie-resonant dielectric nanoparticles made of noncentrosymmetric materials

Volkovskaya I.I., Smirnova D.A.

Institute of Applied Physics, Russian Academy of Sciences, Nizhny Novgorod 603950, Russia
e-mail: volkovskaya@appl.sci-nnov.ru

By combining analytical and numerical approaches, we study resonantly enhanced second-harmonic generation (SHG) by individual spherical high-index dielectric nanoparticles made of noncentrosymmetric materials (AlGaAs and BaTiO₃), which possess large volume quadratic susceptibility of a tensorial form. Excitation of Mie resonances in such nanoparticles allows achieving record-high nonlinear conversion efficiencies at the nanoscale [1].

We focus on Mie-resonant dielectric nanoparticles, whose sizes correspond to the resonant excitation of the leading dipolar modes at the laser fundamental wavelength and discuss the effect of the low-order optical Mie modes on the characteristics of the generated far-field [2]. The problem of linear light scattering by a sphere is solved using the multipolar expansion in accord with Mie theory. We then analyze the induced nonlinear multipolar sources by employing general expressions for the electric and magnetic multipolar coefficients at the SH wavelength as defined by the overlap integrals of the sources with spherical harmonics. We specifically derive an analytical solution for the resonantly enhanced SHG driven by the magnetic dipole (MD) mode. Our calculations show that within the framework of single-mode MD approximation (for the magnetic moment aligned with [010] crystalline axis), the multipolar composition features magnetic quadrupolar (MQ) and electric octupolar (EO) components for the AlGaAs nanoparticle, and electric dipolar (ED), MQ and EO for the BaTiO₃ nanoparticle. Our analytical considerations are confirmed by full-wave numerical modeling performed with the finite-element solver COMSOL Multiphysics, following the procedure described in Refs. [1, 2]. The exemplary results of calculations are shown in Fig. 1.

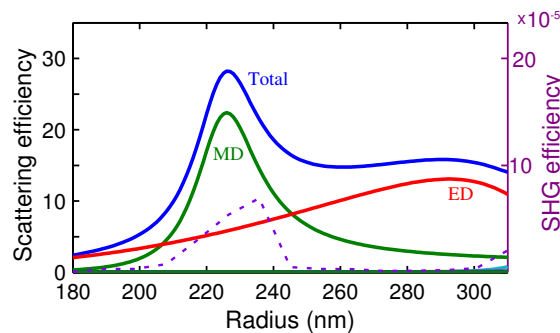


Fig. 1: Total scattered FF (solid blue) and radiated SH (dashed purple) powers spectra calculated for AlGaAs nanoparticle of radius $a = 237$ nm at pump laser wavelength $\lambda_0 = 1550$ nm and incident intensity $I_0 = 1$ GW/cm².

The developed multipolar analysis can be instructive for interpreting the far-field measurements of the nonlinear scattering, and it provides prospective insights into a design of highly-efficient nonlinear nanoantennas and subwavelength light sources, as well as methods of nonlinear diagnostics.

This work was supported by the Russian Foundation for Basic Research (Grant No. 18-02-00381).

References

- [1] S.S. Kruk, R. Camacho-Morales, L. Xu, M. Rahmani, D.A. Smirnova, L. Wang, H.H. Tan, C. Jagadish, D.N. Neshev, Y.S. Kivshar, Nonlinear optical magnetism revealed by second-harmonic generation in nanoantennas, *Nano Lett.*, **17**, 3914–3918 (2017).
- [2] D. Smirnova, A.I. Smirnov, and Y.S. Kivshar, Multipolar second-harmonic generation by Mie-resonant dielectric nanoparticles, *Phys. Rev. A*, **97**, 013807 (2018).

Multi-walled carbon nanotube sheet transparent electrode mediated ionic doping in organic photovoltaics

Voroshilov P.M.^{1,2}, Saranin D.S.³, Simovski C.R.^{1,2}, Zakhidov A.A.^{2,3,4}

¹Aalto University, P.O. 13000, FI-00076, Finland

²ITMO University, 197043, St. Petersburg, Russia

³National University of Science and Technology MISiS, Moscow 119049, Russia

⁴The University of Texas at Dallas, Physics Department and The NanoTech Institute, Richardson 75080, USA

e-mail: p.voroshilov@metalab.ifmo.ru

The main drawbacks of organic solar cells (OSCs) are low efficiency and stability. In this paper, we study the controlled n-doping in OSC by ionic gating of multi-walled carbon nanotube (MWCNT) coated fullerenes. Such electric double layer charging (EDLC) doping, achieved by ionic liquid (IL) charging, allows tuning the electronic concentration in the acceptor layers, increasing it by orders of magnitude [1]. This leads to decreasing both the series and shunt resistances of OPV and allows to use thick (up to 200 nm) electron transport layers, increasing the durability and stability of OPV.

Two stages of OPV enhancement are described, upon increase of gating bias: at small (or even zero) gate voltage the interface between porous transparent MWCNT charge collector with fullerene is improved, becoming an ohmic contact. This changes the S-shaped I-V curve and improves the electrons collection by a MWCNT turning it into a good cathode. The effect further enhances at higher gate voltage due to raising of Fermi level and lowering of MWCNT work function. At next qualitative stage, the acceptor layer becomes n-doped by electron injection from MWCNT and ions penetration into fullerene. At this step the internal built-in field is created within OPV, that helps exciton dissociation and charge separation/transport, increasing further the short-circuit current and the filling factor. Overall power conversion efficiency increases nearly 50 times in classical CuPc/fullerene OPV with bulk heterojunction photoactive layer and MWCNT cathode. Ionic gating of MWCNT-fullerene part of OPV opens a new way to tune the properties of organic devices, based on controllable and reversible doping and modulation of work function.

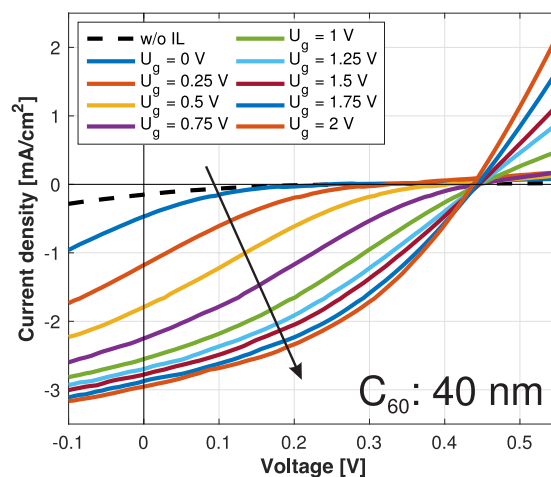
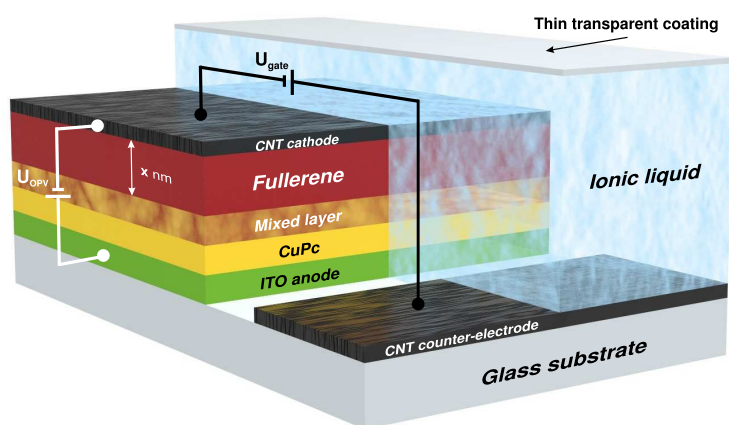


Fig. 1: Side view of the OSC-MWCNT-IL cell (left) and IV curves (right).

References

- [1] A. B. Cook, J. D. Yuen, A. A. Zakhidov, Electrochemically gated organic photovoltaic with tunable carbon nanotube cathodes, *Applied Physics Letters*, **103**, 163301 (2013).

A synthetic dual-frequency self-mixing interferometer

Ming Wang, Junbao Chen, Hui Hao, Dongmei Guo, Wei Xia

Jiangsu Key Lab on Opto-Electronic Technology, Nanjing Normal University, Nanjing 210023, China
e-mail: wangming@njnu.edu.cn, chenjunbao@aliyun.com, huihao@njnu.edu.cn,
guodongmei@njnu.edu.cn, xiaow@njnu.edu.cn

In this paper, a simple scheme of a synthetic dual-frequency self-mixing interferometer for high-precision non-contact displacement measurement is proposed. Previous researches on the self-mixing interference effect in orthogonally polarized dual frequency laser show that the mode competition will affect the phase relationship between the two self-mixing interference signals. If the frequency difference between two modes is greater than the line width of homogeneous broadening gain curve of laser (about 100–300 MHz), the phase relationship of two intensity modulation curves will be mainly determined by phase difference of two modes, and mode competition can be neglected. In this case, the intensity curves of the two orthogonal modes are independent and synthetic wavelength configuration can be brought into the self-mixing interferometer to get rid of the disadvantage of complicacy and high cost in non-contact tiny displacement measurement. An experimental system is set up and nanometer measurement experiment is conducted. In this system, an orthogonally polarized dual frequency laser with a frequency difference of 1 GHz is employed in optical configuration to avoid mode competition. We also design a zero-crossing phase detecting software module to record the temporal point of zero phase difference. The phase difference between the two orthogonally polarized feedback fringes is observed, and the tiny displacement of the object can be measured through the phase change of the synthetic signal. Since the virtual synthetic wavelength is 106 times larger than the operating wavelength, sub-nanometer displacement of the object can be obtained in millimeter criterion measurement without modulation, demodulation and complicated electrical circuits. Experimental results show good agreement with the theoretical analysis and the measurement precision reaches nanometer level with a modest sampling rate within 500 nm displacement range. The error sources of the developed interferometer have been discussed in detail, indicating that the precision of the entire system is mainly limited by the sampling rate of the DAQ card. If a higher sampling rate is used, the resolution of our system might be further improved. We achieve simplicity and good resolution in a synthetic dual-frequency self-mixing interferometer simultaneously, which can provide a potential approach to contactless measurement engineering application.

Flat asymmetric absorbers

Xu-Chen Wang, Ana Díaz-Rubio, Viktor S. Asadchy, Sergei A. Tretyakov

Aalto University, Espoo, Finland

e-mail: sergei.tretyakov@aalto.fi

In this presentation we will discuss how to break the angular symmetry of electromagnetic response of flat thin absorbers without breaking reciprocity. Based on our recent results on multichannel metasurfaces [1], we propose a new concept of asymmetric absorbers in which the absorption coefficient for waves impinging from a given oblique angle is extraordinarily different from that for waves incident from the oppositely tilted direction (see illustration in Fig. 1). The proposed flat structure realizes controllable reflectance (from 0 to 0.99) for waves incident from one direction, exhibiting total absorption when the sign of the incidence angle is reversed. We provide a theoretical and numerical analysis for the asymmetric absorber, including design and numerical validation of its performance. More information about this work can be found in preprint [2].

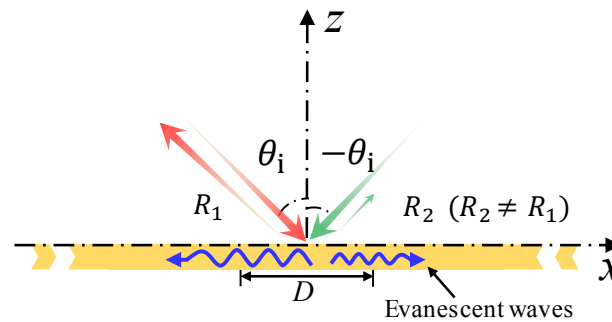


Fig. 1: Illustration of the asymmetric absorber concept. The reflection asymmetry is controlled by engineering the excited evanescent waves, localized at the metasurface.

References

- [1] V. S. Asadchy, A. Díaz-Rubio, S. N. Tsvetkova, D.-H. Kwon, A. Elsakka, M. Albooyeh, S. A. Tretyakov, Flat engineered multichannel reflectors, *Phys. Rev. X*, **7**, 031046 (2017).
- [2] X.-C. Wang, A. Díaz-Rubio, V. S. Asadchy, S. A. Tretyakov, Reciprocal angle-asymmetric absorbers: Concept and design, *arXiv:1801.09397* [physics.app-ph] (2018).

Surface waves of mixed TE-TM polarization at Jerusalem-cross-based anisotropic metasurface in microwaves

Yermakov O., Hurshkainen A., Dobrykh D., Kapitanova P., Iorsh I., Glybovski S., Bogdanov A.

Department of Nanophotonics and Metamaterials, ITMO University, St. Petersburg, Russia
e-mail: o.yermakov@metalab.ifmo.ru

Metasurfaces have recently gained significant attention due to their extraordinary electromagnetic properties to control both propagating plane waves and localized surface waves [1]. Another appealing feature is that spectrum of anisotropic metasurface supports two mixed TE-TM polarized modes [2–4]. This hybridization of TE and TM polarizations for surface waves is the consequence of the anisotropy and accidental degeneracy of the eigenmodes [5]. Moreover, the interplay between hyperbolic dispersion of surface waves and hybrid character of the polarization lead to the multiplicity of the equal frequency contours [2, 6].

In this work we focus on the numerical and experimental characterization of hybrid TE-TM polarized surface waves in the super high frequency range (from 2 to 8 GHz) supported by hyperbolic metasurface representing a two-dimensional array of copper Jerusalem crosses on FR4 substrate. We measure the normal component of electric and magnetic fields by using a coaxial probe and loop, respectively. Then we apply a 2D fast Fourier transform in order to visualize the equal frequency contours [7]. We demonstrate the propagation of two localized surface modes, which have hybrid TE-TM polarization and analyze the degree of a hybridization. We investigate the evolution of equal frequency contours for each eigenmode. The drastical changes of the equal frequency contours shapes, called topological transitions, are observed. Finally, we show that both modes can propagate simultaneously at the same frequency.

The manipulation and control over electromagnetic surface waves are promising for a number of potential applications in optical information technologies, opto-electronic and photonic devices, opto-mechanics, biological sensors etc.

References

- [1] S. B Glybovski, S. A. Tretyakov, P. A. Belov, Y. S. Kivshar, C. R. Simovski, Metasurfaces: From microwaves to visible, *Physics Reports*, **634**, 1–72 (2016).

- [2] O. Yermakov, A. Ovcharenko, M. Song, A. Bogdanov, I. Iorsh, Y. S. Kivshar, Hybrid waves localized at hyperbolic metasurfaces, *Physical Review B*, **91**, 235423 (2015).
- [3] J. S. Gomez-Diaz, M. Tymchenko, A. Alù, Hyperbolic plasmons and topological transitions over uniaxial metasurfaces, *Physical Review Letters*, **114**, 233901 (2015).
- [4] M. Mencagli, E. Martini, S. Maci, Surface wave dispersion for anisotropic metasurfaces constituted by elliptical patches, *IEEE Transactions on Antennas and Propagation*, **63**, 2992 (2015).
- [5] O. Yermakov, A. Ovcharenko, A. Bogdanov, I. Iorsh, K. Bliokh, Y. S. Kivshar, Spin control of light with hyperbolic metasurfaces, *Physical Review B*, **94**, 075446 (2016).
- [6] A. Samusev, I. Mukhin, R. Malureanu, O. Takayama, D. Permyakov, I. Sinev, D. Baranov, O. Yermakov, I. Iorsh, A. Bogdanov, A. Lavrinenko, Polarization-resolved characterization of plasmon waves supported by an anisotropic metasurface, *Optics Express*, **25**, 32631 (2017).
- [7] J. Dockrey, S. Horsley, I. R. Hooper, J. Sambles, A. P. Hibbins, Direct observation of negative-index microwave surface waves, *Scientific Reports*, **6**, 22018 (2016).

Dynamics of solitons and slow light in optical systems with strong light-matter interactions

Yulin A.V., Iorsh, I., Shelykh, I.

ITMO University, St. Petersburg 197101, Russia

e-mail: a.v.yulin@corp.ifmo.ru

Propagation of the waves in waveguides with incorporated two-levels systems (quantum dots or atoms) is considered. In the framework of mean field approximation the system can be described by the equation for the optical field amplitude ϕ and the spin projections S . Under the assumption that the backscattering can be neglected the equation have the form

$$i \frac{\partial \phi^{(R)}}{\partial t} + i \frac{\partial \phi^{(R)}}{\partial x} = \sum_j S_{-,j}^{(R)}(t) \psi_j(x),$$

$$i \frac{\partial S_{-,j}^{(R)}}{\partial t} = -S_{z,j}^{(R)} \int dx \phi^{(R)}(x) \psi_j(x) - \Omega S_{z,j}^{(R)} S_{-,j}^{(L)},$$

$$\frac{\partial S_{z,j}^{(R)}}{\partial t} = -\text{Im} \left(S_{-,j}^{(R)} \int dx \phi^{(R)*}(x) \psi_j(x) \right) - \Omega \text{Im} S_{-,j}^{(R)} S_{-,j}^{(L)*},$$

$$i \frac{\partial S_{-,j}^{(L)}}{\partial t} = -\Omega S_{z,j}^{(L)} S_{-,j}^{(R)}, \quad \frac{\partial S_{z,j}^{(L)}}{\partial t} = -\Omega \text{Im} S_{-,j}^{(L)} S_{-,j}^{(R)*}.$$

The influence of the effective transverse magnetic field resulting in the direct coupling between the atom subsystems is accounted by the normalized frequency Ω .

It is known that in the absence of the magnetic field Ω strong optical pulses in the systems in question split into a number of solitons and the residual radiation. The solitons have different amplitudes and durations, but the product of the amplitude and the duration is a fixed value which provides that after propagation of the solitons no material excitations are left in the medium.

The second material sub-system $S^{(L)}$ creates resonance excitations with the frequency laying in the resonant gap of the dispersion characteristic. The finite coupling Ω broadens the resonance into a narrow zone, the modes belonging to the zone correspond to slow light propagating in the system.

In this work we show that propagating solitons can resonantly excite slow light belonging to the flat branch of the dispersion characteristics. We discuss the scattering of the dispersive waves on the solitons and show that this process allows to transfer slow light belonging to the intermediate branch of the dispersive characteristic into either upper or lower branch of the dispersion characteristic. This opens a possibility to transform pulses of fast light into the slow ones and then to transform the slow light back to a fast propagating mode. This process can be of interest from the point of view of new frequencies generation and for optical writing, storing and reading of information.

Crystalline metamaterials for topological properties at the subwavelength scale

Yves S., Lemoult F., Fink M., Lerosey G.

Institut Langevin, CNRS UMR 7587, ESPCI Paris, PSL Research University, 1 rue Jussieu, 75005 Paris

e-mail: simon.yves@espci.fr

Fleury R.

Laboratory of Wave Engineering, EPFL, Station 11, route cantonale, 1015 Lausanne, Switzerland

e-mail: romain.fleury@epfl.ch

Berthelot T.

KELENN Technology, Antony, France

e-mail: thomas.berthelot@kelenntech.com

In this talk, we will show how going beyond the usual description of locally resonant metamaterials in terms of effective parameters allows to induce topological properties on a subwavelength scale [1]. Without any loss of generality, we take the particular case of quarter-wavelength-resonators in the microwave domain. First we show numerically that, thanks to multiple scattering [2], it is possible to engineer the band structure of a subwavelength scaled lattice of such resonators in order to obtain Dirac cones.

Then, following the previous work of Wu and Hu [3], we operate adiabatic subwavelength structural changes within the metamaterial. We show that these modifications lead to a phenomenon of band inversion which, added to the computation of the topological invariant, is a proof of the topological nature of the metamaterial crystals we designed. This band inversion is demonstrated both numerically and experimentally comparing the symmetries of the measured modes within the samples. This phenomenon is explained from a polaritonic point of view.

Moreover, the interface between media which present different topological behavior supports topological edge modes. Therefore we will show that this phenomenon occurs in the case of our subwavelength microwave topological insulator. We measure experimentally, and corroborate numerically, the propagation of subwavelength topological edge modes along the interface between two topologically different samples. This demonstrate the guiding of microwave on a subwavelength scale. We finally show that this work can be directly transposed to the acoustic domain [4].

References

- [1] S. Yves, R. Fleury, T. Berthelot, F. Lemoult, M. Fink, G. Lerosey, Crystalline metamaterials for topological properties at subwavelength scales, *Nat. Commun.*, **8**, 16023 (2017).
- [2] N. Kaina, F. Lemoult, M. Fink, G. Lerosey, Negative refractive index and acoustic superlens from multiple scattering in single negative metamaterials, *Nature*, **525**, 77–81 (2015).
- [3] L.-H. Wu, X. Hu, Scheme for achieving a topological photonic crystal by using dielectric material, *Phys. Rev. Lett.*, **114**, 223901 (2015).
- [4] S. Yves, R. Fleury, F. Lemoult, M. Fink, G. Lerosey, Topological acoustic polaritons: robust sound manipulation at the subwavelength scale, *New J. Phys.*, **19**, 75003 (2017).

Metal-dielectric nanoantenna for NV-center emission control

Zalogina A.S., Zuev D.A.

ITMO University, Saint-Petersburg, Russia

e-mail: a.zalogina@metalab.ifmo.ru

The emission control of nanoscale quantum sources through metal or high refractive index nanoantennas is a cornerstone of nanophotonics [1, 2]. Recently, we have proposed the concept of reconfig-

urable metal-dielectric (hybrid) nanoantenna [3], which can be a promising platform for luminescence control of nanoscale quantum sources. Here, we numerically investigate the opportunity of emission control of a single nitrogen vacancy (NV) center in a nanodiamond (ND) by the hybrid nanoantenna.

We study the influence of spatial arrangement of ND with single NV-center relatively to hybrid nanoantenna as well as NV-center orientation inside ND on the radiation diagram. We applied diameter of the diamond sphere of 50 nm, Si cone tip radius of 55 nm, height of the Si cone of 220 nm, the radius of the Si cone and Au disk base of 110 nm, the Au disk thickness of 30 nm. The simulation demonstrate 2-fold acceleration of spontaneous emission rate for ND placed on the edge of Au nanodisc for perpendicular orientation of NV-center to substrate, and 4-fold acceleration for parallel one. When ND is located in the center of Au nanodisc the spontaneous emission rate is 20 for perpendicular NV-center orientation and 4 for parallel one.

Thus, we have demonstrated that the developed concept of hybrid nanoantenna is suitable for emission control of NV-center in ND. The proposed approach can be realized by the existing fabrication methods and applied to different nanoscale quantum emitters.

References

- [1] X. W. Chen, Metallodielectric hybrid antennas for ultrastrong enhancement of spontaneous emission, *Physical Review Letters*, **108**, 233001 (2012).
- [2] I. Staude, et al., Shaping photoluminescence spectra with magnetoelectric resonances in all-dielectric nanoparticles, *ACS Photonics*, **2**(2), 172–177 (2015).
- [3] D. A. Zuev, et al., Fabrication of hybrid nanostructures via nanoscale laser-induced reshaping for advanced light manipulation, *Advanced Materials*, **28**(16), 3087–3093 (2016).

Manipulation of robust valley edge transport in ultrathin substrate-integrated photonic crystals

Li Zhang

State Key Laboratory of Modern Optical Instrumentation, and The Electromagnetics Academy at Zhejiang University, Zhejiang University, Hangzhou, China
e-mail: lilyzhang@zju.edu.cn

The birth of topological photonics has revolutionized our view on the propagation and scattering of light, especially giving rise to the unconventional robust backscattering-immune energy transport. However, the majority of previous photonic topological insulators (PTIs) consist of either infinitely long rods array, or complex magnetic components, or multi-mode metal waveguides with large thicknesses, rendering them difficult to compatible with the integrated circuitry. To tackle this problem, here we propose ultra-thin substrate-integrated photonic topological insulators (SIPTIs), exhibiting a single pair of edge modes with different valley chirality, which show high robustness and great compatibility with the traditional substrate-integrated circuitry. Such topological properties have been used to design some functional substrate-integrated components, such as sharp bending waveguides with high transmission, waveguides with disorders. Our studies offer a new route to control both valleys in the substrate-integrated circuitry, and may work as a fundamentally new integration platform for information processing with low cost, easy access, and light weight.

Light-assisted spontaneous birefringence and magnetic domains formation in suspension of gyrotropic nanoparticles

Alexander A. Zharov¹, Nina A. Zharova², Alexander A. Zharov, Jr.¹

¹Institute for Physics of Microstructures, Russian Academy of Sciences, Nizhny Novgorod, 603950 Russia

²Institute of Applied Physics, Russian Academy of Sciences, Nizhny Novgorod, 603950 Russia

e-mail: zharov@ipmras.ru

The new demands of optical fields control at microscale and nanoscale stimulate development design and manufacturing of novel types of metamaterials allowing wider possibilities than traditional optical devices. High tunability and easy reconfiguration are important requirements applicable to metamaterials to be a basis for advanced nanophotonic devices. In this context, liquid metamaterials [1] occupy special niche because of their incredible reconfigurability. Recently, a tunable resonant metamaterial called liquid metacrystal was suggested in [2]. It was supposed that such a material can be made of elongated resonant metallic nanoparticles (meta-atoms) dispersed in viscous liquid. An external DC electric field aligns meta-atoms along one axis that imparts the anisotropic properties to the metamaterial. The reorientation of anisotropy axis leads to the change of effective refraction index of metamaterial that, taking a resonant response into account, may strongly change the conditions of light propagation. Furthermore, meta-atoms can also be reoriented in response to high-frequency electromagnetic field that supposes the presence of strong nonlinearity of LMC. These properties of LMC were predicted in [2–4] and basically demonstrated in experiment [5].

In this report we discuss some unusual optical properties of a liquid metamaterial with spherical gyrotropic (for example, ferromagnetic) meta-atoms. It is well-known that electromagnetic properties of ferromagnetics in optical domain can be described by dielectric tensor similar to dielectric tensor of magneto-active plasma while the magnetic permeability is the unit tensor [6, 7]. We show that linearly polarized light in the suspension of gyrotropic nanoparticles can experience modulation instability, which leads to spatial separation of right- and left-circularly polarized waves. Such a separation preserves zero full angular momentum of electromagnetic field; thus, the time-reversal symmetry is broken only locally. Eventually, this instability results in the formation of the lattice of spatial solitons with alternating right and left circular polarization. As magnetic moments of nanoparticles tend to re-orient parallel to the wavevector in circular polarized light, every spatial soliton captures static magnetic field directed along or opposite to the wavevector depending on the direction of the field angular momentum; therefore, the soliton lattice altogether looks like magnetic domains array with antiferromagnetic ordering.

References

- [1] A. B. Golovin, O. D. Lavrentovich, *Appl. Phys. Lett.*, **95**, 254104 (2009).
- [2] A. A. Zharov, A. A. Zharov, Jr., N. A. Zharova, *J. Opt. Soc. Am. B*, **31**, 559 (2014).
- [3] A. A. Zharov, A. A. Zharov, Jr., N. A. Zharova, *Phys. Rev. E*, **90**, 023207 (2014).
- [4] A. A. Zharov, Jr., N. A. Zharova, A. A. Zharov, *J. Opt. Soc. Am. B*, **34**, 546 (2017).
- [5] M. Liu, K. Fan, W. Padilla, X. Zhang, I. V. Shadrivov, *Adv. Mater.*, **28**, 1553 (2016).
- [6] H. J. Zeiger, G. W. Pratt, *Magnetic Interaction in Solids*, Oxford, New York, 1973, 2009.
- [7] A. A. Zharov, V. V. Kurin, *J. Appl. Phys.*, **102**, 123514 (2007).

Self-focusing of electromagnetic surface waves in gyrotropic liquid metacrystals

Alexander A. Zharov, Jr.¹, Nina A. Zharova², Alexander A. Zharov¹

¹Institute for Physics of Microstructures, Russian Academy of Sciences, Nizhny Novgorod, 603950 Russia

²Institute of Applied Physics, Russian Academy of Sciences, Nizhny Novgorod, 603950 Russia
e-mail: azharov@ipmras.ru

Metamaterials provide a variety of possibilities to control optical fields at microscale and nanoscale unachievable in traditional optical devices, which, in turn, instigates interest of scientific community to this research area. Tunable structures with easily adjustable electromagnetic properties are particularly challenging as they can increase functionality of metamaterial devices. One of possible approaches to realize such structure, namely, liquid metamaterial, was experimentally studied in [1]. Similar concept was theoretically analyzed in [2]. In [2], a tunable metamaterial called liquid metacrystal (LMC) was composed of elongated resonant nanoparticles (meta-atoms) suspended in viscous liquid. The orientation of such particles can be managed by external DC electric field, which provides the ability to control the anisotropy axis direction of the material. The reorientation of meta-atoms in high frequency field leads to strong nonlinearity of LMC. Such properties of LMC as high tunability, strong nonlinearity, ability to support surface and guided waves of new kinds, as well as existence of thermal topological transitions were theoretically studied in [2–5]. Some predicted properties of LMC were experimentally demonstrated in [6].

Current research is devoted to the study of nonlinear propagation of surface plasmons in LMCs with gyrotropic meta-atoms. Such meta-atoms can be described by the Hermitian polarizability tensor with isotropic diagonal part and imaginary non-diagonal elements. It was shown that in this case the orientation of meta-atoms is determined not by external DC electric field but by the presence of the nonzero angular momentum of the electromagnetic field. As TM electromagnetic surface wave (SW) has elliptic polarization (with longitudinal and transverse components of electric field) it causes reorientation of the meta-atoms magnetic moments along the SW angular momentum, thus, leading to the change of SW dispersion properties and emergence of focusing nonlinearity. It can result in lateral self-focusing of SWs and eventually in forming of SW spatial solitons.

References

- [1] A. B. Golovin, O. D. Lavrentovich, *Appl. Phys. Lett.*, **95**, 254104 (2009).
- [2] A. A. Zharov, A. A. Zharov, Jr., N. A. Zharova, *J. Opt. Soc. Am. B*, **31**, 559 (2014).
- [3] A. A. Zharov, A. A. Zharov, Jr., N. A. Zharova, *Phys. Rev. E*, **90**, 023207 (2014).
- [4] N. A. Zharova, A. A. Zharov, A. A. Zharov, Jr., *J. Opt. Soc. Am. B*, **33**, 594 (2016).
- [5] A. A. Zharov, Jr., N. A. Zharova, A. A. Zharov, *J. Opt. Soc. Am. B*, **34**, 546 (2017).
- [6] M. Liu, K. Fan, W. Padilla, X. Zhang, I. V. Shadrivov, *Adv. Mater.*, **28**, 1553 (2016).

Leaky topological states: from near- to far-field investigation

Zhirihin D.V., Gorlach M.A., Slobozhanyuk A.P., Belov P.A.

ITMO University, Saint Petersburg, 197101, Russia

e-mail: d.zhirihin@metalab.ifmo.ru

Ni X., Smirnova D.A., Korobkin D., Alù A., Khanikaev A.B.

The Department of Electrical Engineering, Grove School of Engineering, City College of the City University of New York, New York, 10031, USA

Inspired by the discoveries of the topological phases in condensed matter physics, photonic analogues of topological insulators are currently under active investigation. Their fascinating properties

such as disorder robustness and backscattering-immune propagation of the topological states have opened novel ways to control propagation and internal degrees of freedom of electromagnetic waves.

In the recent years, photonic topological systems have been investigated experimentally from microwave to optical frequencies [1–3], while the conclusions about the topological properties of the structures have been drawn based on the analysis of the topological edge states. Technically, this implies the measurement of the near field distribution from the topological structure.

In this work, we propose an alternative strategy, namely, to retrieve the topological invariants from the *far field*. Specifically, we measure the angle-resolved transmission spectra of the topological metasurfaces [Fig. 1(a,b)] and from these results extract spin Chern number. To verify the proposed technique, we perform proof-of-concept experimental near-field studies of the edge modes in the microwave spectral range [Fig. 1(c)] which confirm the proposed method.

Our results thus give not only an alternative technique to investigate the topological systems, but also provide further insights into the topological states of open non-Hermitian systems.

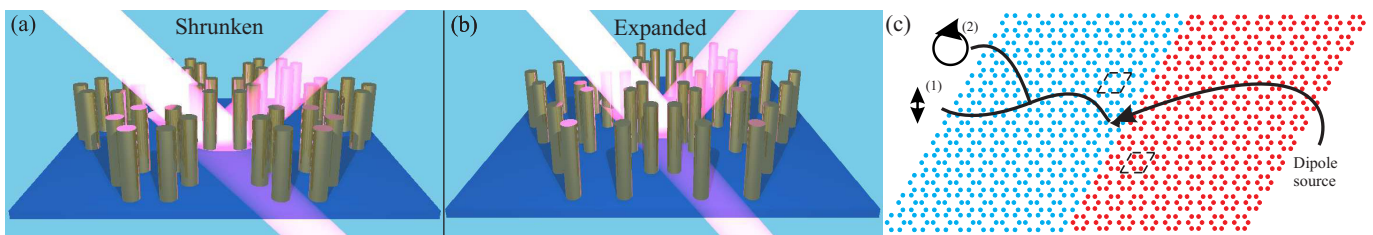


Fig. 1: (a) Shrunken and (b) expanded geometries of a metasurface based on a triangular lattice of hexamers of silicon pillars on a sapphire substrate. (c) A sketch of the metasurface for observation of pseudo-spin polarized edge states in microwave range.

References

- [1] A.P. Slobozhanyuk, et al., Experimental demonstration of topological effects in bianisotropic metamaterials, *Scientific Reports*, **6**, 22270 (2016).
- [2] M. Hafezi, et al., Imaging topological edge states in silicon photonics, *Nature Photonics*, **7**, 1001–1005 (2013).
- [3] M.C. Rechtsman, et al., Photonic Floquet topological insulators, *Nature*, **496**, 196–200 (2013).

Multimode theory of plasmonic distributed feedback laser

A.A. Zyablovsky^{1,2}, E.S. Andrianov^{1,2}, N.E. Nefedkin^{1,2,3}, I.A. Nechepurenko¹, A.V. Dorofeenko^{1,2,3}, A.A. Pukhov^{1,2,3}, A.P. Vinogradov^{1,2,3}

¹Dukhov Research Institute of Automatics, 22 Sushchevskaya, Moscow 127055, Russia

²Moscow Institute of Physics and Technology, 9 Institutskiy per., 141700 Dolgoprudny, Moscow reg., Russia

³Institute for Theoretical and Applied Electromagnetics RAS, 13 Izhorskaya, Moscow 125412, Russia
e-mail: zyablovskiy@mail.ru

In the last years, substantial progress has been made in creating plasmonic distributed feedback (DFB) lasers [1–6]. In these lasers, the role of the resonator is played by the periodic plasmonic structure. These can be metallic films perforated by holes [1, 3, 5, 6] and one- or two-dimensional arrays of plasmonic nanoparticles [2, 4]. The eigenmodes of plasmonic DFB lasers are hybrid plasmon-polariton Bloch modes [1, 2]. These modes can be generated with either continuous [1, 5] or pulsed [2–4, 6] pumping. Owing to its small size the plasmonic DFB lasers are very promising for a wide range of applications, from spectroscopy [6] to optoelectronics [2]. At the same time, a number of problems with the DFB lasers remain unresolved [5].

Here, we develop a multimode theory of the plasmonic DFB laser that takes into account the spontaneous emission of the atoms of the active medium and a nonlinear interaction between the

Bloch modes of the plasmonic structure [7–9]. Based on this theory we find the output power, the spectrum and the radiation pattern of the plasmonic DFB laser. We demonstrate that the spontaneous emission and the multimode nature of the lasing have a strong effect on the radiation properties of the plasmon DFB lasers [8, 9]. Our theory [9] eliminates the existing discrepancies between theoretical [10] and experimental [5] results.

References

- [1] F. van Beijnum, et al., *Phys. Rev. Lett.*, **110**, 206802 (2013).
- [2] W. Zhou, et al., *Nature Nanotech.*, **8**, 506 (2013).
- [3] X. Meng, et al., *Laser Photon. Rev.*, **8**, 896 (2014).
- [4] | A. H. Schokker, A. F. Koenderink, *Phys. Rev. B*, **90**, 155452 (2014).
- [5] V. T. Tenner, et al., *ACS Photonics*, **3**, 942946 (2016).
- [6] P. Melentiev, et al., *Appl. Phys. Lett.*, **111**, 213104 (2017).
- [7] A. A. Zyablovsky, et al., *Phys. Rev. A*, **95**, 053835 (2017).
- [8] A. A. Zyablovsky, et al., *Phys. Rev. B*, **95**, 205417 (2017).
- [9] N. E. Nefedkin, et al., *arXiv:1712.09906* (2017).
- [10] H. Kogelnik, C. Shank, *Journal of Appl. Phys.*, **43**, 2327 (1972).

Author index

- Abdeddaim, R., 116, 144, 182, 189, 201, 220
Abramochkin, E.G., 23, 90
Adenot-Engelvin, A-L., 220
Afanasev, K.N., 203
Afzal, M.U., 117
Akimov, A.V., 118, 147
Alahbakhshi, M., 158
Alekseev, K.N., 118
Alekseev, P.A., 123
Alekseeva, E.L., 24
Alharbi, M., 157
Alkhimenko, A.A., 24
Altaisky, M.V., 25
Alü, A., 119, 174, 230
Amlani, K., 25
Anastasia, R., 25
Andreychenko, A.E., 129
Andrianov, E.S., 140, 187, 231
Anikin, A.Yu., 26, 27
Apostolakis, A., 118
Arkhipkin, V.G., 216
Arseniev, D.G., 111
Artemov, V.V., 152
Asadchikov, V.E., 28
Asadchy, V.S., 224
Auffray, E., 218
Babich, M.V., 29
Badanin, A.V., 30
Baibulov, I.V., 30
Bakharev, F.L., 30, 31
Balanov, A.G., 118
Bandres, M.A., 118
Baranov, D.G., 119, 120
Barhom, H., 121
Barsukova, M.G., 122
Bartley, T.J., 205
Baryshnikova, K.V., 204
Baughman, R.H., 123
Bekshaev, A.Y., 128
Belashov, A.V., 32
Belishev, M.I., 31
Belolipetskaia, A.G., 32
Belous, A.A., 97
Belov, P.A., 230
Beltukov, Y.M., 32
Belyaev G.R., 46
Belyaev, A.K., 24, 33, 86, 111
Benabid, F., 157
Bendahmane, A., 133
Benimetskiy, F.A., 123
Berestennikov, A.S., 124
Berthelot, T., 227
Beruete, M., 126
Besedin, I., 206
Bezus, E.A., 141
Bittner, S., 102
Blagoveshchensky, A.S., 34
Bleu, O., 127
Bliokh, K.Y., 128
Bogdanov, A.A., 128, 196, 197, 225
Boginskaya, I.A., 203
Borzov, V.V., 34
Botkin, N.D., 65
Boyd, R.W., 143
Brezhnev, Yu.V., 35
Brodbeck, S., 194
Brui, E.A., 129
Budiasih, L.K., 36
Budylin, A.M., 30
Bulatov, V.V., 36
Buljan, H., 130
Bulygin, A.N., 37
Burenin, A.V., 84
Bushuev, V.A., 217
Buslov, V.A., 38
Bykov, D.A., 141
Bykov, I.V., 203
Cardin, A., 193
Carluccio, G., 132
Carter, J.D., 42
Chafer, M., 157
Chang, J.-H., 39
Chávez-Rivas, F., 194
Chebotarev, A.Yu., 65
Chehade, S., 40
Chemnitz, M., 163
Chen, J., 224
Chen, Z., 200
Chernomyrdin, N.V., 93
Chestnov, I.Yu., 130
Chong, Y.D., 175
Chubchev, E.D., 131
Collins, C.M., 132
Conforti, M., 133, 178, 184
Copie, F., 184
Dadoenkova, N.N., 134
Dadoenkova, Yu.S., 134
Damaskinsky, E.V., 34
Danilin, A.N., 82
Danilov, V.G., 40
Darmon, M., 40
Debord, B., 157
Dekalchuk, A.A., 65
Demchenko, M.N., 41
Demidchik, V.I., 135
Di Carlo, A., 136, 150
Di Liberto, M., 136
Díaz-Rubio, A., 224
Dietz, B., 102
Dinvay, E., 42
Dmitriev, A.A., 137
Dmitrieva, L.A., 42
Dobrokhotov, S.Yu., 26, 27, 35, 43, 44, 83
Dobrykh, D., 225
Dolganov, P.V., 138
Dolganov, V.K., 138
Dong, J.-W., 139
Dorodnyi, M.A., 44
Dorofeenko, A.V., 131, 231
Doronin, I.V., 140
Doroshenko, O.V., 45
Doskolovich, L.L., 141
Driben, R., 142
Droulias, S., 160
Drozдов, A.A., 143
Dubois, M., 144, 220
Dubtsov, A.V., 164
Dubuc, D., 219
Dugin, N.A., 46
Dujardin, C., 218
Dutykh, D., 42
Dyakov, S.V., 145
Dzhioev, R.I., 187
Economou, E.N., 160
Edemsky, F.D., 87
Egorov, O.A., 145
Ehrhardt, M., 85
Eich, M., 195
Enoch, S., 116, 144, 182, 220
Eremin, A.A., 53
Erni, D., 159, 200
Esselle, K.P., 117
Evtushenko, E.G., 203
Ezhov, A.A., 152, 192
Fan, K., 193
Farafonov, V.G., 47
Fedorov, S.V., 146
Fedotov, A.A., 47, 48
Fedyanin, A.A., 122, 192
Fedyanin, A.E., 147
Ferreira, H., 181
Fetisov, S.N., 96
Fialkovsky, I.V., 49
Filatova, V.M., 82
Filippenko, G.V., 50
Filonov, D., 148
Fink, M., 156, 227
Fistul, M.V., 206
Fleury, R., 227
Fomenko, S.I., 54, 74
Frizyuk, K.S., 149
Fromhold, T.M., 118

- Fuentes, S., 194
 Fujiwara, Y., 187
 Furasova, A.D., 150
Gainutdinov, R.V., 152
 Galyamin, S.N., 56
 Garbuzov, F.E., 32, 50
 García-Etxarri, A., 151
 Gavrikov, A.A., 51
 Gavrilov, S.N., 52
 Gaydukov, R.K., 40
 Generalov, A., 119
 Gerome, F., 157
 Gerrits, T., 205
 Gets, D.S., 151
 Ginzburg, P., 121, 148
 Gippius, N.A., 145
 Glushkov, E.V., 53
 Glushkova, N.V., 53
 Glybovski, S.B., 113, 129, 189, 211, 225
 Golov, A.A., 84
 Golub, M.V., 53, 54
 Gómez, D., 55
 Gomez, L., 187
 Goray, L.I., 28
 Gorkunov, M.V., 152
 Gorlach, A.A., 153
 Gorlach, M.A., 153, 154, 212, 230
 Goupalov, S.V., 187
 Grange, R., 149
 Greenaway, M.T., 118
 Gregorkiewicz, T., 187
 Grekova, E.F., 55
 Grenier, K., 219
 Grigoreva, A.A., 56
 Grishchenko, A.I., 24
 Gubaydullin, A.R., 161, 183
 Gundacker, S., 218
 Guo, D., 224
 Gusev, V.A., 57
 Guy, A., 194
Haemer, G., 132
 Hafezi, M., 155, 175
 Hao, H., 224
 Haroldson, R., 158
 Hayat, A., 194
 Herrmann, H., 205
 Hoffling, S., 194
 Höpker, J.P., 205
 del Hougne, P., 156
 Hurshkainen, A.A., 225
 Husakou, A., 157
Il'in, V.B., 47
 Imani, M.F., 156
 Iorsh, I.V., 124, 167, 225, 226
 Ishkhanyan, A.M., 58
 Ishkhanyan, T.A., 58
 Ishteev, A.R., 151, 158
 Ivanov, A.V., 59, 203
 Ivanov, K.A., 161, 183
 Ivchenko, E.L., 158
Jalali, M., 159
 Jalas, D., 195
 Jouvaud, C., 201
Kall, M., 120
 Kafesaki, M., 160
 Kalashnikova, A.M., 147
 Kalinovich, A.A., 92
 Kalisch, H., 42
 Kaliteevski, M.A., 161, 183
 Kaminer, I., 162
 Kan, V.A., 103
 Kapitanova, P.V., 225
 Kaputkina, N.E., 25
 Karpinski, P., 120
 Kartashov, D., 163
 Katsantonis, I., 160
 Katsnelson, B., 60
 Kavokin, A.V., 130
 Kazakov, A.Ya., 60
 Ken, O.S., 187
 Kent, J., 118
 Kevin, 72
 Khanikaev, A.B., 153, 164, 230
 Khusnutdinova, K.R., 50
 Kirpichnikova, A.S., 61
 Kirpichnikova, N.Ya., 61
 Kiselev, A.D., 164
 Kiselev, A.P., 34, 61, 115
 Kislin, D.A., 62
 Kivshar, Yu.S., 128, 165, 214
 Klimov, V.V., 165
 Klopp, F., 47
 Knyazev, M.A., 62, 143, 166
 Knyazkov D., 63
 Kober, F., 189
 Koli, M.N.Y., 117
 Kolodny, S.A., 167
 Komissarenko, F.E., 199
 Komissarova, M.V., 92
 Kondratov, A.V., 152
 Konotop, V.V., 142, 217
 Korenev, V.L., 187
 Korikov, D.V., 64
 Kornev, R.V., 135
 Korobkin, D., 230
 Korolev, V.I., 199
 Korolkov, A.I., 97
 Koshelev, K.L., 128
 Kosulnikov, S.Yu., 113
 Kotolevich, Y., 194
 Kotov, O.V., 174
 Kovalenko, E.O., 103
 Kovaleva, M., 64
 Kovtanyuk, A.E., 65
 Kozin, V.K., 168
 Kozitskiy, S.B., 66
 Kozlov, S.A., 62, 143, 166
 Kozlov, V.A., 67, 68
 Krafft, C., 69, 112
 Krapick, S., 205
 Krasnok, A.E., 119, 174, 176
 Kretov, E.I., 169
 Kristianto, I.J., 68
 Krizhanovskii, D., 170
 Krylov, V.A., 25
 Kudlinski, A., 133, 178, 184
 Kudrin, A.V., 69
 Kuperin, Yu.A., 42
 Kurochkin, I.N., 203
 Kurseeva, V.Yu., 69
 Kusmartsev, F.V., 118
 Kusrayev, Yu.G., 187
 Kuznetsov, N.G., 70
Lafargue, C., 102
 Lagarkov, A.N., 203
 Lalbakhsh, A., 117
 Lammering, R., 109
 Lampe, R., 65
 Landau, N., 194
 Lannebère, S., 170
 Lapine, M., 171
 Larin, A.O., 172
 Larrat, B., 189, 201
 Lavrinenko, A.V., 173, 196
 Lebeau G., 40
 Lebental, M., 102
 Lecoq, P., 218
 Lee, W., 216
 Lemarchand, F., 182
 Lemoult, F., 227
 Lepeshov, S.I., 174
 Leroi, L., 144, 220
 Lerosey, G., 156, 227
 Leroy, C., 58
 Levin, S.B., 30
 Leykam, D., 175
 Li, S.V., 119, 176
 Liashenko, T.G., 151
 Limonov, M.F., 128, 209
 Lin, J., 187
 Lisyansky, A.A., 140, 187
 Lita, A., 205
 Lobastov, V.G., 46
 Lukashenko, S.Y., 209
 Luk'yanchuk, B.S., 122
 Lumeau, J., 182
 Luo, K.H., 205
 Lyalinov, M.A., 71
 Lysenko, S., 147

- Lyubarov, M.D., 177
 Lyuibchanskii, I.L., 134
MacDiarmid, A.G., 123
 Machnev, A., 121
 Machorro, R., 194
 Magdalena, I., 25, 68, 72
 Mahler, B., 218
 Makarov, S.V., 124, 149–151, 158, 199, 214
 Malléjac, N., 220
 Malpuech, G., 127
 Manevitch, L.I., 64
 Mantsyzov, B.I., 217
 Marest, T., 133, 178
 Markina, D.I., 199
 Martin, F., 219
 Mas Arabí, C., 133, 178
 Maslova, E.E., 180
 Maslovski, S., 181
 Mata-Contreras, J., 219
 Matias, D.V., 72
 Matveenko, S.G., 30
 Matveev, V.B., 73
 Mauconduit, F., 220
 Medvedev, Iu., 181
 Meier, T., 142, 205
 Melchakova, I.V., 129
 Melikhova, A.S., 73
 Merzlikin, A.M., 203
 Miakishcheva, O.A., 74
 Mikhaylov, A.S., 75
 Mikhaylov, V.S., 75
 Mikheev, V.V., 203
 Mikheeva, E., 182
 Milian, C., 178
 Minenkov, D.S., 76
 Miridonov, S., 194
 Mirin, R., 205
 Miroshnichenko, A., 183
 Mittal, S., 175
 Mochalova, Yu.A., 52
 Mogunov, Ia.A., 147
 Moreau, A., 182
 Morgunov, Yu.N., 84
 Morozov, K.M., 183
 Motygin, O.V., 77
 Mukhin, I.S., 123
 Musorin, A.I., 122
 Mussot, A., 133, 178, 184
Nadgaran, H., 159
 Nam, S.W., 205
 Nandan, N., 186
 Naveau, C., 184
 Nazaikinskii, V.E., 26, 27
 Nazarov, S.A., 31, 68, 77, 78
 Nechepurenko, I.A., 231
 Nefedkin, N.E., 187, 231
 Negrov, D.V., 203
 Nestoklon, M.O., 187
 Neves, A. L., 220
 Ni, X., 230
 Nikitin, A., 205
 Nikulin, A., 188, 189, 201
 Nori, F., 128, 190
 Nosikova, V.V., 82
 Noskov, R., 121
 Nosov, P.A., 93
Okhlopkov, K.I., 192
 Orlikovsky, N.A., 192
 Ourir, A., 188, 189, 201
Padilla, W.J., 193
 Panah, M.E.A., 173
 Pankin, P.S., 216
 Panna, D., 194
 Panyaev, I.S., 134
 Papadimitratos, A., 208
 Pasechnik, S.V., 164
 Pastukhova, S.E., 79
 Pavlov, Yu.V., 37
 Pavlova, A.V., 80
 Pelinovsky, E.N., 210
 Perel, M.V., 49
 Pérez, E., 81
 Permyakov, D.V., 196
 Pestov, L.N., 82
 Petranovskii, V., 194
 Petrov, A.Yu., 195
 Petrov, M.I., 149
 Petrov, P.N., 83
 Petrov, P.S., 84, 85, 95
 Petrov, V.A., 86
 Pidgayko, D.A., 196
 Pilipchuk, V., 64
 Pimenov, A., 221
 Plachenov, A.B., 61
 Plamenevskii, B.A., 64
 Poddubny, A.N., 154, 177, 197
 Pogorelskaya, L.Yu., 197
 Polyanskiy, A.M., 86
 Polyanskiy, V.A., 24, 86, 111
 Popov, A.V., 87
 Popov, I.Y., 32, 73
 Popov, M.M., 88
 Porubov, A.V., 89
 Poutrina, E., 198
 Poyser, C.L., 118
 Pozina, G.P., 183
 Prokopovich, I.V., 87
 Prozorova, E.V., 89
 Pukhov, A.A., 187, 231
 Pushkarev, A.P., 199, 214
Raolison, Z., 144, 220
 Razueva, E.V., 23, 90
 Reichelt, M., 205
 Rennings, A., 200
 Repän, T., 173
 Rif'atin, H.Q., 25
 Rogov, O.Y., 152
 de Rosny, J., 188, 189, 201
 Rosshin, B.S., 28
 Rouleux, M., 27
 Rozanov, N.N., 146
 Rubtsov, S.E., 80
 Rudnitskii, A. G., 82
 Rutckaia, V.V., 196
 Ryadovkin, K.S., 91
 Rybak, L., 194
 Rybin, M.V., 128, 137, 180, 186, 209
 Ryzhikov, I.A., 203
Sabouroux, P., 220
 Saburova, N.Yu., 91
 Sadrieva, Z.F., 128
 Sáenz, A.B., 202
 Saksida, P., 92
 Samusev, A.K., 123, 196
 Samusev, K.B., 128, 197, 209
 Sánchez-Lopez, P., 194
 Sannikov, D.A., 199
 Sannikov, D.G., 134
 Sapega, V.F., 187
 Saranin, D.S., 151, 223
 Sarychev, A.K., 203
 Savelev, R.S., 154, 172
 Sazonov, S.V., 92
 Schadko, A.O., 93
 Scherbakov, A.V., 147
 Schilling, J., 196
 Schmidt, M., 163
 Schneider, C., 194
 Schulz, K.M., 195
 Sedov, E.S., 130
 Sedova, M.V., 203
 Segev, M., 118, 204
 Sekerzh-Zenkovich, S.Ya., 44
 Semenov, A.A., 32
 Semenov, A.S., 24
 Semenova, I.V., 32
 Senik, N.N., 94
 Sergeev, S.A., 95
 Sergeeva, N.V., 110
 Setukha, A.V., 96
 Shafrin, P.A., 192
 Shalin, A.S., 204
 Shamkhi, H.K., 204
 Shanin, A.V., 97
 Sharapova, P.R., 205
 Shchelokova, A.V., 129, 169
 Shcherbakov, M.R., 192
 Shchetka, E.V., 48

- Shegai, T., 206
 Shelykh, I.A., 226
 Shirokov, E.A., 98
 Shishkin, I.I., 121
 Shishkina, E.V., 52
 Shkondin, E., 173
 Shmeliova, D.V., 164
 Shorokhov, A.S., 122
 Shpak, A.N., 54
 Shpolyanskiy, Y.A., 62
 Shulga, K.V., 206
 Shuravin, N.S., 138
 Shurgalina, E.G., 210
 Shvets, G., 207
 Sievert, B., 200
 Silberhorn, C., 205
 Silveirinha, M.G., 170
 Simonov, S.A., 31
 Simovski, C.R., 208, 223
 Sinelnik, A.D., 197, 209
 Sinev, I.S., 123, 196
 Skryabin, D.V., 145, 178
 Slavyanov, S.Yu., 29
 Slobozhanyuk, A.P., 129, 153, 169, 230
 Slunyaev, A.V., 99, 210
 Smetanin, N.M., 42
 Smirnova, D.A., 222, 230
 Smith, D.R., 156
 Smolkin, E.Yu., 100
 Snegur, M.O., 100
 Sokolovskaya, M.V., 47
 Sollapur, R., 163
 Solnyshkov, D.D., 127
 Solomakha, G.A., 211
 Soukoulis, C.M., 160
 Spielmann, C., 163
 Starkov, A.S., 100
 Starkov, I.A., 100
 Stavtsev, S.L., 101
 Stepanenko, A.A., 212
 Suenaga, K., 187
 Sukharevsky, I.O., 102
 Sukhorukov, A.A., 213
 Suleymanova, A., 103
 Sun, Y., 172
 Sushchenko, A.A., 103
 Suslina, T.A., 44, 104
 Svejda, J.T., 200
 Sychev, S.K., 196
 Szriftgiser, P., 184
 Tagirdzhanov, A.M., 34
 Takayama, O., 173
 Tarasov, M.G., 149
 Telyatnikov, I.S., 80, 105
 Tiguntseva, E.Y., 124, 214
 Tikhodeev, S.G., 215
 Tikhonov, A.M., 28
 Tikhov, S.V., 106
 Timofeev, I.V., 216
 Todorov, M.D., 107
 Tolchennikov, A.A., 95
 Tolstova, O.L., 44
 Tretyakov, D.A., 24, 86, 111
 Tretyakov, S.A., 224
 Trillo, S., 133, 184
 Tsesses, S., 194
 Tsvetkov, D.M., 217
 Tsvetkova, A.V., 35
 Tulegenov, A.P., 47
 Turtos, R.M., 218
 Tyshchenko, A.G., 85
 Tyukhtin, A.V., 56
 Urbas, A.M., 198
 Ustimov, V.I., 47
 Ustinov, A.V., 206
 Valovik, D.V., 106
 Vargas, C.A., 44
 Vasilchuk, V.Yu., 108
 Vedenyapin, V.V., 108
 Velez, P., 219
 Veretenov, N.A., 146
 Verma, V., 205
 Verre, R., 120
 Vetrov, S.Ya., 216
 Vignaud, A., 144, 220
 Vinogradov, A.P., 131, 140, 187, 231
 Vladimirov Yu.V., 36
 Vladimirov, A.G., 221
 Volkov, Yu.O., 28
 Volkovskaya, I.I., 222
 Vorobev, V.V., 56
 Voroshilov, P.M., 208, 223
 Voznuk, I., 182
 Vu, N.N., 109
 Wang, F., 118
 Wang, M., 224
 Wang, X.-C., 224
 de Weerd, C., 187
 Wenger, J., 182
 Whitehead, A., 158
 Wilde, M.V., 50, 110
 Wiryanto, L.H., 36
 Xia, W., 224
 Xu, G., 133
 Yakovlev, Yu.A., 24, 86, 111
 Yasina, N.F., 112
 Yassievich, I.N., 187
 Yermakov, O.Y., 225
 Yudin, D.I., 167
 Yulin, A.V., 142, 226
 Yves, S., 227
 Zaboronkova, T.M., 46, 69, 112
 Zaitseva, A.S., 69
 Zakharov, D.D., 113
 Zakharova, I.G., 92
 Zakhidov, A.A., 150, 151, 158, 208, 214, 223
 Zalipaev, V.V., 113
 Zalogina, A.S., 227
 Zasedatelev, A.V., 199
 Zavorokhin, G.L., 68
 Zaytsev, K.I., 93
 Zhang, Ch., 54
 Zhang, L., 228
 Zharov, A.A., 229, 230
 Zharov, A.A., Jr., 229, 230
 Zharova, N.A., 229, 230
 Zhirihin, D.V., 153, 230
 Zhuchkova, M.G., 114
 Zlobina, E.A., 115
 Zograf, G.P., 149
 Zubkovi, M.A., 129
 Zuev, D.A., 172, 227
 Zürich, M., 163
 Zyablovsky, A.A., 140, 231
 Zyryanov, V.Ya., 216